

Epoxy silane-modified colloidal silica particle. The particle size of the silica core is 7 nm.

Surface Modifications and Applications of Aqueous Silica Sols

PETER GREENWOOD

Department of Chemical and Biological Engineering
CHALMERS UNIVERSITY OF TECHNOLOGY
Gothenburg, Sweden 2010

Doctoral thesis for the degree of Doctor of Chemical Engineering

Surface Modifications and Applications of Aqueous Silica Sols

Peter Greenwood



Department of Chemical and Biological Engineering
Chalmers University of Technology
Göteborg, Sweden
2010

Surface Modifications and Applications of Aqueous Silica Sols

Peter Greenwood

ISBN 978-91-7385-430-6

© Peter Greenwood, 2010

Doktorsavhandlingar vid Chalmers tekniska högskola

Ny serie nr: 3111

ISSN: 0346-718X

Department of Chemical and Biological Engineering

Chalmers University of Technology

SE-412 96 Göteborg

Sweden

Telephone +46 (0) 31-772 10 00

Cover: Epoxy silane-modified colloidal silica particle. The particle size of the silica core is 7 nm.

Printed by Chalmers Reproservice

Göteborg, Sweden 2010

Surface Modifications and Applications of Aqueous Silica Sols

Peter Greenwood
Department of Chemical and Biological Engineering
Chalmers University of Technology
Göteborg, Sweden

Abstract

Methods of modifying the surface of the particles of colloidal silica were developed and the effects of surface modification on the properties of colloidal silica were studied.

Gamma-glycidoxypropyltrimethoxysilane (GPTMS) readily reacts with water to yield a hydrolysed silane that reacts readily with the silica surface. The epoxy functional groups were not affected during the hydrolysis but subsequent reaction with the silica surface opened the epoxy rings. The presence of silane groups on the particle surface was established by Si-NMR. About 1.5 GPTMS groups per nm² silica surface were needed to affect significantly the properties of colloidal silica. Modification of conventional silica sols improves the stability toward gelling by electrolytes, allows the preparation of mixtures of various lattices with silica sols that are stable toward gelling, increases the hardness of latex coatings, and improves the properties of pigmented coatings.

Methods were developed for making white composite pigments consisting of a silica core with a titania shell. A necessary step was the aluminate modification of the silica particles. With 1.5 aluminosilicate sites per nm² of core surface, well-dispersed composite particles having cores of uniform size in the range of 300 to 500 nm with a titania coating, the thickness of which corresponded to from 150 to 400 wt-% of titania based on the weight of the core, were prepared.

In a third type of modification colloidal silica was prepared with a high degree of structure, i.e. the silica particles having linear dimensions rather than being perfect spheres and being stabilised with amines. Such sols are very effective anionic components in dual retention aids in papermaking. Highly structured silica sols but being stabilised with sodium can be used to make solid electrolytes in lead-acid batteries with improved properties compared with conventional electrolytes.

Colloidal silica of different sizes can be used to improve the properties of concrete mixtures. Modifying colloidal silica to yield sols of wide particle size distributions provides a means to make concrete with improved properties. The small particle fraction of the sol will increase the early strength while the large particle fraction will increase the ultimate mechanical properties.

Keywords: Surface modification, silica sol, colloidal silica, applications, silane, titania, aqueous

List of publications

- I Aqueous Silane Modified Silica Sols: Theory and Preparation**
Peter Greenwood (corresponding author) and Börje S. Gevert
Submitted to Pigment & Resin Technology
- II Novel nano-composite particles: titania-coated silica cores**
Peter Greenwood, Börje S. Gevert , Jan-Erik Otterstedt, Gunnar Niklasson and William Vargas, Pigment & Resin Technology, 2010, Vol. 39, No. 3, pp. 135-40.
- III Modified silica sols: Titania dispersants and co-binders for silicate paints**
Peter Greenwood, Pigment & Resin Technology, 2010, Vol. 39, No. 6 (accepted for publication)
- IV Nano-Particle Reinforced Latex Dispersions With Modified Colloidal Silica**
Peter Greenwood, JCT CoatingsTech, 2008, Vol. 5, No. 2, pp. 44-51.
- V Some Important, Fairly New Uses Of Colloidal Silica/Silica Sol**
Jan-Erik Otterstedt and Peter Greenwood in Bergna, H.E. and Roberts, W. O. (Eds.), Colloidal Silica. Fundamentals and Applications. , 2005, Taylor and Francis, pp. 737-56.
- VI LIGHT SCATTERING IN PIGMENTED COATINGS: EXPERIMENTS AND THEORY,** W.E Vargas, P. Greenwood, J.E. Otterstedt and G. A. Niklasson, Solar Energy, 2000, Vol. 68, No. 6, pp. 553–61.

Contribution Report

- I** Major part of writing the manuscript and major part of experimental work
- II** Major part of writing the manuscript and major part of experimental work
- III** Sole author, experimental work except light scattering measurements
- IV** Sole author and planning of experimental work
- V** Co-author of chapter (review)
- VI** Experimental part: planning of/and sample and film preparation

List of publications related to the area but not discussed in detail

- I Advances in gelled-electrolyte technology for valve-regulated lead-acid batteries.**
D.W.H. Lambert, P.H.J. Greenwood, M.C. Reed,
Journal of Power Sources, 2002, No. 107, pp.173–9.
- II Using Silica to Control Bleed and Segregation in Self-Compacting Concrete.**
C. Bigley and P. Greenwood, Concrete, 2003, Vol. 37, No. 2, pp. 43-5.
- III Enhancement of low VOC floor-coatings with modified colloidal silica.**
Dirk Mestach, Derrick Twene, Peter Greenwood and Hans Lagnemo, Proceedings,
European Coatings Conference Parquet Coatings III, Berlin, November 25th-26th, 2004.
- IV Aggregation of Nanosized Colloidal Silica in the Presence of Various Alkali Cations Investigated by the Electrospray Technique**
Ann-Catrin J. H. Johnson, Peter Greenwood, Magnus Hagström, Zareen Abbas, and Staffan Wall, Langmuir, 2008, No. 24, pp.12798-806.
- V Modified colloidal silica in silicate paint.**
Céline de Lame, Jean-Marie Claeys, Peter Greenwood and Hans Lagnemo, PPCJ, 2010,
No.1 (January), pp. 48-52.

List of patents related to the area but not discussed in detail

Granted patents (invention represented by one of the EP or US patents)

- I Silica based sols**
Peter Greenwood, Magnus Olof Linsten and Hans Johansson-Vestin,
EP 1 242 308 B1
- II Primer coating of steel**
Gerald Howard Davies, Peter Harry Johan Greenwood and Paul Anthony Jackson
EP 1 317 515 B1
- III Composition and method to prepare a concrete composition**
Peter Greenwood, Hans Bergqvist and Ulf Skarp
EP 1 286 929 B1
- IV Mixture of silica sols**
Peter Greenwood, Hans Bergqvist and Ulf Skarp
US 6 596 250 B1
- V Construction Material**
Peter Greenwood, Hans Bergqvist and Ulf Skarp
EP 1 292 547 B1
- VI Sealing composition and its use**
Peter Greenwood, Inger Jansson and Ulf Skarp
US 6 857 824 B1
- VII Injection Grouting**
Peter Greenwood, Inger Jansson and Ulf Skarp
US 7 163 358 B1
- VIII Colloidal Silica Dispersion**
Peter Greenwood
EP 1 554 220 B1
- IX Aqueous Silica Dispersion**
Peter Greenwood and Hans Lagnemo
EP 1 554 221 B1
- X Composition prepared from silica sol and mineral acid**
Peter Greenwood, Hans Lagnemo and Matthew Reed
US 7 674 833 B2
- XI Composition for producing a barrier layer on laminated packing material**
Peter Greenwood and Hans Lagnemo
EP 1 824 937 B1

Granted patents, continued

XII Detergent Composition

Peter Greenwood and Hans Lagnemo
EP 1 733 015 B1

Pending Patents (PCT)

I Pigment Dispersion

Peter Greenwood and Hans Lagnemo
WO 2008/057029

II Coating composition for metal substrates

Victoria Browne, Paul Anthony Jackson, Alistair James Reid and
Peter Harry Johan Greenwood
WO 2008/128932

Table of contents

| | |
|--|-----------|
| 1. Introduction | 1 |
| 2. Colloidal silica | 3 |
| 3. Silanes, especially Silquest A-187 | 6 |
| 4. Modification of the silica surface | 8 |
| 4.1. Silylation of the silica surface..... | 8 |
| 4.2. Titania coating of the silica surface..... | 10 |
| 5. Applications of colloidal silica | 16 |
| 5.1. Applications of silane modified colloidal silica..... | 16 |
| 5.1.1. Silicate paint..... | 16 |
| 5.1.2. Pigment dispersant..... | 18 |
| 5.1.3. 2-k and curable lacquers..... | 23 |
| 5.2. Applications of conventional colloidal silica..... | 29 |
| 5.2.1. Cementitious applications..... | 29 |
| 5.2.2. Paper-making..... | 34 |
| 5.2.3. Lead-acid batteries..... | 40 |
| 5.2.4. Titania coated colloidal silica..... | 47 |
| 6. Outlook | 48 |
| 7. References | 49 |
| 8. Acknowledgements | 57 |

1. Introduction

When Charles C. Payne of the Nalco Chemical Company in the USA was asked, “Where has colloidal silica been used?” he answered that a more pertinent question is, “Where has it not been used?” .The uses of colloidal silica in industry and academic research are too many to be enumerated here but some will be briefly mentioned.

Dilute silica sols were prepared and studied over 75 years ago. Their uses as binders in catalyst preparation, as glazes on ceramics, as coatings on concrete and plaster of Paris, in treatment of paper and textiles, and many other applications were investigated (Griessbach, 1933). These early silica sols contained less than 10 % by weight of silica, were not very stable and did not have reproducible properties. In 1955, Iler predicted that colloidal silica would not be accepted for wide commercial use before these shortcomings were remedied (Iler, 1955). Good stability at high concentrations of silica was probably the most serious weakness of early silica sols.

Product development work in several industrial laboratories resulted in the production of concentrated silica sols of high stability and very reproducible properties (Iler, 1979). The use of colloidal silica could now be expanded to previously inaccessible applications. Colloidal silica is widely used as binder in shell investment casting. Refractory binders can be bonded with colloidal silica to give insulators that have excellent high-temperature resistance. Small amounts of colloidal silica increase the coefficient of friction of surfaces. Carpets and other surfaces coated with colloidal silica resist soiling because the colloidal silica occupies the site that would most likely retain visible soil. The strength and adhesion of latex-based adhesives and paints can be enhanced by the addition of colloidal silica. Beverages, such as wine, beer, or fruit juices can be clarified using colloidal silica as an aid to flocculation and coagulant for proteins.

Fairly recent and important developed applications of colloidal silica, which have been studied in the present work, are the use of colloidal silica to make high quality concrete, as retention aid in papermaking, as polishing agents for silicon wafers, to provide solid electrolytes in lead-acid batteries and as components in high quality coatings.

The coagulation-dispersion behaviour of aqueous silica sols is central to many applications where they are used. Aqueous silica sols are of particular interest in colloidal science because their coagulation-dispersion behaviour is said to be “anomalous”; i.e. their stability in terms of electrolyte-pH control does not follow the pattern followed by almost all other oxide and latex colloidal materials. This characteristic of silica sols has been used by scientists to develop highly concentrated silica sols of remarkable stability.

There are still applications where many of the properties of colloidal silica could be put to good use but cannot, or only with difficulty, because even the outstanding stability of modern silica sols is not high enough. It has, for instance, been found that colloidal silica is an excellent dispersant of pigments but the stability of silica particles in the high solids environment of pigment paste may pose a problem, which may be aggravated by the presence of electrolytes in the system. Low temperatures are another environment in which the stability of conventional silica sols is poor.

One objective of this investigation is therefore to change the nature of the silica particles by chemical modification of their surface. In one approach, stability of colloidal silica toward gelling under exacting conditions of solids content, temperature and electrolyte content was shown to be improved by reacting the particle surface with organofunctional silanes. The structure and reactions of organofunctional silanes are described in section 3. Procedures for modifying the

surface of silica particles that were developed in this work are detailed in section 4.1. The effects of silane modification on the performance of colloidal silica in silica paint, as dispersant in pigment pastes and as an additive in 2-k and curable lacquers are shown in section 5.1.

In another approach, described in section 4.2, the surface of the particles of colloidal silica was modified by reacting it with sodium aluminate to create negatively charged aluminosilicate sites on the surface. The particles of colloidal silica modified in this manner can readily be coated with metal oxides (e.g., titanium dioxide). In section 5.2.4 some of the light scattering properties of such materials are briefly discussed.

Another objective is to describe and explain the use of conventional colloidal silica in some important and fairly recently developed applications as an agent to improve the properties of concrete (section 5.2.1), as retention aid in the paper making process (section 5.2.2), and as a means to provide solid electrolytes in lead-acid batteries (section 5.2.3).

2. Colloidal silica

Aqueous colloidal silica dispersions, silica sols, have been commercially available since the early 1930s when a 10 wt-% silica sol was produced and sold by I.G. Farben. However, they did not find a broader use until the 1950s when these dispersions could be made at higher solid concentrations (e.g., 30 wt-% because of the development in the ion exchange technology that led to reduced levels of destabilising ions/impurities and hence improved colloidal stability) (Iler, 1979; Payne, 1994). The number of uses for colloidal silica as well as the number of different silica sol products has increased since. Today, colloidal silica dispersions are commercially available in a variety of different kinds of products: anionic and cationic and with different types of surface modifications (e.g., aluminate modification and silylated). Commercial silica sols are fluid, with the viscosity typically less than 35 mPas, and stable toward gelling and settling in the pH range between 8 and about 10. They have been stabilized, or brought into this pH range, by adding an alkali (e.g., NaOH, KOH, LiOH, or NH₃) to the sol. The silica particles are negatively charged and charge neutrality is brought about by the presence of positively charged counter ions, such as Na⁺, K⁺, Li⁺, and NH₄⁺. There are also available commercial silica sols consisting of positively charged particles, which have been stabilized at pH of about 4 by adsorption of polycations of, for instance, aluminium onto the surface of the particles. Most commercial silica sols are quite monodisperse and consist of dense, discrete spheres with a range of diameters between about 5 nm and 100 nm. The maximum concentration depends on particle size and is 15 % by weight for 5 nm particles, 30 % by weight for 8 nm particles and at least 50 % by weight for 100 nm particles. There are also commercial sols that have deliberately been made polydisperse or where the particles are not discrete spheres but instead chains of linked spheres. The appearance of silica sols depends on particle size, particle size distribution, and concentration. They look milky if the particle size is large and the concentration is high, opalescent if the size is intermediate or clear, and almost colourless when the diameter of the particles is in the smallest size range.

Colloidal silica dispersions are used in an extensive range of industrial applications covering the most different applications areas, including flocculation applications such as beverage fining and retention aids in papermaking, as a binder in high-temperature applications such as foundry production, ceramics, and catalyts (Dahar and Te, 2009; Bradzil, George and Rosen, 2009; May, Vogel, Siegert, Gaudschun and Quandt, 2009), and recently in fuel cells applications (Larsen, Olsen and Jensen, 2009), as an additive in cementitious applications (Otterstedt and Greenwood, paper V), as an abrasive in wafer polishing (WP) and chemical mechanical planarization (CMP) (Ahn, Yoon, Baek and Kim, 2004; Matijevic' and Babu, 2008; Yang, Oh, Lee, Song, and Kim, 2010), as solid state electrochemical devices (Collinson, Zambrano, Wang and Taussig, 1999), and as a gelling agent when sealing hard-rock tunnels (Funehag and Fransson, 2006; Funehag and Gustafson, 2008; Butrón, Gustafson, Fransson and Funehag, 2010) or solidifying electrolyte in lead-acid batteries (Lambert, Greenwood and Reed, 2002). Furthermore, silica sols are used in a vast number of coating applications to improve mechanical properties as well as anti-blocking, adhesion, and wetting properties just to mention a few.

The nature of the silica surface, the specific surface area, and degree of aggregation are important parameters regardless of application area.

The surface of a silica sol is fully hydroxylated with a maximal amount of silanol groups. The number of silanol surface groups was determined by Zhuralev to be about 4.6 OH per nm² where the measured silanol numbers were ranging from 4.3 up to 5.8 OH per nm² silica surface (Zhuralev, 1993). However, in Zhuralev's study the silica samples were dried and one may expect an even higher silanol number for a silica surface that has never been subject for drying or at least to be in the upper end of this range. The silanol groups may also be of different types: single isolated silanol groups, geminal (silanediol groups) and vicinal types. The silanol groups have a big impact on the surface charge of the silica particles and hence the stability of the silica sol. In addition, they will act as reactive groups enabling chemical grafting of the silica surface or playing an important role in the formation of siloxane bridges between the silica particles during aggregation/gellation processes.

Surface area - high

Colloidal silica dispersions having a high specific surface area (m²/g), i.e. small particle size, have many surface groups that can participate in numerous bonds and reactions, as well as bearing a high electric charge per kg product. Such products are particularly useful in applications of where binder, reactant, and flocculating properties are desirable. The specific surface area for these kinds of products is typically in the range of 200 m²/g and upwards.

Surface area - low

Colloidal silica dispersions of larger particles with a lower specific surface area are typically used in polishing applications, such as an abrasive, where a coarser particle offers a higher removal rate, such as a surface modifier in, for example, anti-skid coatings on paper substrates where enrichment on the substrate surface is favourable or as a carrier/core for metal oxides in composite pigments, catalysts, etc.

Aggregation-structured colloidal silica dispersions

Non-aggregated silica dispersions are preferably used in coating applications in order to enhance properties such as cross-linking density. The effect on hardness and Young's modulus in coatings are highly dependent on the size of the silica particle and aggregation will increase the size of the silica material and hence significantly decrease the effect on the mechanical properties from the particles (Douce, Boilot, Biteau, Scodellaro and Jimenez, 2004). Further, gloss and haze may be compromised if aggregation occurs in the system. The absence of aggregated particles is vital in the polishing field since aggregates may cause scratches and other surface defects.

Structured or aggregated silica dispersions are beneficial in applications where flocculation and gellation is desirable. The degree of aggregation is normally characterised by the S-value, which is a measure of the silica (as per cent) in the disperse phase (Iler and Dalton, 1956). Silica sols used in flocculation applications (e.g., as a retention aid in papermaking) typically has an S-value of 15-35 % (Andersson, Larsson and Lindgren, 1997). In gellation applications, such as solidification of sulphuric acid in lead-acid batteries a typical S-value could be in the range of 30-50 % (Greenwood, Lagnemo and Reed, 2010).

Aluminate modification of the silica surface.

Modification of the silica surface with sodium aluminate gives a fix negative surface charge that is not pH dependant and gives a surface with a higher charge (pH range 3-9) relative to non-modified silica (Iler, 1979). Furthermore, such surface modification lowers the solubility of the silica surface (Iler, 1973) and therefore reduces the Ostwald ripening and hence can be used to stabilise colloidal silica dispersions of high specific surface area. Aluminate modified silica sols with a high specific surface area above 500 m²/g and surface charge are used in the papermaking area (Johansson and Larsson, 1994), whereas aluminate modified silica sols of lower surface area may be used in wine clarification where the modification (Bohm, Genth, Schober, and Simons, 1977) gives a high surface charge at pH 3.5 - 4 (i.e. the pH of wine). In addition to this, aluminate modified silica sols have been found to work well in cementitious applications (e.g., concrete), where strength is enhanced and flowability (Greenwood, Bergqvist and Skarp, 2004) is not compromised relative to non-modified sols.

3. Silanes

Silanes are a group of chemicals that has been around for more than 50 years. They are widely used as coupling agents because of their bi-functional nature (Osterholtz and Pohl, 1992). One organofunctional group, Y, and three hydrolysable groups, X (see Figure 1).

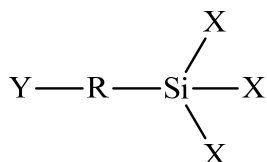


Figure 1: Structure of silane.

There are a number of different hydrolysable groups but the two main groups are chlorosilanes and alkoxy silanes and the most common groups of those are the trialkoxysilanes, Y-R-Si(OR')₃. By hydrolysis in water, the X group is converted to the reactive silanol form, which ultimately condenses to a siloxane bonds. Both reaction rates are strongly dependent on pH, but under the right conditions the hydrolyse step is relatively fast (several minutes); however, the condensation reaction is much slower (several hours).

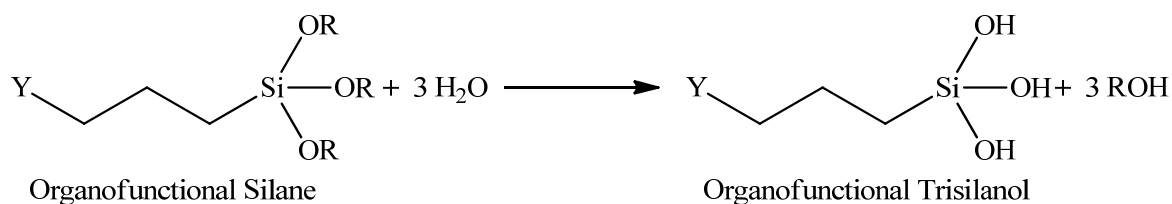


Figure 2: Hydrolysis of silane.

In order to be suitable for silylation of the surface of an aqueous silica sol, one can expect that the silane should be possible to hydrolyse in water, i.e. sufficient solubility and that such hydrolysed silane should be stable enough to avoid self-condensation. The first condition eliminates silane with a too hydrophobic functional group (e.g., long carbon chain). The latter condition normally eliminates the use of chlorosilanes and aminosilanes since these kinds of silanes dramatically affect the pH (due to the release of HCl and alkali, respectively) and hence increase the rate of condensation reactions dramatically (Osterholtz and Pohl, 1992).

In this respect, functional tri-alkoxy silanes are a preferred type of silane, especially epoxy-silanes with the focus on gamma-glycidoxypropyl-trimethoxysilane (Silquest A-187) because of its easiness in preparing stable pre-hydrolysed aqueous solutions of high concentrations in the epoxy-functional group. Pre-hydrolysed solutions of Silquest A-187 are stable for at least a couple of weeks if the pH of the solution is in the range of about 4-7. Condensations reactions are at a minimum under these conditions (see Figure 3).

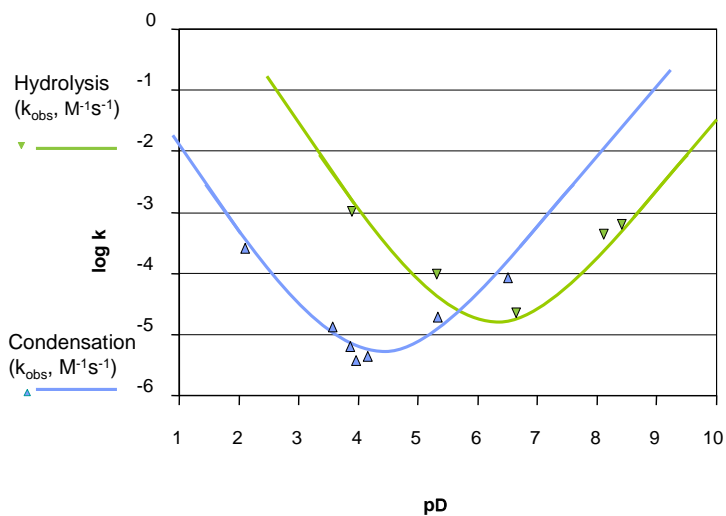


Figure 3: pD - Rate Profile for Combined Hydronium- and Hydroxide-Catalyzed Hydrolysis and Condensation of Silquest A-187 (γ -glycidoxypropyltrimethoxysilane) and Its Triol in D_2O (Plueddemann, 1991). Courtesy of Alain Lejeune, Momentive.

4. Modification of the silica surface

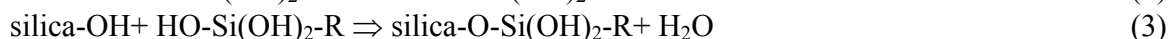
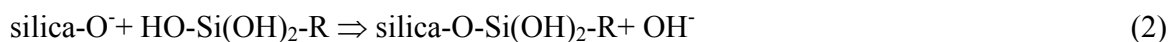
4.1. Silylation of the silica surface (paper I)

The reaction between a hydrolysed silane (e.g., gamma-glycidoxypropyltrialkoxysilane) and the silanol groups of the silica particles is a condensation reaction.



Based on steric reasons, it is unlikely that all three alkoxy groups will react with the silica surface. The reaction is fast in the alkaline pH region (Osterholtz and Pohl, 1992) and can therefore be conveniently carried out at the pH of the sodium-stabilised sol, which is about pH 10. For uniform coverage of the particle surface, it is essential that the silane is present in monomeric form and not as large oligomers or cyclic species (Peeters, 2000). Under moderate conditions of rate of addition of silane and temperature, however, self-condensation and precipitation will not occur. An aqueous silica sol has about 4.6 silanol groups per nm² surface (Zhuralev, 1993), but considering that each silane may react with three surface groups, fewer silane molecules per nm² will be required to react fully with the silica surface. Silylation of the silica surface will reduce the number of silanol groups and hence make silylated sols more stable toward gelling through formation of siloxane bonds between particles.

The shape of the curves in Figure 4 indicates that at least two types of reaction take place during the silylation of the silica surface as suggested by the following reaction schemes:



During the first 5 min of silane addition, pH increased rapidly from 10.1 to almost 10.4 (scheme 2), whereas there was a more gradual increase to 10.6 during the next 135 min (scheme 3), after which time the pH remained constant. In reaction 2 the hydrolysed silane reacted rapidly with the negatively charged sites of the silica surface releasing hydroxyl ions, which raised the pH and created more charged sites on the surface (Iler, 1979). In the slower reaction (reaction 3), probably catalysed by hydroxyl ions, the hydrolysed silane condensed with surface silanol groups.

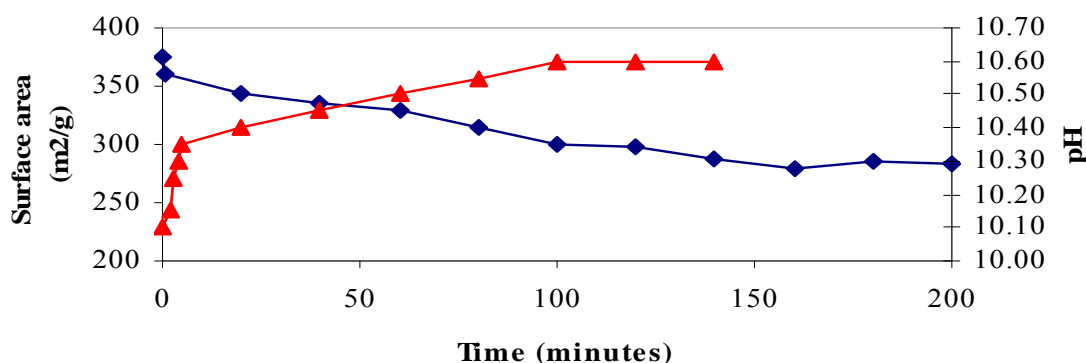


Figure 4: Specific surface area (blue) and pH (red) versus time for a 7 nm silica sol which at the end of the experiment will have 0.6 molecules GPTMS per nm² silica surface as a function of time.

Continuous silane addition

With a higher degree of silylation of the silica surface, which is the preferred route for a surface modification corresponding to 1.4 and 1.7 molecules of GPTMS per nm² silica surface (now commercial products under the names of Bindzil[®] CC30, dp: 7 nm, and Bindzil[®] CC40, dp: 12 nm, respectively), there is a reduction of about 85% of the surface charge as measured by Polybrene titration (Table V, in paper I). This observation is well in line with reported data on zeta potential. Blute, Pugh, van de Pas, and Callaghan (2007) found that Bindzil[®] CC30 had a very low zeta potential (below -10 mV) in the pH range of 2-6 and significantly lower than that of the non-modified silica sol (Bindzil[®] 40/220) in the pH range of 6-11. Blute et al. also found that the low surface charge remained unchanged over time.

The pre-hydrolysed silane was continuously added to the colloidal silica at a reaction temperature of 60 °C, a rate of about 1.4 molecules GPTMS per nm² silica surface and hour and under good agitation. The comparison between the ²⁹Si NMR spectra (Figures 3 and 4 in paper I) reveals a significant reduction in the ratio of silanol groups to bulk siloxane units (Q3/Q4) for a silica sol silylated with 1.4 molecules GPTMS per nm² silica surface relative to a non-silylated sol with a particle size of 7nm. This reduced ratio indicates a covalent bond between the silane and the silica surface. The ²⁹Si NMR spectra were de-convoluted and gave a ratio Q3/Q4 of 0.240 for the non-modified silica sol and 0.140 for the silylated silica sol. The change in the Q3/Q4 ratio, indicating a reduction of Q3 groups by 42%, corresponded fairly well to the drop in specific surface area by 38% (from 369 m²/g for the unmodified sol to 227 m²/g for the silylated sol).

The epoxy-functional group and silane solubility of the silylated silica sol

¹³C NMR confirmed that the alkaline conditions (pH of about 10) during the condensation reaction transformed the functional epoxy group of the silane to a diol group (Figure 5). This finding is consistent with reports that ring opening can take place under alkaline conditions (Riegel et al., 1998).

Further, measurement of the content of free silane monomer by HPLC gave a monomer content of 2600 ppm at pH 10.9 for a silica sol with a particle size of 7 nm and silylated with 1.4 molecules GPTMS per nm² silica surface. In contrast, soluble silica, as measured by the ammonium heptamolybdate method, was found to be 960 ppm. On the other hand, when the pH of the sol was adjusted to about 8 by cation exchange, the monomer content was only about 280 ppm, indicating silane solubility increases at alkaline pH. In the latter case the soluble silica was found to be 87 ppm, close to the theoretical value of a flat silica surface at room temperature. No free silane dimers or oligomers were detected by the HPLC analysis of the silane-modified silica sols. This finding strongly indicates that nearly all of the added silane had reacted with the silica surface because the total amount of added silane corresponds to 53 600 ppm of silane in the silylated sol.

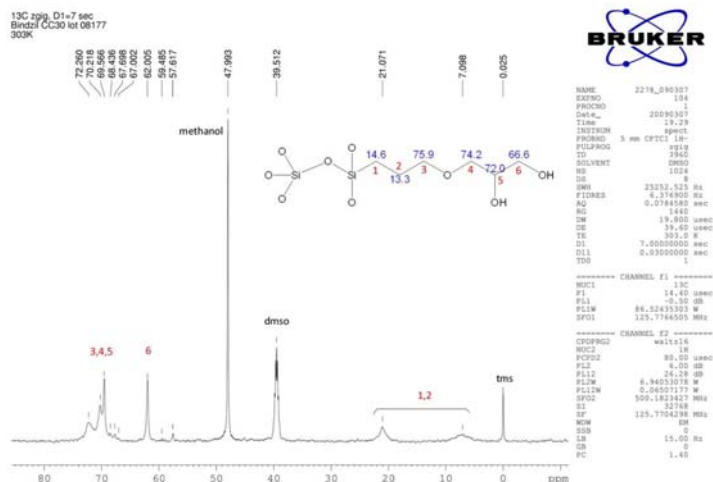


Figure 5: ^{13}C HR/MAS NMR spectrum of 7 nm silica sol silylated with 1.4 GPTMS per nm^2 silica surface (Bindzil[®] CC30).

Effect of rate of addition and amount of silane on sol stability

Lower rates of addition, typically about 0.6 silane molecules per nm^2 added for a 2 h period at room temperature, result in clear stable sols. Even rates of addition as high as 1.4 molecules per nm^2 particle surface area and hour at 60 °C result in clear stable sols. At very high rates of addition (e.g., 4.4 molecules per nm^2 surface of the sol and hour at 70 °C), precipitation of the sol, self-condensing of the silane, or both occurred.

4.2. Titania Coating of the silica surface (paper II)

Titanium dioxide (TiO_2) is the principal white pigment because of its scattering power, which is superior to that of any other white pigment. It occurs in nature in the crystalline form rutile, anatase, and brookite. Rutile and anatase are manufactured in large quantities and are primarily used as pigments but also as catalysts and in the production of ceramics.

Two processes, the sulphate process and the chloride process, are used to make TiO_2 (Braun, Baidin and Marganski, 1992). The major objection against the sulphate process has been the amount of by-product gypsum it produces. The chloride process is considered a more environmentally friendly method of producing TiO_2 . In general, however, the environmental impact of TiO_2 production is mostly a factor of the raw materials used, the effluent treatment processes, and the degree of by-product development a particular plant has.

The scattering of light by TiO_2 particles varies with particle size and reaches a maximum when the particle size is about one-half of the scattered wavelengths of light that are in the 250 to 300 nm size range (Forrest, 2001). For maximum scattering efficiency, commercial TiO_2 pigment should therefore be milled to a particle size narrowly distributed around a value in the 250 to 300 nm size range, which is normally not done (Forrest, 2001). Further, the pigment particles should be well dispersed and not aggregated in order to give optimal light scattering performance (Auger, Barrera, and Stout, 2003). From environmental considerations, it is of interest to use raw

material as little as possible, which is available in limited supply and negatively affects the environment when it is refined to TiO₂. Recently, there have been several papers discussing monodisperse nano-composites obtained by the deposition of titania onto silica cores (Li and Dong; Ryu, Kim, and Koo, 2003; Choi, Park, and Singh, 2005; Kalele et al., 2005). However, the titania source has been expensive titaniumalkoxides and/or the amount of titania coated onto the silica core has been relatively low.

Therefore, an objective of the present investigation was to develop methods for coating silica core particles with TiO₂ in an effort to obtain composite particles with well-defined and carefully controlled ratios between particle diameters and thickness of titania coating.

Because the isoelectric point of silica is between pH 1.7 and 2.0, silica sols have a low surface charge at pH below 7 (Iler, 1979). If, however, negatively charged aluminosilicate sites are generated on the surface by heating the sols with sodium aluminate, the surface will remain negative at pH down to about 2. It is reasonable to assume that positively charged subcolloids or polycations of titania, existing only in quite acidic solutions, would adsorb more readily onto a negatively charged aluminate-modified silica surface than on an almost neutral, unmodified silica surface. To test this hypothesis silica particles with a diameter of 300 nm were heated with a sodium aluminate solution under conditions such that the silica surface contained 0, 0.6, or 1.5 aluminosilicate ions per nm² (sol 1A, 1B and 1C in Table 1). (For sample preparation and experimental methods, see also paper II.) Table 1 shows that the particles containing 1.5 aluminosilicate sites per nm² had the highest charge at pH 2.0 as determined from electrophoretic mobility measurements. Care had to be taken to measure the charge very soon after the pH of the sol had been adjusted to 2.0 because at this pH aluminium will begin to dissolve out from the particle surface. The table also shows that after charge reversal, accomplished by adding the silica sols to a solution of titanium tetrachloride of a pH below 1.5, the silica sol (2C) containing the high amount of aluminium per nm² again had the highest charge but now positive, indicating that this surface adsorbed more positively charged titania species than the other silica sols, i.e. 2A and 2B, with 0 or 0.6 Al per nm². Adjusting the pH of the dispersion of charge-reversed sol to 1.5 (from about 1.4) and heating at 75 °C for about 10 min increased the charge on all three types of sol particle, but somewhat more for the particles containing most aluminium (3C). The titanium concentration in the aqueous phase of this silica sol was lower than in the other silica sols, indicating that particle surfaces having a high surface concentration of negative sites adsorb titania species more effectively compared with 4A-C.

Table 1: Electrophoretic mobility at pH 2.0 ($\text{m}^2 \cdot \text{V}^{-1} \cdot \text{s}^{-1} \cdot 10^8$).

| Step | Silica sol (A) not modified | Silica sol (B) mod.0.6 Al nm^{-2} | Silica sol (C) mod.1.5 Al nm^{-2} |
|---|--------------------------------|---|---|
| 1. Before charge reversal | 0.7 | - 1.2 | - 3.1 |
| 2. After charge reversal | 2.1 | 2.6 | 4.3 |
| 3. After pH adjustment and heating to 75 °C | 2.5 | 2.8 | 4.6 |
| 4. Concentration TiO_2 (ppm) in the supernatants of the sols from point 3 in this table. | 880 | 638 | 230 |

Sol A from step 1 is noted by 1A, and so on in the text.

Figures 6-8 show that after coating the charge-reversed sol with titania, adding titanium chloride at a rate of $0.2 \text{ mmol TiO}_2/(\text{h} \cdot \text{m}^2)$ and in an amount corresponding to 233% titania based on the weight of silica while maintaining the pH at 1.5, the best result was obtained with the sol containing silica core particles with 1.5 Al-sites per nm^2 surface. The particles are discrete and appear to be uniformly coated with a layer of titania (Figure 8). The particles with 0.6 Al-sites per nm^2 surface seem to be somewhat less uniformly coated and somewhat aggregated (Figure 7). If no alumina is present on the particle surface, not all the added titania is deposited on the core particles but form secondary titania particles in the dispersion, which aggregate with themselves and with partially coated core particles (Figure 6).

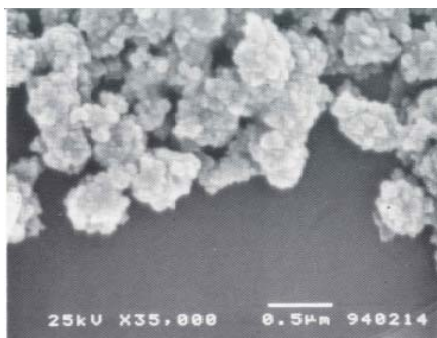


Figure 6: SEM micrograph of a silica core with a particle diameter of 300 nm (not aluminate-modified core surface) coated at pH 1.5 with 233 % titania based on the weight of silica.

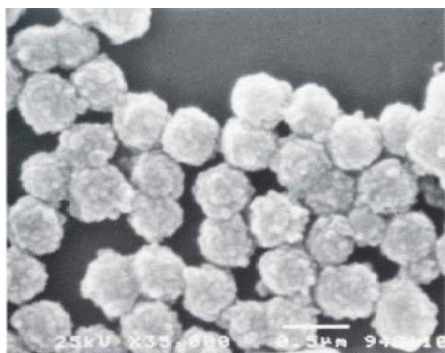


Figure 7: SEM micrograph of a silica core with a particle diameter of 300 nm (aluminate-modified core surface) 0.6 Al per nm² coated at pH 1.5 with 233 % titania based on the weight of silica.

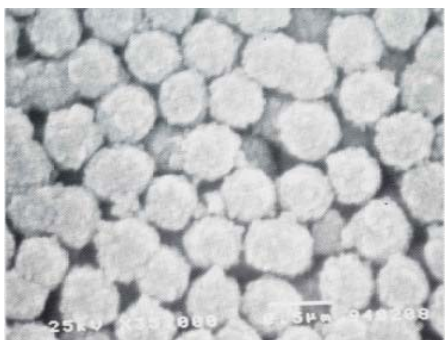
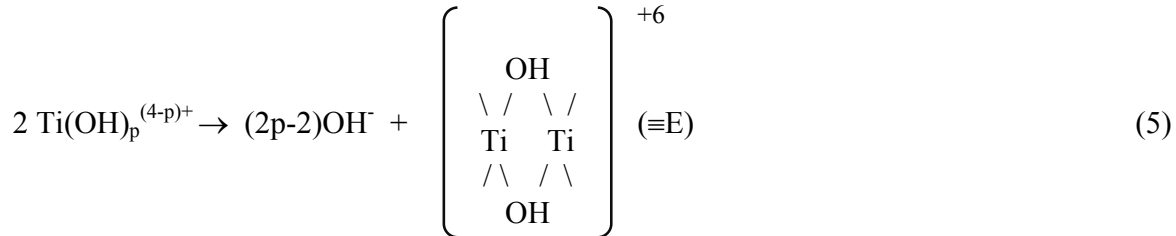


Figure 8: SEM micrograph of a silica core with a particle diameter of 300 nm (aluminate-modified core surface) 1.5 Al per nm² coated at pH 1.5 with 233 % titania based on the weight of silica.

Coating of silica cores with titania has been suggested to take place by heterogeneous nucleation on the core surface (Hsu, Yu, and Matijević, 1993). The following mechanism for the reaction has been proposed and assumed that step five was the rate-determining step and that the rate of reaction increases rapidly with increasing pH (Matijević, Budnik, and Meites, 1977).



pH has been recognised (and also agitation) as an important parameter in the process of coating silica cores with titania (Kohlschütter, Getrost, Hörl, Reich, and Rößler, 1970). Following their lead, the effect of pH on the quality of titania coating on silica cores was investigated. Because the iep of titania is about 5.5 to 6.0, it follows that the positive charge on titania particles decreases with increasing pH (Barringer and Bowen, 1985). Aggregation that is due to diminishing electrostatic repulsion between the particles could therefore occur if coating takes place at pH values approaching the iep from the acid side. On the other hand, it has been reported that uniform coating of silica cores with titania is favoured by low ionic strength (Hsu et al., 1993), which speaks against low pH where the ionic strength is high. Moreover, the solubility of titania increases with decreasing pH (Look and Zukoski, 1992), an event that could lead to substantial losses of titania through the ultrafiltration membrane used in the coating procedure. Obviously, one must find a pH at which the uniformity of the coating is maximised whereas losses of titania and aggregation are minimised. Thus, coating 300 nm aluminium silicate modified silica sols, 3C, using an addition rate of titanium chloride of $0.2 \text{ mmol h}^{-1} \text{ m}^{-2}$ and in an amount corresponding to 233 % titania based on the weight of silica, yielded a more dispersed system at pH 2.0 (Figure 9) than that at pH 1.5 (Figure 8). The concentrations of titania in the aqueous phase at pH 1.5 and 2.0 were 178 and 130 ppm, respectively, suggesting that the losses of titania at pH 1.5 were about 50 % higher than at pH 2.0, although at both pH values the losses were negligible (less than 0.4 % of the titania was lost through the microfiltration membrane at pH 1.5). A higher chloride concentration (e.g., solutions acidified with HCl) has been reported to yield a grainier surface of TiO_2 particles. The particles in Figure 8 are grainier than the particles in Figure 9 (pH 2.0), a finding in accord with those of Look and Zukoski (1992).

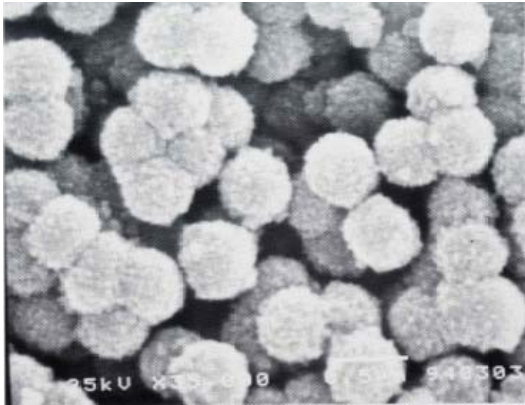


Figure 9: SEM micrograph of a silica core with a particle diameter of 300 nm (aluminate-modified core surface) 1.5 Al per nm² coated at pH 2.0 with 233 % titania based on the weight of silica.

5. Applications of colloidal silica

5.1. Applications of silane modified colloidal silica

5.1.1. Silicate paint (paper III)

Silicate paint is a traditional inorganic concrete paint using potassium silicate as a binder for inorganic fillers (e.g., clays and pigments such as titania and iron oxides). However, the solubility of the silicate binder of the paint in water is at first relatively high because of the high alkali content of the paint, but this problem is reduced over time by the reaction of the paint with calcium-rich surfaces (e.g., concrete surfaces) and the creation of insoluble calcium silicate species. Silicate mineral paints have several advantages (such as high durability because of their inorganic composition, scrub resistance, high vapour water permeability, resistant to mould and fungal growth because of their high alkalinity, odourless, non flammable, free of solvents and biocides, and environmentally friendly). Their major drawbacks are high water absorption and low flexibility.

One way of reducing the solubility of the dried silicate paint binder in water and hence improve the weather resistance of the paint is to add a conventional silica sol to the potassium silicate binder, which increases the molar ratio of silica to the alkali of the binder. Conventional silica sols are currently being used in combination with potassium silicates as binders in wholly inorganic silicate paints (Heiberger and Schl affer, 2001; Rademacher, Pantke, and Wilhelm, 2008).

Adding conventional silica sols to the potassium silicate binders, however, reduces the stability towards gelling and the film-forming properties of the binder. These drawbacks can be minimised by using silane-modified colloidal silica. Table 2 shows that stability toward gelling is significantly improved by silane modification.

Table 2: Viscosity for silicate-silica sol mixtures.

| No. | Molar ratio: SiO ₂ /K ₂ O | Silica sol : Non-surface modified, dp: 7 nm | | Silica sol: Silane modified dp: 7 nm | |
|-----|--|--|------------------------------|---|------------------------------|
| | | Viscosity (mPas), 1 week | Viscosity (mPas), 2 weeks | Viscosity (mPas), 1 week | Viscosity (mPas), 2 weeks |
| 1 | 5.0 | 1287 | Gel | 19 | 131 |
| 2 | 6.0 | 14 | Gel | 6.6 | 10 |
| 3 | 7.0 | 6.7 | Gel | 4.2 | 5.1 |
| 4 | 8.0 | 4.8 | Gel | 3.5 | 3.8 |
| 5 | 9.0 | 4.0 | Gel | 2.9 | 3.0 |
| 6 | 10.0 | 3.7 | Gel | 2.8 | 2.9 |
| 7 | 11.0 | 3.3 | 31 | 2.6 | 2.8 |
| 8 | 12.0 | 3.1 | 13 | 2.5 | 2.5 |

The film forming properties of silicate binders deteriorate with increasing ratio. When a silica sol has been used to increase the ratio of the binder, silane-modified sol, in comparison with a

conventional sol, yields somewhat improved film-forming properties. Poorer film-forming properties at higher ratios may be rectified to some extent by the addition of a wetting agent* (Table 3 and paper III).

Table 3: Film properties for silicate-silica sol mixtures.

| No. | Molar Ratio: SiO ₂ /K ₂ O | Colloidal silica - Silane modified | Colloidal silica non- surface modified |
|-----|--|---------------------------------------|---|
| 1 | 5.0 | Film | Film |
| 2 | 6.0 | Film | Film |
| 3 | 7.0 | Film | Film |
| 4 | 8.0 | Film | No film* |
| 5 | 9.0 | Cracks* | No film* |
| 6 | 10.0 | No film* | No film |
| 7 | 11.0 | No film | No film |
| 8 | 12.0 | No film | No film |

*: Film was formed when wetting agent was added.

The water resistance is normally improved when the molar ratio SiO₂/K₂O is increased (i.e. lower alkali content). As shown in Table 3, at a given molar ratio, silane-modified colloidal silica improves the water resistance relative to non-modified colloidal silica.

Table 4: Water resistance of film from silicate-colloidal silica mixes.

| No. | Molar Ratio: SiO ₂ /K ₂ O | Colloidal silica - Silane modified | Colloidal silica non- surface modified |
|-----|--|---------------------------------------|---|
| 1 | 5.0 | 0 | 0 |
| 2 | 6.0 | 0 | 0 |
| 3 | 7.0 | 1-2 | 1 |
| 4 | 8.0 | 2 | --- |
| 5 | 9.0 | --- | --- |
| 6 | 10.0 | --- | --- |
| 7 | 11.0 | --- | --- |
| 8 | 12.0 | --- | --- |

----: No film 0: Film “dissolved”. 1: Severe impact on the film.

2: Some impact on the film 3: No impact on the film.

Another property that can be enhanced by using silane-modified colloidal silica in silicate paint is dirt pick-up resistance. Recent findings (De Lame, Claves, Greenwood, and Lagnemo, 2009) indicate that a dramatic improvement, from 0.39 to 0.95, in dirt pick-up resistance could be achieved when replacing 2/3 of the potassium silicate binder with silane modified colloidal silica, Bindzil[®] CC30, on dry base, as indicated by Figure 10 below. In addition, De Lame et al., (2009) found that stress forces during drying were significantly lower for paint formulations containing silane modified silica sols.

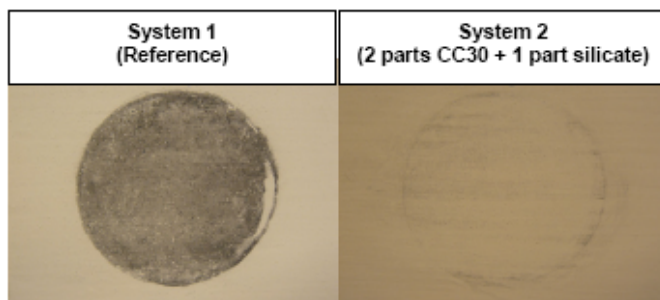


Figure 10: Surface aspects for the different systems after dirt pickup (De Lame et al., 2009).

5.1.2. Pigment dispersant (paper III)

The surfactant effects of silica sols are well known and thus may be used as a dispersing agent in the manufacture of certain organic copolymers (Iler, 1979)

More recently, colloidal silica has been shown to be an excellent dispersant for TiO₂ pigments (Bolt, 1999). Silica sol is added to the pigment slurry to coat the surfaces of the TiO₂ particles with discrete particles of silica. In applications of this kind the silica particles are introduced into a system of high solids content and the stability toward gelling of the silica particles may be low. The problem of stability may be aggravated by the presence of electrolytes in the system. In contrast to conventional colloidal silica, silanes modified silica sols give good pigment spacing and have high dispersing power even in systems of high solid content, as indicated by Figure 11.

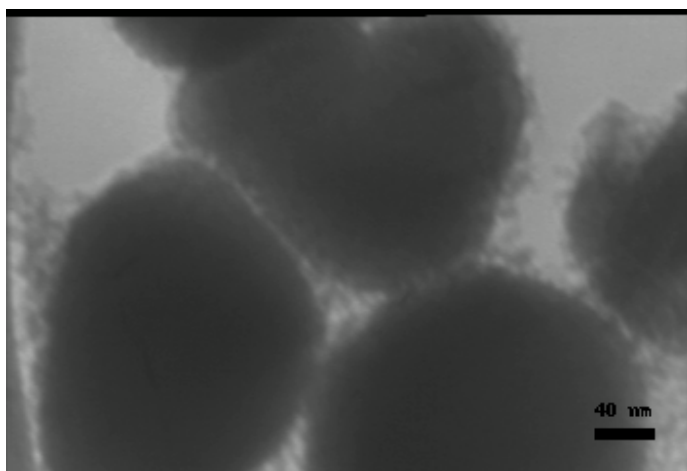


Figure 11. TEM Micrograph: Titania pigment dispersed by 5 nm silane modified silica sol (pigment paste number 1, see paper III).

Using silane-modified colloidal silica as a dispersant, pigments pastes containing 75 % by weight TiO₂ could be prepared with improved stability and fluidity as compared with using conventional silica sols as dispersing aids.

In general, all things being equal, the stability of colloidal silica decreases with increasing specific surface area, i.e. decreasing particle size, which is also the case when silica sols are used as dispersing agents in pigment pastes. It is, however, desirable to use small particles rather than larger ones as dispersants for pigments because they cover the surface of the big pigment particles more efficiently (Hansen and Matijevic, 1980). For paste and film preparation, see paper III.

The stabilising effect of silane-modified silica sols as dispersants in TiO₂ pastes is twofold. On the one hand, compared with conventional silica, silane-modified silica significantly improves the stability toward gelling of the sol, even in environments of high solids content. On the other, good dispersion of the pigment requires that there are enough silica particles present to cover the surface of the TiO₂ particles with a surface coverage exceeding a certain critical value. Tables 5 and 6 show that stable pigments pastes require that the silane modifications of the silica dispersants correspond to at least 1 molecule of GPTMS/nm² particle surface. Specifically, the stable pastes number 1, 2, 4, 13, and 15 show that the degree of surface modification of the silica sols is at least 1 molecule of GPTMS/nm² and that the surface coverage of titania particles with silica particles exceeds 100 %.

Table 5: Dispersant used for and notes about the pigments pastes.

| Paste No. | Sol particle size and degree of silane modification (GPTMS/nm² surface) | Paste stability |
|------------------|---|---|
| 1 | 5 nm, 2.0 | Stable low viscous paste after 9 days |
| 2 | 5 nm, 1.0 | Stable for 1 day, thereafter thixotropic |
| 3 | 4 nm, 0.7 | Gels after 1 day |
| 4 | 4 nm, 1.4 | Stable for 1 day, thereafter thixotropic |
| 5 | 5 nm, no silane | Gels during paste preparation |
| 6 | 7 nm, no silane | Gels during paste preparation |
| 7 | 7 nm, 1.4 | Gels during paste preparation |
| 8 | 12 nm, no silane | Gels during paste preparation |
| 9 | 12 nm, 1.7 | Gels during paste preparation |
| 10 | Dispex 40 N, 0.53 % on TiO ₂ (reference) | Thixotropic after 1 day, phase separated after 9 days |
| 11 | 5 nm, 2.0 | Thixotropic paste after 3 h |
| 12* | 5 nm, 2.0 | Gels during paste preparation |
| 13 | 5 nm, 2.0 | Stable low viscous paste after 6 days |
| 14 | 12 nm, no silane | Gels during paste preparations |
| 15 | 12 nm, 1.7 | Stable low viscous, fluid after 26 days. |

*: Paste No 12 had a titania content of 78 %.

Although the stability of the pastes treated with silane-modified silicas improved significantly, all the pastes studied in Table 6 were found to settle with time. After 7.5 months, they had all formed sludge at the bottom.

However, the sludges containing silane-modified silicas in required amounts could readily be re-dispersed. The other pastes, including paste number 10 containing Dispex N40 with a surface coverage of 165 %, were much more difficult to re-disperse.

Table 6: Silica Surface coverage of titania pigments particles of 300 nm particle size.

| Paste No. | Number of silica particles needed for full surface coverage of one pigment particle, N_{\max} | Weight per cent silica dispersant needed for full TiO_2 pigment coverage | Weight per cent added of silica dispersant based on TiO_2 | Pigment surface coverage in per cent of full monolayer coverage |
|------------------|---|---|--|--|
| 1 | 13492 | 3.19 | 4.47 | 141 |
| 2 | 13492 | 3.19 | 4.47 | 141 |
| 3 | 20943 | 2.54 | 4.47 | 176 |
| 4 | 20943 | 2.54 | 4.47 | 176 |
| 5 | 13942 | 3.19 | 4.47 | 141 |
| 6 | 6973 | 4.53 | 4.47 | 99 |
| 7 | 6973 | 4.53 | 4.47 | 99 |
| 8 | 661 | 17.3 | 4.47 | 26 |
| 9 | 661 | 17.3 | 4.47 | 26 |
| 10 | ----- | 0.32* | 0.53 | 165 |
| 11 | 13492 | 3.19 | 1.49 | 47 |
| 12 | 13492 | 3.19 | 3.83 | 120 |
| 13 | 13492 | 3.19 | 4.47 | 141 |
| 14 | 661 | 17.3 | 20.0 | 116 |
| 15 | 661 | 17.3 | 20.0 | 116 |

*: Assuming 1.2 monomers/nm² titania pigment for full surface coverage corresponding to an adsorption of 0.7 mg Dispex N40 per m² of pigment surface (Boisvert, Persello, Foissy, Castaing, and Carbane, 2000; Boisvert, Persello, Castaing, and Carbane, 2001)

Pigments particles must be well dispersed and not aggregated to give optimal light-scattering performance (Auger et al., 2003). For maximum scattering efficiency, commercial TiO₂ pigments should therefore be milled to a particle size narrowly distributed around a value in the range 250 to 300 nm (Forrest, 2001). Silane-modified colloidal silica as a dispersing agent can enhance pigment efficiency compared with the conventional polyacrylate-based dispersing agent Dispex N40. Figure 12 shows that sample paste number 1 (blue), dispersed with 5 nm silica particles and modified with 2 molecules of GPTMS/nm² particle surface, scattered light much more efficiently than the reference paste number 10 (red) containing 0.53 % Dispex N40 based on titania – the dosage recommended by the supplier. The relative enhancing effect on the reflectance is about 50-60% and constant over the range of solids contents. Thus, a 10 % silica dispersed paste scatters light as effectively as a 15 % Dispex N40 dispersed paste and a 35 % silica dispersed paste reflects light as effectively as a 50 % Dispex N40 dispersed paste.

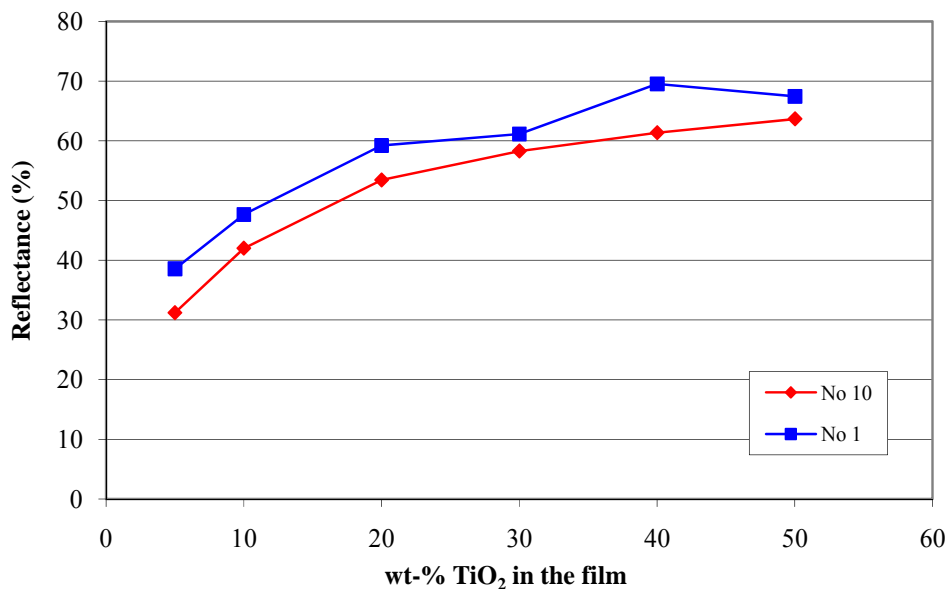


Figure 12: Reflectance (%) versus titania content, λ : 300 nm - 700 nm. Coatings based on pigments pastes number 1 and 10.

For a given degree of silane modification, the improvement in pigment efficiency increases with decreasing particle size down to about 5 nm, corresponding to a specific surface area of 500 m²/g. Figure 13 shows that 4 nm particles with a specific surface area of 750 m²/g scattered light somewhat less efficiently over most of the range of solids contents but at 40% solids and above the reflectance dropped sharply, probably because of aggregation that is caused by the very small particle size.

For a given particle size, and independent of particle size, the stability of the pastes to aggregation, and as a consequence also the reflectance, increases with increasing degree of silane modification, reaching a plateau at between 1 and 2 GPTMS/nm².

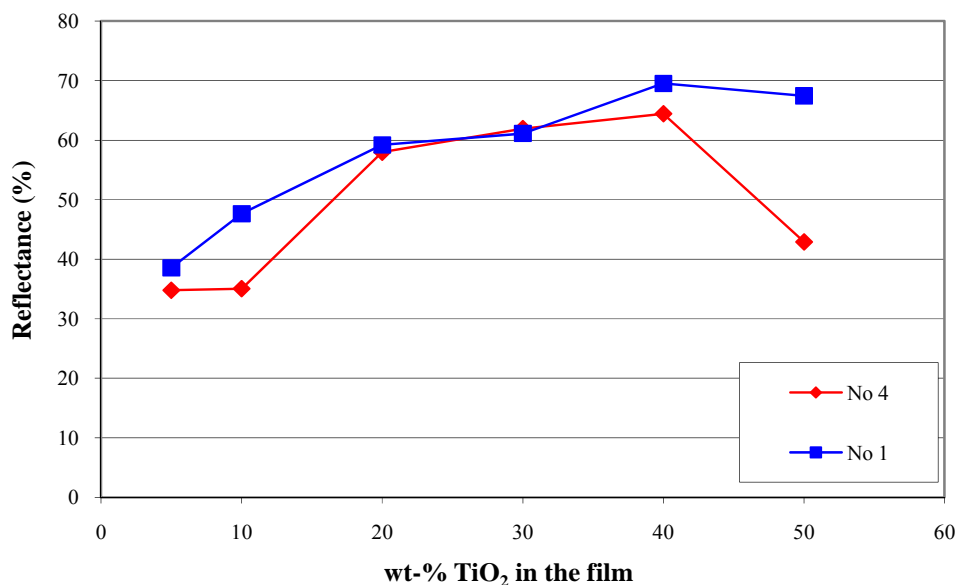


Figure 13: Reflectance (%) versus titania content, λ : 300 nm - 700 nm. Coatings based on pigments pastes number 1 and 4.

Degree of dispersing energy and level of dispersant

Water is by far the most common dispersing medium in titania pigments pastes. Titania powder is added to water containing a dispersing agent and the slurry that results is agitated by powerful dispersers. Using a conventional dispersing agent, such as Dispex N40, considerable input of energy is required to bring about complete dispersion of the titania, i.e. a paste in which each titania particle of about 300 nm is surrounded by dispersant molecules and completely separated from the other titania particles in the paste. A minimum amount of energy is required to obtain a completely dispersed paste.

With silane-modified colloidal silica as a dispersing agent, however, much less energy is needed to obtain a completely dispersed paste. It is well known that silanes (e.g., gamma-glycidoxypropyltrimethoxysilane) readily react with the OH groups on the surface of titania particles. Therefore, we speculate that the reason for silane-modified colloidal silica being more effective dispersants for titania pigments is that the silica particles adhere more strongly to the titania surfaces than conventional dispersants, which are hydrogen-bonded to the surface of the pigments. In addition to forming hydrogen bonds with the titania surfaces, the silica particles may form chemical bonds with the surfaces when silane molecules, chemically attached to the silica surfaces, react with hydroxyl groups on the titania surfaces.

In a well dispersed titania pigment paste with high titania content the optimal average size of a spacer/extender component of the particles is about 5-30 nm depending on the titania content (Braun, 1988). The particles constantly bump into each other but are prevented from associating or aggregating by the steric stabilisation provided by the dispersant.

Silane-modified silica sols provide much more effective steric stabilisation than conventional dispersing agents (such as Dispex N40) because the silica particles are much larger than the dispersant molecules, i.e. they are much larger “spacers”.

For a given particle size, say 5 nm, silane-modified sols can be prepared with 20-25 % higher solid contents compared with unmodified particles, indicating that silane modification weakens interactions between the silica particles (see paper I). It is therefore to be expected, and we have shown it to be the case in this investigation, that for a given solids content, pastes dispersed with silane-modified sols have less tendency to settle and form hard sludges than pastes dispersed with dispersing agents such as Dispex N40.

Moreover, 5 nm silica particles modified with 1 to 2 GPTMS/nm² may be the optimum dispersing agent for titania pigments. With larger particles, stable pastes cannot be prepared with the highest solids contents because the pigment particles will be less densely packed. With smaller particles, the stability toward aggregation and settling will be compromised.

5.1.3. 2-k and curable lacquers (paper IV)

In the past, there have been numerous investigations on the use of silica nano-particles in resin-based systems. Water-free systems of silane modified colloidal silica particles have been found to enhance mechanical properties of coatings (Vu, La Ferté and Eranian, 2005; Chisholm and Resue, 2003). Silane modified fumed silica has been used to enhance coating properties (Bauer et al, 2004) and organosols have been used to improve scratch resistance in clear coatings by surface enrichment (Anderson et al, 2002). Aqueous colloidal silica has been used in co-polymerisation of resins (Percy et al, 2000) and co-polymerised colloidal silica resin hybrids are also used to enhance a variety of coating properties, including hardness, anti-blocking, and reduced dirt-pickup (Leuniger, Tiarks, Wagner, and Wiese, 2006). Silica particles made from TEOS have recently been investigated in co-polymerisation of hybrid coatings where hardness and adhesion properties were found to be improved (Yeh, Weng, Liao, and Mau, 2006). Non-surface modified colloidal silica has been tested as nano-filler in latex coatings with encouraging results concerning mechanical properties (Oberdisse, 2002). In addition silane modified silica sols have been used in polymerisation of styrene and acrylic polymers, (Schmid, Tonnar, and Armes, 2008; Schmid, Armes, Carlos, and Galembeck, 2009; Schmid, Scherl, Armes, Carlos, and Galembeck, 2009). However, there have been very few studies done on the use silane modified water-based colloidal silica used in formulations of waterborne coatings.

Recently, there has been great interest in such particles in waterborne lacquers since they often provide benefits such as anti-blocking and “anfeuerung” in acrylic emulsion-based wood coatings. It is also very desirable to improve mechanical properties, such as hardness and abrasion resistance, in coatings without affecting appearance (e.g., gloss and haze) in a negative way. To this end, highly cross-linked systems such as two-pack or 2-k, systems are often required. Addition of colloidal silica dispersions to waterborne lacquers provides coatings with excellent mechanical properties.

It has been reported in the literature that colloidal silica in water-based wood coatings comprising colloidal silica, organosilane, and latex emulsion can penetrate into the wood substrate (De Lame, 2005). As indicated in Figure 14, that the addition of epoxysilane-modified 7 nm silica particles to waterborne one-pack coating formulations containing acrylic binders enhance and complement

the wood grain structure by “anfeuerung”, giving an appearance similar to solvent-based coating systems. This valuable aesthetic effect can be expected to be present also with waterborne two-pack coating systems based on acrylic binders to which silica particles have added, combined with the excellent mechanical properties characteristic of such systems.



Figure 14: 1-pack water-based lacquer formulated on acrylic resin without (left) and with (right) 20% SiO₂ addition of epoxy-silane modified colloidal silica.

Concentrated epoxysilane-modified colloidal silica in the form of aqueous sols is one of most readily available sources of nano-particles for the coating area. Such sols are characterised by high solids content, least 30 % by weight of silica depending on particle size, which ranges from about 5 nm to 100 nm. Compared with conventional silica sols, silane modified colloidal silica has greater stability toward aggregation and gelling, both as is and in latex-based coating formulations.

Finally, from an environmental point of view, it is advantageous to use colloidal silica in latex-based coating formulations. This is because less resin will be needed in that it is partially replaced by silica, with accompanying lower amounts of VOC. Softer resins can be used since silica addition will improve their mechanical properties to the level of those of harder resins obviating the use of potentially hazardous film-forming agents such as NMP or glycol ethers. Addition of silane modified silica sol into two-pack coating formulations, product weights are given in grammes, are exemplified by Tables 7 and 8. For additional details, see paper IV.

Table 7: Two-pack coating formulation based on Bindzil® CC30 and Setalux 6510.

| Formulation A | <i>Reference</i> | <i>10 % SiO₂</i> | <i>20 % SiO₂</i> |
|-------------------------------------|------------------|-----------------------------|-----------------------------|
| C1 Setalux 6510 | 100 | 100 | 100 |
| Solvesso 100 | 2.14 | 2.14 | 2.14 |
| Butyl acetate | 5.19 | 5.19 | 5.19 |
| Butyl glycol acetate | 4.66 | 4.6 | 4.6 |
| TINSTAB BL 277 (1% ds Solvesso 100) | 1.00 | 1.00 | 1.00 |
| Bindzil® CC30 | 0 | 14.48 | 14.48 |
| | | | |
| C2 Rhodocoat X EZ-D401 | 43.17 | 43.17 | 43.17 |

Table 8: Two-pack coating formulation based on Bindzil® CC30 and Setalux 6510.

| Formulation B | <i>Reference</i> | <i>10 % SiO₂</i> | <i>20 % SiO₂</i> |
|-------------------------------------|------------------|-----------------------------|-----------------------------|
| C1 Setalux 6511 | 100 | 100 | 100 |
| Butylglycol | 1.96 | 1.96 | 1.96 |
| Butyl acetate | 2.83 | 2.83 | 2.83 |
| Butyl glycol acetate | 0.84 | 0.84 | 0.84 |
| TINSTAB BL 277 (1% ds Solvesso 100) | 1.00 | 1.00 | 1.00 |
| Bindzil® CC30 | 0 | 16.21 | 32.42 |
| | | | |
| C2 Rhodocoat X EZ-D401 | 48.09 | 48.09 | 48.09 |

There is little or no change in gloss or even an increase in gloss upon silica addition, indicating good compatibility of the silica with the resin for formulations A and B as can be seen in Table 9.

Table 9: Gloss 20° /Haze index (Gloss 60° - Gloss 20°) in gloss units, GU

| Formulation | Reference | 10% SiO₂ | 20% SiO₂ |
|--------------------|------------------|----------------------------|----------------------------|
| No A | 127/57 | 130/56 | 112/8 |
| No B | 108/60 | 99.2/57 | 129/50 |

There is no proportionality between the amount of added inorganic particles and the property response. To achieve good improvement in hardness it is important to have good interaction/cross-linking between the resin and the silica particle as well as to build a structure, such as a skeleton, of silica in the resin matrix. In such cases it is possible to significantly improve the mechanical properties even at low silica additions as indicated in Figures 15 and 16.

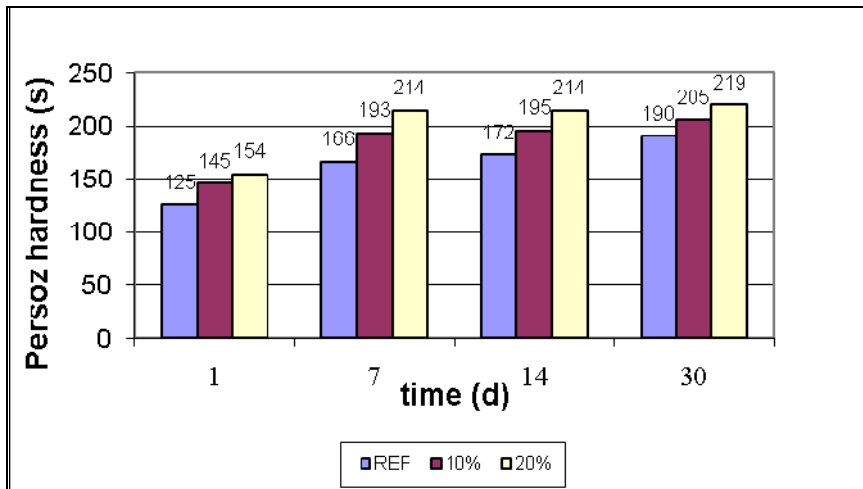


Figure 15: Formulation A. Persoz hardness in function of coating composition and drying time at ambient temperature.

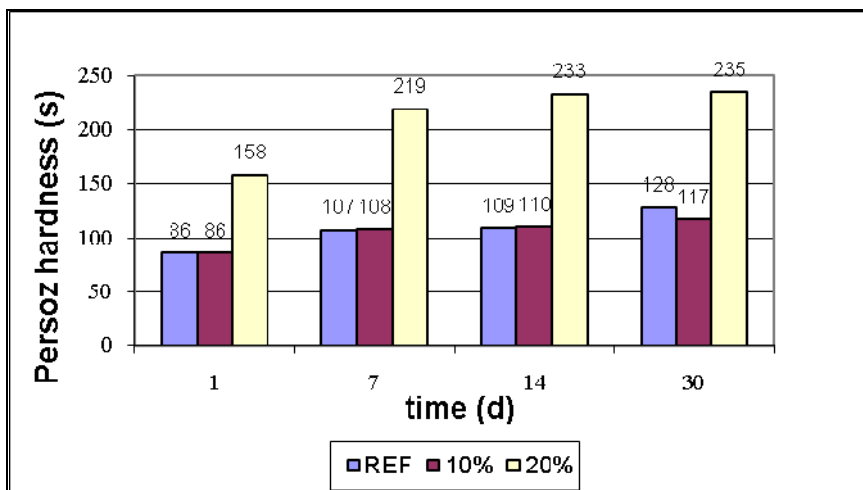


Figure 16: Formulation B. Persoz hardness in function of coating composition and drying time at ambient temperature.

Although it is quite dependant on the type of resin, the effect of silica on abrasion resistance is not clear. For formulation A, there is improvement at 10 % but some deterioration at 20 % addition of silica. For formulation B, the reverse is true. Basically, one would like to say that abrasion resistance increases as the energy required to tear the resin apart, i.e. the energy at break, increases. There are, however, many other factors, including surface enrichment of the filler particles, the effect of the filler particles on the friction coefficient, and clustering of the particles to large aggregates in the resin that affect abrasion resistance in a major way.

Table 10: Taber Abrasion resistance – weight loss mg (ASTM D4060). The test was performed after 30 days of drying at ambient temperature. An abrasive wheel, CS17, under 1 kg load was used.

| Formulation | Reference | | | 10 % SiO ₂ addition | | | 20 % SiO ₂ addition | | |
|-------------|-----------------------|-----|------|--------------------------------|-----|------|--------------------------------|-----|------|
| | Number of revolutions | | | Number of revolutions | | | Number of revolutions | | |
| | 100 | 500 | 1000 | 100 | 500 | 1000 | 100 | 500 | 1000 |
| No A | 3 | 33 | 60 | 2 | 17 | 37 | 3 | 33 | 64 |
| No B | 3 | 37 | 83 | 2 | 40 | 88 | 3 | 33 | 68 |

Silica structure in the resin matrix – Effect on hardness and abrasion resistance.

Transmission electron microscopy has been used to visualise the structure of the inorganic part embedded in the organic matrix. In Figures 17 and 18, the structure of the inorganic part embedded in Setalux 6510 (formulation A) varnish with 10 and 20 wt-%, SiO₂ based on dry resin of Bindzil[®] CC30, respectively, are displayed. In Figures 19 to 20, the Setalux 6511 (formulation B) varnish with 10 and 20 wt-% SiO₂ based on dry resin of Bindzil[®] CC30 are presented. The resin – air interface cannot be seen in the pictures but it extends in from about the midpoint of the upper edge to the lower left corner in Figure 17; from below the midpoint of the left edge of the picture to somewhat to the right of the lower edge in Figure 18; and from well to the right of the midpoint of the upper edge in Figure 19 to about the midpoint of the left edge of the picture. No interface can be seen in Figure 20.

Formulation A

Figures 17 and 18 show that the particles are not accumulated at the resin-air interface. They are moderately aggregated and the aggregates are somewhat larger at 20 % addition of silica than at 10 % addition. The Perzos hardness increases with increased addition of silica, whereas there is a significant improvement of the abrasion resistance only at 10 % addition of silica, whereas 20 % addition affects the abrasion resistance only in a minor way.

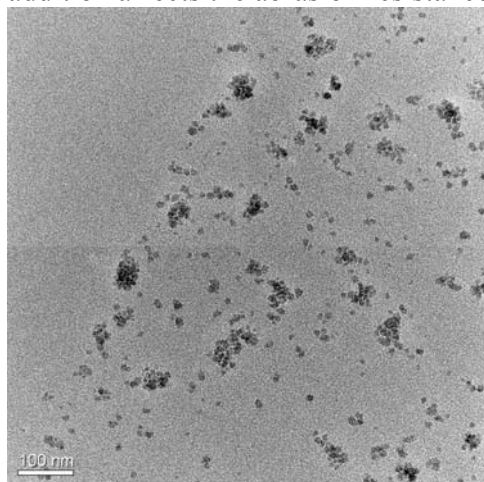


Figure 17: Formulation A with 10% SiO₂.

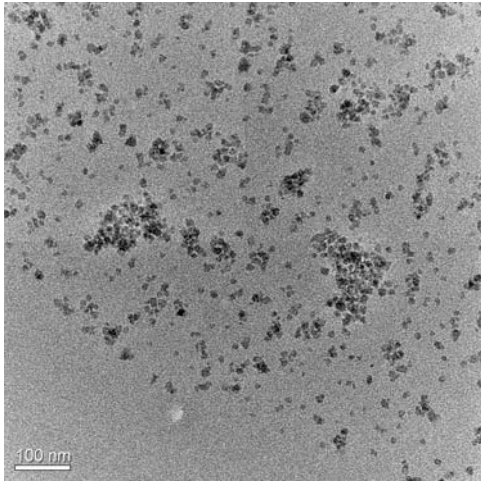


Figure 18: Formulation A with 20% SiO₂.

Formulation B

Setalux 6511, like the resin, Setalux 6510, in formulation A is an acrylic polyol and the silica particles are not accumulated or enriched at the binder-air interface. However, in contrast to the situation with first resin, Figures 19-20 show that the silica particles have clustered around droplets, most likely of the polyisocyanate hardener, perhaps preventing them from reacting effectively with the binder. There is no enhancement of the abrasion resistance at 10 % and only modest improvement at 20 % silica addition on resin, as might be expected from poor interaction between the silica and resin. On the other hand, the effect of the silica particles on the Persoz hardness, small or non-existent at 10 %, is quite large at 20 % addition of silica. The increase in hardness of the resin by the larger aggregates of silica particles at 20 % silica addition may therefore be analogous to the observation that aggregation of nano-particles leads to increase in Young's modulus, especially by creating some occluded volumes in the matrix which augment the effective fraction of nano-filler (Reynaud, 2000).

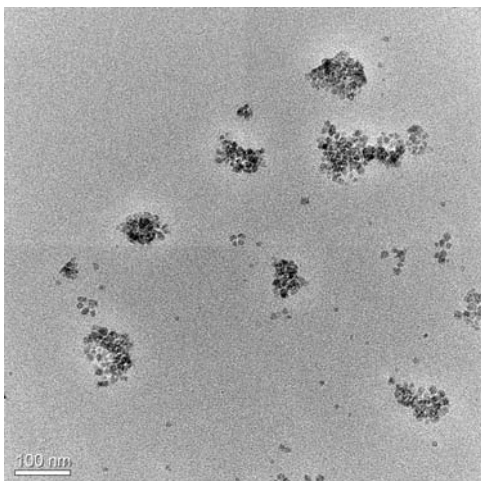


Figure 19: Formulation B with 10% SiO₂.

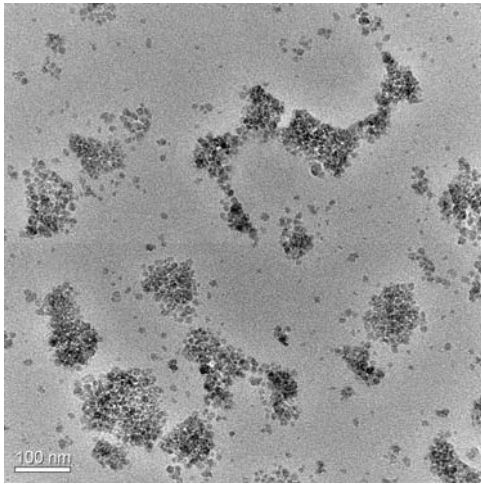


Figure 20: Formulation B with 20% SiO₂.

5.2. Applications of conventional colloidal silica

5.2.1. Cementitious applications (paper V)

Already in ancient times, it was known that the reaction between calcium oxide, also called lime or quicklime, and water could yield a binder in building construction. The Etruscans, for instance, added water to lime to form calcium hydroxide, or slaked lime, which they mixed with sand and stone into what today would be called a primitive concrete. The Romans discovered a way to improve cement making by burning a mixture of volcanic ash, which essentially consisted of silica and lime. The many impressive constructions that have lasted to our own time testify to the durability of their cement.

However, the Roman cement technology fell into oblivion and high quality cement became available first in 1824 when the Englishman, Joseph Aspdin, invented Portland cement, or modern cement. Modern cement is made by grinding a mixture of limestone and clays, with a weight ratio of about 80 to 20, and several other minor components with water to a slurry. This slurry is passed down a rotating kiln and first loses water and then carbon dioxide as the temperature gradually increases downward the kiln. In the last temperature zone, where the temperature is 1200 to 1500 °C, the material sinters and melts to clinker. After cooling, the clinker is ground, together with a small amount of gypsum, which controls the reactivity of the cement with water, into a fine powder (Cotterill, 1985). The specific surface area of the particles, normally measured by air permeability (Keyes, 1946), e.g., on a Blaine apparatus, which is inversely proportional to particle size, determines the rate of reaction when water is added to the powder. The different grades of commercial cement powder are usually given designations that indicate how rapidly the cement paste becomes rigid and gains strength. Table 11 shows the composition and specific surface area of three common grades of Swedish cement.

Table 11: Composition and specific surface area of three Swedish cements (courtesy of Euroc Research AB).

| Compound | OPC Sl | OPC Sk | SRPC D |
|------------------------------------|--------|--------|--------|
| CaO (%) | 62.2 | 64.3 | 54.6 |
| SiO ₂ (%) | 20.0 | 19.8 | 21.6 |
| Al ₂ O ₃ (%) | 4.53 | 5.21 | 3.46 |
| Fe ₂ O ₃ (%) | 2.23 | 3.04 | 4.75 |
| K ₂ O (%) | 1.42 | 1.30 | 0.75 |
| MgO (%) | 3.37 | 1.45 | 1.02 |
| Na ₂ O (%) | | 0.11 | 0.06 |
| Blaine (m ² /kg) | 363 | 400 | 323 |

Manufacturer: Sl=Slite, Sk=Skövde, D=Degerhamn

OPC: Ordinary Portland Cement

SRPC: Sulphate Resistant Portland Cement

The metals oxides in Table 11 are not present as such in cement powder but instead as four major compounds: alite, $3\text{CaO}\cdot\text{SiO}_2$, 50-70 % by weight; belite, $2\text{CaO}\cdot\text{SiO}_2$, 15-30 % by weight; aluminate, $3\text{CaO}\cdot\text{Al}_2\text{O}_3$, 5 -10 % by weight; and ferrite, $4\text{CaO}\cdot\text{Al}_2\text{O}_3\cdot\text{Fe}_2\text{O}_3$, 5-15 % by weight (Taylor, 1997). Small amounts, a fraction of a percent usually, of free lime, magnesium oxide, sodium sulphate, and potassium sulphate are also present. These trace compounds can influence the final properties of the material (e.g., concrete) to a much higher degree, and sometimes in a negative way, than their abundance in the cement powder might suggest. Gypsum, which is added when the clinker is ground to a powder, is present in amounts between 2 and 5 % by weight.

Modern cement (e.g., Portland cement, OPC) contains more components and is a much better binder than the primitive cement. Another important difference between Portland cement and the primitive cement is that the former will set and harden under water. Cement paste, i.e. a slurry of cement powder and water is usually mixed with sand or stone when it is used in building construction. The term sand refers to particles smaller than 2 mm and the term stone refers to particles larger than 2 mm. A mixture of inorganic materials, which may include sand and stone and having a particle size distribution ranging from about 0.01 mm to 100 mm, is called an aggregate (Bergqvist and Sandra, 1999). Mortar is a mixture of cement paste and sand. If aggregate is added to cement paste, the mixture is called concrete. The weight ratio of cement paste to aggregate in concrete is usually in the range up to 1:6. Concrete may contain additives, such as setting and hardening additives, usually called accelerators, or workability additives, usually called superplasticiser. The worldwide production of cement amounts to about 2.5 billion metric tons per annum (Komiya and Kraines, 2008).

Silica in cement

For reasons of utilising waste materials and decreasing overall energy consumption, certain inorganic materials, called mineral additives, such as fly ash and ground granulated blast furnace slag are added to the cement paste. Mineral additives take part in the hydration reaction and thereby make a substantial contribution to the hydration product. For reasons of obtaining durability and strength above the normal range, silica in the form of silica fume or colloidal silica is being used. Cement containing mineral additives is often called composite cement.

Silica fume in cement

Silica fume is a by-product, in the form of a very finely particulate powder, of the production of silica or silica alloys in an electric furnace. High-quality silica fume consists of spherical particles, which have a density of about 2200 kg/m³ and a BET specific surface area of about 18 m²/g and an average particle size from about 300 nm to 400 nm (Papadakis, 1999). The chemical composition of silica fume is shown in Table 13.

Table 13: Chemical composition of silica fume. Adapted from Rahhal, Cabrera, Talero, and Delgado, 2007.

| Compound | %,weight | Compound | %,weight |
|--------------------------------|----------|-------------------|----------|
| SiO ₂ | 92 | MgO | 0 |
| Al ₂ O ₃ | 0.7 | K ₂ O | 0 |
| Fe ₂ O ₃ | 0.4 | Na ₂ O | 0 |
| CaO | 0 | SO ₃ | 0.1 |

Silica fume, like other mineral additives, has pozzolanic activity, i.e. it reacts with Ca(OH)₂, formed during the hydration of alite and belite, (see Table 57.2 in paper V) and produces more calcium-silicate aquagel, the actual binder material in cement. However, being made in high heat, the surface of the silica fume particles contains very few hydroxyl groups, or silanol groups, which are necessary for reaction with water and calcium hydroxide. It will therefore take some time before the particle surface has become re-hydroxylated in the warm, highly alkaline environment of the cement paste and the pozzolanic activity of silica fume typically reaches a high value first in the period 7-14 days after mixing.

The fine particles of silica fume fill spaces between clinker grains, producing a denser paste. It also densifies the interfacial transition zone between cement paste and aggregate, which increases strength and lowers permeability. Papadakis, (1999) investigated the effect of adding between 5 and 15 % by weight of silica fume to concrete and found that the compressive strength increased by 10 % at 5 % addition and by 20 % at 15 % addition.

Colloidal silica in cement

In contrast to silica fume, or micro silica, the surface of the particles of colloidal silica is fully hydroxylated and contains 4.6 OH silanol groups per nm². This fact, together with the much higher specific surface area, makes the pozzolanic activity of colloidal silica much higher than that of silica fume (Campillo, Dolado, and Porro, 2003). Wagner and Hauck (1994) mixed 15 nm colloidal silica with cement paste and noted a significant increase compared with a reference paste without colloidal silica of the early strength, i.e. the early strength development during the first 1-7 days. In fact, others (Skarp and Sarkar, 2001) pointed out that ultrafine silica particles will harden the cement paste very fast because most of the available water is consumed in the early stage of gel formation, which is due to the very high pozzolanic activity of colloidal silica. The resulting high early strength, however, is gained at the expense of low final strength as caused by the pore structure created during the very rapid early gel formation. On the other hand, they claim that this problem that is caused by excessively high pozzolanic activity of colloidal

silica has been solved and they report that small amounts of colloidal silica added to the concrete mixture, 0.15-0.20 % silica based on the weight of the cement, significantly increased the final strength, reduced the chloride ion permeability, and increased the sulphate resistance of the concrete. The properties of the colloidal silicas used are given in Table 14. Accelerating effects, especially in early hydration, in cement upon addition of small amounts of colloidal silica have also been confirmed by others (Björnström Martinelli, Matic, Börjesson, and Panas, 2004) where the silica particles are believed to act as nucleation sites for the C-S-H gel.

Table 14: Physical Properties of Colloidal Silica. (Skarp and Sarkar, 2001).

| Product | Sp. Surface Area, m ² /g | Solids, % | Average Particle Size, nm |
|---------|-------------------------------------|-----------|---------------------------|
| A | 400 | 24 | 35 |
| B | 80 | 50 | 45 |

Had the sols contained spherical particles of uniform size the particle sizes of sols A and B would have been 7 nm and 34 nm, respectively. Instead, the average particle sizes are considerably higher, more so for A than for B, indicating that the sols are polydisperse, sol A being the most polydisperse and containing the smallest particles. The cement pastes, with or without colloidal silica, had a water to cement ratio of 0.35 and contained sulphonated naftalene formaldehyde resin (NSF) superplasticiser. The colloidal silica was added to the concrete mixture after the superplasticiser in order to minimise premature gelling. The compressive strengths of the concrete samples are listed in Table 15.

Table 15: Effect of Colloidal Silica on the Compressive Strength (psi) of Concrete. Adapted from Skarp and Sarkar, 2001.

| Type Silica | SiO ₂ , % | 1 Day | % Increase | 7 Days | 28 Days | % Increase |
|-------------|----------------------|-------|------------|--------|---------|------------|
| -(Sample1)) | - | 4,300 | - | 6,840 | 8,680 | - |
| A(Sample2) | 0.15 | 5,300 | 23 | 8,010 | 9,680 | 12 |
| B(Sample3) | 0.15 | 5,580 | 30 | 8,030 | 9,840 | 13 |
| B(Sample4) | 0.20 | 4,470 | 4 | 8,280 | 9,970 | 15 |

Addition of colloidal silica increases the 1 day strength by up to 30 % and the 28 days strength by up to 15 %. Colloidal silica of type B may be somewhat more effective than type A, although the increase of the 1 day strength is only 4 % at 0.20 % of type B as compared with 30 % at only 0.15 % of the same type of silica sol. Obviously, judicious choice of the average particle size and the particle size of silica sols make it possible to fine-tune the pozzolanic activity of the silica so that significant increases of both the early stage strength and the final strength of the concrete can be accomplished. Tables 16 and 17 show that the addition of colloidal silica to a concrete mixture substantially reduces chloride ion permeability and enhances sulphate resistance.

Table 16: Effect of Colloidal Silica on the Chloride Ion Permeability of Concrete (28 days). Adapted from Skarp and Sarkar, 2001.

| | | | | |
|------------------------------------|------|------|------|------|
| Silica, % | 0 | 0.1 | 0.15 | 0.20 |
| Chloride ion permeability, coulomb | 3600 | 3200 | 2400 | 1700 |

Table 17: Effect of Colloidal Silica on the Sulphate Resistance of Concrete. Adapted from Skarp and Sarkar, 2001.

| Weeks | Control % expansion | Sol A, 0.13 % SiO ₂ , % expansion | Sol B, 0.13 % SiO ₂ % expansion |
|-------|---------------------|--|--|
| 4 | 0.01 | < 0.01 | < 0.01 |
| 8 | 0.021 | <0.01 | < 0.01 |
| 12 | 0.036 | 0.015 | 0.014 |
| 16 | 0.050 | 0.017 | 0.016 |

Greenwood, Bergqvist, and Skarp, (2003) showed that the smaller particles in the sol provided most of the sulphate resistance, whereas the larger particles provided the chloride resistance, but the two particle size regions appeared to interact and gave rise to a significant synergism.

The availability of modern workability additives (e.g., superplasticiser such as polycarboxylates) has made it possible to develop highly fluid concrete, HFC, which does not bleed or segregate in use. Self-compacting concrete, SCC, (in the USA: self-consolidating concrete) is a particular type of HFC, which achieves significant benefits and advantages in many types of construction. Thus, by using SCC, it is possible to fill the mould completely and uniformly, even moulds of difficult and complicated shapes. There is no need to vibrate the material to eliminate voids and holes formed when conventional, often sluggish concrete is poured into the form. Moreover, the quality of the concrete surface is often very good, minimising the need for expensive and time-consuming after treatment.

Skarp and Sarkar (2001), however, pointed out that poor stability, i.e. bleeding or segregation and loss of workability are two main concerns when working with SCC. A concrete mixture is said to be workable if it can be maintained in fluid form until the casting moment. The term workability time is defined as the time the concrete mixture remains workable. They attribute the instability to deficiencies in mix design and the loss of workability to incompatibility between the cement and the superplasticiser.

Greenwood, Bergqvist, and Skarp, (2002) showed that small amounts (0.2 % by weight of SiO₂) of colloidal silica of small particle size, corresponding to a specific surface area of 900 m²/g, significantly increased the workability time of concrete mixtures containing polycarboxylates as superplasticiser. It required much larger amounts of colloidal silica of larger particle size, corresponding to a specific surface area of 80 m²/g, 1.25 % by weight of SiO₂, or of fumed silica, 10 % by weight of SiO₂, to achieve the same results. In contrast to the control that contained no silica, the concrete mixtures containing either colloidal or fumed silica showed no bleeding. These findings indicating the high activity for colloidal silica relative (e.g., silica fume) have been confirmed by others (Colleparidi, Ogoumah Olagot, Skarp, and Troli, 2002; Thomas,

Jennings, and Chen, 2009). Additionally, silica sols have been found to offset some of the retarding effects of the cement reactions from the addition of polycarboxylate superplasticiser, (Björnström and Panas, 2007).

Improved concrete through modified silica sols

Aluminium-modified sols, compared with unmodified sols of the same specific surface area, as additives in concrete mixture containing polycarboxylates as superplasticiser achieved not only increased workability time but also improved strength (Greenwood, Bergqvist, and Skarp, 2004).

5.2.2. Paper-making (paper V)

Different paper machines have various configurations at the wet end of the machine (Figure 21 shows a schematic representative setup). In the mixing chest fibres and paper chemicals are mixed to an aqueous slurry (the furnish) containing about 0.5-2 % fibre. Some of the chemicals may be added at a later stage, e.g., to the machine chest or before, or into a pump. From the head box, the furnish is filtered on a wire screen, where the fibres adhere weakly to one another. When more water is removed from the mat formed on the screen by suction, the sheet becomes stronger, but is still relatively weak. When the sheet is dried, it becomes still stronger, and becomes the material known as paper. Modern paper machines produce an endless paper sheet, up to 10 m wide, at a speed of over 20 m/s, i.e. one hectare (more than two acres) every 50 sec. The machine is more than 100 m long and produces about 250,000 metric tons per year.

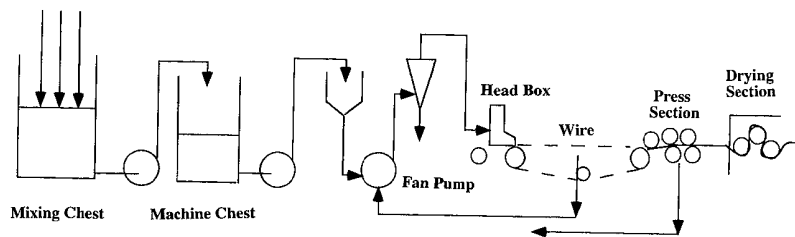


Figure 21. The wet end of a paper machine. (Otterstedt and Brandreth, 1998). Courtesy of Plenum Press.

Environmental and economic pressures have reduced water usage in paper production in the last 30-40 years from 80-90 m³ per metric ton to less than 10 m³ per metric ton. During the past decade, many efforts have been made to reduce the use of water even more, with the ultimate objective of achieving a paper mill that is 100 % closed.

The problem

The achievement of a closed or nearly closed paper mill with respect to water usage is intimately related to the retention of fibre fines and chemicals and other additives in the furnish on the wire. Poor retention will cause the fines and other small particles to go through the wire with the water and make reuse of the backwater difficult or impossible (see Figure 21). The nature of the problem is further illustrated in Figure 22, showing the dimensions in the wet end,

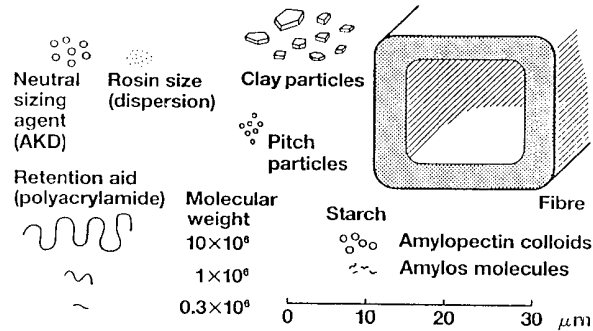


Figure 22. Dimensions in the wet end of the papermaking process (Otterstedt and Brandreth, 1998). Courtesy of Plenum Press.

and Figure 23, which compares the size of the holes in the wire with the sizes of the cellulose fibres, fines, filler particles, and the various chemical additives present in the furnish.

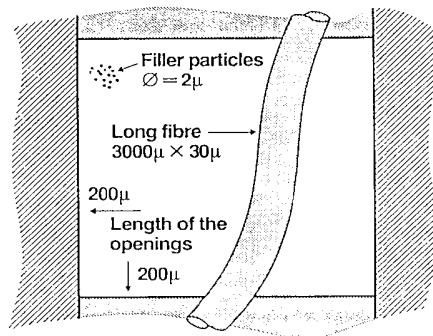


Figure 23. Small particles on the wire in the papermaking process (Otterstedt and Brandreth, 1998). Courtesy of Plenum Press.

The difficulty in retention is further aggravated by the fact that all the particles of the furnish are negatively charged and therefore have no bonding to each other to form aggregates large enough not to pass through the holes of the wire. The obvious solution to the problem is to put particles or additives of opposite charge into the system to cause agglomeration of the paper components to larger clumps that cannot go through the wire. This is accomplished by retention aids.

Retention, retention mechanisms and retention aids.

The term retention refers to the holding back of the components of the stock during dewatering. The fibres are retained on the wire while fillers, fines, and additives of colloidal size may be washed through the mat formed on the screen. Retention is accomplished by a combination of mechanical means, i.e. filtration in conjunction with the physico-chemical mechanism of agglomeration or flocculation.

Mechanical retention during sheet formation on the wire may be considered a filtration process. The fibres in the stock, which are 500-4000 μm long and 20-100 μm thick, are captured on the wire and form a three-dimensional network consisting of 2-100 layers of fibres on the wire. As the layers form, they capture progressively smaller fibres and other colloidal particles in the stock suspension, making the pore structure gradually finer with the largest pores on the wire side and the finest on the top side. Mechanical retention is least efficient in the beginning of the sheet formation and, although it becomes more effective as more layers form, it cannot retain a satisfactorily high proportion of the finest components of the stock. The losses for newsprint are typically about 50 %.

By adding special chemicals (retention aids) to the stock, the fines and other colloidal components can be made to flocculate or aggregate into agglomerates too large to go through the wire. Retention aids may consist of either one component or two components. They can act by changing the electrostatic repulsion forces between colloidal particles or affect the stability of colloids by adsorbing on two or more particles causing them to form larger aggregates.

Although good retention is most likely attained by the joint action of more than one mechanism and a given retention aid may act by several mechanisms, it is still useful to distinguish between some principal types of aggregation mechanisms.

There are no sharp distinctions between the terms coagulation and flocculation, but here coagulation denotes aggregation by the action of low molecular weight electrolytes, whereas flocculation implies aggregation brought about by polymers, which can be natural or synthetic.

In high-speed modern paper machines the floc is subjected to high shear, which may tear the floc apart. The trend toward reduced water usage in the production of paper increases the amounts of soluble anionic wood polymers and electrolytes in the stock, which will also affect the retention on the wire.

Dual retention aid systems

Cationic natural and synthetic polymers have long been used to improve retention of fines and fillers on the wire of paper machines. Such polymers, i.e. cationic starch or cationic polyacrylamide, produce a high degree of flocculation in the furnish. This floc, however, is not very strong and is easily broken and re-dispersed by hydraulic shear. Furthermore, when long-chain polymers are used, chain rupture and rearrangement of the polymer fragments on the particle surfaces may occur. Nevertheless, single-component retention aids improve the first-pass retention though not to the same degree as dual retention aid systems.

Such systems have been used in the paper industry for many years. Component one, a cationic polymer, usually of the patching type, is first added to the furnish, followed by the addition of the second component, an anionic polymer of the bridging type. Figure 24 schematically compares single-component and dual retention aid systems. The application of retention aids has been optimised in the sense that the retention maximum in the figure corresponds to a zeta potential of

zero value, i.e. the charges on the positive components in the system exactly balance the charges on the negative component, which may be difficult to accomplish in an actual situation. When an optimal amount of cationic component, in this case cationic starch, in the single-component system is added, the furnish system has no charge and flocculation and retention are maximised. In the dual system cationic starch has to be present in the furnish in order to reach zero-potential after the given amount of the second component, an anionic polymer, has been added. Thus, the maximum in flocculation and retention is not only higher than for the single-component system but it also occurs at larger dosages of cationic starch, which is beneficial since starch is not only a retention aid but is also an additive that increases the dry strength of paper.

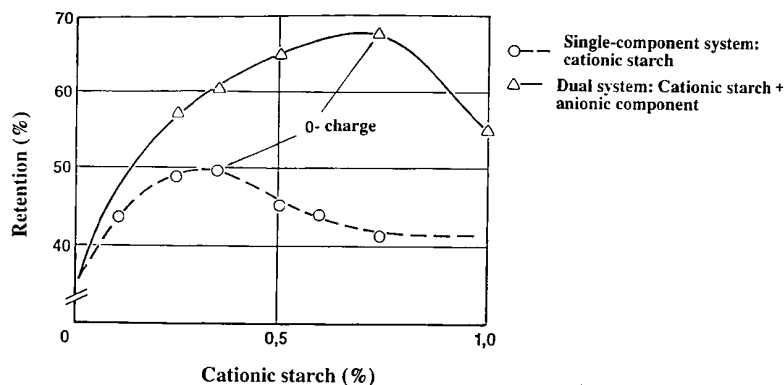


Figure 24. Single-component and dual retention aid systems (Andersson and Larsson, 1984). Courtesy of Arbor Publications.

In the past 10-15 years a special kind of dual retention aid, a micro particle-containing flocculant system, often referred to as micro-particulate retention/dewatering aid, was developed. A commonly used commercial system, the Compozil@ system, comprises colloidal silica in combination with cationic starch or cationic synthetic polymers (Andersson and Larsson, 1984; Andersson and Lindgren, 1996). In this system the cationic polymer is added first and the extensive flocs then formed are broken down and partially re-dispersed by high-shear forces. The anionic micro-particles are added just before the paper is formed and cause final flocculation of the furnish. A dual retention system, having colloidal silica as the anionic component, has the following characteristics (Lindström, Hallgren, and Hedborg, 1989):

- strong, reversible flocculation
- more effective dewatering in the wire and press sections
- formation on the wire yields sheets of higher porosity and permeability.

The Compozil@ system was recently studied by Andersson and Lindgren (1996). They used a Britt Dynamic Drainage Jar to investigate the retention effects of combinations of various types of anionic colloidal silica (ACS) with either cationic starch or polyacrylamides of different charge density. The furnish consisted of a 60/40 mixture of fully bleached birch and pine sulphate pulps with 30 % (based on total solids) chalk as the filler. The solids content was 0.5 % and the pH of the furnish 8.1. The polyacrylamides had charge densities from 2 - 25 % cationicity,

corresponding to between 0.25 and 3.0 meq/g, and a molecular weight of 5×10^6 . The cationic starch had a degree of cationic substitution of 0.4, corresponding to 0.25 meq/g.

The anionic colloidal silica used in this study was either monodisperse colloidal silica with a particle size of about 4 nm or structured colloidal silica, consisting of linear aggregates of about 4 nm particles. Structured colloidal silica is, like monodisperse colloidal silica, characterised by its specific surface area and charge density, which decreases with pH but can be maintained high even at pH as low as 3 and 4 by aluminising the colloidal silica with sodium aluminate, but also by some other properties. One such property is the S-value, which is defined as the percentage of silica in the dispersed phase and can be obtained from viscosity measurements (Iler and Dalton, 1956). A high S-value indicates well-dispersed, non-aggregated colloidal particles, whereas a low value suggests that the primary particles have formed micro-aggregates, perhaps linear structures containing up to 7-8 primary particles. Another property is the average size of the micro-aggregates, A, as determined by dynamic light scattering (DLS). Other ones are the length, L, and the width, W, of the micro-aggregates as determined by DLS and viscosity measurements. From their results, Andersson and Lindgren concluded that for both the cationic starch-ACS and CPAM-ACS systems the main flocculation mechanisms were electrostatic interactions (e.g., charge neutralisation and bridging).

Andersson and Lindgren also used their data to construct a model for the system CPAM-ACS shown in Figure 25 for a constant dosage of CPAM. Each curve shows the predicted retention for an ACS with a constant S-value. As expected, maximum retention increases with increasing structure or degree of micro-aggregation of the ACS.

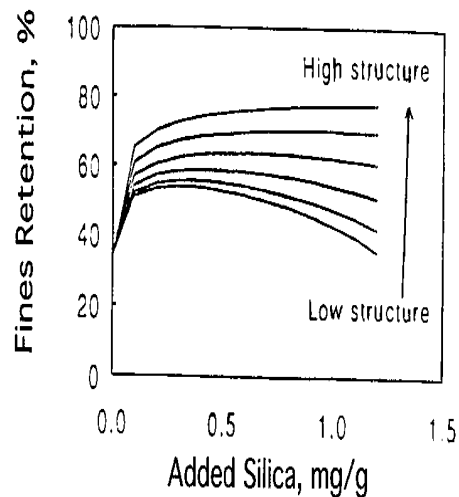


Figure 25. Retention model for the CPAM-ACS system, (Andersson and Lindgren, 1996). Courtesy of Arbor publication.

Improved retention through modified silica sols

Relatively recently, Paul Fish (2005) made an exposé over the development of the silica nano-particles used in the retention application from the early 1980s to the present. In that overview the first generation of silica sols used as retention aids was a 5 nm non-surface modified silica sol, second generation, silica sol was aluminate modified followed by third generation that was based on a smaller silica sol of about 3 nm that was aluminate modified with a degree of structure. In the latest generations of silica nano-particles for this application the surface area and structure have been optimised to boost performance.

Greenwood, Linsten, and Johansson-Vestin, (2002) showed that chemical modification of ACS, comprising stabilisation of structured colloidal silica by amines instead of by NaOH, which is the most common method, not only improved the retention but also the dewatering on the wire of the paper machine. They found that quaternary amines gave the best results, followed by tertiary and secondary amines. In addition to these findings, silica sols with high surface could be made at significantly higher solid content at a given specific surface area, i.e. a higher “wet surface area” than was possible before. The wet surface area is the surface area on product base: the specific surface area x solid content. The wet surface area was increased from about 100-110 m²/g for a conventional silica sol to about 200-250 m²/g by stabilising the silica particles with amines. The effect was dramatic: on a dry silica base dosage could be reduced by more than 50 % (see Table 18). Taking into account that these products in addition could be supplied at significantly higher silica content, the potential reduction in product dosage is big. One explanation could be that the quaternary ammonium ions are strongly adsorbed and cause coagulation at neutral pH at small concentrations while the free base can act as a stabiliser at pH 9-10, being adsorbed onto the silica surface and thus providing steric stabilisation (Iler, 1979). The effect could be expected to be less pronounced for tertiary and lower amines.

Additionally, the use of oxidation of mercapto group from silane as a mean of creating silica sols with highly charged sulphonic acid surface groups has been found to improve dewatering properties significantly (Meisner et al., 2005). Highly structured silica nano-particles by combining high specific surface area, low S-value, and high axial ratio (above 10) has recently been reported to be a very efficient flocculent (Persson, Hansson, Pal, Lindahl, and Carlén, 2008). Other microparticles, such as highly structured aluminosilicates, have found a new interest in the field (Lee and Hubbe, 2008; Lee and Hubbe, 2009).

Table 18: Dewatering of fine paper furnish (Greenwood, Linsten, and Johansson-Vestin, 2002).

| Silica-based sol (silica content, specific surface area and structure – S-value, modification/stabilisation) | | Drainage time (sec) at SiO ₂ dosage of | | |
|--|--|---|----------|----------|
| | | 0.25 kg/t | 0.5 kg/t | 1.0 kg/t |
| Ref. 1 | 8 % SiO ₂ , 900 m ² /g,S: 25 %, aluminate | 12.20 | 10.40 | 8.76 |
| Ref. 2 | 10 % SiO ₂ , 880 m ² /g,S: 36 % | 11.60 | 9.83 | 8.28 |
| No. 1 | 9 % SiO ₂ , 820 m ² /g,S: 20 %, choline-OH | 9.11 | 7.19 | 5.74 |
| 2 | 5 % SiO ₂ , 1330 m ² /g,S: 28 %, choline-OH | 8.65 | 6.79 | 5.76 |
| 3 | 9 % SiO ₂ , 850 m ² /g,S: 20 %, TMA-OH | 9.34 | 7.30 | 6.30 |
| 4 | 13 % SiO ₂ , 1140 m ² /g,S: 27 %, TMA-OH | 8.82 | 6.97 | 5.86 |
| 5 | 8 % SiO ₂ , 930 m ² /g,S: 21%, TEA-OH | - | 7.74 | - |
| 6 | 8 % SiO ₂ , 820 m ² /g,S: 24 %, TPA-OH | - | 8.98 | - |
| 7 | 8 % SiO ₂ , 795 m ² /g,S: 15 %, triethanolamine | 10.3 | 8.77 | 6.66 |
| 8 | 9 % SiO ₂ , 800 m ² /g,S: 25 %, triethylamine | 10.3 | 8.31 | 7.02 |
| 9 | 9 % SiO ₂ , 860 m ² /g,S: 26 %, dimethylethanolamine | 9.90 | 8.80 | 7.90 |
| 10 | 9 % SiO ₂ , 875 m ² /g,S: 22 %, diethanolamine | 10.00 | 8.21 | 7.07 |
| 11 | 9 % SiO ₂ , 880 m ² /g,S: 22 %, diethylamine | 10.00 | 8.04 | 7.28 |
| 12 | 9 % SiO ₂ , 885 m ² /g,S: 25 %, diisopropylamine | 9.87 | 7.97 | 6.85 |
| 13 | 9 % SiO ₂ , 880 m ² /g,S: 25 %, pyrrolidine | 9.60 | 7.85 | 6.30 |
| 14 | 9 % SiO ₂ , 855 m ² /g,S: 30 %, dipropylamine | 10.70 | 8.80 | 7.80 |
| 15 | 9 % SiO ₂ , 870 m ² /g,S: 24 %, ethanolamine | 10.70 | 8.80 | 7.51 |
| 16 | 9 % SiO ₂ , 880 m ² /g,S: 24 %, cyclohexylamine | 10.30 | 8.13 | 6.75 |
| 17 | 9 % SiO ₂ , 850 m ² /g,S: 28 %,methoxyethylamine | 10.50 | 8.80 | 7.70 |
| 18 | 9 % SiO ₂ , 875 m ² /g,S: 26 %, AEEA | 10.60 | 9.20 | 8.20 |

Choline hydroxide: Trimethylethanolammoniumhydroxide
AEEA: aminoethylethanolamine

5.2.3. Lead-acid batteries (paper V)

Lead-acid batteries are one of the most common types of batteries. Most lead-acid batteries are flooded, i.e. they have a liquid electrolyte such as in standard car batteries, but a significant and growing number have a solid electrolyte. Some of the advantages of a solid electrolyte in lead-acid batteries are little or no spill or splashing of highly corrosive sulphuric acid in case of accidents, no leakage if the battery is placed sideways or even upside-down and longer life time because there is no accumulation of precipitated lead sulphate at the bottom of the battery, which may cause discharge.

The electrochemical process in a lead-acid battery is well known (Garche, 1990);

Negative electrode (charging):



Positive electrode (charging):



There are two methods of immobilising the electrolyte, i.e. making a solid electrolyte, in valve-regulated lead-acid (VRLA) batteries. The first method involves AGM-VRLA batteries, where the electrolyte is immobilised by being absorbed in absorptive glass-fibre mats placed between the electrodes. This type of battery can produce high starting currents and be rapidly recharged. Such batteries can be used in, e.g., uninterrupted power supply systems (UPS). VRLA batteries must be carefully managed in order to prevent ever increasing charge current and temperature rise effects, i.e. thermal runaway. AGM-VRLA batteries, as opposed to their GEL-VRLA counterparts, are much more susceptible to this potentially catastrophic phenomenon (Lambert et al, 2002; Wagner 2007).

The second method involves GEL-VRLA batteries, where the electrolyte is immobilised by being absorbed within the very fine pores of a silica gel, which can be made from different silica materials. GEL-VRLA batteries have long life span, good cycling characteristics, and relatively low current. Moreover, they are used in applications such as telecommunication and solar energy devices, as well as motive power applications (e.g., golf cars, wheel chairs, and loading trucks) (Lambert et al., 2002). GEL-VRLA batteries are predicted to be used as a second battery in cars to supply steady, non-surging power to the increasing number of electronic components in modern cars. Wagner (2007) points out that two of the key benefits of a gel battery are its very long service life, up to 15-18 years at room temperature, and its high reliability even under severe circumstances (e.g., high temperatures or deep discharges as well as long storage at room temperature without any charging).

Electrochemical processes that take place in a battery during charging are well known (Garche, 1990) Since the electrolyte is solid and ion mobility is very limited, the oxygen cycle (Bagshaw 1990) is important in lead-acid batteries with gelled electrolyte (Hardman, 1988). In fact, the gelled battery will not work optimally until the gel has hardened and cracked sufficiently (micro-cracks) to allow oxygen transportation in the battery (Mrha, 1989).

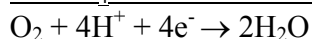
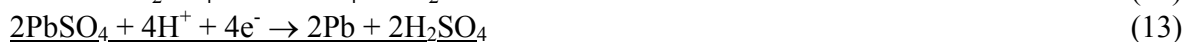
Positive electrode

Oxygen cycle (charging)



Negative electrode

Oxygen cycle (charging)



Silica gels can be made from different starting materials, typically from fumed silica or silica sols. Judging from the patent literature, fumed silica traditionally appears to be the most common starting material for making silica gels for GEL-VRLA batteries. However, in the past several years, some very promising work has been reported on making silica gels for batteries from colloidal silica in the form of silica sols. Fumed silica is dusty powder with low density and hence puts high demands on the handling and filling procedures, including vacuum filling equipment of the battery (immediate viscosity increases because of the thickening effect of the

rod-like silica) in contrast to colloidal silica. Colloidal silica tends to replace fumed silica during recent years (Toniazzo, 2006).

Gelling of silica sols

At the ACS National Meeting in Washington, D.C. in 1990, Paul Yates gave a talk on the “Kinetics of Gel Formation of Silica Sols”. He described that the gellation of silica sols is kinetically quite different from that of soluble silicates, although the same factors are important, i.e. silica concentration, pH, salt content, temperature, and the particle size of the sols. Expressions were derived for the quantitative prediction of the gel times for colloidal silica dispersions over a wide range of these variables. The following is a summary of Yates presentation. It is very difficult to study a gel in detail of concentrated sulphuric acid. A typical sulphuric acid concentration in a gelled lead-acid battery is 38 wt-% (or about 5 M). This will destroy most equipment such as SEM/TEM and viscometers. Empirical based methods for characterising the gellation process of silica sols under conditions similar or close to those in a lead-acid battery are therefore of most importance.

Types of Gel

There are three types of silica gel, of which the first results from neutralising dilute aqueous solutions of a silicate and is formed by the polymerisation of silicic acid. The polysilicate ions extend as a three-dimensional cross-linked network throughout the solution. The second type results from the collision of preformed colloidal silica particles to form three-dimensional chains of such particles, bonded at their junction points with siloxane bonds (Figure 26). The third type is a hybrid of the first two with polysilicic acid chains joining preformed colloidal silica particles. Hybrid gels are formed by neutralisation of mixtures of silicates and colloidal silica sols.

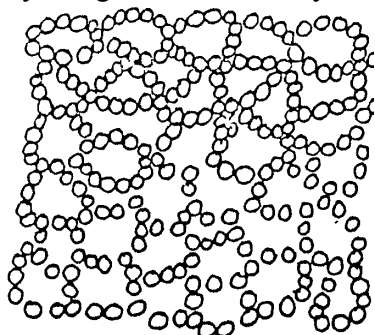


Figure 26. Structure of collision gel (Yates, 1990).

Common Features in Gel Formation

Although the quantitative kinetic expressions for each of the three types of gel are different, they respond qualitatively in a similar way to most of the important variables. For all types of gel, gel times become shorter at higher temperatures, at higher silica concentrations, and in the presence of increasing concentrations of neutral salts.

The effect of pH is complex. Starting with strongly acid (low pH) systems, gel times initially decrease rapidly as the OH concentration is increased, then pass through a minimum, and finally,

increase rapidly as the pH continues to increase. For all types of gel, the effect salts in decreasing gel times are much more pronounced on the basic side than on the acid side, and the location of the minimum in the gel time versus pH curve is a very sensitive function of the neutral salt content and even of the specific salt employed.

The Central Mechanism in Gel Formation

The similarities described exist because the central polymerisation mechanism is essentially the same for all types of gel. This mechanism also shows the key role played by the hydroxyl ion.

The First Role of Hydroxyl Ions - As a Catalyst

A silicon atom in silicic acid or at a surface normally has a coordination number of 4. The coordination number can be momentarily expanded by adsorption of a hydroxyl ion simultaneously with adsorption of a sixth group, such as a silanol group belonging to another silicic acid molecule or colloidal particle. This transition complex is unstable and water condenses out between the two silanol groups to form a permanent siloxane bond. The coordination number drops back to 4 and the hydroxyl ion is desorbed, regenerating it to continue its catalytic role elsewhere in the solution.

The Second Role of Hydroxyl Ions - Charge Repulsion

If the only role played by hydroxyl ions were a catalytic one, gel times would continuously decrease as the pH increased. The observed minimums in gel times and their rapid increase at high pH show that the hydroxyl ion plays a dual role in the mechanism of formation of silica gels.

The conditions of gellation of sols in a very strong acidic environment (such as in sulphuric acid) differ, significantly from the ones present under Yate's investigation. At pH below 2, silica sols are positively charged and the role of hydroxyl ion is taken over by the proton (Brinker, 1994) as indicated by the formulas below. In addition, the negatively charged sulphate ion will take over the role of sodium as the ion to "balance" the positive charge of the particles.

Gellation of silica above pH 2



Gellation of silica below pH 2



Kinetics of Collision Gels

Gels formed by the collision of colloidal silica particles in solutions containing only traces of silicate ions have entirely different kinetics than the other two types of gel. Under comparable conditions, gel times are 100 to several thousand times as long. The quantitative response to variables (e.g., concentration, salt content, pH, and the surface area silica) is also quite different. The equation derived (Yates, 1990) for gels prepared from deionised "Ludox HS" mixtures of varying concentrations, pH values, and salt contents is given below as Equation 18.

$$\log t = 5.85 - \text{pH} - \log(\Phi/(1-2.58\Phi)) + (1.333-1.482\Phi)(0.032-0.1183\log c) \times (\text{pH}-2.34)^2. \quad (18)$$

Where

t = gel time in minutes, Φ = volume fraction of silica, and c = salt concentration. This equation reproduced the gel times of 39 gels from solutions containing 10, 20, 30, and 40 wt % SiO_2 at pH values of 3.5, 5.0, 6.0, 7.0, and 8.5, and salt concentrations of .01 N, .03 N, 0.1 N, and 0.3 N, with an average error of 0.11 units in the log gel time value. This is within the probable experimental reproducibility of these data.

Figure 27 shows the ability of this equation to reproduce gel times at a constant (0.1 normal) salt concentration over a range of pH and silica concentrations. The solid lines were calculated from Equation 18.

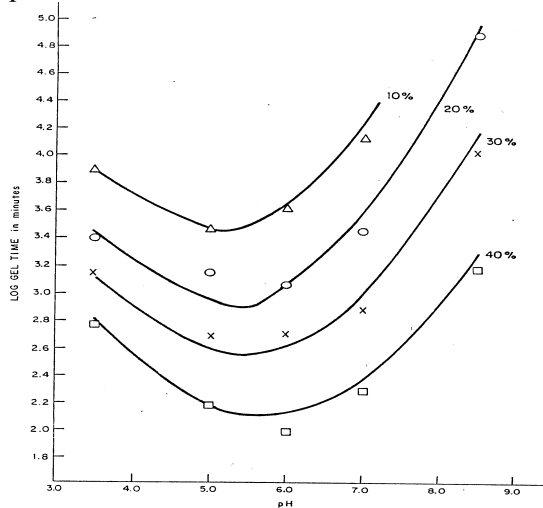


Figure 27. Effect of silica concentration on the gel time of collision gels at 0.1 normal salt concentration (Yates, 1990).

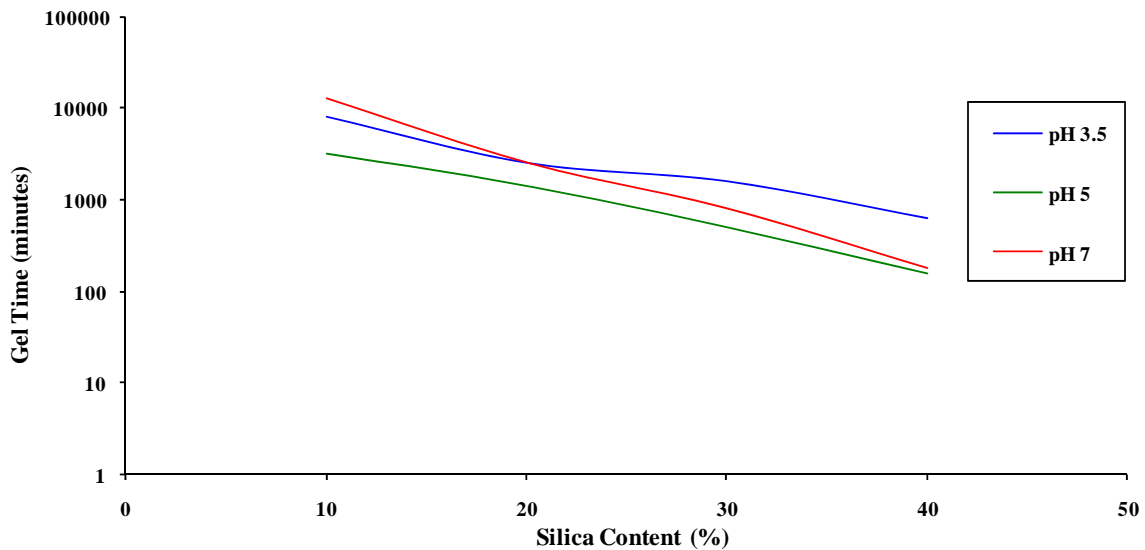


Figure 28. Gel time versus silica content for Ludox HS at different pH values at 0.1 normal salt concentration (based on Figure 27).

However, in highly acidic sulphuric acid the picture is a bit different. In 38 wt-% sulphuric acid the gel times (at 20°C) in minutes are shown in Figure 29. In Figure 29, the relation between the gel times and the silica contents is significantly more pronounced than in Figure 28 (the slopes are steeper) and the impact of electrolyte concentration in equation 18 is relatively small. Similar experiments at a 50 wt- % sulphuric acid concentration for one of the silica sols (11 nm in size) revealed that it gelled about 5 times faster under otherwise similar conditions.

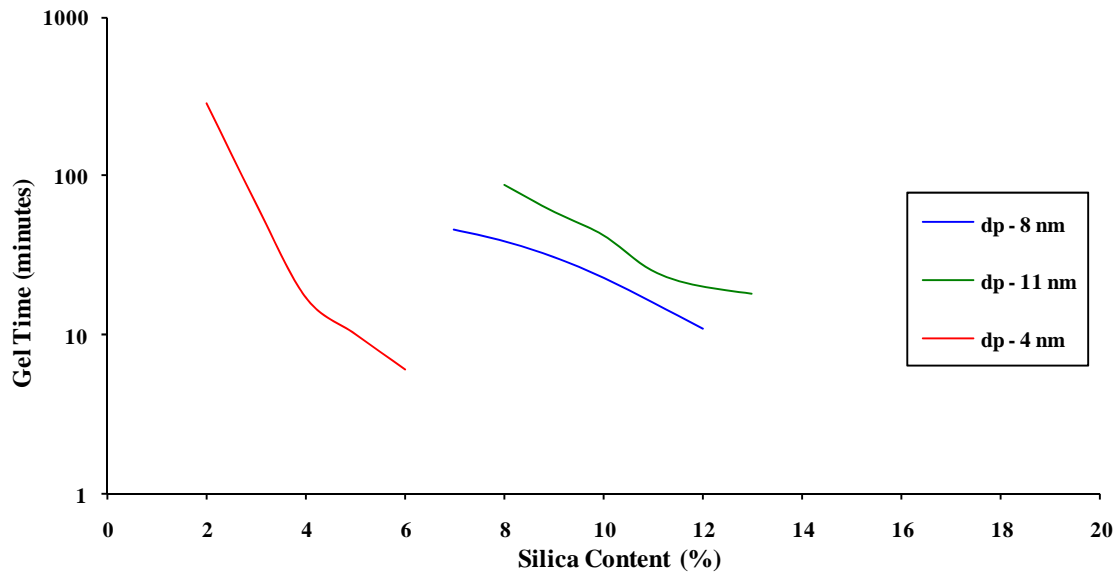


Figure 29. Gel time versus silica content for silica sols of different particle sizes in 38 wt-% sulphuric acid.

Obviously, equation 18 is at best only heuristically useful at very acidic conditions. At these conditions, the various terms in the equation would be the same, but the actual values of the constants would have to be re-calculated in order to make the equation fit experimental data more closely.

Improved battery performance by modified silica sols

Silica sols with a high specific surface of 750 m²/g (dp: 4 nm) and a high degree of structure (a S-value below 50) have been found to be very suitable for this application, combining an efficient silica usage with a reasonable fast gel time (Greenwood et al., 2010) as indicated in Figure 30. Gel structure has been found to play a vital role for battery performance as confirmed by others (Chen, Chen, Shu, and Finlow, 2008) working with the degree of dispersion for fumed silica.

As indicated, gel strength is the second important parameter of the silica in a gel battery. Because of the severe conditions in the gelled acid, gel strength is measured by a special method: a lead bullet (diameter 4.4 mm and weight of 0.50 g) is dropped from the height of 23 cm on a 24 hours old gel. The impact in mm is measured and an impact of 2 mm or less is normally considered to give a gel of sufficient strength. Using fumed silica, this typically requires a silica load of about 5-6 % in the gel to obtain a gel with sufficient strength.

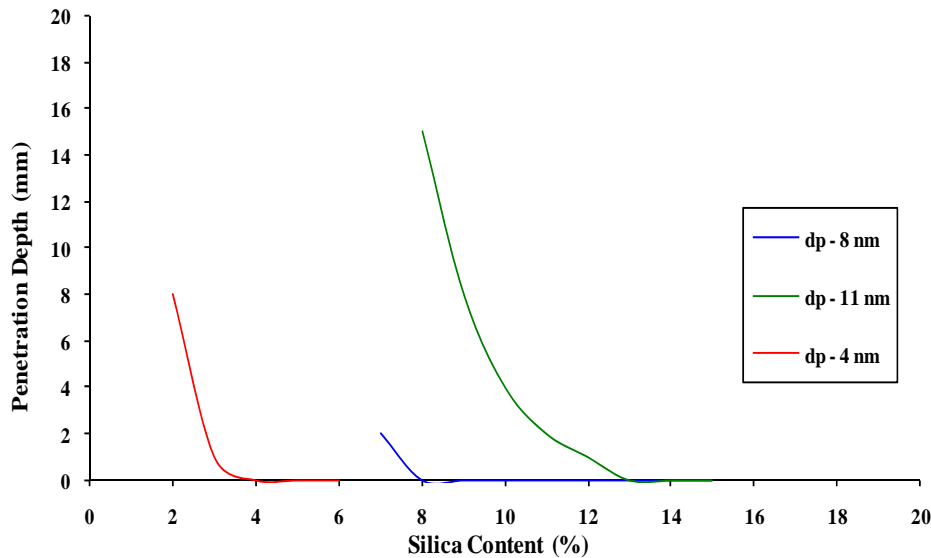


Figure 30. Gel strength versus silica content for silica sols of different particle sizes in 38 wt-% sulphuric acid.

Sielemann, Niepraschk, and Nemeč-Losert (1997) compared solid electrolytes consisting of collision gels made either from silica sols with a specific surface area between 100 to 500 m²/g or from fumed silica in lead-acid batteries. The solid electrolyte made from the silica sol was prepared directly in the battery container, whereas the one made from fumed silica had to be made in a separate step. The fumed silica, in the form of a very light, fluffy powder, was mixed with the sulphuric acid and the other components of the solid electrolyte in a special vessel. The slow-gelling mixture was then poured into the battery container where it eventually solidified. The performances of lead-acid batteries containing the two types of solid electrolyte were very similar, perhaps with a slight edge for the silica sol battery since it had a somewhat higher discharge current.

Lambert et al. (2002) carried out a comparative study of solid electrolytes made from silica sol and fumed silica and suggested the following advantages for electrolytes made with silica sol:

- Simplified handling and mixing of the electrolyte
- No liquid separates from the gel after solidification
- High silica concentration in gelling additive
- Increased residual gel strength
- Controlled gel time
- Less impurities (e.g., iron and chloride)

5.2.4 Titania coated colloidal silica (paper VI)

The advancement of high technology composite particles (e.g., new titania-silica pigments) could be used in, for instance, inks and coatings to optimise particle size and light scattering performance. The pigment size distribution should be monodisperse and of optimal size in that a conventional titania pigment is about 300 nm. In practise, most pigments are distributed around 200-400 nm (Nelson, 2008). Titania is one of the most important photocatalysts (Kalele, 2005) and using a silica core can enhance the performance further (Lee et al., 2008). Titania particles have recently been reported to reduce NO_x emissions in traffic when used on surface treatment of pavements (Murata, Kamitani, Tawara, Obata, and Yamada, 2002; Hellman, 2009). Composite particles may enhance performance further since particle size and titania efficiency may be controlled.

Another application area for white composite pigments of titania-silica can be white ink applications in which settling is a severe problem and limitation because of, high particle density and large particle size, for using pure titania pigments.

Vargas, Greenwood, Otterstedt, and Niklasson (2000), (paper VI in this thesis), studied the performance of commercial TiO₂ pigments and TiO₂ coated SiO₂ particles (as described in 4.2) hosted in a copolymer of ethylene and vinyl acetate. Spectrophotometric measurements were used to calculate solar (R_{sol}) and luminous (R_{lum}) reflectances of films containing commercial rutile pigments and composite anatase pigments. The reflectance was reported as a function of $F \cdot h$, where F is the pigment weight fraction and h denotes the film thickness. At low $F \cdot h$, the reflectance increases rapidly but levels off to a constant value for $F \cdot h > 15 \mu\text{m}$. The composite anatase pigments are less scattering than the commercial rutile pigments but the difference is not large and becomes even smaller at high $F \cdot h$. As expected, the reflectance increases with the thickness of the TiO₂ coating on the SiO₂ core. The highest solar reflectances were close to 0.7 for the composite pigments and between 0.75 and 0.8 for the rutile pigments.

The main reason for the difference in scattering power between the two types of pigment is the lower refractive index of anatase (2.52 and 2.74 for rutile). Fresnel's equation, $R = (n_1 - n_2)^2 / (n_1 + n_2)^2$ gives that the scattering power of the two phases of TiO₂ in polymer films, where n_2 is 1.38 for the polymer (Vargas, 1997), has been compared and it was found that rutile scatters light about 30 % more efficiently than anatase. In addition, any aggregation is detrimental for light scattering efficiency and any change in pigment particle size (from optimal) dramatically reduces the efficiency (Nelson and Yulin, 2008).

6. Outlook

The future is very bright for aqueous silica sols. Colloidal silica dispersions are inorganic materials made from sand, soda, and water as raw material all readily available. Each year there are one or several new applications or developments of these exiting silica nano-particles, in many cases driven by environmental reasons/legislations. Though the debate over the risks from nano-materials has been intense during recent years, nothing has been found until now indicating that these materials should be harmful to health or environment in contrast to such materials as e.g., carbon nanotubes.

The largest potentials for silica sols are likely to be in high value applications where relatively small amounts of materials are needed: for example, in coatings, WP/CMP, lead acid batteries or flocculation applications, as well as in special construction applications such as oil well cementing. To cite Charles C. Payne (1994); “Colloidal silica will continue to be a versatile product with an applicability limited only by the imagination of the researcher”.

7. References

- Ahn, Y., Yoon, J-Y., Baek, C-W. and Kim, Y-K., (2004), "Chemical mechanical polishing by colloidal silica-based slurry for micro-scratch reduction", *J. Wear*, Vol. 257, No. 7-8, pp. 785-9.
- Andersson, K., Larsson, B. and Lindgren, E., (1997), "Silica sols and the use of silica sols", US patent 5,603,805.
- Andersson, K. and Larsson, H., (1984), "Nya kemikaliesystem för fyllda finpapper", *Nordisk Cellulosa*, No.1, pp. 55-9.
- Andersson, K. and Lindgren, E., (1996), "Important properties of colloidal silica in microparticulate systems", *Nord. Pulp Pap. Res. J.*, No. 1, pp. 15-21.
- Anderson, L.G., Barkac, K.A., Chasser, A.M., Desaw, S.A., Hartman, M.E., Hayes, D.E., Hockswender, T.R., Kuster, K.L., Montague, R.A., Nakajima, M., Olson, K.G., Richardson, J.S., Sadvary, R.J., Simpson, D.A., Tyebjee, S. and Wilt, T-F., (2002), "Cured coatings having improved scratch resistance, coated substrates and method thereto", U.S. patent 6,387,519.
- Auger, J-C., Barrera, R.G. and Stout, B., (2003), "Scattering efficiency of clusters composed by aggregated spheres", *J. Quant. Spectrosc. Radiat. Transfer*, Vol. 79-80, pp. 521-31.
- Bagshaw, N.E., (1990), "Lead/acid recombination batteries: principles and applications", *J. Power Sources*, Vol. 31, No. 1-4, pp. 23-33.
- Barringer, E.A. and Bowen, H. (1985), "High-Purity, Monodisperse TiO₂ Powders by Hydrolysis of Titanium Tetraethoxide. 2. Aqueous Interfacial, Electrochemistry and Dispersion Stability", *Langmuir*, Vol. 1, No 4, pp. 420-8.
- Bauer, F., Ernst, H., Hirsh, D., Naumov, S., Pelzing, M., Sauerland, V. and Mehnert, R., (2004) "Preparation of Scratch and Abrasion Resistant Polymeric Nanocomposites by Monomer Grafting onto Nanoparticles", *Macromol. Chem. Phys.*, Vol. 205, No. 12, pp. 1587-93.
- Bergqvist, H. and Chandra, S., (1999), "Method for preparation of a hardening composition", U.S. patent 5,932,000.
- Björnström, J., Martinelli, A., Matic, A., Börjesson, L. and Panas, I., (2004), "Accelerating effects of colloidal nano-silica for beneficial calcium-silicate-hydrate formation in cement", *Chem. Phys. Lett.*, Vol. 392, No. 1-3, pp. 242-8.
- Björnström, J. and Panas, I., (2007), "Antagonistic effect of superplasticizer and colloidal nano-silica in the hydration of Alite and Belite pastes", *J. Mater. Sci.*, Vol. 42, No. 11, pp. 3901-7.
- Blute, I., Pugh, R.J., Pas, J. and Callaghan, I., (2007), "Silica nanoparticle sols 1. Surface chemical characterization and evaluation of the foam generation (foamability)", *J. Colloid Interface Sci.*, Vol. 313, No. 2, pp. 645-55.

Bohm, B., Genth, H., Schober, P. and Simons, P., (1977), "Finishing with aluminate modified silica-sol", US patent 4027046.

Boisvert, J.-P., Persello, J., Foissy, A., Castaing, J.-C. and Cabane, B. (2000), "Effect of surface charge on the adsorption mode of sodium poly(acrylate) on alumina-coated TiO₂ used as coating pigment", *Colloids Surf., A*, Vol. 168, No. 3, pp. 287–96.

Boisvert, J.-P., Persello, J., Castaing, J.-C. and Cabane, B. (2001), "Dispersion of alumina-coated TiO₂ particles by adsorption of sodium polyacrylate", *Colloids Surf., A*, Vol. 178, No. 1-3, pp. 187–98.

Bolt, J.D., (1999), "Titanium dioxide particles having substantially discrete inorganic particles dispersed on their surfaces", US patent 5 886 069.

Brazdil, J. F., George, R.J. and Rosen, B.I., (2009), "Catalyst composition and use thereof in ethane oxidation", US patent application 2009/0292139.

Braun, J. H. (1988), "Crowding and Spacing of Titanium dioxide Pigments", *J. Coat. Technol.* Vol. 60, No.758, pp. 67-71.

Braun, H., Baidins, A. and Marganski, R.E. (1992), "TiO₂ pigments technology: a review", *Prog. Org. Coat.*, Vol. 20, No. 2, pp. 105-38.

Brinker, C.J., (1994), "Sol-Gel Processing of Silica" in Bergna, H.E. (Ed.), *The Colloid Chemistry of Silica, Advances in Chemistry Series 234*; American Chemical Society: Washington D.C, pp. 361-402.

Butrón, C., Gustafson, G., Fransson, Å. and Funehag, J., (2010), "Drip sealing of tunnels in hard rock; A new concept for the design and evaluation of permeation grouting", *Tunnelling Underground Space Technol.*, Vol. 25, No. 2, pp. 114-21.

Campillo, I., Dolado, J.S. and Porro, A., (2004), "High-performance nanostructured materials for construction", in Bartos, P.J.M., Hughes, J.J., Trtik, P. and Zhu, W. (Eds.), *Nanotechnology in Construction*, The Royal Society of Chemistry, Cambridge, pp. 215-25.

Chen, M.Q., Chen, H.Y., Shu, D., Li, A.D. and Finlow, D.E., (2008), "Effects of preparation condition and particle size distribution on fumed silica gel valve-regulated lead-acid batteries performance", *J. Power Sources*, Vol. 181, No. 1, pp. 161–71.

Chisholm, B. and Resue, J., (2003), "UV-curable, Hybrid organic-inorganic Coatings", *Proceedings 30th International Waterborne, High-Solids, and Powder Coatings Symposium*, New Orleans, USA.

Choi, H.-H., Park, J. and Singh, R.K., (2005) "Nanosized titania encapsulated silica particles using an aqueous TiCl₄ solution", *Appl. Surf. Sci.*, Vol. 240, No. 1, pp. 7-12.

Collinson, M.M., Zambrano, P. J., Wang, H. and Taussig, J. S., (1999), "Diffusion Coefficients of Redox Probes Encapsulated within Sol-Gel Derived Silica Monoliths Measured with Ultramicroelectrodes", *Langmuir*, vol. 15, No. 3, pp. 662-8.

Collepari, M., Ogoumah Olagot, J.J., Skarp, U. and Troli., R., "Influence of amorphous colloidal silica on the properties of self compacting concretes", (2002), *Proceed. International Conference "Challenges in concrete construction – innovation and developments in concrete materials and construction"*, Dundee, Scotland, September 9-11th, pp. 473-83.

Cotterill, R. (1985), *The Cambridge guide to Material World*, Cambridge University Press, Cambridge, pp. 124-31.

Dahar, S. and Te, M., (2009), "Articles comprising tetragonal zirconia and methods of making the same", US patent application 2009/0305882.

De Lame, C., (2005), "Water-based hybrid organic/inorganic coatings", presented at ATIPIC-NVVT Nanotechnology and Coatings meeting, Brecht, Belgium.

De Lame, C., Clayes, J-M., Greenwood, P. and Lagnemo, H., (2009), "Modified colloidal silica in silicate paints", 19th SLF Congress, September 7-9th, Sandefjord, Norway.

Douce, J., Boilot, J-P., Biteau, J., Scodellaro, L. and Jimenez, A., (2004), "Effect of filler size and surface condition of nano-sized silica particles in polysiloxane coatings", *Thin Solid Films*, Vol. 466, No. 1-2, pp. 114 – 122.

Fish, P., (2005), "Colloidal Silica", in Rodriguez, J., M. (Ed.), *Micro and Nanoparticles in Papermaking*, Tappi Press, Atlanta, pp. 55 -73.

Forrest S., (2001), "The development of titanium pigments", *Surf. Coat. Australia*, Vol. 38 No. 10, pp. 16-22.

Funehag, J. and Fransson, Å. (2006), "Sealing narrow fractures with a Newtonian fluid: Model prediction for grouting verified by field study", *Tunnelling Underground Space Technol.*, Vol. 21, No. 5, pp. 492-8.

Funehag, J. and Gustafson, G., (2008), "Design of grouting with silica sol in hard rock – New design criteria tested in the field, Part II", *Tunnelling Underground Space Technol.*, Vol. 23, No. 1, pp. 9-17.

Gao, Z., Zhao, Z., Ou, Y., Qi, Z. and Wang, F., (1996), "Preparation of StyreneMaleic Anhydride Copolymer/Si-O Network Nanocomposites by the Sol-Gel Process", *Polym. Int.*, Vol. 40, No. 3, pp. 187-92.

Garche, J., (1990), "On the historical development of the lead/acid battery, especially in Europe", *J. Power Sources*, Vol. 31, No. 1-4, pp. 401-6.

Greenwood, P., Linsten, M. O and Johansson-Vestin, H. E., (2002), "Silica-based sols", U.S. patent 6,379,500.

Greenwood, P., Bergqvist, H. and Skarp, U., (2002), "Composition and method to prepare a concrete composition", US patent 6,387,173.

Greenwood, P., Bergqvist, H. and Skarp, U., (2003), "Mixture of silica sols", US patent 6,596,250.

Greenwood, P. Bergqvist, H. and Skarp, U., (2004), "Construction material", US patent 6,800,130.

Greenwood, P., Lagnemo, H. and Reed, M., (2010), "Composition prepared from silica sol and mineral acid", US patent 7,674,833.

Griessbach, R., (1933), "Lösungen kolloidaler Kieselsäure und ihre Anwendung in der Technik. 1.", Chem. Ztg., Vol. 57, No. 26, pp 253-60, 274-6.

Hansen, F.K. and Matijevic, E., (1980), "Heterocoagulation. Part 5.— Adsorption of a carboxylated polymer latex on monodispersed hydrated metal oxides", J. Chem. Soc., Faraday Trans. 1, Vol. 76, pp. 1240-62.

Hardman, A.M. , (1988), "A comparison of flooded, gelled and absorptive separator lead/acid cells", J. Power Sources, Vol. 23, No. 1-3, pp. 127 – 34.

Heiberger, F. and Schläffer, H., (2001), "Silicatic Coating Mass with Improved Stability", PCT WO 2001/53419.

Hellman, F.,(2009), "Use of TiO₂ nanoparticles for self cleaning of roads – A short literature survey", VTI (Swedish National Road and Transport Research Institute), VTI notat 11-2009.

Hsu, P.W., Yu, R. and Matijevic', E., (1993), "Paper Whiteners", J. Colloid Interface Sci., Vol. 156, No. 1, pp. 56-65.

Iler, R.K., (1973), "Effect of Adsorbed Alumina on the Solubility of Amorphous Silica in Water", J. Colloid Interface Sci., Vol. 43, No 2, pp. 399-408

Iler, R.K., (1955), The colloid chemistry of silica and silicates, 1st Ed., Cornell University Press, New York.

Iler, R.K., (1979), The Chemistry of Silica: Solubility, Polymerization, Colloid and Surface Properties, 1st Ed., Wiley and Sons, New York.

Iler, R.K. and Dalton, R.L., (1956), "Degree of hydration of particles of colloidal silica in aqueous solution", J. Phys. Chem., Vol. 60, No. 7, pp. 955-7.

- Inglis, G.E., (1913), “Stresses in a plate due to the presence of cracks and sharp corners”, Trans. Inst. Nav. Archit., Vol. 55, pp. 219-30.
- Johansson, H.V. and Larsson, B. V., (1994), “Silica sols having high surface area”, US patent 5,368,833.
- Kalele, S., Dey, R., Hebalkar, N., Urban, J., Gosavi, S.W. and Kulkarni, S.K., (2005), “Synthesis and characterization of silica-titania core-shell particles”, PRAMANA J. Phys., Vol. 65, No.5, pp.787-91.
- Keyes, W.F., (1946), “Determination of specific surface area by permeability measurements”, Ind. Eng. Chem., Vol. 18, No.1, pp. 33-4.
- Kohlshütter; H., Getrost, H., Hörl, W., Reich, W. and Rößler, H., (1970), “ Verfahren zur Herstellung von Titandioxid –bzw. Titandioxidaquatüberzügen“ German. Patent. 2 009 566.
- Komiyama, H., Kraines, S., (2008), Vision 2050 Roadmap for a Sustainable Earth, 1st Ed., Springer, Tokyo, pp. 81-3.
- Lambert D. W.H., Greenwood, P.H.J and Reed, M.C., (2002), “Advances in gelled-electrolyte technology for valve-regulated lead-acid batteries”, J. Power Sources, Vol. 107, No. 2, pp. 173-9.
- Larsen, J.G., Olsen, C. and Jensen, M.D. (2009), “Fuel cell stack”, European patent application 2.109,173.
- Lee, S.Y., and Hubbe, M.A., (2008), “Polyelectrolyte titrations of synthetic mineral microparticle suspensions to evaluate charge characteristics”, Colloids Surf., A, Vol. 331, No. 3, pp. 175-82.
- Lee, S.Y., and Hubbe, M.A., (2009), “Morphologies of synthetic mineral microparticles for papermaking as a function of synthetic conditions”, Colloids Surf., A, No. 1-3, pp. 118-25.
- Lee, J.W., Othman, M.R., Eom, Y., Lee, T.G., Kim, W.S. and Kim, J. , (2008), “The effects of sonification and TiO₂ deposition on the micro-characteristics of the thermally treated SiO₂/TiO₂ spherical core-shell particles for photo-catalysis of methyl orange”, Microporous Mesoporous Mater., Vol. 116, No. 1-3, pp. 561–8.
- Leuniger, J., Tiarks, F., Wagner, O., Jahns, E. and Wiese, H., (2006) “Nano-Composite dispersions - The Col 9. Technology for Water-based Coatings”, Proc.18th SLF Congress, Helsingör, Denmark.
- Li, Q. and Dong, P., (2003), “Preparation of nearly monodisperse multiply coated submicrospheres with a high refractive index”, J. Colloid Interface Sci., Vol. 261, No. 2, pp. 325-9.
- Lindström, T., Hallgren, H. and Hedborg, F., (1989), “Aluminium based microparticulate retentionaid systems”, Nord. Pulp Pap. Res. J., Vol. 4, No. 2, pp. 99-103.

Look J.L. and Zukoski C.F., (1992), "Alkoxide-Derived Titania Particles: Use of Electrolytes to Control Size and Agglomeration Levels", *J. Am. Ceram. Soc.*, Vol. 75, No. 6, 1587-95.

Matijević E. and Babu, S.V., (2008), "Colloid aspects of chemical-mechanical planarization", *J. Colloid Interface Sci.*, Vol. 320, No. 1, pp. 219-37.

Matijević E., Budnik, M. and Meites, L., (1977), "Preparation and mechanism of formation of titanium dioxide hydrosols of narrow size distribution", *J. Colloid Interface Sci.*, Vol. 61, No. 2, pp. 302-11.

May, A., Vogel, B., Siegert, H., Gaudschun, K-A. and Quabdt, T., (2009), "Katalysator zur Umsetzung von Carbonsäurenitrilen", German patent application DE 10 2008 001 319.

Meisel, K., Thiele, B., Renner, G-F., Kijlstra, J., Nennemann, A. and Hübbe, T., (2005), "Paper production with modified silica gels as microparticles", PCT WO2005/003455.

Murata, Y., Kamitani, K., Tawara, H., Obata, H. and Yamada, Y., (2002), "NO_x removing pavement structure", US patents 6454489.

Mrha, J., Micka, K., Jindra, J. and Musilová, M., (1989), "Oxygen cycle in sealed lead-acid batteries", *J. Power Sources*, Vol. 27, No. 2, pp. 91-117.

Nelson, K. and Yulin, D., (2008), "Effect of polycrystalline structure of TiO₂ particles on the light scattering efficiency", *J. Colloid Interface Sci.*, Vol. 319, No. 1, pp.130-9.

Oberdisse, J., (2002), "Structure and Rheological Properties of Latex-Silica Nanocomposite Films: stress-Strain Isotherms", *Macromol.*, Vol. 35, No. 25, pp. 9441-50.

Osterholtz, F.D. and Pohl, E.R., (1992), "Kinetics of the hydrolysis and condensation of organofunctional alkoxysilanes: a review", *J. Adhes. Sci. Technol.*, Vol. 6, No. 1, pp. 127-49.

Otterstedt, J-E. and Brandreth, D.A., (1998), *Small Particles Technology*; Plenum Press: New York, pp. 407-29.

Papadakis, V. G., (1999), "Experimental investigation and theoretical modeling of silica fume activity in concrete", *Cem. Concr. Res.*, Vol. 29, pp. 79-86.

Payne, C.C. (1994), "Applications of Colloidal Silica: Past, Present, and Future" in Bergna, H.E. (Ed.), *The Colloid Chemistry of Silica*, Advances in Chemistry Series 234; American Chemical Society: Washington D.C, pp. 581 – 94.

Peeters, M.P.J., (2000), "An NMR Study of MeTMS Based Coatings Filled with Colloidal Silica", *J. Sol-Gel Sci. and Tech.* Vol.19, No. 1-3, pp. 131-5.

Percy, M.J., Barthet, C., Lobb, J.C., Khan, M.A., Lacelles, S.F. and S.P. Armes, (2000), "Synthesis and Characterization of Vinyl Polymer-Silica Colloid Nanocomposites", *Langmuir*, Vol. 16, No. 17, pp. 6913-20.

Persson, M., Hansson, F., Pal, A.V., Lindahl, L. and Carlén, J., (2008), "Silica-based sols", PCT WO 2008/150230.

Plueddemann E., P., (1991), Silane Coupling Agents, 2nd Ed., Plenum Press, New York

Rahhal, V., Cabrera, O., Talero, R. and Delgado, A., (2007), "CALORIMETRY OF PORTLAND CEMENT WITH SILICA FUME AND GYPSUM ADDITIONS", J. Therm. Anal. Calorim., Vol. 87, No. 2, pp. 331–6.

Rademacher, I., Pantke, D. and Wilhelm, P., (2008), "Innovativer Einsatz von Kieselsole in der Bauchemie Fassadenfarben, Bautenschutz, Oberflächenbehandlung", Proceedings of Gesellschaft Deutscher Chemiker Fachgruppen Bauchemie und Lackchemie, GEMEINSAME TAGUNG, Koblenz, September 22nd- 24th, pp. 91 -100.

Reynaud, E., (2000), "Etude des relations Structure-Propriétés mécaniques de thermoplastiques renforcés par des particules inorganiques nanoscopiques", PhD thesis, L'Institut National des Sciences Appliquées de Lyon, France, in French.

Riegel, B., Blittersdorf, S., Kiefer, W., Hofacker, S., Müller, M. and Schottner, G., (1998), "Kinetic investigations of hydrolysis and condensation of the glycidoxypropyltrimethoxysilane-aminopropyltriethoxysilane system by means of FT-Raman spectroscopy I", J. Non-Cryst. Solids, Vol. 226, No. 1-2, pp. 76-84.

Ryu, R.D., Kim, S.C. and Koo, S.M., D.P., (2003), "Deposition of Titania Nanoparticles on Spherical Silica", J. Sol-Gel Sci. and Tech., Vol. 26, No. 1-3, pp. 489-93.

Sielemann, O., Niepraschk, H. and Nemeč-Losert, P., (1997), "Process for the production of a lead accumulator", US. Patent 5,664,321.

Schmid, A., Tonnar, J. and Armes, S. P. (2008), "A New Highly Efficient Route to Polymer-Silica Colloidal Nanocomposite Particles", Adv. Mater., Vol. 20, No. 17, pp. 3331-6.

Schmid, A., Armes, S. P., Carlos, A.P.L. and Galembeck, F. (2009), "Efficient Preparation of Polystyrene/Silica Colloidal Nanocomposite Particles by Emulsion Polymerization Using a Glycerol-Functionalized Silica Sol", Langmuir, Vol. 25, No. 4, pp. 2486-94.

Schmid, A., Scherl, P., Armes, S. P., Carlos, A.P.L. and Galembeck, F. (2009), "Synthesis and Characterization of Film-Forming Colloidal Nanocomposite Particles Prepared via Surfactant-Free Aqueous Emulsion Copolymerization", Macromol., Vol. 42, No. 11, pp. 3721-8.

Schottner, G., (2001), "Hybrid Sol-Gel-Derived Polymers: Applications of Multifunctional Materials", Chem. Mater., Vol. 13, No. 10, pp. 3422-35.

Skarp, U. and Sarkar, S., (2001), "Enhanced properties of concrete containing colloidal silica" Presented at The World of Concrete, Las Vegas, February 27- March 2.

Taylor, H.F.W, (1997), *Cement chemistry*, 2nd Ed., Thomas Telford Services Ltd, London.

Toniazzo, V., (2006), “The key to success: Gelled-electrolyte and optimized separators for stationary lead-acid batteries”, *J. Power Sources*, Vol. 158, No. 2, pp. 1124–32.

Thomas, J.J., Jennings, H.M. and Chen, J.J., (2009), “Influence of nucleation seeding on the hydration mechanisms of tricalcium silicate and cement “”, *J. Phys. Chem. C*, Vol.113, No. 11, pp. 4327–34.

Vu, C., La Ferté, O. and Eranian, A., (2005), “High Performance UV Multi-Layer Coatings Using Inorganic Nanoparticles”, *Proc. RadTech Europe*.

Vargas, W. E., (1997), “Light Scattering and Absorption in Pigmented Coatings, Theory and Experiments”, *Dissertation Uppsala University, Faculty of Science and Technology*, pp. 56

Wagner, R., (2007), “Stationary applications. I. Lead-acid batteries for telecommunications and UPS”, in Broussely, M. and Pistoia, G. (Eds.), *Industrial Applications of Batteries from Cars to Aerospace and Energy Storage*, Elsevier, Amsterdam, pp. 395-454.

Wagner, J-P and Hauck, H.G, (1994), “Nanosilica - ein Zusatz für dauerhaften Beton”, *Wiss. Z. Hochsch. Archit. Bauwes. – Weimar*, Vol. 40, 5/6/7, pp.183-7.

Yates, P. C.; “Kinetics of Gel Formation of Colloidal Silica Sols”, *Ralph K. Iler Memorial Symposium on the Colloidal Chemistry of Silica*, ACS National Meeting, Washington D.C., 1990.

Yang, J.C., Oh, D.W., Lee, G.W., Song, C.L. and Kim, T., (2010), “Step height removal mechanism of chemical mechanical planarization (CMP) for sub-nano-surface finish”, *J. Wear*, Vol. 268, No. 3-4, pp. 505-10.

Yeh, J-M., Weng, C-J., Liao, W-J. and Mau, Y-W., (2006), “Anticorrosively enhanced PMMA-SiO₂ hybrid coatings prepared from the sol-gel approach with MSMA as the coupling agent”, *Surf. Coat. Technol.*, Vol. 201, No. 3-4, pp. 1788-95.

Zhuralev, L.T., (1993), “Surface characterization of amorphous silica- a review of work from the former USSR”, *Colloids Surf., A*, Vol. 74, No. 1, pp. 71-90.

8. Acknowledgement

Thanks to my family for understanding and patience over the years to complete this project.

A great thanks to my mentor and friend, Professor Emeritus Jan-Erik Otterstedt, Chalmers University of Technology, for all his fruitful discussions, as a priceless source of references (sometimes out of press), and valuable input and comments.

In addition, I would like to extend my gratitude to all colleagues at Industrial Specialties, Eka Chemicals (Akzo Nobel), especially to Mr. Bo Larsson, Mrs. Inger Jansson, Mr. Roy Hammer-Olsen, and Mr Olle Sörensson for giving me the time and support needed for finalising this intellectual journey.

I would also like to acknowledge my supervisor, Professor Börje Gevert, for his support over the years.

Professor Arne Roos and Dr. Andreas Jonsson, The Ångström Laboratory, Uppsala University, are being acknowledged for light scattering measurements related to pigments pastes. Mr. Martin Lagnemo is acknowledged for his support with graphic work.

Finally, I wish to express my gratitude to all other colleagues that has supported my over the years in one way or another.

Paper I

Aqueous Silane Modified Silica Sols: Theory and Preparation

Peter Greenwood (corresponding author) and Börje S. Gevert

Submitted to Pigment & Resin Technology



Aqueous Silane Modified Silica Sols: Theory and Preparation

| | |
|------------------|--|
| Journal: | <i>Pigment & Resin Technology</i> |
| Manuscript ID: | PRT-03-2010-0027 |
| Manuscript Type: | Original Article |
| Keywords: | Aqueous, Silane , Surface Modification, Silica Sol, Colloidal Silica |
| | |



Review

Aqueous Silane Modified Silica Sols: Theory and Preparation

ABSTRACT

Purpose – The objectives of this work were to study methods of reacting the surface of the particles of silica sols with silanes, primarily gamma-glycidoxypropyltrimethoxysilane (GPTMS) and study some basic properties of the modified sols and the nature and structure of the silane groups attached to the particle surface.

Design/methodology/approach - The surface of the silica particles was modified by reacting the silica sols with aqueous solutions of silanes, chiefly GPTMS. The presence and structure of silane groups on the particle surface were established by Si-NMR and C-NMR, respectively.

Findings - Several silanes were studied but silica sols could be readily modified only with GPTMS and glycidoxypropylmethoxydiethoxysilane (GPMDES), most readily if the silanes were pre-hydrolysed in water. Higher degrees of silylation were preferably done by continuous addition of silane. Lower degrees of modification can be achieved at room temperature by the stepwise addition of the silane solution. The silylation of the silica surface with GPTMS significantly reduces the number of charged surface groups and silanol groups. GPTMS binds covalently to the silica surface and the epoxy ring opens and transforms into a diol. Silica sols modified with GPTMS and GPMDES are stable toward aggregation.

Research limitations/implications – Only organo-reactive silanes were studied.

Originality/value – This is the first work to study the modification by silanes of silica aquasols with high concentrations of silica. The silane modification can extend the use of silica to areas of applications previously inaccessible to silica sols.

Practical implications - Stable, high-performing, surface-modified silica sols for use in waterborne lacquers, resin polymerisation, as inorganic pigments dispersants and in emulsion stabilisation.

Keywords – Silane, Surface Modification, Silica Sol, Colloidal Silica, Aqueous

Paper type – Research paper

For Peer Review

INTRODUCTION

Concentrated colloidal silica in the form of aqueous sols is one of the cheapest and most readily available sources of nanoparticles. Such sols are characterised by high-solids content (up to at least 50% by weight of silica, which depends on particle size ranging from about 5 nm to 100 nm) in combination with remarkable stability toward gelling. Because they are colloidal particles in water, water-based silica sols are often sensitive to salt (Hunter, 1995) and aggregation at high silica concentrations or when exposed to freezing temperatures (Iler, 1979).

In many applications, especially coating applications, water-based silica sols have not reached their full potential because of two important drawbacks: decreased water resistance and problems of stability. First, because silica sols have a surface that is fully hydroxylated (Iler, 1979), they normally decrease water resistance of a coating when incorporated into the same. This problem can be overcome by the addition of a hardener to the system. Second, and more important, severe long-term stability problems of the coating composition often occur when incorporated into polymer latices. Silica sols adsorb neutral surfactants by hydrogen bonding onto their sol surface (Hasan and Huang, 1997) and probably destabilising the coating composition by stripping the latex emulsion of stabilising surfactants. This is one of the main reasons why conventional silica sols are used in, e.g., latex emulsions for making packaging films (Steiner, 1977) and photo films that do not require long-term stability of the lacquer, but not in clear

coatings (such as in furniture or parquet lacquers) in which the coating composition requires a shelf-life of at least one year.

Silane grafting of dry silica powder has been done for many years, such as in the treatment of silica in the production of rubber tires. Studies of surface adsorption of gamma-glycidoxypropyltrimethoxysilane (GPTMS) on colloidal silica have been done in alcohol-based systems in the past (Daniels and Francis, 1998; Daniels et al, 1999). Furthermore, silane-modified silica particles in mainly alcohol-based systems have been reported to be used as fillers in hard-coat systems for polycarbonate (Wu et al, 2008). Recently, silane modifications of aqueous silica sols with poor stability for use in sol-gel coating have been reported (Na et al, 2008). In addition, water-free systems of silane-modified colloidal silica particles have been found to enhance mechanical properties of coatings (Vu, La Ferté and Eranian, 2005; Chisholm and Resue, 2003). Organosols have been used to improve scratch resistance in clear coatings by surface enrichment (Anderson et al, 2002) in solvent-borne clear coatings. Until now, very little has been reported on the basic properties or the nature of stable aqueous silane-modified silica sols. One of the reasons for the lack of research may be that silanes are normally not stable in the presence of water. Water promotes hydrolysis and condensation reactions, making surface modification of aqueous colloidal silica much more complicated than in solvent-borne systems.

Although colloidal silica is an especially preferred nano material in clear coatings and resins since it combines a high solid concentration (30-40 % by weight), at small particle sizes of 7 to 12 nm in combination with a low refractive index of 1.45 for SiO₂, poor stability toward gelling may be a problem in some applications. Other properties,

including performance in clear coatings (Greenwood, 2008), pigment dispersant (Greenwood, 2010), emulsion polymerisation (Schmid, Tonnar and Armes, 2008; Schmid, Armes, Carlos and Galembeck, 2009; Schmid, Scherl, Armes, Carlos and Galembeck, 2009) and foam and emulsion stabilisation (Whitby, Djerdjev, Beattie and Warr, 2006; Blute, Pugh, van de Pas and Callaghan (2009a, 2009b), have recently been reported for these kinds of modified aqueous silica sols.

In industrial use trialkoxysilanes, $\text{RSi}(\text{OR})_3$, are most common. They hydrolyse stepwise in water to give the corresponding silanols, which ultimately condense to siloxanes. Both reaction rates strongly depend on pH, but under optimal conditions



Hydrolysis (1) is relatively fast (several minutes), whereas the condensation reaction is much slower (several hours); both reactions are strongly pH dependant. Higher alkoxy silanes hydrolyse very slowly in water because they are strongly hydrophobic, but even in a homogeneous solution in water-miscible solvents they hydrolyse more slowly than the lower alkoxy silanes. Gamma-glycidoxypropyltrialkoxysilane is the preferred silane in this study because it reacts readily with water and the rate of hydrolysis is fast at both alkaline and acidic pH (Brinker and Scherer, 1990). The rate of hydrolysis is relatively slow in the pH region of 6-8.5. The chain length of the alkoxy group determines the rate of hydrolysis (Osterholtz and Pohl, 1992): trimethoxysilane hydrolysis is faster than triethoxysilane. When fully hydrolysed, GPTMS will have released three moles of methanol for each mole of silane as indicated above.

Before reaction with, for instance, an inorganic surface, silanes are often pre-hydrolysed by mixing them in water with a silane: water mol ratio of about 10:1, which, in the case

of gamma-glycidoxypropyltrialkoxysilane, corresponds to a weight ratio of about 1:1. The solution of pre-hydrolysed silane will have a pH of about 7 and will be stable toward self-condensation for at least 2 weeks.

The reaction between a hydrolysed silane (e.g., gamma-glycidoxypropyltrialkoxysilane) and the silanol groups of the silica particles is a condensation reaction.



The reaction is fast in the alkaline pH region (Osterholtz and Pohl, 1992) and can therefore be conveniently carried out at the pH of the sodium-stabilised sol, which is about pH 10. For uniform coverage of the particle surface, it is essential that the silane is present in monomeric form and not as large oligomers or cyclic species (Peeters, 2000). Under moderate conditions of rate of addition of silane and temperature, self-condensation and precipitation will not occur, however. An aqueous silica sol has about 4.6 silanol groups per nm² surface (Zhuralev, 1993), but considering that each silane may react with three surface groups, fewer silane molecules per nm² will be required to react fully with the silica surface. Silylation of the silica surface will reduce the number of silanol groups and hence make silylated sols more stable toward gelling through formation of siloxane bonds between particles.

Epoxy functional groups are stable during hydrolysis and condensation reactions (Gao, Zhao, Ou, Qi and Wang, 1996) but are believed to react/open up at elevated temperatures during the curing process of coatings containing, for instance, GPTMS

(Gao et al, 1996; Schottner, 2001). Cross-linking with other particles or molecules will cause an increase in viscosity or turbidity and is thus easy to detect.

EXPERIMENTAL

Materials used in the experiments

Colloidal silica dispersions - silica sols.

The following commercial silica sols (pH ranged from 9 to 11), supplied by Eka Chemicals AB (Akzo Nobel), were used.

Bindzil® 15/750 with a specific surface area of 750 m²/g: particle size 4 nm and a silica content of 15 % by weight.

Bindzil® 15/500 with a specific surface area of 500 m²/g: particle size 5 nm and a silica content of 15 % by weight.

Bindzil® 30/360 with a specific surface area of 360 m²/g: particle size 7 nm and a silica content of 30 % by weight.

Bindzil® 40/220 with a specific surface area of 220 m²/g: particle size 12 nm and a silica content of 40 % by weight.

Bindzil® 305/220 with a specific surface area of 220 m²/g: particle size 12 nm and a silica content of 30 % by weight. The surface is modified with sodium aluminate.

Silanes

Silquest® A-187: GPTMS, MW: 236 g/mole,

Silquest® Wetlink 78: gamma-glycidoxypropyl metoxydiethoxy silane (GPMDES), MW: 255 g/mole,

Silquest® A-1106: aqueous amino alkyl silicone solution; MW: proprietary information of supplier,

Silquest® Y-9669 N: N-phenyl-gamma-aminopropyl trimethoxysilane, MW: 255 g/mole and

Coatosil® 1770: beta-(3,4 epoxycyclohexyl) ethyl triethoxysilane, MW: 288 g/mole, were used, which were kindly supplied free of charge by Momentive Performance Materials.

Preparation of pre-hydrolysed silane

In a typical preparation 1000 g of silane were added to 1000 g of de-ionised water in a 3 L beaker with moderate agitation, corresponding to a water:silane molar ratio of 13:1. Agitation for 1 h resulted in a transparent solution with pH from 5 to 7.

Silanes are generally poorly soluble in water and hydrolysis is therefore facilitated by using a heel of hydrolysed silane, which contains up to about 20 % by weight of a lower aliphatic alcohol. Therefore, 50 to 70 g of hydrolysed GPTMS were placed in a 3 L beaker. 1000 g of silane were added in about 20 sec to the heel and 1000 g of de-ionised water were then added in about 20 sec with moderate agitation. After a few minutes, a transparent solution was obtained, indicating that hydrolysis had taken place.

Preparation of silane-modified sols

In one procedure the undiluted silane was rapidly added over a period of a few minutes to the undiluted sol with good agitation and, for comparison, with poor stirring at 25 °C. In another study a pre-hydrolysed 1:1 weight mixture of silane in water was added to the undiluted sol with good agitation. In a preferred method a pre-hydrolysed 1:1 weight mixture of silane in water was added to 5000 g of the undiluted sol (e.g., Bindzil®

30/360) with good agitation and a controlled rate of addition. Three addition rates and two reaction temperatures were used: 600 g/h and 2000 g/h at 60 °C and 1500 g/h at 70 °C. The silica sols were concentrated by vacuum evaporation at 60 °C in a 20 L evaporator for about 2 h. Typically, a 7 nm sol and a 5 nm sol, both silylated with GPTMS, could be concentrated to 40 and 26 wt-% SiO₂-content, respectively, with good stability as shown in Table I. (Take in Table I.)

Stability toward gelling

The stability behaviour of the sols was tested as stability toward gelling upon addition of salt solution (salt stability) measured as gel time. The gel time is defined as the time to obtain a rigid gel, i.e. the beaker containing the gel can be tilted 90 ° without inversion of the gel.

Stability under freezing conditions

A sample of 100 ml sol was put in a freezer for 24 h at -20 °C (deep-frozen) and then allowed to stand for 16 h in room temperature (to thaw) before evaluation. The procedure was repeated once. The samples were evaluated visually.

Characterisation of the silica sols

The silica sols were characterised by measuring pH, specific surface area by Sears' titration (Sears, 1956), viscosity with a Brookfield Viscometer and alcohol content by HPLC, Shimadzu Class 10 LC AD VP series equipped with a La Chrome L-7490 detector from Merck. The silica content was determined by XRF on a PaNalytical Magix PW 2450 instrument. ²⁹Si-MAS NMR spectra were obtained on a 400 MHz Varian NMR System

(Direct Drive™) operating with a 6 mm HX Chemagnetics (HX DR mode) and ¹³C-NMR spectra on a Bruker 500 MHz Ultrashield Advance III system equipped with a ATM/TCI probe. Particle charges were measured by cationic polyelectrolyte titration (Morgan, Forster and Evison, 1990) on a Mütek Particle Charge Detector. The sample concentration was 5 g per litre, titrated with a Polybrene solution of 4 g per litre in concentration. Levels of soluble (or monomeric) silica were determined using the ammonium heptamolybdate method (Iler, 1979).

RESULTS AND DISCUSSION

Of the five silanes evaluated, only silylation with the two glycidoxysilanes -- GPTMS and GPMDES -- resulted in stable sols. N-phenyl-gamma-aminopropyl trimethoxysilane, beta-(3,4 epoxy cyclohexyl) ethyl triethoxysilane and the aqueous amino alkyl silicone solution caused rapid reaction (green and brown colour), precipitation of the sols, or both. Not only did GPTMS dissolve more readily in water than GPMDES but it also seemed to react more promptly with the silica surface. One reason for the differences may be that GPTMS hydrolyses much faster in water than GPMDES.

Pre-hydrolysed silane simplified the silane modification process significantly since such silane will more readily adsorb and react with the silica surface, which would reduce the level of free silane and associated self-cross-linking.

Pre-hydrolysis of silane

At pH 10 and dilute conditions, GPTMS hydrolyses rapidly (about 100 min) and becomes fully hydrolysed in water as indicated by the formation of 3 moles methanol per mole silane, whereas the time of hydrolysis was considerably longer at pH 7 (Table II). High silane concentrations (e.g., 50 wt-% silane in a water mixture) speed up hydrolysis. After about 30 min, the silane is fully hydrolysed, even at neutral pH. Table II shows that more than 3 moles methanol (3.2-3.3) are formed per mole silane and that the initial methanol content should be about 0.2-0.3 mole per mole GPTMS under diluted conditions. This “extra” methanol probably originates as an “impurity” in the silane starting material, GPTMS. Regrettably, a small heel of pre-hydrolysed silane did not further reduce the preparation time for a fully hydrolysed solution of GPTMS as shown in Table II, although transparency indicated faster reactions. The rate of hydrolysis depends on the solubility of the silane in water. The addition of pre-hydrolysed silane to the silane/water mixture was expected to increase the solubility somewhat and thus reduce the time of hydrolysis. On the other hand, the fast hydrolysis reaction may have made such time differences too small to detect. The use of heel, however, did give a clearer solution of hydrolysed silane as indicated by the lower turbidity values. During the preparation, the temperature increased from 20 °C to 30 °C, indicating an exothermic reaction. These results are consistent with the findings of de Buyl and Kretschmer (2008), who have done work on dilute GPTMS at pH 5.6. (Take in Table II.)

Self-condensation reaction of the hydrolysed silane

Self-condensation, which can cause gelling of hydrolysed silane solutions, proceeds very slowly in the acid region but fast at alkaline pH (Brinker and Scherer, 1990). For reasons

of stability, hydrolysed silane solution should be kept at a pH below 7, preferably in the range from 4 to 6. This range is low enough to avoid self-condensation but not low enough to promote opening of the epoxy ring (de Buyl and Kretschmer, 2008) and reaction of the diol groups of the opened ring with silanol groups of the hydrolysed silane (Horr and Reynolds, 1997). ^{29}Si NMR studies revealed that the stability of the pre-hydrolysed silane (at neutral pH) appeared to be good, at least for the first couple of weeks (Table III), indicating a high amount of dimers (T1). The amount of oligomeric content had increased significantly (T2 and T3) in the solution that was aged for 5 months. During hydrolysis of the silane, the epoxy functional group is not affected as depicted in Figure 1. (Take in Table III.) (Take in Figure 1.)

Condensation reaction of (non-pre-hydrolysed) silane with the silica surface at room temperature

When the silane is added to the sol over a short time (1 – 2 min) and in higher doses (2 – 10 g of silane to 100 g sol), corresponding to about 0.6 – 2.5 silane molecules per nm^2 of particle surface area, the sols turned opaque. The higher the amount of silane, the faster the sol turned opaque, taking about 10 min for the highest dosage. Good agitation reduced the degree of opaqueness for a given amount of silane added to the sol at a given temperature. Self-condensation of the silane molecules before they have time to react with the silica surface is the most likely reason for the appearance of opacity.

Condensation reaction of pre-hydrolysed silane with the silica surface

Batch-wise silane addition – low degree of modification

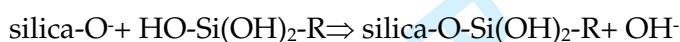
The course of the reaction between the silica sol and a particular silane was studied by measuring the specific surface area and pH value during the addition of silane.

Table III and Figure 2 show changes in pH and specific surface area during the course of silylation of a 7 nm sol (Bindzil 30/360), with pre-hydrolysed GPTMS to yield 0.6 molecules of silane per nm² silica surface. The silane addition was completed in a few seconds under good agitation at room temperature.

(Take in Table IV.)

In the Sears' titration method for determining the specific surface area (originally based on BET) of aqueous silica sols the adsorption of hydroxyl ions on the silanol groups of the particle surface is measured in the pH range 4 – 9 in a nearly saturated salt solution. This solution permits the surface charge density to approach a maximum 1.26 negatively charged OH groups per nm² surface area at pH 9.0 (Sears, 1956). The silanol number, i.e. the number of OH groups per nm² of silica particle surface, has been determined to be 4.6 for silica sols (Zhuralev, 1993). Accordingly, the number of silanol groups present in a given silica sol is directly proportional to its specific surface area. If, for any reason (e.g., reacting the silica surface with silanes), the number of silanol groups in the system decreases, this reduction will show up as a decrease in the specific surface area as measured by Sears' titration. A degree of silylation of 0.6 molecules of GPTMS per nm² particle surface corresponds to one molecule of GPTMS per eight silanol groups. The reduction in the specific surface area from 376 m²/g to 280 m²/g after the completed addition of silane corresponds to a decrease in the silanol number by 1.2 units, i.e. from 4.6 to 3.4 silanol groups per nm² silica surface, indicating that each molecule of GPTMS reacts with 2.0 silanol groups. Fully hydrolysed GPTMS contains three hydroxyl groups, of which two may react with one silanol group each, leaving one unreacted OH group

on each GPTMS molecule. A less likely possibility is that each GPTMS molecule reacts with three silanol groups but that a small fraction of the fully hydrolysed GPTMS molecules in the pre-hydrolysed silane undergoes self-condensation to siloxanes. Self-condensation is low because the pre-hydrolysed GPTMS remains a clear, stable solution for months provided the methanol produced during the hydrolysis is not removed from the system. Once it is removed, however, the pre-hydrolysed silane will turn turbid and gel within 24 h. The shape of the curves in Figure 2 indicates that at least two types of reaction take place during the silylation of the silica surface as suggested by the following reaction schemes:



(3)



During the first 5 min of silane addition, pH increased rapidly from 10.1 to almost 10.4 (scheme 3), whereas there was a more gradual increase to 10.6 during the next 135 min (scheme 4), after which time the pH remained constant. In reaction 3 the hydrolysed silane reacted rapidly with the negatively charged sites of the silica surface releasing hydroxyl ions, which raised the pH and created more charged sites on the surface (Iler, 1979). In the slower reaction (reaction 4), probably catalysed by hydroxyl ions, the hydrolysed silane condensed with surface silanol groups. (Take in Figure 2.)

Continuous addition of silane – high degree of modification

With a higher degree of silylation of the silica surface, this is the preferred route as for a surface modification corresponding to 1.4 and 1.7 molecules of GPTMS per nm² silica surface (now commercial products under the names of Bindzil[®]CC30, dp: 7 nm, and

Bindzil® CC40, dp: 12 nm, respectively), there is a reduction of about 85% of the surface charge as measured by Polybrene titration (Table V). This observation is well in line with reported data on zeta potential. Blute et al found that Bindzil® CC30 had a very low zeta potential (below -10 mV) in the pH range of 2-6 and significantly lower than that of the non-modified silica sol (Bindzil® 40/220) in the pH range of 6-11 (Blute, Pugh, van de Pas and Callaghan, 2007). The authors also found that the low surface charge remained unchanged over time. (Take in Table V.)

The pre-hydrolysed silane was continuously added to the colloidal silica at a reaction temperature of 60 °C, a rate of about 1.4 molecules GPTMS per nm² silica surface and hour and under good agitation. The comparison between the ²⁹Si NMR spectra in Figures 3 and 4 reveals a significant reduction in the ratio of silanol groups to bulk siloxane units (Q3/Q4) for silica sol, silylated with 1.4 molecules GPTMS per nm² silica surface relative to non-silylated sol with a particle size of 7nm. This reduced ratio indicates a covalent bond between the silane and the silica surface. The ²⁹Si NMR spectra in Figures 3 and 4 were de-convoluted and gave a ratio Q3/Q4 of 0.240 for the non-modified silica sol, whereas the ratio of Q3/Q4 for the silylated silica sol was 0.140. The change in the Q3/Q4 ratio, indicating a reduction of Q3 groups by 42%, corresponded fairly well to the drop in specific surface area by 38%, from 369 m²/g for the unmodified sol to 227 m²/g for the silylated sol. (Take in Figure 3.) (Take in Figure 4.)

The epoxy functional group and silane solubility of the silylated silica sol

¹³C NMR confirmed that the alkaline conditions (pH of about 10) during the condensation reaction transformed the functional epoxy group of the silane to a diol

group (Figure 5). This finding is consistent with reports that ring opening can take place under alkaline conditions (Riegel, Blittersdorf, Kiefer, Hofacker, Müller and Schottner, 1998). (Take in Figure 5.)

Further, measurement of the content of free silane monomer by HPLC gave a monomer content of 2600 ppm at pH 10.9 for a silica sol with a particle size of 7 nm and silylated with 1.4 molecules GPTMS per nm² silica surface. In contrast, soluble silica, as measured by the ammonium heptamolybdate method, was found to be 960 ppm. On the other hand, when the pH of the sol was adjusted to about 8 by cation exchange, the monomer content was only about 280 ppm, indicating silane solubility increases at alkaline pH. In the latter case the soluble silica was found to be 87 ppm, close to the theoretical value of a flat silica surface at room temperature. No free silane dimers or oligomers were detected by the HPLC analysis of the silane-modified silica sols. This finding strongly indicates that all of the added silane had reacted with the silica surface because the total amount of added silane corresponds to 53 600 ppm of silane in the silylated sol.

Effect of rate of addition and amount of silane on sol stability

Lower rates of addition, typically about 0.6 silane molecules per nm² added for a 2 h period at room temperature, result in clear stable sols. Even rates of addition as high as 1.4 molecules per nm² particle surface area and hour at 60 °C result in clear stable sols. At very high rates of addition (e.g., 4.4 molecules per nm² surface of the sol and hour at 70 °C), precipitation of the sol, self-condensing of the silane, or both occurred.

Viscosity and silica content of silylated sols

Normally, stability of unmodified silica sols is achieved by strong electrostatic repulsion between the particles at pH above 8. Silylation of the particle surface provides steric hindrance as a complement to electrostatic repulsion for stabilising silica sols. The results in Figure 6 show that steric stabilisation, or a combination of steric and ionic stabilisation, was more effective than ionic repulsion alone. (Take in Figure 6)

Concentrations of conventional sols and sols silylated with GPMTS were increased stepwise by vacuum evaporation. The viscosities of the sols in each step were measured immediately and after 4 months. The results, which are summarised in Table I, show that silylation substantially improved the stability of silica sols. In fact, the improvements in stability and the subsequent increases in solids content were so large, in particular for very small particle sols, that the use of such sols (e.g., 5 nm sols) can be expanded into new areas of applications where the unmodified sols could not be used because of the low solids content.

Stability toward gelling upon salt addition

Like other colloidal systems, silica sols are sensitive to the presence of electrolytes. Addition of, e.g., sodium chloride will cause the silica sol to gel by compression of the electrostatic double layer around the silica particles. It may be expected that sterically stabilised colloids are less sensitive to electrolytes than electrostatically stabilised colloids. Table VI shows that the increase in stability toward gelling, expressed as gel time, of silane-modified sols was dramatic when compared with non-modified sols, even at a relatively moderate addition of GPTMS. To obtain maximal stability the addition level should be in the order of 1.4 molecules per nm^2 sol surface. The reason for

the stability increase is probably a combination of steric stabilisation of the sol and a reduced number of reactive surface groups as previously mentioned. Moreover, the silane-modified silica surface has probably lower silica solubility, causing the coalescence of silica particles to take place at a much slower rate. (Take in Table VI.)

Stability toward gelling/precipitation under freezing conditions

Freeze stability is something that normally is not possible to achieve for sodium-stabilised and aluminate-modified water-based sols. The freezing point can be lowered by the addition of alcohol (e.g., ethylene glycol). However, if the sol freezes to a solid body, it will normally coagulate and be irreversibly aggregated (Iler, 1979). The results from the freezing tests, as given in Table VII, show that the sols with a high degree of silane modification can be frozen and then thawed with no apparent changes in properties, even when the procedure was repeated. When frozen, reference samples of non-treated sol are irreversibly aggregated/precipitated. Sols with a smaller amount of silane added (e.g., about 0.6 molecules per nm² surface area) or sols with a very high specific surface area in combination with structure/aggregation have somewhat reduced freeze stability. The improved stability under freezing conditions is probably a function of improved steric hindrance that prevents particles from coming to close, in combination with a less reactive surface that does not create siloxane bridges very easily with other silica particles. The improved stability is also a strong indication that the silane is covalent, and not hydrogen-bonded to the silica surface. (Take in Table VII.)

CONCLUSIONS

1. Full hydrolysis of GPTMS can be achieved with practical rates at a high concentration (50 wt-%), at room temperature and at neutral pH. Pre-hydrolysed silane solutions will be stable for several weeks toward condensation reactions.
2. Silane surface modification of the silica sols could only be achieved with GPTMS and GPMDES and with the silanes preferably pre-hydrolysed in water.
3. The epoxy functional groups of the silanes are not affected during hydrolysis.
4. Higher degrees of silylation, about 1.4 silane molecules per nm² silica surface or more, are preferably done with continuous addition of silane solution at a rate of about 1.4 – 1.7 silane molecules per nm² silica surface and hour at 60 °C. Lower degrees of silane modification, about 0.6 molecules per nm² silica surface, can be achieved at room temperature by stepwise addition of the silane solution.
5. The silylation of the silica surface with GPTMS significantly reduces the number of charged surface groups and silanol groups.
6. During the silylation reaction, GPTMS binds covalently to the silica surface and the epoxy ring opens and transforms into a diol.
7. Silica sols modified with GPTMS and GPMDES are very stable toward aggregation by salts and exhibit good stability under freezing conditions. They also show improved long-term stability at high silica concentrations compared with corresponding non-silylated sols.

ACKNOWLEDGEMENT

The authors thank professor emeritus Jan-Erik Otterstedt, Chalmers University of Technology, for valuable discussions and fruitful input. The authors also thank Dr

Kenneth Larsson and Mr Robert Butler for HPLC measurements, as well as Mrs Elsemarie Johnsson for surface charge measurements.

REFERENCES

Anderson, L.G. , Barkac, K.A. , Chasser, A.M. , Desaw, S.A. , Hartman, M.E. , Hayes, D.E. , Hockswender, T.R. , Kuster, K.L. , Montague, R.A. , Nakajima, M. , Olson, K.G. Richardson, J.S. , Sadvary, R.J., Simpson, D.A., Tyebjee, S. and Wilt, T-F. (2002), "CURED COATINGS HAVING IMPROVED SCRATCH RESISTANCE, COATED SUBSTRATES AND METHODS THERETO", *US Patent 6 387 519*.

Blute, I., Pugh, R.J., van de Pas, J. and Callaghan, I (2007), " Silica nanoparticle sols 1. Surface chemical characterization and evaluation of the foam generation (foamability)", *Journal of Colloid Interface Science*, Vol. 313, No. 2, pp. 645-55.

Blute, I., Pugh, R.J., van de Pas, J. and Callaghan, I. (2009a), "Industrial manufactured silica nanoparticle sols. 2: Surface tension, particle concentration, foam generation and stability", *Colloids and Surfaces A: Physicochemical and Engineering Aspects*, Vol. 337, No. 1-3, pp. 127-35.

Blute, I., Pugh, R.J., van de Pas, J. and Callaghan, I (2009b), "Silica nanoparticle sols. Part 3: Monitoring the state of agglomeration at the air/water interface using

the Langmuir–Blodgett technique”, *Journal of Colloid Interface Science*, Vol. 336, No. 2, pp. 584-91.

Brinker, C.J. and Scherer, G.W. (1990), *Sol-Gel Science The physics and Chemistry of Sol-Gel Processing*, Academic Press, San Diego

de Buyl, F. and Kretschmer, A. (2008), “Understanding Hydrolysis and Condensation Kinetics of γ -Glycidoxypropyltrimethoxysilane”, *The Journal of Adhesion*, Vol 84, No. 2, pp. 125-42.

Chisholm, B. and Resue, J. (2003), “UV-CURABLE, HYBRID ORGANIC-INORGANIC COATINGS”, *Proceedings 30th International Waterborne, High-Solids, and Powder Coatings Symposium*, New Orleans, USA, pp. 261-81.

Daniels, M.W. and Francis, L.F. (1998), “Silane Adsorption Behavior, Microstructure, and Properties of Glycidoxypropyltrimethoxysilane-Modified Colloidal Silica Coatings”, *Journal of Colloid Interface Science*, Vol. 205, No. 1, pp. 191-200.

Daniels, M.W., Sefcik, J., Francis, L.F. and McCormick, A.V. (1999), “Reactions of a Trifunctional Silane Coupling Agent in the Presence of Colloidal Silica Sols in Polar Media”, *Journal of Colloid Interface Science*, Vol. 219, No. 2, pp. 351-6.

Gao, Z., Zhao, Z., Ou, Y., Qi, Z. and Wang, F. (1996), "Preparation of StyreneMaleic Anhydride Copolymer/Si-O Network Nanocomposites by the Sol-Gel Process", *Polymer International*, Vol. 40, No. 3, pp.187-92.

Greenwood, P. (2008), "Nano-Particle Reinforced Latex Dispersions with Modified Colloidal Silica", *Journal of Coatings Technology Coatings Tech*, Vol. 5, No. 2, pp. 44-51.

Greenwood, P. (2010), "Modified Silica Sols: Titania Dispersants and Co-binders for Silicate Paints", *Pigment & Resin Technology*, Vol. 39, No. 6, article in press.

Iler, R.K. (1979), *The Chemistry of Silica: Solubility, Polymerization, Colloid and Surface Properties*, 1st Ed., Wiley and Sons, New York.

Hasan, F.B. and Huang, D.D (1997), "Characterization of Colloidal Silica and Its Adsorption Phenomenon with Silicon-Base Surfactants with Relation to Film Strength", *Journal of Colloid Interface Science*, Vol. 190, No. 1, pp. 161-70.

Horr, T.J. and Reynolds, G.D. (1997), "The reactions of 3-glycidoxypropyltrimethoxysilane in acidic solutions on polymerization and in the presence of silica", *Journal of Adhesion Science Technology*, Vol. 11, No. 7, pp. 995-1009.

Hunter, R.J. (1995), *Foundations of Colloid Science*, 1st Ed., Oxford University Press, New York, Vol. 1.

Morgan, J. W., Forster, C. F. and Evison, L. (1990), "A COMPARATIVE STUDY OF THE NATURE OF BIOPOLYMERS EXTRACTED FROM ANAEROBIC AND ACTIVATED SLUDGES", *Water Research*, Vol. 24, No. 6, pp. 743-50.

Na, M., Park, H., Kang, D. and Ahn, M. (2008), "Properties of Nano-Hybrid Sol-Gel Coating Films Synthesized with Colloidal Silica and Organoalkoxy Silanes", *Materials Science Forum*, Vol. 569, pp. 69-72.

Osterholtz, F. D. and Pohl, E. R. (1992), "Kinetics of the hydrolysis and condensation of organofunctional alkoxy silanes: a review", *Journal of Adhesion Science and Technology*, Vol. 6, No. 1, pp. 127-49.

Peeters, M.P.J. (2000), "An NMR Study of MeTMS Based Coatings Filled with Colloidal Silica", *Journal of Sol-Gel Science and Technology*, Vol.19, No. 1-3, pp. 131-5.

Riegel, B., Blittersdorf, S., Kiefer, W., Hofacker, S., Müller, M. and Schottner, G. (1998), "Kinetic investigations of hydrolysis and condensation of the glycidoxypropyltrimethoxysilane-aminopropyltriethoxy-silane system by means of FT-Raman spectroscopy I", *Journal of Non-Crystalline Solids*, Vol. 226, No. 1-2, pp. 76-84.

Schmid, A., Tonnar, J. and Armes, S. P. (2008), "A New Highly Efficient Route to Polymer-Silica Colloidal Nanocomposite Particles", *Advanced Materials*. Vol. 20, No. 17, pp. 3331-6.

Schmid, A., Armes, S. P., Carlos, A.P.L. and Galembeck, F. (2009), "Efficient Preparation of Polystyrene/Silica Colloidal Nanocomposite Particles by Emulsion Polymerization Using a Glycerol-Functionalized Silica Sol", *Langmuir*, Vol. 25, No. 4, pp. 2486-94.

Schmid, A, Scherl, P., Armes, S. P., Carlos, A.P.L. and Galembeck, F. (2009), "Synthesis and Characterization of Film-Forming Colloidal Nanocomposite Particles Prepared via Surfactant-Free Aqueous Emulsion Copolymerization", *Macromolecules*, Vol. 42, No. 11, pp. 3721-8.

Schottner, G. (2001), "Hybrid Sol-Gel-Derived Polymers: Applications of Multifunctional Materials", *Chemistry of Materials*, Vol. 13, No. 10, pp. 3422-35.

Sears, G.W. Jr (1956), "Determination of Specific Surface Area of Colloidal Silica by Titration with Sodium Hydroxide", *Journal of Analytical Chemistry*, Vol. 28, No. 12, pp.1981-3.

Steiner, R.H. (1977), "HEAT SEALABLE THERMOPLASTIC FILMS", *US patent 4 058 645*.

Vu, C., La Ferté, O. and Eranian, A. (2005), "High Performance UV Multi-Layer Coatings Using Inorganic Nanoparticles", *Proceedings RadTech Europe*, Barcelona, Spain

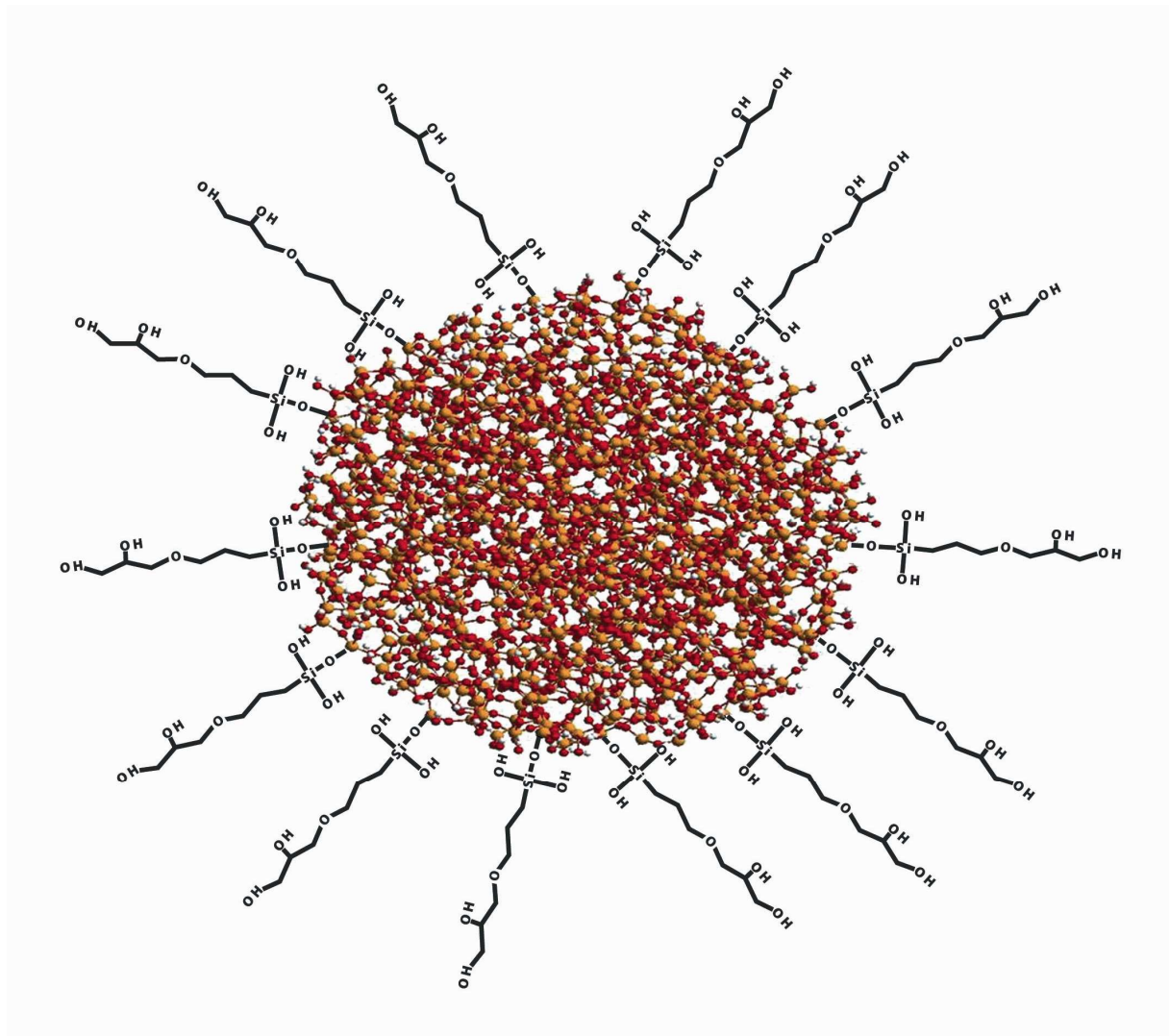
Available http://www.radtech-europe.com/templates/mercury.asp?page_id=1613

Whitby, C., Djerdjev, A.M., Beattie, J.K. and Warr, G.G. (2006), "Nanoparticle adsorption and stabilisation of surfactant-free emulsions", *Journal of Colloid Interface Science*, Vol. 301, No. 1, pp. 342-5.

Wu, L.Y.L., Chwa, E., Chen, Z. and Zeng, X.T. (2008), "A study towards improving mechanical properties of sol-gel coatings for polycarbonate", *Thin Solid Films*, Vol. 516, No. 6, pp. 1056-62.

Zhuravlev, L.T. (1993), "Surface characterization of amorphous silica- a review of work from the former USSR", *Colloids and Surfaces A: Physicochemical and Engineering Aspects*, Vol. 74, No. 1, pp. 71-90.

Graphical abstract



Epoxy silane modified colloidal silica particle. The particle size of the silica core is 7 nm.

Tables

Table I. Maximal SiO₂ content (weight-%) of conventional and silylated silica sols.

| Particle size (nm) | Without silane modification | With silane modification | Increase of solids content, % | Silane per nm ² surface area | Weight ratio Silane/Colloid. Silica |
|--------------------|-----------------------------|--------------------------|-------------------------------|---|-------------------------------------|
| 4 | 16 | 20 | 25 | 1.4 | 0.40 |
| 5 | 22 | 26 | 18 | 2.0 | 0.40 |
| 7 | 32 | 40 | 25 | 1.4 | 0.20 |
| 12* | 40 | 47 | 18 | 0.6 | 0.05 |

Maximum SiO₂ content is defined as the SiO₂ content at which the viscosity increase is less than 1 cP (20 °C) during a period of 4 months.

*: Aluminate-modified sols

Table II. Hydrolysis rate in water. Mole methanol per mole GPTMS formed at room temperature.

| Time (minutes) | 3 -wt % GPTMS, Water pH 10.6 | 3 -wt % GPTMS, Water pH 7 | 50 -wt % GPTMS, Water pH 7 | 50 -wt % GPTMS, Water pH 7, heel |
|----------------|------------------------------|---------------------------|----------------------------|----------------------------------|
| 2 | 0.30 | 0.21 | 1.15 | 1.16 |
| 30 | 1.74 | 0.28 | 2.82 | 2.78 |
| 60 | 2.59 | 0.35 | 2.86 | 2.84 |
| 90 | 2.97 | 0.45 | 2.90 | 2.88 |
| 120 | 3.12 | 0.58 | 2.89 | 2.89 |

Table III. ²⁹Si HR/MAS NMR spectrum of GPTMS, 50 % by weight hydrolysed silane solution, neutral pH.

| | 3-week-old solution | 5-month-old solution |
|----------------|---------------------|----------------------|
| T ¹ | 35.02 % | 4.33 % |
| T ² | 54.61 % | 51.41 % |
| T ³ | 10.36 % | 44.26 % |

Table IV. The course of silylation of a silica sol of particle size 7 nm with 0.6 molecules of silane per nm² silica surface.

| No. | Time (minutes) | Specific surface area(m ² /g) | pH |
|-----|------------------------|--|-------|
| 1. | Before silane addition | 376 | 10.10 |
| 2. | 0 | 361 | 10.10 |
| 3. | 2 | ---- | 10.15 |
| 4. | 3 | ---- | 10.25 |
| 5. | 4 | ---- | 10.30 |
| 6. | 5 | ---- | 10.35 |

| | | | |
|-----|-----|-----|-------|
| 7. | 20 | 344 | 10.40 |
| 8. | 40 | 336 | 10.45 |
| 9. | 60 | 329 | 10.50 |
| 10. | 80 | 315 | 10.55 |
| 11. | 100 | 301 | 10.60 |
| 12. | 120 | 298 | 10.60 |
| 13. | 140 | 288 | 10.60 |
| 14. | 160 | 280 | ----- |
| 15. | 180 | 285 | ----- |
| 16. | 200 | 284 | ----- |

Table V. Particle charge as meq/g for conventional and silylated silica sols

| Colloidal silica, size (nm) | Charge meq/g | pH | Silane per nm ² surface area | SiO ₂ -content (weight-%) |
|--|--------------|-----|---|--------------------------------------|
| 7 nm, non-silylated (Bindzil® 30/360) | 577 | 9.2 | 0 | 30 |
| 7 nm, silylated (Bindzil® CC30) | 93 | 8.5 | 1.4 | 30 |
| 12 nm, non-silylated (Bindzil® 40/220) | 334 | 8.9 | 0 | 40 |
| 12 nm, silylated (Bindzil® CC40) | 52 | 8.2 | 1.7 | 40 |

Table VI. Gel time versus NaCl concentration for silica sols of different particles sizes, dp (nm), and degree of silylation, sd, as GPTMS/nm² surface.

| Added NaCl conc. (weight-%) in sol | Silica sol No (as by Table 9) | | | | |
|------------------------------------|-------------------------------|-----------------------|-----------------------|---------------------|-----------------------|
| | 1 dp: 7 sd: 0 | 2 dp: 7 sd: 0.6 | 3 dp: 7 sd: 1.4 | 4 dp: 4 sd: 0 | 5 dp: 4 sd: 1.4 |
| 1.33 | 56 min | ---- | > 3 m | 26 min | > 3 m |
| 1.67 | 18 min | ---- | > 3 m | 5 min | > 3 m |
| 2.00 | 6 min | 126 h | > 3 m | 2 min | > 3 m |
| 2.33 | 2 min | 83 h | > 3 m | 1 min | > 3 m |
| 8.33 | ---- | ---- | 29 d | ---- | 72 h |
| 12.50 | ---- | ---- | 42 h | ---- | 2 h |

m: months, d: days, h: hours and min: minutes

Table VII. Stability under freezing conditions, silica sols of particle size of 7 nm

| No | Silica Sol Degree of silylation: (GPTMS/nm ² surface) | Observation cycle 1 | Observation cycle 2 |
|----|--|---------------------|---------------------|
| | | | |

| | | | |
|---|-----|--|--|
| 1 | 0 | White precipitates – no sol | White precipitates – no sol |
| 2 | 0.6 | Very few small flakes/ some precipitates. | Very few small flakes/ some precipitates. |
| 3 | 1.4 | Clear, low viscous | Clear, low viscous |

For Peer Review

Figures

Figure 1: ¹³C suspended-state NMR spectra under MAS condition with HPDEC of GPTMS 50 weight-% hydrolysed silane solution three weeks old (neutral pH).

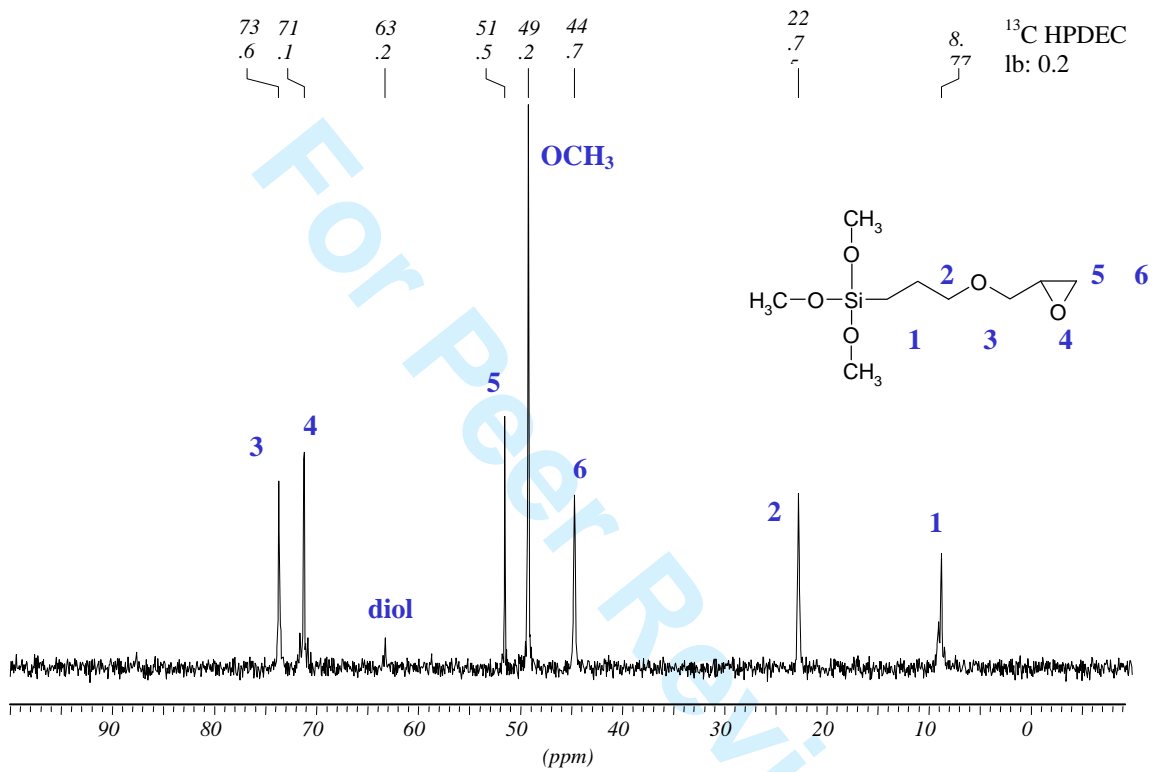
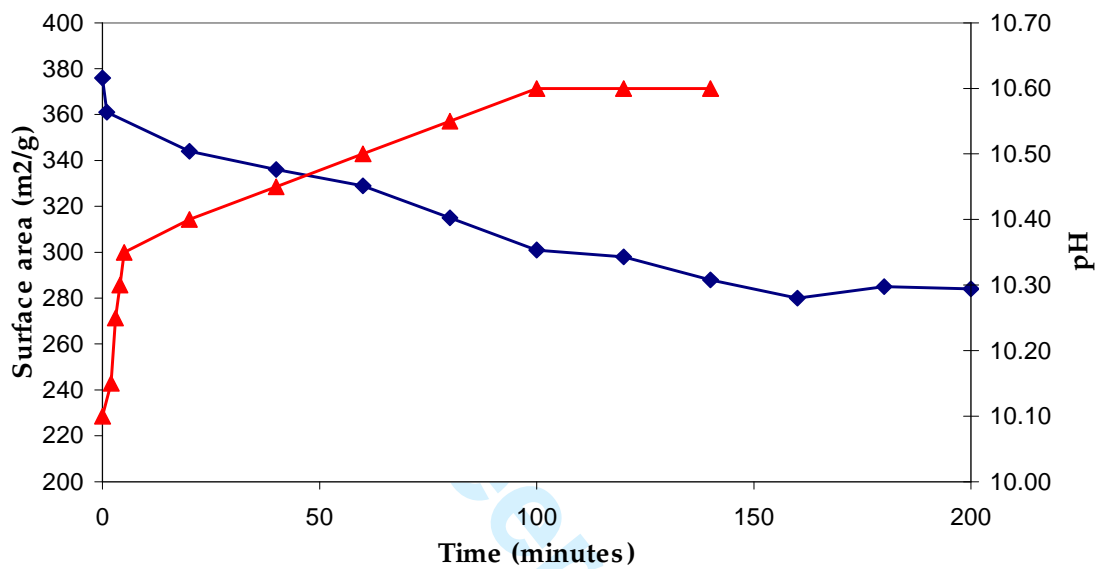


Figure 2: Specific surface area and pH versus time during silylation of surface of a 7

nm silica sol, with 0.6 molecules of GPTMS per nm² silica.

Figure 3: ²⁹Si-MAS NMR, 7 nm silica sol silylated with 1.4 GPTMS per nm² silica surface (Bindzil® CC30).

```

sample1
bindzil CC30/Lot 08177
250uL / 6mm spinner
MAS 3.5kHz
    
```

```

exp6 onepul
    
```

```

SAMPLE
date Mar 3 2009
temp not used
srate 4000.0
file exp
    
```

```

ACQUISITION
tn 5129
sfrq 79.454046
tof -3760.5
tpwr 54
sw 40322.6
at 0.019840
np 1600
dl 300.000000
nt 180
ct 180
ss 0
rd 5.0
ad 5.0
ax90 2000
pwx90 10.0
    
```

```

DECOUPLE
dn H1
dfrq 399.942645
dof -4369.0
dpwr 57
ah90 2000
pwh90 5.0
    
```

```

DECOUPLE2
dn2 N15
dfrq2 40.530048
dof2 0
dpwr2 0
ay90 0
pwy90 0
    
```

```

TPPM
ahppm 1200
pwHppm 6.0
phHppm 6.00
    
```

```

PROCESSING
fn 32768
phfid not used
rp -66.52
lp 0
lb 30.0
    
```

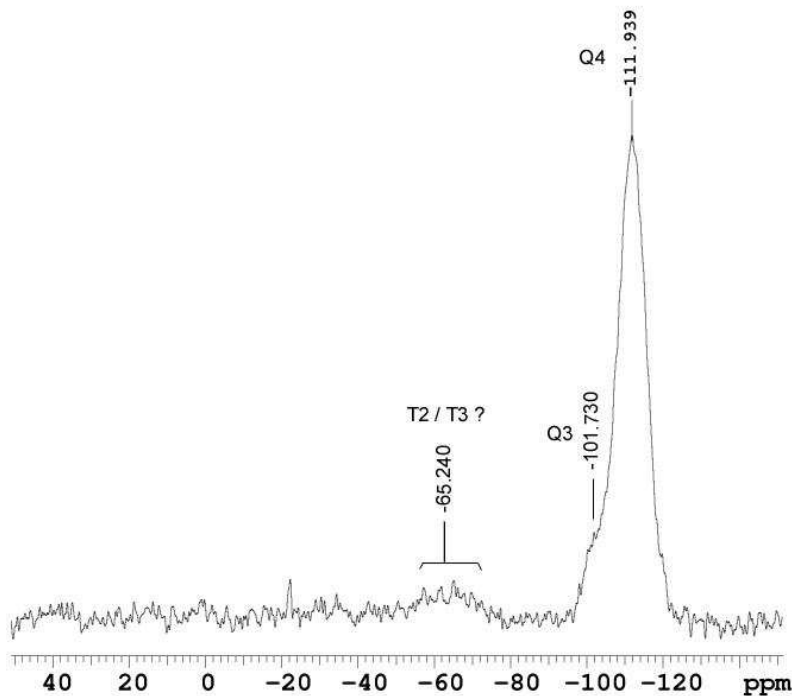


Figure 4: ^{29}Si -MAS NMR, 7 nm silica sol not silylated (Bindzil® 30/360).

```
sample3
bindzil 30/360 Lot 08115
250uL / 6mm spinner (47M1025)
MAS 3.5kHz

exp8 onepul

SAMPLE
date Mar 4 2009
temp not used
srate 4000.0
file exp
ACQUISITION
tn si29
sfrq 79.454046
tof -3760.5
tpwr 54
sw 40322.6
at 0.019840
np 1600
dl 300.000000
nt 144
ct 144
ss 0
rd 5.0
ad 5.0
aX90 2000
pwX90 10.0
DECOUPLE
dn H1
dfrq 399.942645
dof -4369.0
dpwr 57
aH90 2000
pwH90 5.0
DECOUPLE2
dn2 N15
dfrq2 40.530048
dof2 0
dpwr2 0
aY90 0
pwY90 0
TPPM
aHtppm 1200
pWtppm 6.0
pHtppm 6.00
PROCESSING
fn 32768
phfid not used
rp -57.56
lp 0
lb 30.0
```

Spinnovation
NMR Service, Equipment and Supplies

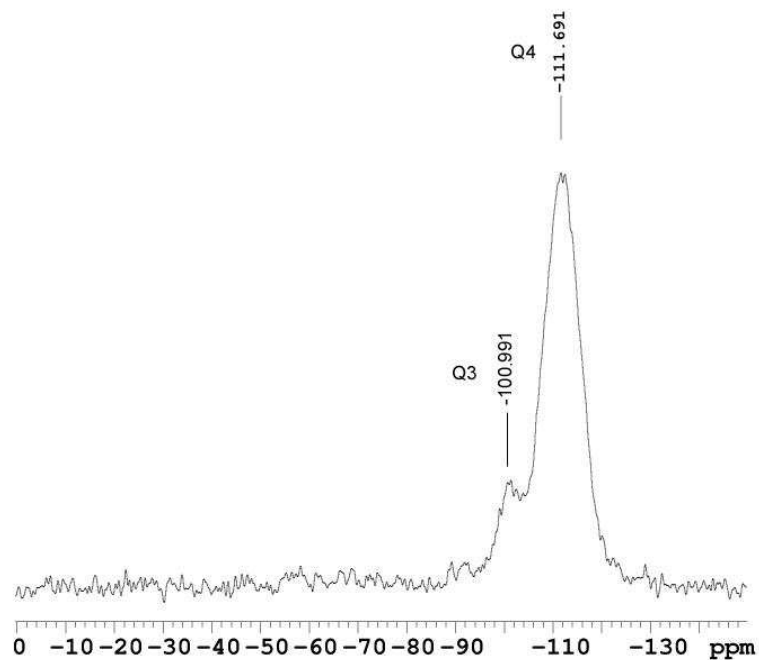
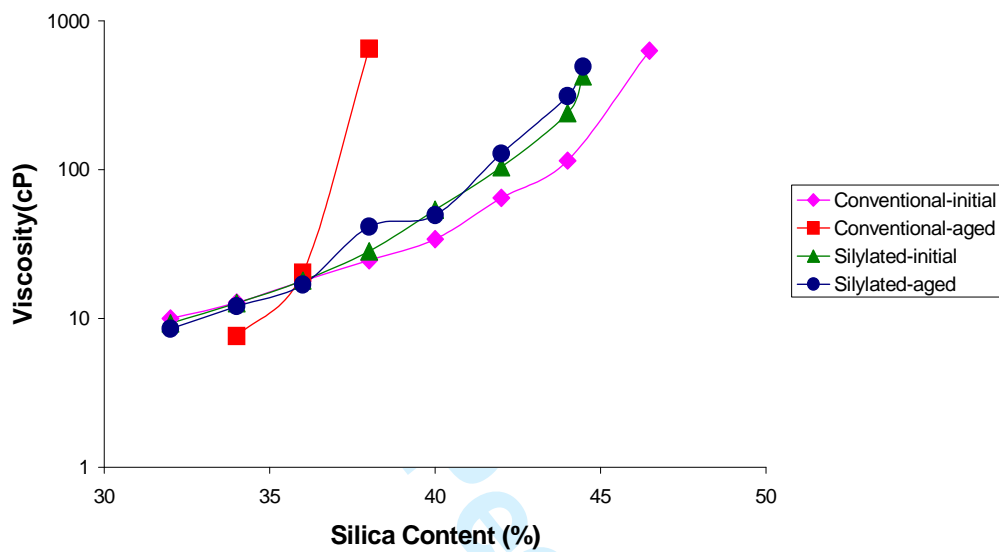


Figure 6: Viscosity initially and after 4 months versus silica content for conventional and modified 7 nm sols silylated with 1.4 GPTMS per nm² silica surface.



Paper II

Novel nano-composite particles: titania-coated silica cores

Peter Greenwood, Börje S. Gevert , Jan-Erik Otterstedt, Gunnar Niklasson and William Vargas, *Pigment & Resin Technology*, 2010, Vol. 39, No. 3, pp. 135-40.

Novel nano-composite particles: titania-coated silica cores

Peter Greenwood

Department of Chemical and Biochemical Engineering, Chalmers University of Technology, Gothenburg, Sweden,
Department of Materials Science, Uppsala University, Uppsala, Sweden and
Eka Chemicals, Bohus, Sweden

Börje S. Gevert and Jan-Erik Otterstedt

Department of Chemical and Biochemical Engineering, Chalmers University of Technology, Gothenburg, Sweden, and

Gunnar Niklasson and William Vargas

Department of Materials Science, Uppsala University, Uppsala, Sweden

Abstract

Purpose – The purpose of this paper is to develop methods to produce white composite pigments consisting of a silica core with a titania shell.

Design/methodology/approach – Silica cores were coated with titanium dioxide (TiO₂) via forced hydrolysis of a solution prepared from titanium tetrachloride (TiCl₄). The morphology, surface charge and particle size of obtained composite particles were studied.

Findings – Dispersions of well-dispersed composite particles, having silica cores of uniform size in the range from 300 to 500 nm with a homogeneous titania coating are obtained. The coating thickness corresponded to 150-400 per cent by weight of titania based on the core. Modification of the silica core by incorporation of 1.5 aluminosilicate sites per square nanometre of core surface proves to be favourable in achieving a homogeneous coating on the silica core. Deposition of such titania coating is also favoured by agitating the dispersion well, keeping electrolyte content low, maintaining pH at 2.0 and the temperature at 75°C during the coating process.

Research limitations/implications – Only TiCl₄ is used as titania source. In addition, only silica cores obtained by Stöber synthesis are used while commercially available silica solutions made from sodium silicate are not used.

Practical implications – The process offers a method of producing a white composite pigment with a narrow particle size distribution in order to maximise light scattering as well as using a core with lower density than the shell. This kind of particle would be of interest for coating applications and white inorganic inks.

Originality/value – The developed method provides a straightforward process to produce well-defined composite particles.

Keywords Minerals, Silicates, Light, Surface mount technology, Composite materials, Coatings

Paper type Research paper

Introduction

Titanium dioxide (TiO₂) is the principal white pigment because of its scattering power, which is superior to that of any other white pigment. It occurs in nature in the crystalline form rutile, anatase and brookite. Rutile and anatase are manufactured in large quantities and are primarily used as pigments but also as catalysts and in the production of ceramics.

Two processes, the sulphate process and the chloride process, are used to make TiO₂ (Braun *et al.*, 1992). The major objection against the sulphate process has been the amount of by-product gypsum it produces. The chloride process is considered as a more environmentally friendly method of producing TiO₂. In general, however, the environmental impact of TiO₂ production is mostly a factor of the raw materials used, the effluent treatment

processes and the degree of by-product development a particular plant has.

The scattering of light by TiO₂ particles varies with particle size and reaches a maximum when the particle size is about one-half of the scattered wavelengths of light that are in the 250-300 nm size range (Forrest, 2001). For maximum scattering efficiency, commercial TiO₂ pigment should therefore be milled to a particle size narrowly distributed around a value in the 250-300 nm size range, which is normally not done (Forrest, 2001). Furthermore, the pigment particles should be well dispersed and not aggregated in order to give optimal light scattering performance (Auger *et al.*, 2003). From environmental considerations, it is of interest to use raw material as little as possible, which are available in limited supply and negatively affect the environment when they are refined to TiO₂. Recently, there have been several papers discussing monodisperse nano-composites obtained by the deposition of titania onto silica cores (Li and Dong, 2003; Ryu *et al.*, 2003; Choi *et al.*, 2005). However, the titania source has been expensive titaniumalkoxides and the amount of titania coated onto the silica core has been relatively low.

Therefore, an objective of the present investigation was to develop methods for coating silica core particles with TiO₂ in an effort to obtain composite particles with well-defined and

The current issue and full text archive of this journal is available at www.emeraldinsight.com/0369-9420.htm



Pigment & Resin Technology
39/3 (2010) 135–140
© Emerald Group Publishing Limited [ISSN 0369-9420]
[DOI 10.1108/03699421011040758]

carefully controlled ratios between particle diameters and thickness of titania coating.

Experimental

Materials

Tetraethyl ortosilicate (TEOS), technical grade: minimum 98 wt%, from Hüls Sverige AB. Titanium tetrachloride (TiCl_4), technical grade: minimum 99.8 wt%, from Tioxide Ltd Sodium silicate ratio: 3.3, technical grade with a dry content of 36.0 wt%, from Akzo-Nobel. Sodium aluminate, NaAlO_2 , purum, containing 55 wt% Al_2O_3 from KEBO LAB AB. All other chemicals were of pro analar grade.

Preparation of titania-coated particles

Silica core particles

Uniform silica core particles of well-defined mean diameters in the range from 0.3 to 0.5 μm were prepared by hydrolysis of TEOS in an aqueous medium containing ammonia as a catalyst (Stöber *et al.*, 1968). The reaction temperature was varied to give different mean particle diameters. The obtained water-based silica solution had a concentration of SiO_2 of about 5 wt%.

Aluminosilicate sites

Sodium aluminate was used to introduce aluminosilicate sites onto the surface of the silica cores (Iler, 1976). A solution of sodium aluminate was prepared by dissolving 11.66 g sodium aluminate powder in 24.82 g water under heating and stirring. While stirring vigorously, various amounts of sodium aluminate solution were slowly added to the silica solutions (the cores), from the previous section, in order to provide 0.6 and 1.5 aluminosilicate sites per nm^2 of silica surface (Table I). The solutions were heated at 90°C for 2 h whereby aluminate ions were exchanged into the silica surface. The initial pH of the silica solutions was about 8.5 and the pH increased by 0.1 to 0.2 units during aluminate modification.

Charge reversal

Unmodified and aluminosilicate modified silica solutions were charge-reversed by adding the silica solutions (the cores) to a freshly made solution of TiCl_4 under stirring at room temperature. One litre of silica solution, from the previous section, was added to approximately 20 ml of a TiCl_4 solution. The amount of TiCl_4 used corresponded to a $\text{TiO}_2/\text{SiO}_2$ weight ratio of 0.03.

Table I Electrophoretic mobility at pH 2.0 ($\text{m}^2 \text{V}^{-1} \text{s}^{-1} \times 10^8$)

| Step | Silica sol (A) not modified | Silica sol (B) modified (0.6 Al nm^{-2}) | Silica sol (C) modified (1.5 Al nm^{-2}) |
|--|-----------------------------|--|--|
| 1 Before charge reversal | 0.7 | −1.2 | −3.1 |
| 2 After charge reversal | 2.1 | 2.6 | 4.3 |
| 3 After pH-adjustment and heating to 75°C | 2.5 | 2.8 | 4.6 |
| 4 TiO_2 concentration (ppm) in the super-natants of the sols from point 3 in this table | 880 | 638 | 230 |

Note: Sol A from step 1 will be noted by 1 A and so on in the text

The TiCl_4 solution was prepared by dissolving 150 g TiCl_4 in 114 ml concentrated hydrochloric acid (12 mol/dm^3). After diluting the solution with distilled water to 1,000 ml a clear solution of 0.79 mol/dm^3 in TiCl_4 and 1.37 mol/dm^3 in HCl was obtained. After charge reversal, the solid content of the charge-reversed silica solution was adjusted to 4 per cent SiO_2 by dilution with distilled water.

Titania coating of the silica core

The charge-reversed silica cores were pH-adjusted to pH 1.5 or 2.0 and the temperature was raised to 75°C, over a period of approximately 10 min. A freshly made solution of TiCl_4 was added at a rate of 0.2 mmol TiO_2/m^2 of core surface area and hour. The solution of TiCl_4 used in the experiments was the same as that used in the earlier section. The pH was maintained at pH 1.5 or 2.0 by continuously adding a solution of 3.75 mol/dm^3 NaOH. The ionic strength was kept low by continuous ultrafiltration of the solutions during the coating process through a fluoropolypropylene membrane, with a cut-off of 100,000 g/mol in minilab ten units from DOW Denmark A/S to give a more uniform coating (Iler, 1976). The operation was performed at a constant volume by adding water, the pH of which had been adjusted to either 1.5 or 2.0.

Dispersal of the titania-coated silica cores

The solutions of titania-coated silica cores were charge-reversed by adding the solutions to a solution of 3.3 molar ratio sodium silicate, containing 3.0 per cent SiO_2 by weight under stirring at room temperature. The amount of sodium silicate corresponds to a $\text{SiO}_2/\text{TiO}_2$ -coated core weight ratio of 0.03. The pH was always higher than 9.0 during the charge reversal and was afterwards adjusted to pH 9.5. Using ultrafiltration as described above, the solutions (coated cores) were concentrated and washed with water of pH 9.5 and containing 150 ppm SiO_2 . They were further concentrated to solids contents above 25 per cent by weight using vacuum evaporation.

Material characterisation

The size of the solution particles was determined by dynamic light scattering (Brookhaven BI-90 particle sizer). Scanning electron microscopy (JEOL JSM-5200) was used to determine the particle size distribution and to study the surface of the particles. The electrophoretic mobility of the particles was measured at pH 2.0 in 10 mM HCl and at all other pH values in 10 mM NaCl, using a Zetasizer IIc Particler Electrophoresis Analyser (Malvern Instruments Inc., Southborough, Massachusetts, USA). The concentrations of titania and silica in the permeates and supernatant liquids were determined spectroscopically by measuring the absorbance at 410 nm of complexes between titania and hydrogen peroxide (Charlot, 1964) and between silica and ammonium heptamolybdate (Iler, 1979), respectively, using a Shimadzu UV-160 A, spectrophotometer. A Siemens D5000 powder X-ray diffractometer was used for the X-ray diffraction measurements.

Results and discussion

Coating of the silica core with titania

The effect of the incorporation of aluminosilicate sites onto the silica surface

Because the isoelectric point of silica is between pH 1.7 and 2.0, silica solutions have a low surface charge at pH below 7 (Iler, 1979). If, however, negatively charged aluminosilicate sites are generated on the surface by heating the solutions with

sodium aluminate, the surface will remain negative at pH down to about 2 (Iler, 1979). It is reasonable to assume that positively charged subcolloids or polycations of titania, existing only in quite acidic solutions, would adsorb more readily onto a negatively charged aluminate-modified silica surface than on an almost neutral, unmodified silica surface. To test this hypothesis silica particles with a diameter of 300 nm were heated with a sodium aluminate solution under conditions such that the silica surface contained 0, 0.6 or 1.5 aluminosilicate ions per nm^2 (solution 1 A, 1 B and 1 C) in Table I. Table I shows that the particles containing 1.5 aluminosilicate sites/ nm^2 had the highest charge at pH 2.0 as determined from electrophoretic mobility measurements. Care had to be taken to measure the charge very soon after the pH of the solution had been adjusted to 2.0 because at this pH aluminium will begin to dissolution out from the particle surface. (It takes only about 3-4 min for the aluminate-modified particles to lose their charge at pH 2.) The table also shows that after charge reversal, accomplished by adding the silica solutions to a solution of TiCl_4 of a pH below 1.5, the silica solution (2 C) containing the high amount of aluminium per nm^2 again had the highest charge but now positive, indicating that this surface adsorbed more positively charged titania species than the other silica solutions, i.e. 2 A and 2 B, with 0 or 0.6 Al/nm^2 . Adjusting the pH of the dispersion of charge-reversed solution to 1.5 (from about 1.4) and heating at 75°C for about 10 min increased the charge on all three types of solution particle, but somewhat more for the particles containing most aluminium (3 C). The titanium concentration in the aqueous phase of this silica solution was lower than in the other silica solutions indicating that particle surfaces having a high surface concentration of negative sites adsorb titania species more effectively compared with 4 A-C.

Figures 1-3 show that after coating the charge-reversed solution with titania, adding titanium chloride at a rate of $0.2 \text{ mmol TiO}_2 \text{ h}^{-1} \text{ m}^{-2}$ and in an amount corresponding to 233 per cent titania, based on the weight of silica while

Figure 1 SEM micrograph, silica core with a particle diameter of 300 nm, not aluminate-modified core surface, coated at pH 1.5 with 233 per cent titania based on the weight of silica

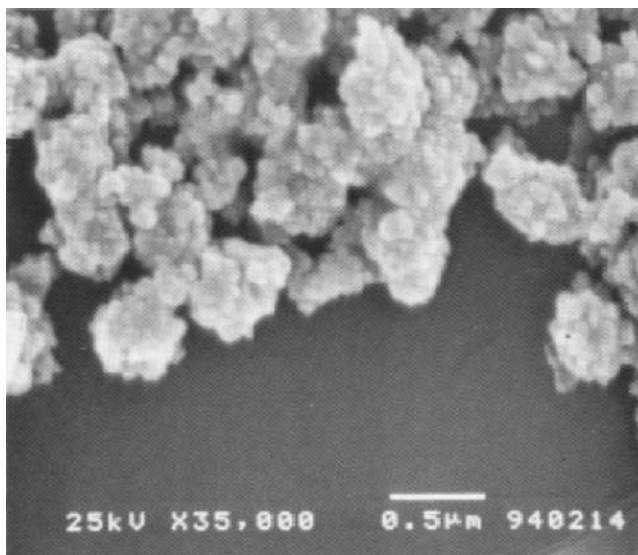


Figure 2 SEM micrograph, silica core with a particle diameter of 300 nm, aluminate-modified core surface $0.6 \text{ Al}/\text{nm}^2$, coated at pH 1.5 with 233 per cent titania based on the weight of silica

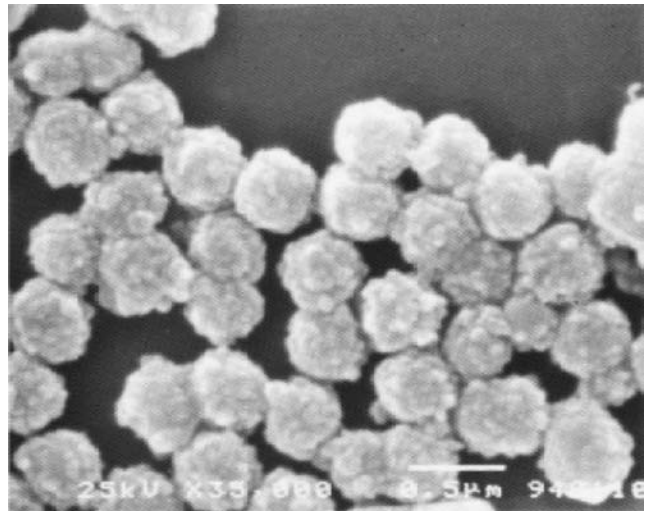
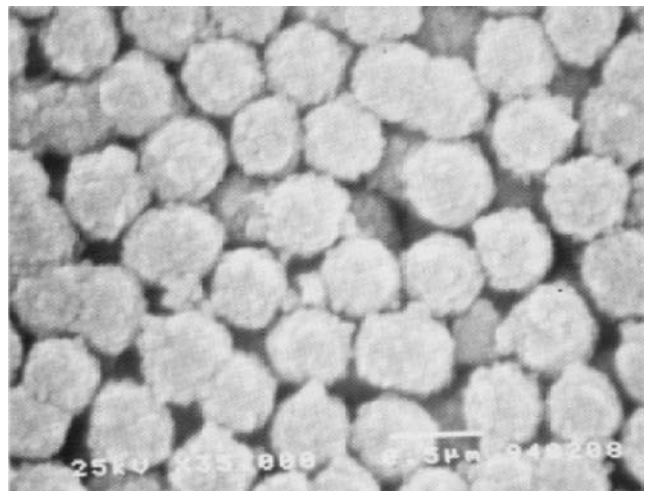


Figure 3 SEM micrograph, silica core with a particle diameter of 300 nm, aluminate-modified core surface $1.5 \text{ Al}/\text{nm}^2$, coated at pH 1.5 with 233 per cent titania based on the weight of silica

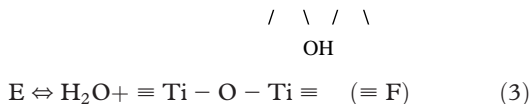
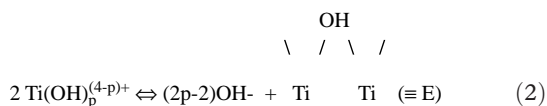


maintaining the pH at 1.5, the best result was obtained with the solution containing silica core particles with $1.5 \text{ Al}/\text{nm}^2$ surface. The particles are discrete and appear to be uniformly coated with a layer of titania (Figure 3). The particles with $0.6 \text{ Al}/\text{nm}^2$ surface seem to be somewhat less uniformly coated and also somewhat aggregated (Figure 2). If no alumina is present on the particle surface, not all the added titania is deposited on the core particles but form secondary titania particles in the dispersion, which aggregate with themselves and with partially coated core particles (Figure 1).

The effect of the pH in the coating stage

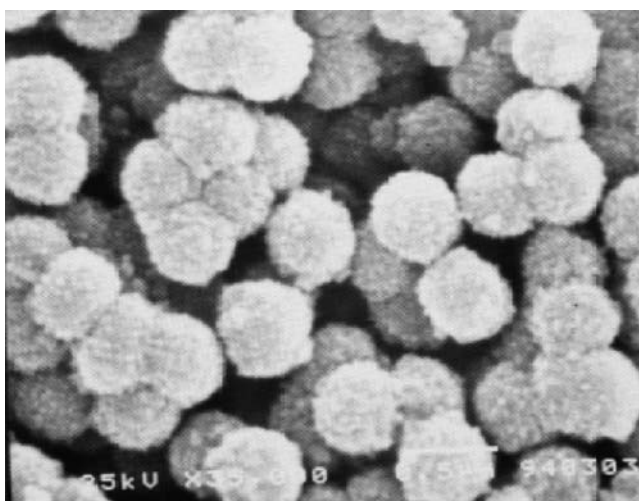
Coating of silica cores with titania has been suggested to take place by heterogeneous nucleation on the core surface (Hsu *et al.*, 1993). The following mechanism for the reaction has

been proposed and assumed that step 2 was the rate determining step and that the rate of reaction increases rapidly with increasing pH (Matijeć *et al.*, 1977):



pH has been recognised (and also agitation, see next section) as an important parameter in the process of coating silica cores with titania (Kohlschütter *et al.*, 1970). Following their lead, the effect of pH on the quality of titania coating on silica cores was investigated. Because the iep of titania is about 5.5-6.0 it follows that the positive charge on titania particles decreases with increasing pH (Barringer and Bowen, 1985). Aggregation that is due to diminishing electrostatic repulsion between the particles could therefore occur if coating takes place at pH values approaching the iep from the acid side. On the other hand, it has been reported that uniform coating of silica cores with titania is favoured by low ionic strength (Hsu *et al.*, 1993), which speaks against low pH where the ionic strength is high. Moreover, the solubility of titania increases with decreasing pH (Look and Zukoski, 1992), an event that could lead to substantial losses of titania through the ultrafiltration membrane used in the coating procedure. Obviously, one must find a pH at which the uniformity of the coating is maximised whereas losses of titania and aggregation are minimised. Thus, coating 300 nm aluminium silicate modified silica solutions, 3 C, using an addition rate of titanium chloride of 0.2 mmol h⁻¹ m⁻² and in an amount corresponding to 233 per cent titania based on the weight of silica, yielded a more dispersed system at pH 2.0 (Figure 4) than that at pH 1.5 (Figure 3). The concentrations of

Figure 4 SEM micrograph, silica core with a particle diameter of 300 nm, aluminate-modified core surface 1.5 Al/nm², coated at pH 2.0 with 233 per cent titania based on the weight of silica



titania in the aqueous phase at pH 1.5 and 2.0 were 178 and 130 ppm, respectively, suggesting that the losses of titania at pH 1.5 were about 50 per cent higher than at pH 2.0, although at both pH values the losses were negligible (less than 0.4 per cent of the titania was lost through the microfiltration membrane at pH 1.5). A higher chloride concentration (e.g. solutions acidified with HCl) has been reported to yield a grainier surface of TiO₂ particles. The particles in Figure 3 are grainier than the particles in Figure 4 (pH 2.0), a finding in accord with those of Look and Zukoski (1992).

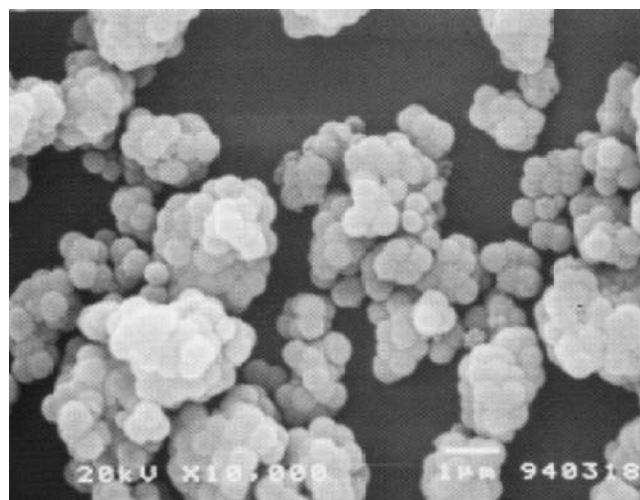
The effect of agitation

Agitation is a common, and often necessary, means of maintaining a colloidal system in a highly dispersed state during its formation or while it is being modified, such as in the case of coating a colloidal dispersion of silica cores with titania. To investigate the importance of agitation on the degree of dispersion 300 nm aluminosilicate modified silica cores, 3 C, were coated at pH 2.0 at 75°C with 400 per cent TiO₂ at a coating rate of 0.2 mmol TiO₂ m⁻² h⁻¹ with no other agitation than that provided by the circulation pump of the ultrafiltration unit and with moderate additional agitation provided by a mechanical stirrer. Figure 5 shows that the titania-coated silica cores made with no extra agitation were quite aggregated whereas even moderate stirring considerably improved the state of dispersion (Figure 6).

The coating thickness

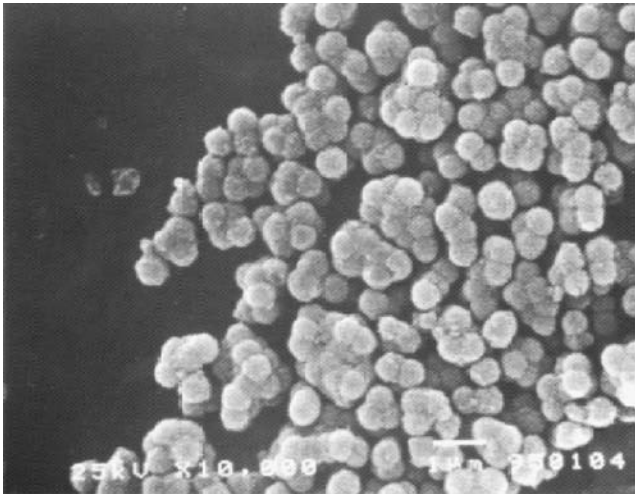
In the previous section, the effect of the pH in the coating stage, the effect of the ionic strength of the titania coating was discussed. A high ionic strength, such as, at low pH or high salt concentrations, is detrimental to the uniformity of the coating and to the high degree of dispersion of the colloidal particles (Figure 7, Hsu *et al.*, 1993). By using ultrafiltration to wash out salts, it is possible to achieve uniformly coated silica cores (Figure 8) with up to 400 per cent titania based on the weight of silica and at solids contents of at least 8 per cent by weight (Figures 6 and 9).

Figure 5 SEM micrograph, silica core with a particle diameter of 300 nm, aluminate-modified core surface 1.5 Al/nm², coated at pH 2.0 with 400 per cent titania based on the weight of silica



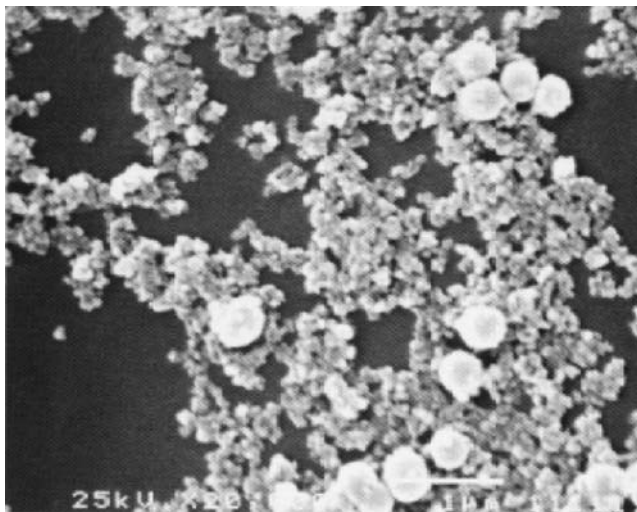
Note: No agitation during the coating process

Figure 6 SEM micrograph, silica core with a particle diameter of 300 nm, aluminate-modified core surface 1.5 Al/nm^2 , coated at pH 2.0 with 400 per cent titania based on the weight of silica



Note: Moderate agitation during the coating process

Figure 7 SEM micrograph, titania coating at pH 1.0, 233 wt% TiO_2 based on SiO_2 , core diameter: 300 nm



The dispersion of the titania particles

To obtain an optimal scattering efficiency it is vital that the titania coated silica particles are well dispersed. Measurements of the hydrodynamic diameter of the titania-coated cores dispersed in sodium silicate solution, being negatively charged, and comparing it with the theoretical diameter (Table II) indicated that the titania-coated silica particles were well dispersed when considering that dynamic light scattering depends strongly on particle size. If only a smaller amount of the particles were twins, they would give a substantial contribution to light scattering and therefore give a larger mean particle diameter.

Light scattering in pigmented coatings

The measurements and the four-flux model used to calculate reflectances of commercial TiO_2 pigments and TiO_2 coated

Figure 8 SEM micrograph, titania coating at pH 2.0, 233 wt% TiO_2 based on SiO_2 , core diameter: 300 nm

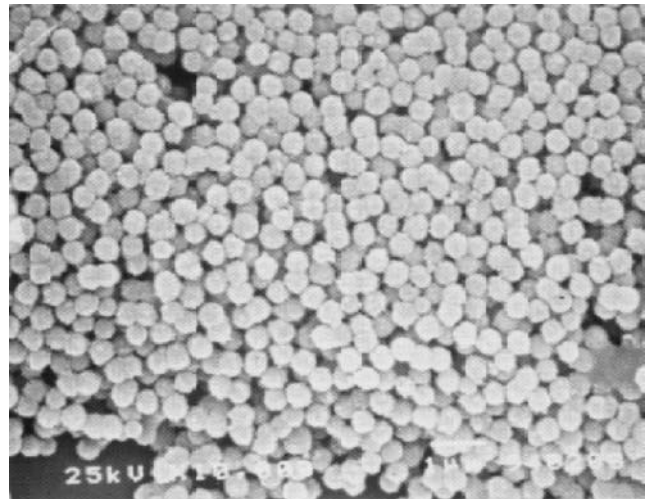
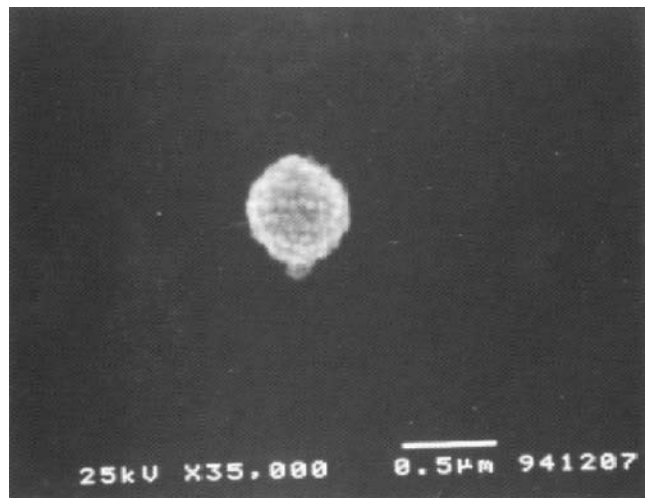


Figure 9 SEM micrograph, titania coating at pH 2.0, 400 wt% TiO_2 based on SiO_2 , core diameter: 300 nm



SiO_2 particles hosted in a copolymer of ethylene and vinyl acetate have been described elsewhere (Vargas *et al.*, 2000).

Conclusions

- It is possible to produce a well-dispersed composite titania-silica particle of desired size and titania/silica ratio by coating a silica core via forced hydrolysis of the TiCl_4 solution.
- To obtain a homogeneous titania coating it is important that the silica surface is aluminate-modified, in an amount corresponding to about 1.5 aluminosilicate sites per nm^2 silica surface.
- The aluminate-modified silica solution should be charge-reversed before the coating process starts.
- It is also important to perform the coating under such conditions that the electrolyte content is kept low (e.g. by continuous wash-out by ultra-filtration) and to keep the pH

Table II Measured diameter, theoretical diameter and the surface charge expressed as the electrophoretic mobility at pH 9.5

| Core diameter (nm), amount titania wt% based on the core (%) | Electrophoretic mobility ($10^8 \text{ m}^2 \text{ V}^{-1} \text{ s}^{-1}$) | Measured particle diameter (nm) | Theoretical particle diameter (nm) |
|--|---|---------------------------------|------------------------------------|
| 300, 150 | -4.29 | 540 | 360 |
| 300, 325 | -4.21 | 556 | 410 |
| 300, 400 | -4.05 | 608 | 430 |
| 407, 81.8 | -3.98 | 659 | 450 |
| 407, 170 | -3.98 | 655 | 490 |
| 407, 233 | -4.05 | 630 | 520 |
| 500, 81.8 | -3.27 | 695 | 560 |
| 500, 138 | -3.12 | 660 | 590 |

Notes: $dp_{\text{theoretical}} = dp_{\text{core}}(1 + \text{amount titania on the core} \times \rho_{\text{SiO}_2} / \rho_{\text{TiO}_2})^{1/3}$; ρ_{TiO_2} (anatase) = 3.9 g/cm^3 (Forrest, 2001); ρ_{SiO_2} (Stöber sols) = 1.8 g/cm^3 (Coen and Kruijff, 1988)

in the region of 2.0 to obtain a uniform titania coating of the silica core.

- Good agitation is needed to prevent agglomeration of particles during the coating process.

References

- Auger, J., Barrera, R.G. and Stout, B. (2003), "Scattering efficiency of clusters composed by aggregated spheres", *Journal of Quantitative Spectroscopy & Radiative Transfer*, Vols 79-80, pp. 521-31.
- Barringer, E.A. and Bowen, H. (1985), "High-purity, monodisperse TiO_2 powders by hydrolysis of titanium tetraethoxide. 2. Aqueous interfacial, electrochemistry and dispersion stability", *Langmuir*, Vols 1 No. 4, pp. 420-8.
- Braun, H., Baidins, A. and Marganski, R.E. (1992), "TiO₂ pigments technology: a review", *Progress in Organic Coatings*, Vol. 20, pp. 105-38.
- Charlot, C. (1964), *Colorimetric Determination of Elements*, Elsevier, Amsterdam, pp. 408-10.
- Choi, H.-H., Park, J. and Singh, R.K. (2005), "Nanosized titania encapsulated silica particles using an aqueous TiCl_4 solution", *Applied Surface Science*, Vol. 240, pp. 7-12.

- Coen, S. and Kruijff, C.G. (1988), "Synthesis and growth of colloidal silica particles", *Journal of Colloid Interface Science*, Vol. 124 No. 1, pp. 104-10.
- Forrest, S. (2001), "The development of titanium pigments", *Surface Coatings Australia*, Vol. 38 No. 10, pp. 16-22.
- Hsu, P.W., Yu, R. and Matijević, E. (1993), "Paper whiteners", *Journal of Colloid Interface Science*, Vol. 156, pp. 56-65.
- Iler, R.K. (1976), "The effect of surface aluminosilicate ions on the properties of colloidal silica", *Journal of Colloid Interface Science*, Vol. 55, pp. 25-34.
- Iler, R.K. (1979), *The Chemistry of Silica*, Wiley, New York, NY.
- Kohlshütter, H., Getrost, H., Hörl, W., Reich, W. and Rößler, H. (1970), "Verfahren zur herstellung titandioxid - bzw. titandioxidaquatüberzeugen", German Patent No. 2 009 566.
- Li, Q. and Dong, P. (2003), "Preparation of nearly monodisperse multiply coated submicrospheres with a high refractive index", *Journal of Colloid Interface Science*, Vol. 261, pp. 325-9.
- Look, J.L. and Zukoski, C.F. (1992), "Alkoxide-derived titania particles: use of electrolytes to control size and agglomeration levels", *Journal of American Ceramic Society*, Vol. 75 No. 6, pp. 1587-95.
- Matijević, E., Budnik, M. and Meites, L. (1977), "Preparation and mechanism of formation of titanium dioxide hydrosols of narrow size distribution", *Journal of Colloid Interface Science*, Vol. 61 No. 2, pp. 302-11.
- Ryu, R.D., Kim, S.C. and Koo, S.M. (2003), "Deposition of titania nanoparticles on spherical silica", *Journal of Sol-Gel Science and Technology*, Vol. 26, pp. 489-93.
- Stöber, W., Fink, A. and Bohn, E. (1968), "Controlled growth of monodisperse silica spheres in the micron size range", *Journal of Colloid Interface Science*, Vol. 26, pp. 62-9.
- Vargas, W., Greenwood, P., Otterstedt, J.E. and Niklasson, G. (2000), "Light scattering in pigmented coatings: experiments and theory", *Solar Energy*, Vol. 68, pp. 553-61.

Further reading

- Baes, C.F. and Mesmer, R.E. (1976), *The Hydrolysis of Cations*, Wiley, New York, NY, pp. 147-52.

Corresponding author

Peter Greenwood can be contacted at: peter.greenwood@akzonobel.com

Paper III

Modified silica sols: Titania dispersants and co-binders for silicate paints

Peter Greenwood, Pigment & Resin Technology, 2010, Vol. 39, No. 6 (accepted for publication)

Modified silica sols: Titania dispersants and co-binders for silicate paints

*Peter Greenwood*¹

Eka Chemicals AB (a business unit within AkzoNobel), S-44580 Bohus, Sweden

Abstract

Purpose - The purpose was to investigate epoxysilane modified silica sols as surfactant-free inorganic pigments dispersants and as co-binders/reinforcing agents for silicate paints.

Design/methodology/approach - The performance of epoxysilane-modified silica sols as dispersants for titania was studied using a polyacrylate-based dispersant as reference. Furthermore, the effect of the addition of silica sols, with or without silane modification, to potassium silicate on binder properties was investigated.

Findings - Significant improvements were obtained in stability towards settling in water-based titania pigments pastes and in light scattering efficiency (as much as 50%) for the optimal size of the silica particle of 5 nm. The number of silane molecules per nm² silica particle surface must exceed a critical value of at least 1 molecule of epoxysilane per nm² particle surface. Additionally, improved stability towards gelling, water resistance and film-forming properties of sol-silicate binder mixes were achieved for epoxysilane modified silica sols.

Research limitations/implications - Only epoxy silane modified silica sols were studied in this report. Titania pigment was examined but other important pigments (e.g., iron oxides) remain to be studied. In addition, only sol-silicate mixes were investigated and not fully formulated silicate paints.

Originality/value - The present method provides an easy route to obtain stable surfactant-free inorganic pigments pastes, as well as makes stable high ratio sol-silicate mixes/paints.

Practical implications - A method that produces stable, high-performing, surfactant-free inorganic pigments pastes. Furthermore, stable high ratio sol-silicate binders can be obtained with improved water resistance and film properties for use in silicate paints.

¹ E-mail: peter.greenwood@akzonobel.com

© Emerald Group Publishing Limited

Keywords - Titania, Pigment, Dispersion, Silica, Colloids, Paint

Paper type - Research paper

Introduction

R.K. Iler lists numerous well-established uses of silica sol in his definitive book on *The Chemistry of Silica* (Iler, 1979), some of which are: catalyst bases and adsorbents, stiffening and binding agents in precision casting moulds, anti-sticking, anti-blocking and antistatic effects on polymer films, antisoiling agents which provide an ultra smooth, oleophobic surface on porous materials, such as in painted surfaces, by filling micropores to exclude dirt particles, reinforcing agents in latex-based coatings, and many others. Otterstedt and Greenwood describe in detail some specific, more recent applications of colloidal silica, including the production of cement, lead-acid batteries, paper, and industrial coatings and polishing (Otterstedt and Greenwood, 2005). In most of these applications conventional silica sols work very well but in some (e.g., as additives to polymer latices and inorganic binders) there are sometimes problems with long-term stability towards gelling. In such cases, the particles of colloidal silica are combined with complicated surfactant systems (such as in polymer latices), exposed to high concentrations of electrolyte (such as alkali silicates in inorganic binders) or find themselves exposed to very high solids contents when they are used as dispersants in pigments pastes.

Non-surface modified silica sols have been used as dispersants of pigments for many years in applications where the use of surfactants is undesirable. Such applications are typically coating applications in which a foaming problem may occur as well as a decrease in the chemical resistance of a coating that is caused by high loads of surfactants. Until now, the drawback of using conventional silica sols as pigments dispersants has been aggregation/gellation of the systems and hence a drop in performance. This decrease in performance occurs because the stability of the colloidal systems has not been sufficient.

Silane modification may improve the stability of colloidal silica in many applications. In a recent study I reported the effect on the properties of the particles of colloidal silica by reacting their silanol groups with various commercially available organo-reactive silanes. In another study I reported the effect of silane modification of the surface silica particles on the stability of colloidal systems when such particles are used as reinforcing fillers in latex

polymer binders, especially as water-based, two-pack coating formulations (Greenwood, (2008).

In this investigation we will study the effect of silane modification of silica sols on the stability of colloidal systems when such sols are used as reinforcing fillers in alkali-silicate-based inorganic binders and as dispersants for inorganic pigments.

Experimental

Materials used in the experiments

Colloidal silica dispersions - silica sols

The following commercial silica sols (pH ranged from 9 to 11), supplied by Eka Chemicals AB (Akzo Nobel), were used:

Bindzil® 15/750 with a specific surface area of 750 m²/g; particle size 4 nm and a silica content of 15 % by weight.

Bindzil® 15/500 with a specific surface area of 500 m²/g; particle size 5 nm and a silica content of 15 % by weight.

Bindzil® 257/360 with a specific surface area of 360 m²/g; particle size 7 nm and a silica content of 25 % by weight; the surface is modified with sodium aluminate.

Bindzil® 30/360 with a specific surface area of 360 m²/g; particle size 7 nm and a silica content of 30 % by weight.

Bindzil® 40/220 with a specific surface area of 220 m²/g; particle size 12 nm and a silica content of 40 % by weight.

Potassium silicate

The potassium silicate used had a silica content of 23.8 % by weight and a K₂O content of 11.1 % by weight corresponding to a molar ratio of SiO₂/K₂O of 3.36 (supplied by Askania AB).

Silane

Silquest® A-187: gamma-glycidoxypropyl trimethoxy silane (GPTMS), MW: 236 g/mole was used, which was kindly supplied free of charge by former General Electric Silicones (now Momentive).

Resin

Setalux® 6774, kindly supplied free of charge by Nuplex Resins.

Pigment

The titania pigment, supplied by Univar, was highly milled and surface treated with Al₂O₃ and ZrO₂ titania pigment, Tiona 595.

Pigment Dispersant

Dispex N40, Sodium polyacrylate (NaPA, Ciba Specialty Chemicals, Switzerland) of average molecular weight of 3500 g/mole was used as reference.

Preparation of materials

Preparation of pre-hydrolysed silane

In a typical preparation 1000 g of silane were added to 1000 g of de-ionised water in a 3 L beaker with moderate agitation, corresponding to a water/silane molar ratio of 13:1.

Silanes are generally poorly soluble in water and hydrolysis is therefore facilitated by using a heel of hydrolysed silane, which contains up to about 20 % by weight of a lower aliphatic alcohol. Therefore, 50 to 70 g of hydrolysed silane were placed in a 3 L beaker. 1000 g silane was first added for about 20 seconds to the heel and then 1000 g of de-ionised water were added for about 20 seconds with moderate agitation. After about 1 hour, a clear solution was obtained, indicating complete hydrolysis.

Preparation of silane modified sols

As described previously, the calculated amount of the hydrolysed silane solution in water was added to 5000 g of undiluted silica sol (e.g., Bindzil® 30/360) with good agitation and a controlled rate of addition. The addition rate and reaction temperature were 600 g/h and 60 °C, respectively.

Characterisation of the sols

The silica sols were characterised by measuring pH, specific surface area by titration (Sears, 1956), viscosity at Brookfield Viscometer, and silica content by XRF. (Table I)

(Take in Table I)

Mixtures of silica sols and soluble silicate

Preparation of mixtures of silica sols and potassium silicate

Silica sols were diluted with water before blending them with the potassium silicate solution under stirring in order to adjust overall silica content to 20 % by weight (see formulations in Table II).

(Take in Table II)

Stability of silica sol- silicate solution mixtures

The stability was measured as viscosity using a Brookfield Viscometer at 20 °C. A sample was considered to have gelled if the viscosity was higher than 2000 mPas.

The water resistance of sol-silicate films

The water resistance was evaluated after 24 hours on 24 hour old films that had been dried at room temperature. Films with a wet film thickness of 200 microns were cast on glass plates with a film applicator for evaluation of film properties and water resistance. The water resistance was measured by visual inspection after 24 hours.

The scale was 0: Film “dissolved”; 1: Severe impact on the film; 2: Some impact on the film; 3: No impact on the film.

Pigments dispersants

Colloidal silica dispersions – silica sols

The silica sols used are as described in table I but their silica content was adjusted to 13.4 % by weight (unless otherwise stated) before they were used as pigment dispersants.

Preparation of pigments pastes.

300 g of titanium dioxide were added under moderate agitation for about 20 sec to 100 g of diluted silica sol to yield a 75 % pigment paste unless otherwise stated (Table III). The pigment was dispersed for 10 min at 1400 rpm with a 40 mm diameter dissolver turbine to render a well-dispersed pigment paste.

(Take in Table III)

Coating composition series

The pastes were incorporated into a resin emulsion to form coating compositions for optical evaluations. The coating compositions contained 5, 10, 20, 30, 40, and 50 % titania pigment on weight base in the dried coating (Table IV). Each coating series had a serial number corresponding to the number of the pigment paste, as given in Table III. Films were cast by using a film applicator with a 100 microns opening. A non-pigmented coating was cast as a

control. Each coating composition contained 50 g of resin emulsion (equal to 22 g of dry resin).

(Take in Table IV)

Evaluation of pigmented films.

Optical measurements were carried out for wavelengths in the visible range (from 300 nm - 700 nm). The reflectance spectrum of the pigmented coatings was measured by a Beckman Acta 5240 spectrophotometer equipped with an integrating sphere and using barium sulphate as the reflectance reference.

Coating compositions made from resin and pigment pastes number 1, 2, 3, 4, 10, 11, and 13 were evaluated. Pigment pastes number 5, 6, 7, 8, 9 and 12 were not stable. Pigments pastes number 14 and 15 were not prepared in conjunction with the other samples and were therefore not evaluated regarding their light-scattering properties.

Results and discussion

Potassium silicate – silica sol inorganic paint binders

Silicate paint is a traditional inorganic concrete paint using potassium silicate as a binder for inorganic fillers, e.g. clays, and pigments such as titania and iron oxides. However, the solubility of the silicate binder of the paint in water is at first relatively high because of the high alkali content of the paint, but this problem is reduced over time by the reaction of the paint with calcium-rich surfaces (e.g., concrete surfaces) and the creation of insoluble calcium silicate species.

One way of reducing the solubility of the dried silicate paint binder in water and hence improve the weather resistance of the paint, is to add a conventional silica sol to the potassium silicate binder, which increases the molar ratio of silica to the alkali of the binder.

Conventional silica sols are currently being used in combination with potassium silicates as binders in wholly inorganic silicate paints (Heiberger and Schläffer, 2001).

Stability of silica sols in silicate solutions: Viscosity for silicate-silica sol mixtures

Adding conventional silica sols to the potassium silicate binders, however, reduces the stability towards gelling and the film-forming properties of the binder.

These drawbacks can be minimised by using silane-modified colloidal silica. Table V shows that stability towards gelling is significantly improved by silane modification.

(Take in Table V)

Film properties

The film forming properties of silicate binders deteriorate with increasing ratio. When a silica sol has been used to increase the ratio of the binder, silane-modified sol, in comparison with a conventional sol, yields somewhat improved film-forming properties. Poorer film-forming properties at higher ratios may be rectified to some extent by the addition of a wetting agent (Table VI). (This problem can be reduced further in fully formulated silicate paint with a high load of inorganic pigments and fillers.)

(Take in Table VI)

Water resistance of films

The water resistance is normally improved when the molar ratio $\text{SiO}_2/\text{K}_2\text{O}$ is increased (i.e. lower alkali content). As shown in Table VII, at a given molar ratio, silane-modified colloidal silica improves the water resistance relative to non-modified colloidal silica.

(Take in Table VII)

Dispersant of titania pigments

The surfactant effects of silica sols are well known and thus may be used as a dispersing agent in the manufacture of certain organic copolymers (Iler, 1979)

More recently, colloidal silica has been shown to be an excellent dispersant for TiO_2 pigments (Bolt, 1999). Silica sol is added to the pigment slurry to coat the surfaces of the TiO_2 particles with discrete particles of silica. In applications of this kind the silica particles are introduced into a system of high solids content and the stability toward gelling of the silica particles may be low. The problem of stability may be aggravated by the presence of electrolytes in the system. In contrast to conventional colloidal silica, silanes modified silica sols give good pigment spacing and have high dispersing power even in systems of high solid content, as indicated by Figure 1.

(Take in Figure 1)

Stability of pigments pastes

Using silane-modified colloidal silica as dispersant, pigments pastes containing 75 % by weight TiO_2 could be prepared with improved stability and fluidity as compared to using conventional silica sols as dispersing aids.

In general, with all other things being equal, the stability of colloidal silica decreases with increasing specific surface area, i.e. decreasing particle size, which is also the case when silica sols are used as dispersing agents in pigment pastes. It is, however, desirable to use small particles rather than larger ones as dispersants for pigments because they cover the surface of the big pigment particles more efficiently (Matijevic and Hansen, 1980).

The stabilising effect of silane-modified silica sols as dispersants in TiO₂ pastes is twofold. On the one hand, compared with conventional silica, silane-modified silica significantly improves the stability towards gelling of the sol, even in environments of high solids content. On the other, good dispersion of the pigment requires enough silica particles present to cover the surface of the TiO₂ particles with a surface coverage exceeding a certain critical value. Tables VIII and IX show that stable pigments pastes require that the silane modifications of the silica dispersants corresponds to at least 1 molecule of GPTMS/nm² particle surface. Specifically, the stable pastes number 1, 2, 4, 13, and 15 show that the degree of surface modification of the silica sols is at least 1 molecule of GPTMS/nm² and that the surface coverage of titania particles with silica particles exceeds 100 %.

Although the stability of the pastes treated with silane-modified silicas improved significantly, all the pastes studied in Table IX were found to settle with time. After 7.5 months, they had all formed sludge at the bottom.

The sludges containing silane-modified silicas in required amounts could, however, readily be re-dispersed. The other pastes, including paste number 10 containing Dispex N40 with a surface coverage of 165 %, were much more difficult to re-disperse.

(Take in Tables VIII and IX)

Light-scattering efficiency of the pigmented resin films

Pigment particles must be well dispersed and not aggregated to give optimal light-scattering performance (Auger *et al.*, 2003). For maximum scattering efficiency, commercial TiO₂ pigments should therefore be milled to a particle size narrowly distributed around a value in the range 250 to 300 nm (Forrest, 2001). Silane-modified colloidal silica as a dispersing agent can enhance pigment efficiency compared to the conventional polyacrylate-based dispersing agent Dispex N40. Figure 2 shows that sample paste number 1 (blue), dispersed with 5 nm silica particles and modified with 2 molecules of GPTMS/nm² particle surface, scattered light much more efficiently than the reference paste number 10 (red), containing 0.53 % Dispex N40 based on titania – the dosage recommended by the supplier. The relative

enhancing effect on the reflectance is about 50-60% and constant over the range of solids contents. Thus, a 10 % silica dispersed paste scatters light as effectively as a 15 % Dispex N40 dispersed paste and a 35 % silica dispersed paste reflects light as effectively as a 50 % Dispex N40 dispersed paste.

(Take in Figure 2)

For a given degree of silane modification, the improvement in pigment efficiency increases with decreasing particle size down to about 5 nm, corresponding to a specific surface area of 500 m²/g. Figure 3 shows that 4 nm particles, with a specific surface area of 750 m²/g, scattered light somewhat less efficiently over most of the range of solids contents but at 40% solids and above the reflectance dropped sharply, probably because of aggregation that is caused by the very small particle size.

For a given particle size, and independent of particle size, the stability of the pastes to aggregation, and as a consequence also the reflectance, increases with increasing degree of silane modification, reaching a plateau at between 1 and 2 GPTMS/nm².

(Take in Figure 3)

Degree of dispersing energy and level of dispersant

Water is by far the most common dispersing medium in titania pigments pastes. Titania powder is added to water containing a dispersing agent and the slurry that results is agitated by powerful dispersers. Using a conventional dispersing agent, such as Dispex N40, it requires considerable input of energy to bring about complete dispersion of the titania, i.e. a paste in which each titania particle of about 300 nm is surrounded by dispersant molecules and completely separated from the other titania particles in the paste. A minimum amount of energy is required to obtain a completely dispersed paste.

With silane-modified colloidal silica as a dispersing agent, however, much less energy is needed to obtain a completely dispersed paste. It is well known that silanes (e.g., gamma-glycidoxypropyltrimethoxysilane) readily react with the OH groups on the surface of titania particles. Therefore, we speculate that the reason for silane-modified colloidal silica being more effective dispersants for titania pigments is that the silica particles adhere more strongly to the titania surfaces than conventional dispersants, which are hydrogen-bonded to the pigments surfaces. In addition to forming hydrogen bonds with the titania surfaces, the silica particles may form chemical bonds with the surfaces when silane molecules, chemically attached to the silica surfaces, react with hydroxyl groups on the titania surfaces.

In a well dispersed titania pigment paste with high titania content the optimal average size of a spacer/extender component of the particles is about 5-30 nm depending on the titania content (Braun, 1988). The particles constantly bump into each other but are prevented from associating or aggregating by the steric stabilisation provided by the dispersant.

Silane-modified silica sols provide much more effective steric stabilisation than conventional dispersing agents (such as Dispex N40) because the silica particles are much larger than the dispersant molecules, i.e. they are much larger “spacers”.

For a given particle size, say 5 nm, silane-modified sols can be prepared with 20-25 % higher solid contents compared with unmodified particles, indicating that silane modification weakens interactions between the silica particles (Greenwood and Gevert, 2009). It is therefore to be expected, and we have shown it to be the case in this investigation, that for a given solids content, pastes dispersed with silane-modified sols have less tendency to settle and form hard sludges than pastes dispersed with dispersing agents such as Dispex N40.

Moreover, 5 nm silica particles modified with 1 to 2 GPTMS/nm² may be the optimum dispersing agent for titania pigments. With larger particles, stable pastes cannot be prepared with the highest solids contents because the pigment particles will be less densely packed. With smaller particles, the stability towards aggregation and settling will be compromised.

Conclusions

1. It is possible to obtain stable silica sol-potassium silicate mixes using silane modified silica sols in molar ratio, SiO₂:K₂O of 5-12.
2. Films from such mixes have improved film properties and better water resistance.
3. Silane modified silica sols are excellent pigments dispersants for titania pigments, giving stable pigments pastes.
4. Optimal particle size of the silica used as dispersants is about 5 nm.
5. A certain degree of silane modification of from 1 to 2 GPTMS/nm² is required for optimal performance as pigments dispersants.
6. A surface coverage of the pigments particles of 120-140 % of the theoretical calculated level is required, depending on the particle size of the silica sol.

References

- Auger, J.-C., Barrera, R.G. and Stout, B. (2003), "Scattering efficiency of clusters composed by aggregated spheres", *Journal of Quantitative Spectroscopy & Radiative Transfer*, Vol. 79-80, pp. 521-31.
- Boisvert, J.-P., Persello, J., Foissy, A., Castaing, J.-C. and Cabane, B. (2000), "Effect of surface charge on the adsorption mode of sodium poly(acrylate) on alumina-coated TiO₂ used as coating pigment", *Colloids and Surfaces A: Physicochemical Engineering Aspects*, Vol. 168, pp. 287-96.
- Boisvert, J.-P., Persello, J., Castaing, J.-C. and Cabane, B. (2001), "Dispersion of alumina-coated TiO₂ particles by adsorption of sodium polyacrylate", *Colloids and Surfaces A: Physicochemical and Engineering Aspects*, Vol. 178, pp. 187-98.
- Bolt, J.D. (1999), "Titanium dioxide particles having substantially discrete inorganic particles dispersed on their surfaces", *US patent 5 886 069*.
- Braun, J.H. (1988), "Crowding and spacing of titanium dioxide pigments", *Journal of Coatings Technology*, Vol. 60 No. 758, pp.67-71.
- Forrest, S. (2001), "The development of titanium pigments (a great balancing act or one size fits all)", *Journal of Surface Coatings Australia*, Vol. 38 No. 10, pp. 16-22.
- Greenwood, P. (2008), "Nano-particle reinforced latex dispersions with modified colloidal silica", *Journal of Coatings Technology Coatings Tech*, Vol. 5 No. 2, pp. 44-51.
- Greenwood, P. and Gevert, B. (2009), "Results to be published"
- Heiberger, F. and Schläffer, H. (2001), "Silicatic coating mass with improved stability", *European Patent 1 222 234*.
- Iler, R.K. (1979), *The Chemistry of Silica: Solubility, Polymerization, Colloid and Surface Properties*, 1st Ed., Wiley and Sons, New York.
- Matijevic, E. and Hansen, F.K. (1980), "Heterocoagulation. Part 5.- Adsorption of a carboxylated polymer latex on monodispersed hydrated metal oxides", *Journal of the Chemical Society, Faraday Transactions 1: Physical Chemistry in Condensed Phases*, Vol. 76, pp.1240-62.

Otterstedt, J.-E. and Greenwood, P. (2005), "Some important, fairly new uses of colloidal silica/silica sol" in Bergna, H.E. and Roberts, W.O. (Eds.), *Colloidal Silica. Fundamentals and Applications.*, Taylor and Francis, pp. 737-56.

Sears, G.W. Jr. (1956), "Determination of specific surface area of colloidal silica by titration with sodium hydroxide", *Journal of Analytical Chemistry*, Vol. 28 No. 12, pp.1981-3.

Table I Description of colloidal silica dispersions used in the application evaluations

| Silica sol No. | Dp (nm), based on specific surface area before modification | SiO₂ content (wt-%) | Modification degree: (GPTMS/nm² surface) |
|-----------------------|--|---------------------------------------|--|
| 1 | 4 | 15 | 0.7 |
| 2 | 4 | 15 | 1.4 |
| 3 | 5 | 15 | 0 |
| 4 | 5 | 15 | 1.0 |
| 5 | 5 | 15 | 2.0 |
| 6 | 7 | 30 | 0 |
| 7 | 7 | 25* | 0 |
| 8 | 7 | 30 | 1.4 |
| 9 | 7 | 30 | 0 |
| 10 | 12 | 40 | 1.7 |

*: Aluminate modified sol

Table II Formulations

| No. | Silica sol (g) | Waterglass (g) | Water (g) | Molar ratio SiO₂/K₂O |
|------------|-----------------------|-----------------------|------------------|---|
| 1 | 10.72 | 28.50 | 10.78 | 5.0 |
| 2 | 14.35 | 23.52 | 12.13 | 6.0 |
| 3 | 16.96 | 20.16 | 12.88 | 7.0 |
| 4 | 18.91 | 17.64 | 13.45 | 8.0 |
| 5 | 20.44 | 15.68 | 13.88 | 9.0 |
| 6 | 21.65 | 14.11 | 14.24 | 10.0 |
| 7 | 22.65 | 12.83 | 14.52 | 11.0 |
| 8 | 23.48 | 11.76 | 14.76 | 12.0 |

Table III Experimental pigments pastes

| Paste No. | Silica sol No., as given in Table I | Sol particle size and degree of silane modification (GPTMS/nm² surface) | Note |
|------------------|--|---|--|
| 1 | 5 | 5 nm, 2.0 | |
| 2 | 4 | 5 nm, 1.0 | |
| 3 | 1 | 4 nm, 0.7 | |
| 4 | 2 | 4 nm, 1.4 | |
| 5 | 3 | 5 nm, no silane | |
| 6 | 7 | 7 nm, no silane | Aluminate modified sol |
| 7 | 8 | 7 nm, 1.4 | |
| 8 | 9 | 12 nm, no silane | |
| 9 | 10 | 12 nm , 1.7 | |
| 10 | ----- | Dispex 40 N, 0.53 % on TiO ₂ | Reference |
| 11 | 5 | 5 nm, 2.0 | Silica content reduced by 2/3 to 4.46 % |
| 12 | 5 | 5 nm, 2.0 | 350 g TiO ₂ in paste |
| 13 | 5 | 5 nm, 2.0 | Dispersion for 20 min at 2000 rpm. |
| 14 | 9 | 12 nm, no silane | Non-diluted silica sol, 200 g TiO ₂ |
| 15 | 10 | 12 nm, 1.7 | Non-diluted silica sol, 200 g TiO ₂ |

Table IV Pastes used in coatings series

| No. | Wt-% TiO₂ | TiO₂(g) | Paste (g) |
|------------|-----------------------------|---------------------------|------------------|
| A | 5 | 1.16 | 1.54 |
| B | 10 | 2.44 | 3.26 |
| C | 20 | 5.50 | 7.33 |
| D | 30 | 9.43 | 12.57 |
| E | 40 | 14.67 | 19.56 |
| F | 50 | 22.00 | 29.33 |

Table V Viscosity of silicate-silica sol mixtures

| No. | Molar ratio: SiO ₂ /K ₂ O | Silica sol non- surface modified, dp: 7 nm, (sol No. 6 in Table I) | | Silica sol- Silane modified dp: 7 nm, (sol No. 8 in Table I) | |
|-----|--|--|------------------------------------|---|---------------------------------|
| | | Viscosity (mPas), 1 week | Viscosity (mPas), 1 weeks | Viscosity (mPas), 1 week | Viscosity (mPas), 2 weeks |
| 1 | 5.0 | 1287 | Gel | 19 | 131 |
| 2 | 6.0 | 14 | Gel | 6.6 | 10 |
| 3 | 7.0 | 6.7 | Gel | 4.2 | 5.1 |
| 4 | 8.0 | 4.8 | Gel | 3.5 | 3.8 |
| 5 | 9.0 | 4.0 | Gel | 2.9 | 3.0 |
| 6 | 10.0 | 3.7 | Gel | 2.8 | 2.9 |
| 7 | 11.0 | 3.3 | 31 | 2.6 | 2.8 |
| 8 | 12.0 | 3.1 | 13 | 2.5 | 2.5 |

Table VI Film properties for silicate-silica sol mixtures

| No. | Molar Ratio: SiO₂/K₂O | Colloidal silica - Silane modified | Colloidal silica non- surface modified |
|------------|--|---|---|
| 1 | 5.0 | Film | Film |
| 2 | 6.0 | Film | Film |
| 3 | 7.0 | Film | Film |
| 4 | 8.0 | Film | No film* |
| 5 | 9.0 | Cracks* | No film* |
| 6 | 10.0 | No film* | No film |
| 7 | 11.0 | No film | No film |
| 8 | 12.0 | No film | No film |

*: Addition of wetting agent to the formulation may give film-forming compositions

Table VII Water resistance of film from silicate-colloidal silica mixes

| No. | Molar Ratio: SiO₂/K₂O | Colloidal silica - Silane modified | Colloidal silica non- surface modified |
|------------|--|---|---|
| 1 | 5.0 | 0 | 0 |
| 2 | 6.0 | 0 | 0 |
| 3 | 7.0 | 1-2 | 1 |
| 4 | 8.0 | 2 | --- |
| 5 | 9.0 | --- | --- |
| 6 | 10.0 | --- | --- |
| 7 | 11.0 | --- | --- |
| 8 | 12.0 | --- | --- |

---: No film

Table VIII Dispersant used for and notes about the pigments pastes

| Paste No. | Silica sol number as given in Table I. | Sol particle size and degree of silane modification; (GPTMS/nm² surface) | Paste stability |
|------------------|---|--|---|
| 1 | 5 | 5 nm, 2.0 | Stable low viscous paste after 9 days |
| 2 | 4 | 5 nm, 1.0 | Stable for 1 day, thereafter thixotropic |
| 3 | 1 | 4 nm, 0.7 | Gels after 1 day |
| 4 | 2 | 4 nm, 1.4 | Stable for 1 day, thereafter thixotropic |
| 5 | 3 | 5 nm, no silane | Gels during pigment paste preparation |
| 6 | 7 | 7 nm, no silane | Gels during pigment paste preparation |
| 7 | 8 | 7 nm, 1.4 | Gels during pigment paste preparation |
| 8 | 9 | 12 nm, no silane | Gels during pigment paste preparation |
| 9 | 10 | 12 nm, 1.7 | Gels during pigment paste preparation |
| 10 | ----- | Dispex 40 N, 0.53 % on TiO ₂ (reference) | Thixotropic after 1 day, phase separated after 9 days |
| 11 | 5 | 5 nm, 2.0 | Thixotropic paste after 3 h |
| 12 | 5 | 5 nm, 2.0 | Gels during pigment paste preparation |
| 13 | 5 | 5 nm, 2.0 | Stable low viscous paste after 6 days |
| 14 | 9 | 12 nm, no silane | Gels during pigment paste preparations |
| 15 | 10 | 12 nm, 1.7 | Stable low viscous, fluid after 26 days. |

Table IX Silica surface coverage of titania pigments particles of 300 nm particle size

| Paste No. | Number of silica particles needed for full surface coverage of one pigment particle, N_{\max} | Weight per cent silica dispersant need for full TiO_2 pigment coverage | Weight per cent added of silica dispersant based on TiO_2 | Pigment surface coverage in per cent of full mono-layer coverage |
|------------------|---|---|--|---|
| 1 | 13492 | 3.19 | 4.47 | 141 |
| 2 | 13492 | 3.19 | 4.47 | 141 |
| 3 | 20943 | 2.54 | 4.47 | 176 |
| 4 | 20943 | 2.54 | 4.47 | 176 |
| 5 | 13942 | 3.19 | 4.47 | 141 |
| 6 | 6973 | 4.53 | 4.47 | 99 |
| 7 | 6973 | 4.53 | 4.47 | 99 |
| 8 | 661 | 17.3 | 4.47 | 26 |
| 9 | 661 | 17.3 | 4.47 | 26 |
| 10 | ----- | 0.32* | 0.53 | 165 |
| 11 | 13492 | 3.19 | 1.49 | 47 |
| 12 | 13492 | 3.19 | 3.83 | 120 |
| 13 | 13492 | 3.19 | 4.47 | 141 |
| 14 | 661 | 17.3 | 20.0 | 116 |
| 15 | 661 | 17.3 | 20.0 | 116 |

*: Assuming 1.2 monomers/nm² titania pigment for full surface coverage corresponding to an adsorption of 0.7 mg Displex N40 per m² of pigment surface (Boisvert *et al.*, 2000; Boisvert *et al.*, 2001)

$$N_{\max} = 2\pi[(a_1 + a_2)/a_2]^2/\sqrt{3}$$

weight ratio: $N_{\max} \times (\rho_{\text{SiO}_2} / \rho_{\text{TiO}_2}) \times (a_2 / a_1)^3$

$\rho_{\text{SiO}_2} = 2.2 \text{ kg/dm}^3$ an, $\rho_{\text{TiO}_2} = 4.3 \text{ kg/dm}^3$

$a_1 = 150 \text{ nm}$ (radius of titania pigment particle of 300 nm size)

$a_2 =$ radius of dispersant particle

Figure 1 TEM Micrograph: Titania pigment dispersed by 5 nm silane modified silica sol; pigment paste number 1

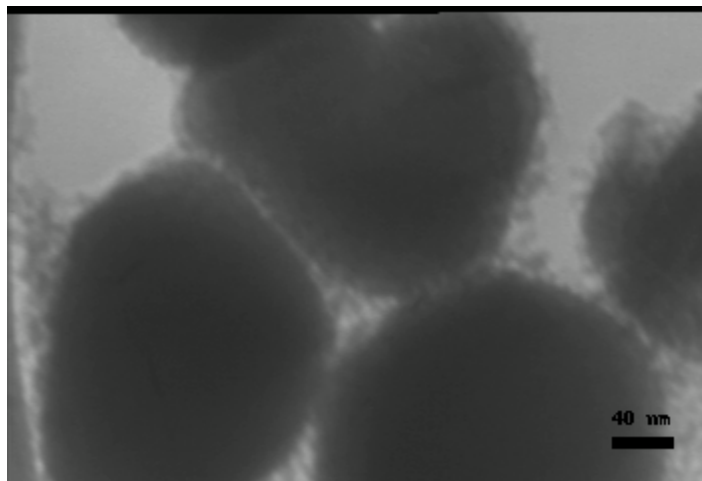


Figure 2 Reflectance (%) versus titania content, λ : 300 nm - 700 nm. Coatings based on pigments pastes number 1 and 10

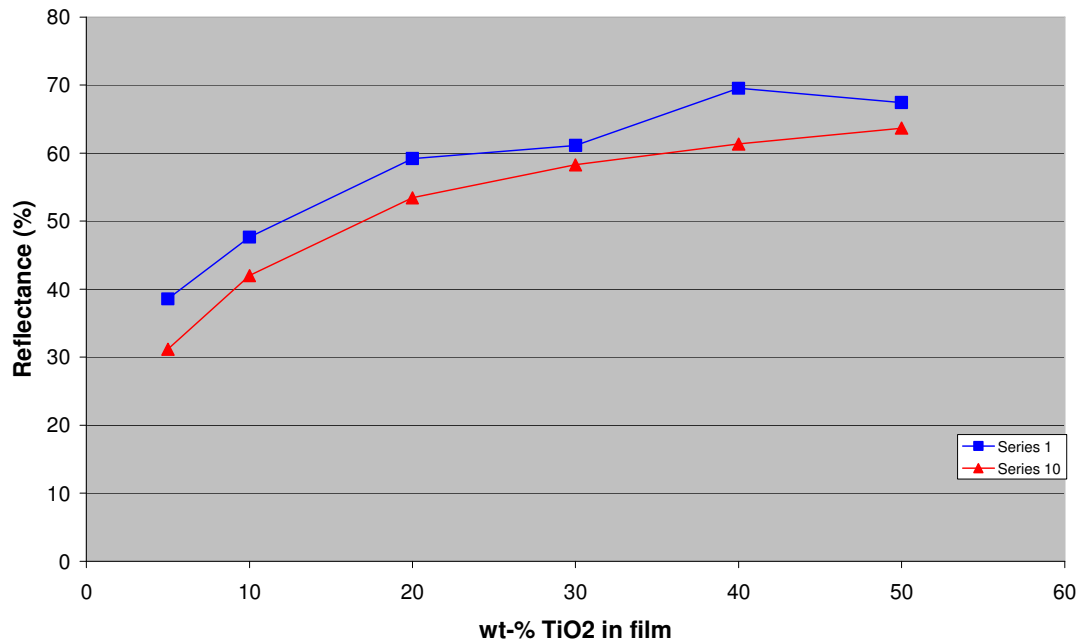
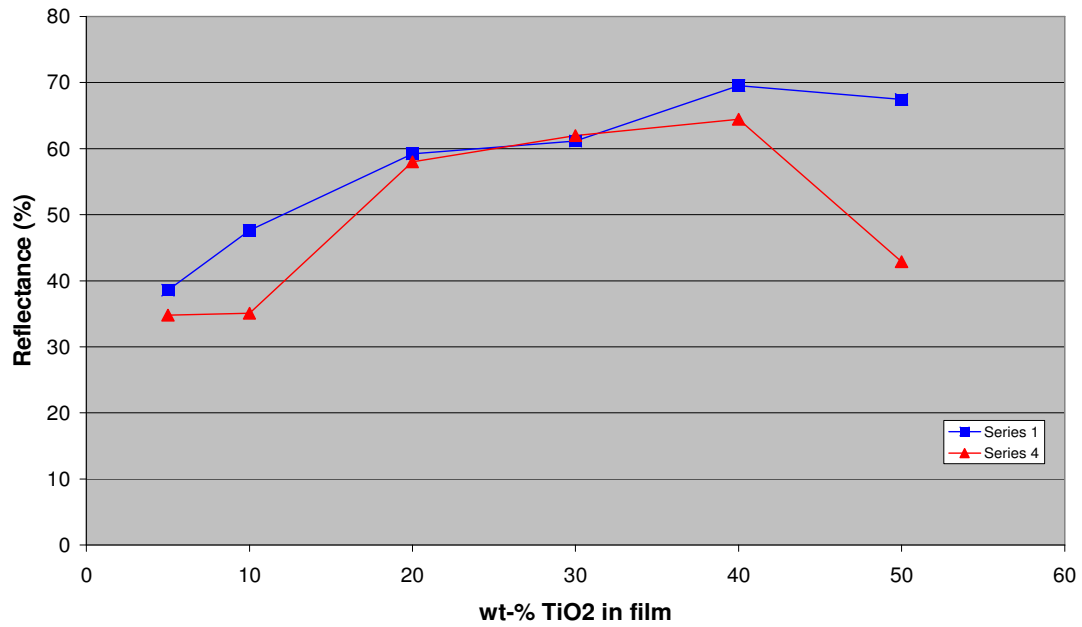


Figure 3 Reflectance (%) versus titania content, λ : 300 nm - 700 nm. Coatings based on pigments pastes number 1 and 4



Paper IV

Nano-Particle Reinforced Latex Dispersions With Modified Colloidal Silica
Peter Greenwood, JCT CoatingsTech, 2008, Vol. 5, No. 2, pp. 44-51.



Nano-Particle Reinforced Latex Dispersions With Modified Colloidal Silica

by Peter Greenwood
Eka Chemicals AB, a Business
Unit within Akzo Nobel*

The impact of adding epoxysilane-modified colloidal silica to water-based coating formulations on the mechanical properties of resin films was studied. In general, the effect of the silica particles depended strongly on the resin and other components of the coating formulation but very significant improvements of hardness could be observed. The effect on the abrasion resistance of the coatings was less clear but still noticeable in many coating systems. Also, the modification ensures good compatibility with the resins and that the aesthetic properties of the coating (gloss and haze) are not compromised.

Addition of silica particles to waterborne wood lacquers enhances the grain structure in a manner similar to solventborne lacquers.

INTRODUCTION

In the past, there have been numerous investigations on the use of silica nano-particles in resin-based systems. Water-free systems of silane-modified colloidal silica particles have been found to enhance the mechanical properties of coatings.^{1,2} Silane-modified fumed silica has been used to enhance coating properties.³ Organosols have been used to improve scratch resistance in clear coatings by surface enrichment.⁴ Aqueous colloidal silica has been utilized in copolymerization of resins,⁵ and copolymerized colloidal silica resin hybrids are also used to enhance a variety of coatings properties like hardness, anti-blocking, and reduced dirt-pickup.⁶ Silica particles made from TEOS have recently been investigated in copolymerization of hybrid coatings where hardness and adhesion properties were found to be improved.⁷ Non-surface modified colloidal silica has been tested as a nano-filler in latex coatings with encouraging results concerning mechanical properties.⁸ However, there have been very few studies done on the use of silane-modified water-based colloidal silica used in formulations of waterborne coatings.

Presented at the 2007 FutureCoat! Conference, sponsored by Federation of Societies for Coatings Technology, in Toronto, Ont., Canada, October 3-5, 2007.

*445 80 Bohus, Sweden.

Recently, there has been great interest in such particles in waterborne lacquers since they often provide benefits like anti-blocking and "anfeuerung" in acrylic emulsion-based wood coatings. It is also very desirable to improve mechanical properties, such as hardness and abrasion resistance, of coatings. To this end, highly crosslinked systems like two-pack, or 2-k, systems are often required. Addition of colloidal silica dispersions to waterborne lacquers provides coatings with excellent mechanical properties.

Concentrated epoxysilane-modified colloidal silica in the form of aqueous sols is one of the most readily available sources of nano-particles for the coating area. Such sols are characterized by high solids content, up to at least 50% by weight of silica depending on particle size, which ranges from about 5 to 100 nm. Compared with conventional silica sols, silane-modified colloidal silica provides greater stability towards aggregation and gelling, both as is and in latex-based coating formulations.⁹⁻¹¹

Finally, from an environmental point of view, it is advantageous to use colloidal silica in latex-based coating formulations. Less resin will be needed as it is partially replaced by silica, with accompanying lower amounts of VOC. Softer resins can be used since silica addition will improve their mechanical properties to the level of those of harder resins, obviating the use of potentially hazardous film-forming agents such as NMP or glycol ethers.

EXPERIMENTAL

2-K Systems

The varnish formulations are detailed in *Tables 1 to 8*. Product weights are given in grams. The varnishes were applied by means of an applicator on aluminum substrates at dry film thicknesses between 40 and 50 μm . Persoz hardnesses were measured after the following drying times: 1 day, 7 days, 2 weeks, and 1 month at ambient temperature. Gloss measurements were performed after 30 days of drying. Before testing, all the samples were conditioned at 23°C and 50% RH during 24 hours. The resistances to abrasion were also determined by means of a Taber abraser after 30 days of drying at ambient temperature. The addition of colloidal silica was 0, 10, and 20% by weight calculated as dry silica based on dry resin.

Materials

RESINS: The resins used are shown in *Table 9*.

HARDENERS: Hardeners used included:

- Rhodocoat X EZ-D401 (a water-dispersible aliphatic polyisocyanate)

- Rhodocoat X EZ-M501 (a water-dispersible aliphatic polyisocyanate; more hydrophobic than Rhodocoat X EZ-D401)

SILICA: Silane-modified colloidal silica dispersion: Bindzil® CC30; epoxy silane-modified colloidal silica, 1.40 GPTMS/nm² colloidal silica surface, pH 7, particle size: 7 nm, silica content 30 wt%.

Lacquer Formulations—Two-Pack Systems

Lacquer formulations for the two-pack systems are shown in *Tables 1–8*.

Gloss and Haze

Gloss (20°) was measured of coatings applied on aluminum plates after 30 days of drying at ambient temperature. Haze index, defined as a gloss difference, was calculated from gloss measurements at 20° and 60° following ASTM D 4039 test (reflection haze of high-gloss surfaces).

Hardness—Persoz Hardness

The hardness of the different varnishes was determined by means of a "Persoz pendulum" according to ASTM D 4366. The gloss of the varnishes was determined as the average of five measurements.

Abrasion Resistance—Taber Abrasion

The resistance to abrasion of the different varnishes with and without addition of epoxy silane-modified colloidal silica applied on aluminum plates was determined by means of a Taber abraser following ASTM D 4060. The test was performed after 30 days of drying at ambient temperature. An abrasive wheel, CS17, under 1 kg load was used. The weight loss of the samples was measured after 100, 500, and 1000 revolutions. The weight loss was determined as the average of two measurements. In some cases, the test was stopped before 1000 revolutions were reached due to delamination of the films or due to local substrate baring.

RESULTS AND DISCUSSION

Compatibility—Gloss and Haze

The results of gloss and haze measurements are given in *Tables 10 and 11*. These results are very dependent on the resin used. For two of the resins, No. 2 and No. 3, there is a big decrease in gloss when silica nanoparticles are added to the resin. For the other resins, there is little or no change in gloss or even an increase

Table 1—Formulation for Resin No. 1

| Resin No. 1 | Reference | 10% SiO ₂ | 20% SiO ₂ |
|--|-----------|----------------------|----------------------|
| C1 Setalux 6741 | 100 | 100 | 100 |
| Dowanol PnB | 2.81 | 2.81 | 2.81 |
| Dowanol DPM | 2.81 | 2.81 | 2.81 |
| TINSTAB BL 277 (1% ds Solvesso 100) | 1.00 | 1.00 | 1.00 |
| Bindzil CC30 | 0 | 14.83 | 29.66 |
| C2 Rhodocoat X EZ-D401 | 21.85 | 21.85 | 21.85 |

Table 2—Formulation for Resin No. 2

| Resin No. 2 | Reference | 10% SiO ₂ | 20% SiO ₂ |
|--|-----------|----------------------|----------------------|
| C1 Setalux 6756 | 100 | 100 | 100 |
| Dowanol PnB | 1.96 | 1.96 | 1.96 |
| Dowanol DPM | 1.96 | 1.96 | 1.96 |
| TINSTAB BL 277 (1% ds Solvesso 100) | 1.00 | 1.00 | 1.00 |
| Bindzil CC30 | 0 | 13.79 | 27.58 |
| C2 Rhodocoat X EZ-D401 | 20.33 | 20.33 | 20.33 |

Table 3—Formulation for Resin No. 3

| Resin No. 3 | Reference | 10% SiO ₂ | 20% SiO ₂ |
|--|-----------|----------------------|----------------------|
| C1 Setalux 6762 | 100 | 100 | 100 |
| Butylglycol | 9.19 | 9.19 | 9.19 |
| Dowanol DPnB | 3.34 | 3.34 | 3.34 |
| Butyldiglycol | 4.93 | 4.93 | 4.93 |
| TINSTAB BL 277 (1% ds Solvesso 100) | 1.00 | 1.00 | 1.00 |
| Bindzil CC30 | 0 | 15.17 | 30.34 |
| C2 Rhodocoat X EZ-D401 | 22.36 | 22.36 | 22.36 |

Table 4—Formulation for Resin No. 4

| Resin No. 4 | Reference | 10% SiO ₂ | 20% SiO ₂ |
|--|-----------|----------------------|----------------------|
| C1 Setalux 6778 | 100 | 100 | 100 |
| Dowanol DPnB | 6.60 | 6.60 | 6.60 |
| TINSTAB BL 277 (1% ds Solvesso 100) | 1.00 | 1.00 | 1.00 |
| Bindzil CC30 | 0 | 15.17 | 30.34 |
| C2 Rhodocoat X EZ-D401 | 22.36 | 22.36 | 22.36 |

Table 5—Formulation for Resin No. 5

| Resin No. 5 | Reference | 10% SiO ₂ | 20% SiO ₂ |
|--|-----------|----------------------|----------------------|
| C1 Setalux 6510 | 100 | 100 | 100 |
| Solvesso 100 | 2.14 | 2.14 | 2.14 |
| Butyl acetate | 5.19 | 5.19 | 5.19 |
| Butyl glycol acetate | 4.66 | 4.66 | 4.66 |
| TINSTAB BL 277 (1% ds Solvesso 100) | 1.00 | 1.00 | 1.00 |
| Bindzil CC30 | 0 | 14.48 | 28.96 |
| C2 Rhodocoat X EZ-D401 | 43.17 | 43.17 | 43.17 |

Table 6—Formulation for Resin No. 6

| Resin No. 6 | Reference | 10% SiO ₂ | 20% SiO ₂ |
|--|-----------|----------------------|----------------------|
| C1 Setalux 6511 | 100 | 100 | 100 |
| Butylglycol | 1.96 | 1.96 | 1.96 |
| Butyl acetate | 2.83 | 2.83 | 2.83 |
| Butyl glycol acetate | 0.84 | 0.84 | 0.84 |
| TINSTAB BL 277 (1% ds Solvesso 100) | 1.00 | 1.00 | 1.00 |
| Bindzil CC30 | 0 | 16.21 | 32.42 |
| C2 Rhodocoat X EZ-D401 | 48.09 | 48.09 | 48.09 |

Table 7—Formulation for Resin No. 7

| Resin No. 7 | Reference | 10% SiO ₂ | 20% SiO ₂ |
|--|-----------|----------------------|----------------------|
| C1 Neopac E-180 | 100 | 100 | 100 |
| Butyldiglycol | 8.00 | 8.00 | 8.00 |
| TINSTAB BL 277 (1% ds Solvesso 100) | 1.00 | 1.00 | 1.00 |
| Bindzil CC30 | 0 | 11.38 | 22.76 |
| C2 Rhodocoat X EZ-M501 | 45.92 | 45.92 | 45.92 |

Table 8—Formulation for Resin No. 8

| Resin No. 8 | Reference | 10% SiO ₂ | 20% SiO ₂ |
|--|-----------|----------------------|----------------------|
| C1 Neorez R-2135 | 100 | 100 | 100 |
| Dowanol DPnB | 6.00 | 6.00 | 6.00 |
| TINSTAB BL 277 (1% ds Solvesso 100) | 1.00 | 1.00 | 1.00 |
| Bindzil CC30 | 0 | 12.07 | 24.14 |
| C2 Rhodocoat X EZ-M501 | 48.7 | 48.7 | 48.7 |

Figure 1—Persoz hardness in function of coating composition and drying time at ambient temperature.

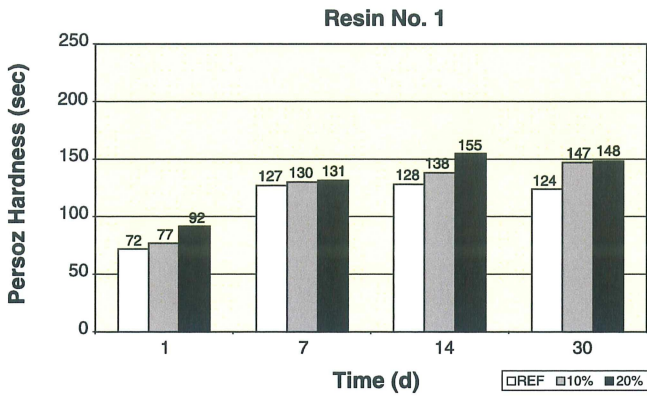


Figure 4—Persoz hardness in function of coating composition and drying time at ambient temperature.

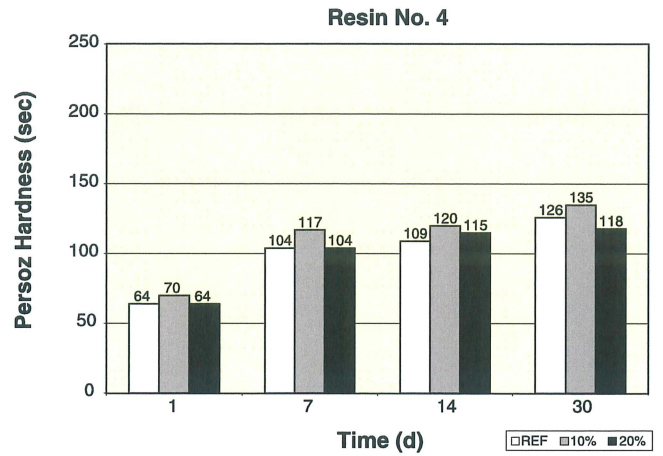


Figure 2—Persoz hardness in function of coating composition and drying time at ambient temperature.

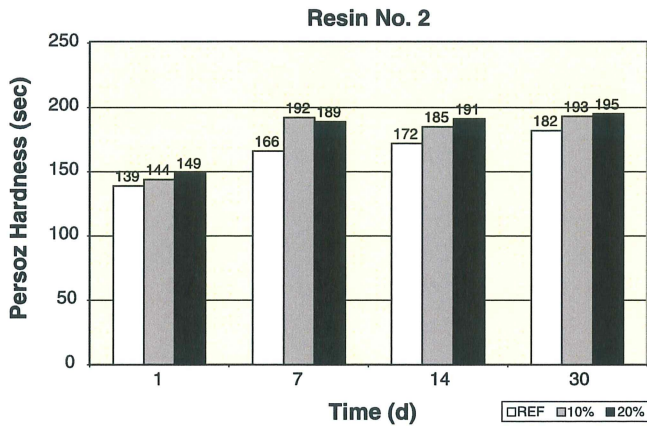


Figure 5—Persoz hardness in function of coating composition and drying time at ambient temperature.

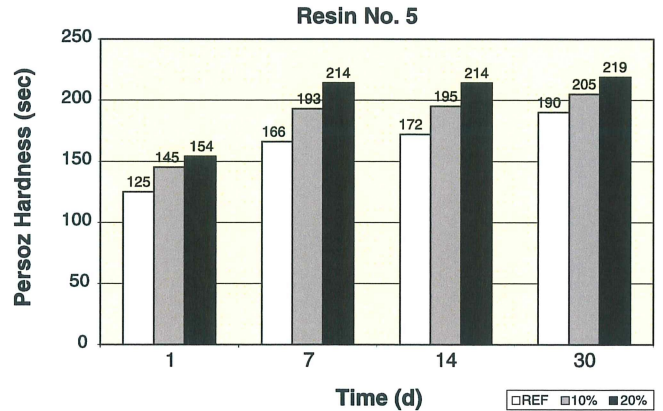


Figure 3—Persoz hardness in function of coating composition and drying time at ambient temperature.

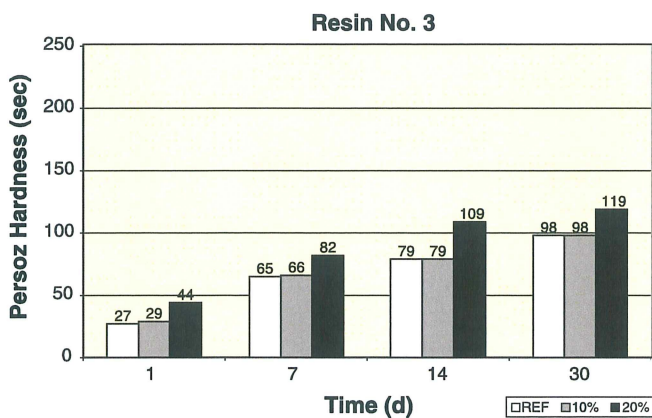


Figure 6—Persoz hardness in function of coating composition and drying time at ambient temperature.

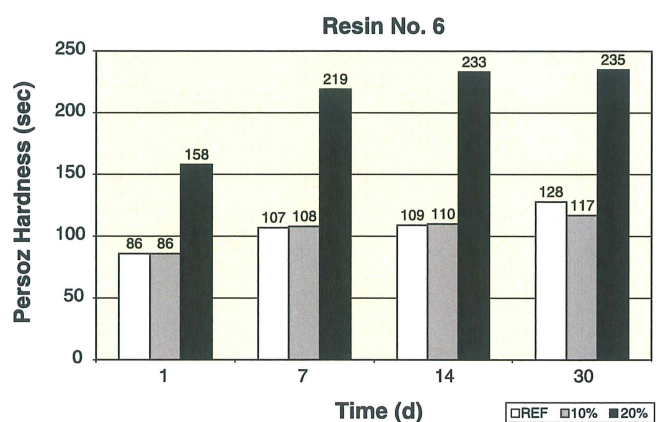


Figure 7—Persoz hardness in function of coating composition and drying time at ambient temperature.

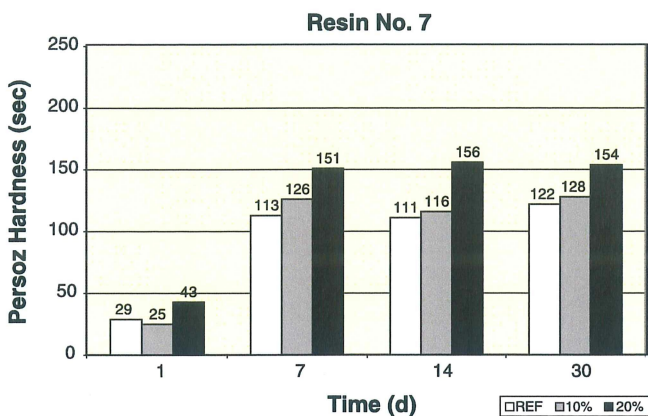
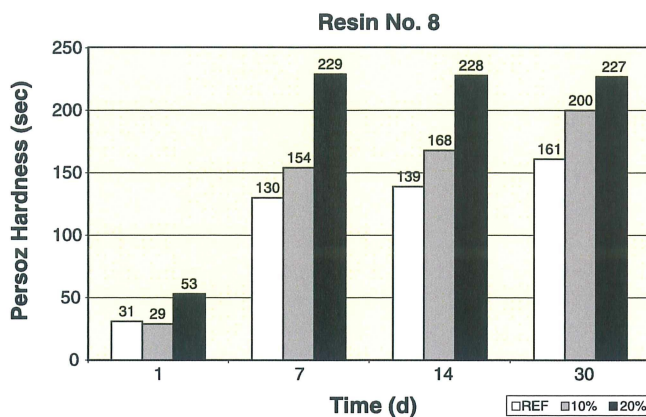


Figure 8—Persoz hardness in function of coating composition and drying time at ambient temperature.



in gloss upon silica addition, indicating good compatibility of the silica with the resin.

Hardness—Persoz Hardness

Evolution of hardness as a function of drying time and coating composition is presented for the different resins in Figures 1–8. The mean hardness values for each varnish are noted on the different graphs.

The effect of silica addition seems to be most pronounced for resins No. 5–8. For these resins, the effect of epoxysilane-modified colloidal silica is most pronounced for the 20 wt% silica addition to the resin (dry on dry). There is no proportionality between the amount of added inorganic particles and the property response. To achieve good improvement in hardness it is important to have good interaction/crosslinking between the resin and the silica particle, as well as to build a structure, like a skeleton, of silica in the resin matrix. In such cases it is possible to significantly improve the mechanical properties even at low silica additions.¹²

With the exception of resin No. 4, and in particular for resin No. 6, addition of 20 wt% of epoxysilane-

modified silica improves the hardness of the coatings at all drying times studied. The increase in hardness was particularly noticeable at shorter drying times. Silica addition accelerates the development of the final hardness of the films, which is probably due to increased interactions/crosslinking between the components of the system, e.g., resin No. 8 with 20% silica addition will reach the ultimate hardness in seven days instead of 28 days.

The surface of the epoxysilane-modified silica particles contains diol groups, which can react/crosslink with carboxyl, hydroxyl, and isocyanate groups on the organic components of the system. Addition of silica to the acrylic binders 2 and 4 increases hardness considerably less than it does for the acrylic polyol binders 5 and 6. The polyol component of the latter type of binders contributes more reactive groups to the system than the pure acrylic binders 2 and 4. For resin No. 4, the hardness improvement is insignificant or nonexistent at all drying times at 20% addition of silica, whereas 10% addition causes a moderate increase of hardness. The seemingly inconsistent response of hardness to the amount of silica added may be due to aggregate formation. Above a certain critical concentra-

Table 9—Resins

| Resin No. | Type | Solid Content (%) | pH | Note |
|-----------|--------------------------------|-------------------|------|---|
| 1 | .Setalux 6741: Acrylic | 43% | pH 8 | |
| 2 | .Setalux 6756: Acrylic | 40% | pH 8 | Surfactant free, self-crosslinking |
| 3 | .Setalux 6762: Styrene-acrylic | 44% | pH 8 | |
| 4 | .Setalux 6778: Acrylic | 44% | pH 9 | Gradient particle morphology, self-crosslinking |
| 5 | .Setalux 6510: Acrylic polyol | 42% | pH 8 | Acid value: 7.8–9.9 mg KOH/g |
| 6 | .Setalux 6511: Acrylic polyol | 47% | pH 8 | Acid value: 6.6–8.5 mg KOH/g |
| 7 | .NeoPac E-180: Acrylic-PU | 33% | pH 8 | Copolymer |
| 8 | .NeoRez-2135: PU | 35% | pH 8 | Aliphatic PU dispersion |

Table 10—Gloss 10°

| Resin | Reference | 10% SiO ₂ | 20% SiO ₂ |
|-----------------|-----------|----------------------|----------------------|
| No. 1 | 97 | 111 | 86.8 |
| No. 2 | 39.2 | 16.1 | 21 |
| No. 3 | 111 | 60.6 | 60.1 |
| No. 4 | 117 | 117 | 114 |
| No. 5 | 127 | 130 | 112 |
| No. 6 | 108 | 99.2 | 129 |
| No. 7 | 2.9 | 3.3 | 4.4 |
| No. 8 | 4.5 | 5.2 | 6.3 |

tion of silica particles, which depends on the type of resin in the binder, the particles will cluster to aggregates of such size that the silica will no longer act as a nano-filler but will instead perform as conventional fillers, which are known to sometimes deteriorate the mechanical properties of the resins to which they are added (see also the following section on Silica Structure in the Resin Matrix).

Abrasion Resistance—Taber Abrasion

The effect of silica on abrasion resistance, although it is quite dependant on the type of resin, is not clear. For some of the resins (No. 2, 3, and 4), it is detrimental. For another (No. 5), there is improvement at 10% but some deterioration at 20% addition of silica. For others still (No. 6 and 7), the reverse is true. Only resin No. 8 shows modest improvement at the two levels of silica addition. The effect of nano-fillers on the abrasion resistance of resins is even more difficult to explain, let alone predict, than their effect on other mechanical properties, like hardness. Basically, one would like to say that abrasion resistance increases as the energy required to tear the resin apart, i.e., the energy at break, increases. There are, however, many other factors—for instance, surface enrichment of the filler particles, the effect of the filler particles on the friction coefficient, and clustering of the particles to large aggregates in the resin—that affect abrasion resistance in a major way. The results are detailed in Table 12.

Silica Structure in the Resin Matrix—Effect on Hardness and Abrasion Resistance

Transmission electron microscopy has been used to visualize the structure of the inorganic part embedded in

Table 11—Haze Index (Gloss 60°–Gloss 20°)

| Resin | Reference | 10% SiO ₂ | 20% SiO ₂ |
|-----------------|-----------|----------------------|----------------------|
| No. 1 | 83 | 76 | 26.2 |
| No. 2 | 54.8 | 31.5 | 38.1 |
| No. 3 | 63 | 58.5 | 36.8 |
| No. 4 | 8 | 8 | 9 |
| No. 5 | 57 | 56 | 8 |
| No. 6 | 60 | 56.8 | 50 |
| No. 7 | 4.7 | 5.4 | 7.6 |
| No. 8 | 7.1 | 8.2 | 9.8 |

the organic matrix. In Figures 9 and 10, the structure of the inorganic part embedded in Setalux 6510 (No. 5) varnish with 10 and 20 wt%, SiO₂ based on dry resin, Bindzil CC30, respectively, are displayed. In Figures 11–13, the Setalux 6511 (No. 6) varnish with 10 and 20 wt% SiO₂ based on dry resin, Bindzil CC30, are presented. The resin–air interface cannot be seen in the figures, but it extends in Figure 9 from about the midpoint of the upper edge to the lower left corner; from below the midpoint of the left edge of the picture to somewhat to the right of the lower edge in Figure 10; and in Figure 11 from well to the right of the midpoint of the upper edge to about the midpoint of the left edge. No interface can be seen in Figure 12. The interface in Figure 13 extends from about the midpoint of the upper edge to the lower left corner.

RESIN NO. 5: Figures 9 and 10 show that the particles are not accumulated at the resin–air interface. They are moderately aggregated and the aggregates are somewhat larger in size at 20% addition than at 10% addition of silica. The Persoz hardness increases with increased addition of silica, whereas there is a significant improvement of the abrasion resistance only at 10% addition of silica while 20% addition of silica affects the abrasion resistance only in a minor way.

RESIN NO. 6: Similar to resin No. 5, resin No. 6 is an acrylic polyol and the silica particles are not accumu-

Table 12—Taber Abrasion Resistance—Weight Loss Mg

| Resin | Reference | | | 10% SiO ₂ Addition | | | 20% SiO ₂ Addition | | |
|-------|-----------------------|-----|------|-------------------------------|-----|------|-------------------------------|-----|------|
| | Number of Revolutions | | | Number of Revolutions | | | Number of Revolutions | | |
| | 100 | 500 | 1000 | 100 | 500 | 1000 | 100 | 500 | 1000 |
| No. 1 | 17 | — | — | 15 | — | — | 15 | 82 | — |
| No. 2 | 5 | 83 | 187 | 20 | 103 | 202 | 15 | 89 | 199 |
| No. 3 | 9 | 70 | 141 | 16 | 83 | — | 17 | 89 | 160 |
| No. 4 | 12 | 69 | — | 10 | 76 | — | 15 | — | — |
| No. 5 | 3 | 33 | 60 | 2 | 17 | 37 | 3 | 33 | 64 |
| No. 6 | 3 | 37 | 83 | 2 | 40 | 88 | 3 | 33 | 68 |
| No. 7 | 5 | 24 | 47 | 2 | 25 | 52 | 1 | 20 | 45 |
| No. 8 | 3 | 23 | 43 | 2 | 14 | 29 | 1 | 19 | 37 |

Figure 9—Resin No. 5 with 10% SiO₂.

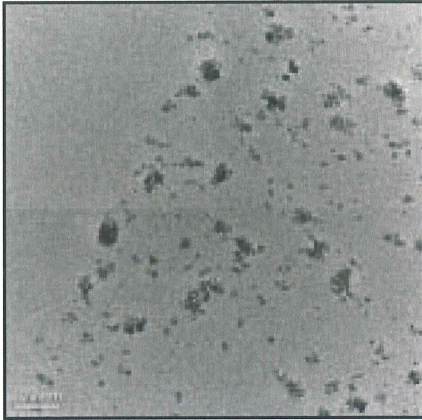


Figure 10—Resin No. 5 with 20% SiO₂.

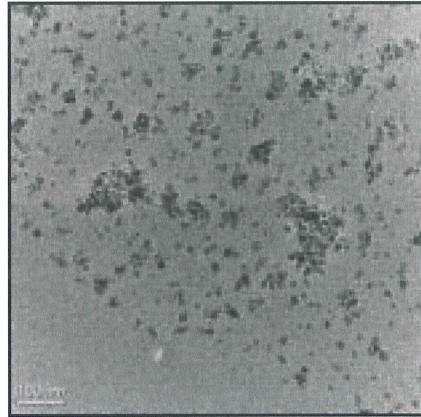


Figure 11—Resin No. 6 with 10% SiO₂.

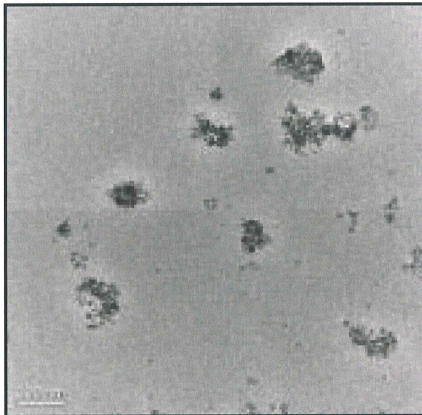


Figure 12—Resin No. 6 with 20% SiO₂.

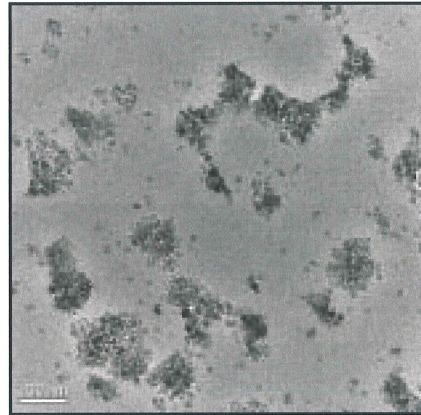
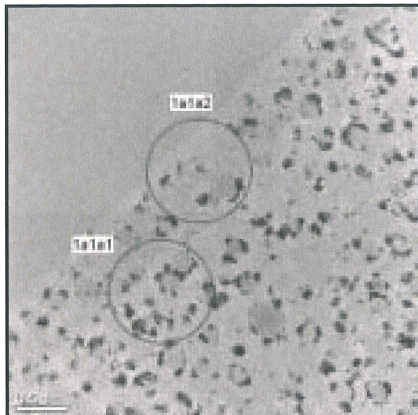


Figure 13—Resin No. 6 with 20% SiO₂.



lated or enriched at the binder-air interface. However, in contrast to the situation with resin No. 5, Figures 11–13 show that the silica particles have clustered around the droplets of the polyisocyanate hardener, perhaps preventing them from reacting effectively with the binder. There is no enhancement of the abrasion resistance at 10% and only modest improvement at 20% silica addition on resin, as might be expected from poor interaction between the silica and resin. On the other hand, the effect of the silica particles on the Persoz hardness while small or non-existent at 10%, is quite large at 20% addition of silica. The increase in hardness of the resin by the larger aggregates of silica particles at 20% silica addition may therefore be analogous to the observation that aggregation of nano-particles leads to increase in Young's modulus, especially by creating some occluded volumes in the matrix which augment the effective fraction of nano-filler.¹³

Anfeuerung—Enhancement of Grain Structure and “Anfeuerung” by Wood Lacquers

It has been reported in literature that colloidal silica in water-based wood coatings comprising colloidal silica, organosilane, and latex emulsion can penetrate into the wood substrate.¹² As indicated in Figure 14, that addition of epoxysilane-modified 7 nm silica particles to waterborne one-pack coating formulations containing acrylic binders enhances and complements the wood grain structure by so-called “anfeuerung,” giving an appearance similar to solvent-based coating systems. This valuable aesthetic effect can be expected to be present also with waterborne two-pack coating systems based on acrylic binders to which silica particles have been added, combined with the excellent mechanical properties characteristic of such systems.

Figure 14—1-K water-based lacquer formulated on resin No. 2 without (left) and with (right) 20% SiO₂ addition of epoxy-silane modified colloidal silica.



ACKNOWLEDGMENTS

The author thanks professor emeritus Jan-Erik Otterstedt, Chalmers University of Technology, for valuable discussions and fruitful input. [G1](#)

References

- (1) Vu, C., La Ferté, O., and Eranian, A., "High Performance UV Multi-Layer Coatings Using Inorganic Nanoparticles," *Proc. RadTech Europe*, 2005.
- (2) Chisholm, B. and Resue, J., "UV-curable, Hybrid Organic-Inorganic Coatings," *Proc. 30th International Waterborne, High-Solids, and Powder Coatings Symposium*, New Orleans, 2003.
- (3) Bauer, F., Ernst, H., Hirsh, D., Naumov, S., Pelzing, M., Sauerland, V., and Mehnert, R., "Preparation of Scratch and Abrasion Resistant Polymeric Nanocomposites by Monomer Grafting onto Nanoparticles," *Macromol. Chem. Phys.*, 205, p. 1587-1593 (2004).
- (4) Anderson, L.G., Barkac, K.A., Chasser, A.M., Desaw, S.A., Hartman, M.E., Hayes, D.E., Hockswender, T.R., Kuster, K.L., Montague, R.A., Nakajima, M., Olson, K.G., Richardson, J.S., Sadvary, R.J., Simpson, D.A., Tyebjee, S., and Wilt, T-F., "Cured Coatings Having Improved Scratch Resistance, Coated Substrates, and Method Thereof," U.S. Patent #6 387 519, 2002.
- (5) Percy, M.J., Barthet, C., Lobb, J.C., Khan, M.A., Lacelles, S.F., and Armes, S.P., "Synthesis and Characterization of Vinyl Polymer-Silica Colloid Nanocomposites," *Langmuir*, 16, p. 6913-6920 (2000).
- (6) Leuniger, J., Tiarks, K., Wagner, O., and Wiese, H., "Nano-Composite Dispersions —The Col 9. Technology for Water-Based Coatings," *Proc. 18th SLF Congress*, Helsingör, Denmark, 2006.
- (7) Yeh, J-M, Weng, C-J., Liao, W-J. and Mau, Y-W, "Anticorrosively Enhanced PMMA-SiO₂ Hybrid Coatings Prepared from the Sol-Gel Approach with MSMA as the Coupling Agent," *Surface Coat. Technol.*, 201, p. 1788-1795 (2006).
- (8) Oberdisse, J., "Structure and Rheological Properties of Latex-Silica Nanocomposite Films: Stress-Strain Isotherms," *Macromol.*, 35, pp. 9441-9450, 2002.
- (9) Greenwood, P., "Colloidal Silica Dispersion," W.O. patent application 2004035473 A1, 2004.
- (10) Greenwood, P. and Lagnemo, H., "Aqueous Silica Dispersion," W.O. patent application 2004035474 A1, 2004.
- (11) Greenwood, P., result to be published.
- (12) de Lame, C., "Water-Based Hybrid Organic/Inorganic Coatings," ATIPIC-NVVT Nanotechnology and Coatings meeting, Brecht, Belgium, 2005.
- (13) Reynaud, E., PhD thesis, L'Institut National des Sciences Appliquées de Lyon, France, 2000.

Paper V

Some Important, Fairly New Uses Of Colloidal Silica/Silica Sol

Jan-Erik Otterstedt and Peter Greenwood in Bergna, H.E. and Roberts, W. O. (Eds.), *Colloidal Silica. Fundamentals and Applications.* , 2005, Taylor and Francis, pp. 737-56.

57 Some Important, Fairly New Uses of Colloidal Silica/Silica Sol

Jan-Erik Otterstedt

Chalmers University of Technology

Peter Greenwood

Eka Chemicals (Akzo Nobel)

CONTENTS

| | | | |
|--|-----|--|-----|
| Colloidal Silica in Cement and Concrete | 738 | The First Role of Hydroxyl Ions — As a Catalyst | 748 |
| Cement | 738 | The Second Role of Hydroxyl Ions — Charge Repulsion | 748 |
| What Is Cement and Concrete? | 738 | The Role of Neutral Salts — Screening of Charge Repulsion | 748 |
| Hydration of Cement | 738 | Specific Salt Effects — Effect of Cations | 749 |
| Flaws in Cement | 740 | Effect of Anions | 749 |
| Silica in Cement | 740 | The Salt Effect Is Proportional to the pH | 749 |
| Silica Fume | 740 | The Effect of Temperature | 749 |
| Colloidal Silica | 741 | Differences between the Polymerization and Collision Mechanisms of Gel Formation | 749 |
| Colloidal Silica as Retention Aid in | | Kinetics of Collision Gels | 749 |
| Paper Making | 743 | Colloidal Silica in Coatings | 751 |
| Fillers | 743 | Shop Primers for Steel Substrates | 751 |
| Paper-Making | 743 | Inorganic Paints | 752 |
| The Problem | 744 | Hard, Scratch-Resistant Thin Coatings | 752 |
| Retention, Retention Mechanisms and Retention Aids | 744 | Colloidal Silica in Polymer Latices | 753 |
| Dual Retention Aid Systems | 745 | Colloidal Silica and Ink Jet | 753 |
| Colloidal Silica in | | Colloidal Silica as Polishing Agent for Electronic Products | 754 |
| Lead-Acid Batteries | 747 | References | 755 |
| Gelling of Silica Sols | 747 | | |
| Types of Gels | 747 | | |
| Common Features in Gel Formation | 748 | | |
| The Central Mechanism in Gel Formation | 748 | | |

Dilute silica sols were prepared and studied over 70 years ago. Their uses as binders in catalyst preparation, as glazes on ceramics, as coatings on concrete and plaster of Paris, as agents for treating paper and textiles, and several other applications were investigated [1]. These early silica sols contained less than 10% by weight of silica, were fairly unstable and did not have reproducible properties. Iler [2] predicted that colloidal silica would not be accepted for wide commercial use before these shortcomings were remedied.

Product development work in several industrial laboratories resulted in the production of concentrated

silica sols of high stability and very reproducible properties. Iler [3] describes numerous applications of such sols.

Otterstedt and Brandreth [4] discusses functions that can be achieved by using colloidal silica in various applications. Most of these functions depend on the presence of a high specific surface area of a special chemical nature.

Here we will focus our attention on the use of colloidal silica to make high quality concrete, as retention aid in paper making, as polishing agents for silicon wafers, to provide solid electrolytes in lead-acid batteries and

as components in high quality coatings because these applications are very large, relatively new and/or fast growing.

COLLOIDAL SILICA IN CEMENT AND CONCRETE

CEMENT

The following outline of cement is an adapted extract from Rodney Cotterill's fascinating odyssey into the material world [5].

What Is Cement and Concrete?

Already in ancient times it was known that the reaction between calcium oxide, also called lime or quicklime, and water could yield a binder in building construction. The Etruscans, for instance, added water to lime to form calcium hydroxide, or slaked lime, which they mixed with sand and stone into what today would be called a primitive concrete. The Romans discovered a way to improve cement making by burning a mixture of volcanic ash, which essentially consisted of silica, and lime. The many impressive constructions that have lasted to our days testify to the durability of their cement.

However, the Roman cement technology fell into oblivion and high quality cement became available first in 1824 when an Englishman Joseph Aspdin invented Portland cement, or modern cement. Modern cement is made by grinding a mixture of limestone and clays, with a weight ratio of about 80 to 20, and several other minor components with water to a slurry. This slurry is passed down a rotating kiln and first loses water and then carbon dioxide as the temperature gradually increases downward the kiln. In the last temperature zone, where the temperature is 1200–1500°C, the material sinters and melts to clinker. After cooling, the clinker is ground, together with a small amount of gypsum, which controls the reactivity of the cement with water, into a fine powder. The specific surface area of the particles, which is inversely proportional to particle size, determines the rate of reaction when water is added to the powder. The different grades of commercial cement powder are usually given designations that indicate how rapidly the cement paste becomes rigid and gains strength. Table 57.1 shows the composition and specific surface area of three common grades of Swedish cement.

The metals oxides in Table 57.1 are not present as such in cement powder but instead as four different major compounds, alite, $3\text{CaO}\cdot\text{SiO}_2$, 40–65% by weight, belite, $2\text{CaO}\cdot\text{SiO}_2$, 10–25% by weight, aluminate, $3\text{CaO}\cdot\text{Al}_2\text{O}_3$, up to 10% by weight, and ferrite, $4\text{CaO}\cdot\text{Al}_2\text{O}_3$, also up to 10% by weight. There are also present small amounts, a fraction of a percent usually, of free lime, magnesium oxide, sodium sulfate and potassium

TABLE 57.1
Composition and Specific Surface Area of Swedish Cements

| Compound | OPC SI | OPC Sk | SRCP D |
|------------------------------------|--------|--------|--------|
| CaO (%) | 62.2 | 64.3 | 54.6 |
| SiO ₂ (%) | 20.0 | 19.8 | 21.6 |
| Al ₂ O ₃ (%) | 4.53 | 5.21 | 3.46 |
| Fe ₂ O ₃ (%) | 2.23 | 3.04 | 4.75 |
| K ₂ O (%) | 1.42 | 1.30 | 0.75 |
| MgO (%) | 3.37 | 1.45 | 1.02 |
| Na ₂ O (%) | | 0.11 | 0.06 |
| Blaine (m ² /kg) | 363 | 400 | 323 |

Manufacturer: SI = Slite, Sk = Skövde, D = Degerhamn.

Note: Courtesy Euroc Research AB.

sulfate. These trace compounds can influence the final properties of the material, for example, concrete, to a much higher degree, and sometimes in a negative way, than their abundance in the cement powder might suggest. Gypsum, which is added when the clinker is ground to a powder, is present in amounts between 2 and 5% by weight.

Modern cement, for example, Portland cement, contains more components and is a much better binder than primitive cement. Another important difference between Portland cement and primitive cement is that the former will set and harden under water. Cement paste, that is, a slurry of cement powder and water is usually mixed with sand or stone when it is used in building construction. The term sand refers to particles smaller than 2 mm and the term stone refers to particles larger than 2 mm. A mixture of inorganic materials, which may include sand and stone, and having a particle size distribution in the range from about 0.01 to 100 mm, is called an aggregate [6]. Mortar is a mixture of cement paste and sand. If aggregate is added to cement paste, the mixture is called concrete. The weight ratio of cement paste to aggregate in concrete is usually in the range up to 1:6. Concrete may contain additives such as setting and hardening additives, usually called accelerators, or workability additives, usually called superplasticizers. The worldwide production of cement amounts to about 1.5 billion metric tons.

Hydration of Cement

What happens when water reacts with the different components of the cement powder is a central question in cement science. In order to answer this complicated question scientists have studied the rates of reaction and heat liberation when water has been added to the different compounds separately.

Alite reacts with water to form calcium silicate hydrate and calcium hydroxide, which is also known as portlandite. The hardened paste has high strength when the reaction is completed, and because alite is the most abundant compound in cement, it also makes the dominant contribution to the mechanical properties of the final product. The hydration reaction proceeds at an appreciable rate a few hours after the addition of water and lasts up to about 20 days. The reaction of alite with water is accelerated by aluminate and gypsum.

Belite reacts with water at a slower rate than alite but the end product is the same. It takes about 2 days for the hardening process to get started and about a year to be completed. The mechanical strength of fully hydrated belite is similar to that of hydrated alite.

The hydration of the aluminate phase is very fast and it is essentially over within the first few hours. The contribution of the final product to the mechanical strength of the hardened cement paste is fairly low. It is also susceptible to attack by sulfate ions, which leads to expansion and weakening of the final product.

The final product of the reaction of ferrite with water is not known but its contribution to the ultimate strength of the paste is modest. Like alite and belite it is not attacked by dissolved sulfates.

The main features of the hydration reaction of the main components in cement are shown in Table 57.2.

In the hydration reaction alite absorbs about 40% by weight of water, of which 24% is chemically bound, and releases 500 J/g. For belite, 21% by weight of water is chemically absorbed, only 250 J of heat per gram are released, and less than half the amount of slaked lime is formed compared with the reaction of alite with water. Hydration of the aluminate phase is the reaction, which consumes most water, up to twice its own weight of water can be absorbed in the final product, and releases most heat, 900 J/gram.

When water is added to the mixture of cement powder and aggregate the reaction of the main components, as well as some others, which will be discussed subsequently, will get under way. Although the hydration process is not understood down to the finest detail, much insight and understanding has been gained by the advent of modern analytical equipment, for example, the scanning electron microscope. The initial hydration, lasting a few minutes, involves the alite-water and aluminate-water reactions and rapidly leads to formation of a hydrous gel of colloidal silica and alumina particles at the interface between the water and the cement grains. The gel envelops the cement particles and the doubly charged calcium ions diffuse rapidly out of the gel and into the surrounding water, where the calcium ion concentration is controlled by the precipitation of crystals of calcium hydroxide. Removing calcium ions from the originally homogeneous gel, resulting in a gel, which essentially is a silica gel, leads to a build up of osmotic pressure, which periodically causes rupture of the water-gel interface. When this happens, the calcium hydroxide and silica components are brought together, and a precipitate of calcium silicate is formed in a shape similar to a volcano crater. Repeated rupturing of the water-gel interface at the craters leads to the formation of hollow needle-shaped projections, known as fibrils, sticking out from the cement grains like the burs of a burdock. The fibrils can lock together by a Velcro-like mechanism, forming a strong bond between the cement particles.

Gypsum is an important extra factor in the hydration process. Although a minor component of the cement powder, present in an amount corresponding to between 2 and 5% of the total weight, it effectively regulates the activity of the aluminate phase. A few minutes after the addition of water, needle-shaped crystals of ettringite, $3\text{CaO}\cdot\text{Al}_2\text{O}_3\cdot 3\text{CaSO}_4\cdot 3\text{H}_2\text{O}$, appear at the surface of the aluminate particles, slowing down the aluminate-water reaction. The alite-water reaction proceeds at its slower

TABLE 57.2
Hydration Reactions

| | Chemically bound water weight % | Heat of hydration joules/g ^a | Ca(OH) ₂ formed weight % |
|---|------------------------------------|--|--|
| $2(3\text{CaO}\cdot\text{SiO}_2) + 6\text{H}_2\text{O} = 3\text{CaO}\cdot 2\text{SiO}_2 + 3\text{Ca}(\text{OH})_2$ Alite aquagel of Ca-silicate | 24 | 500 | 48.7 |
| $2(2\text{CaO}\cdot\text{SiO}_2) + 4\text{H}_2\text{O} = 3\text{CaO}\cdot 2\text{SiO}_2 + \text{Ca}(\text{OH})_2$ Belite aquagel of Ca-silicate | 21 | 250 | 21.5 |
| $3\text{CaO}\cdot\text{Al}_2\text{O}_3 + 6\text{H}_2\text{O} = 3\text{CaO}\cdot\text{Al}_2\text{O}_3\cdot 6\text{H}_2\text{O}$ Aluminate aquagel of Ca-aluminate | 40 | 900 | — |
| Typical values for fully hydrated Portland cement | 25 | 400 | 15–25 |

^aHeats of hydration after 28 days.

rate, as does the belite-water reaction with its still slower rate, producing calcium-silicate hydrate fibrils. Eventually, the ferrite-water reaction gets started, producing final products, the structures of which are still unknown. In addition to the crystals of ettringite, plate-shaped crystals of monosulfate are also formed. After about 5 hr the cement paste is set into an open three-dimensional network, filled with colloidal particles. At this point the strength is quite low but the paste is mechanically stable. The hardening process now begins and lasts up to about a month. The hydration products increase in amount and the fibrils, which are either amorphous or fine-grain crystalline, increase in length. The number and size of the calcium sulfate crystals increase. As these reactions proceed, more and more of the available volume becomes filled, and ultimately there is a considerable amount of interaction and bonding between the individual structures, i.e., the various hydration products and the aggregate particles.

Flaws in Cement

Cement and concrete are ceramics and are therefore brittle, which is a consequence of their hardness, but not weak materials. On the contrary, they are very strong materials for example modern concrete, which in this case means a concrete containing superplasticizers and having low water to cement ratio, for example, 0.3, has a compressive strength of up to 100 MPa per square meter. However, defects, for example, in the form of holes or gaps between particles, will seriously weaken the material. Applied stresses will concentrate at the tip of a flaw and will wedge and propagate it right through the ceramic material. In order to estimate the effect of flaws on the mechanical properties of materials [7] studied the distribution of stress in a large plate with a defect in the form of an elliptical hole of length, L , and radius of curvature, r , at the narrow end. He calculated that the stress, which was uniformly applied to the material, far from the hole, was increased by a factor of $2(L/r)^{0.5}$ near the narrow end of the hole. The compressive strength of hardened cement made from a paste containing too much water – for example, a water-cement ratio of 0.7 instead of a more suitable value of about 0.4 – may well drop to about 10 MPa per square meter, due to a cement structure containing many pores. A reduction of the compressive strength by a factor of 10, because stress at the narrow end of the pores has increased by the same factor, would for instance correspond to elliptical holes of length $5\ \mu\text{m}$ and radius of curvature of $0.2\ \mu\text{m}$. Holes of that size and roughly that shape can be seen in incorrectly made concrete [8].

A necessary condition for concrete to obtain its ultimate strength is thus that it is able to form the densest possible structure, that is, a structure as free from pores as

possible, during the hardening process. Now, there are several reasons why the structure of hardened cement may deviate from this ideal structure. Too much water in the cement paste is one. A water-cement ratio of about 0.4 corresponds to the minimum amount of water required to react with the individual components of the paste and keep the paste workable, which corresponds to a paste containing conventional flow additives, plasticizers or water reducers. With so called superplasticizers, the water-cement-ratio can be reduced to about 0.3. However, more water in the paste makes it easier to handle and some builders may be tempted to add extra water so as to make their job easier, but this extra water is not used up in the hydration reactions, and this leads to a rather porous solid with a strength below the ultimate. Reactions that are accompanied by an increase in volume are detrimental. Any expansion that occurs when the solidification processes of the other components are underway can open small cracks, which can seriously weaken the hardened cement. The aluminate phase reacts vigorously with water under strong heat evolution and expansion. Gypsum moderates the activity of the aluminate phase and is a critical component in modern cement. Moreover, the aluminate phase is susceptible to attack by sulfates, which interact with it and causes expansion. The minor components, see [Table 57.1](#), do not always exert an advantageous influence, and modern cement standards specify a maximum content of these compounds. The reactions of the free oxides of calcium and magnesium with water to hydroxides are accompanied by an increase in volume. The other two minor components in cement, sodium sulfate and potassium sulfate, accelerate the hydration reaction and promote rapid setting of the paste. Early congealing is inconsistent with high ultimate strength.

SILICA IN CEMENT

For reasons of utilizing waste materials and decreasing overall energy consumption certain inorganic materials, called mineral additives, such as fly ash and ground granulated blast furnace slag are added to the cement paste. Mineral additives take part in the hydration reaction and thereby make a substantial contribution to the hydration product. For reasons of obtaining durability and strength above the normal range, silica in the form of silica fume or colloidal silica is being used. Cement containing mineral additives is often called composite cement.

Silica Fume

Silica fume is a by-product, in the form of a very finely particulate powder, of the production of silica or silica alloys in an electric furnace. High-quality silica fume consists of spherical particles, which have a density of $2200\ \text{kg m}^{-3}$ and a BET specific surface area of $15\text{--}25\ \text{m}^2\ \text{g}^{-1}$, corresponding to an average particle size

TABLE 57.3
Chemical Composition of Silica Fume

| Compound | % Weight | Compound | % Weight |
|--------------------------------|-----------|-------------------|----------|
| SiO ₂ | 94–98 | K ₂ O | 0.2–0.7 |
| Al ₂ O ₃ | 0.1–0.4 | Na ₂ O | 0.1–0.4 |
| Fe ₂ O ₃ | 0.02–0.15 | C | 0.2–1.3 |
| MgO | 0.3–0.9 | S | 0.1–0.3 |
| CaO | 0.08–0.3 | | |

Source: Adapted from reference [9].

from about 100 to 200 nm [9]. The chemical composition of silica fume is shown in Table 57.3.

Silica fume, like other mineral additives, has pozzolanic activity, that is, it reacts with Ca(OH)₂, formed during the hydration of alite and belite (see the first two equations, Table 57.2), and produces more calcium-silicate aquagel, the actual binder material in cement. However, being made in high heat, the surface of the silica fume particles contains very few hydroxyl groups, or silanol groups, which are necessary for reaction with water and calcium hydroxide. It will therefore take some time before the particle surface has become rehydroxylated in the warm, highly alkaline environment of the cement paste and the pozzolanic activity of silica fume typically reaches a high value first in the period 7–14 days after mixing.

The fine particles of silica fume fill spaces between clinker grains, producing a denser paste. It also densifies the interfacial transition zone between cement paste and aggregate, which increases the strength and lowers the permeability. Papadakis [10] investigated the effect of adding between 5 and 15% by weight of silica fume to concrete and found that the compressive strength increased by 10% at 5% addition and by 20% at 15% addition.

Colloidal Silica

Iler [11] defines colloidal silica as stable dispersions or sols of discrete particles of amorphous silica in water, called aquasols or hydrosols, or in an organic solvent, then called organosols. Commercial silica sols are fluid, the viscosity is less than 35 mPas, and stable toward gelling and settling in the pH range between 8 and 10. They have been stabilized, or brought into this pH range, by adding an alkali, for example NaOH, KOH, LiOH, or NH₄OH, to the sol. The silica particles are negatively charged and charge neutrality is brought about by the presence of positively charged counter ions, for example, Na⁺, K⁺, Li⁺, and NH₄⁺. There are also available commercial silica sols consisting of positively charged particles, which have been stabilized at pH of about 2 by adsorption

of polycations of for instance aluminium onto the surface of the particles. Most commercial silica sols are quite monodisperse and consist of dense, discrete spheres with a range of diameters between about 5 and 100 nm. The maximum concentration depends on particle size and is 15% by weight for 5 nm particles, 30% by weight for 8 nm particles and at least 50% for 100 nm particles. There are also commercial sols that have deliberately been made polydisperse or where the particles are not discrete spheres but instead chains of linked spheres. The appearance of silica sols depends on particle size, particle size distribution and concentration. They look milky if the particle size is large and the concentration is high, opalescent if the size is intermediate or clear and almost colorless when the diameter of the particles is in the smallest size range.

In contrast to silica fume, the surface of the particles of colloidal silica is fully hydroxylated and contains 4.6 OH silanol groups per nm² [12]. This fact, together with the much higher specific surface area, makes the pozzolanic activity of colloidal silica much higher than that of silica fume. Wagner and Hauk [13] mixed 15 nm colloidal silica with cement paste and noted a 36% increase, compared with a reference paste without colloidal silica, of the early strength, that is the early strength development during the first 1–7 days. In fact, Skarp and Sarkar [14] pointed out that ultrafine silica particles will harden the cement paste very fast because most of the available water is consumed in the early stage of gel formation, due to the very high pozzolanic activity of colloidal silica. The resulting high early strength, however, is gained at the expense of low final strength, caused by the pore structure created during the very rapid early gel formation. On the other hand, they claim that this problem, caused by excessively high pozzolanic activity of colloidal silica, has been solved and they report that small amounts of colloidal silica added to the concrete mixture, 0.15–0.20% silica based on the weight of the concrete mixture, significantly increased the final strength, reduced the chloride ion permeability and increased the sulfate resistance of the concrete. The properties of the colloidal silicas used are shown in Table 57.4.

Had the sols contained spherical particles of uniform size the particle sizes of sols A and B would have

TABLE 57.4
Physical Properties of Colloidal Silica

| Product | Sp. Surface area (m ² /g) | Solids (%) | Particle size (nm) |
|---------|--------------------------------------|------------|--------------------|
| A | 400 | 24 | 35 |
| B | 80 | 50 | 45 |

Source: From reference [14].

TABLE 57.5
Effect of Colloidal Silica on the Compressive Strength (psi) of Concrete

| Type silica | SiO ₂ , % | 1 Day | % Increase | 7 Days | 28 Days | % Increase |
|-------------|----------------------|-------|------------|--------|---------|------------|
| -(Sample1) | — | 4.300 | — | 6.840 | 8.680 | — |
| A(Sample2) | 0.15 | 5.300 | 23 | 8.010 | 9.680 | 12 |
| B(Sample3) | 0.15 | 5.580 | 30 | 8.030 | 9.840 | 13 |
| B(Sample4) | 0.20 | 4.470 | 4 | 8.280 | 9.970 | 15 |

Source: Adapted from Skarp and Sarkar [14].

been 7 and 34 nm, respectively. Instead the average particle sizes are considerably higher, more so for A than for B, indicating that the sols are polydisperse, sol A being the most polydisperse and also containing the smallest particles.

The cement pastes, with or without colloidal silica, had a water to cement ratio of 0.35 and contained sulfonated naftalene formaldehyde resin (NSF) superplasticizer. The colloidal silica was added to the concrete mixture after the superplasticizer so as to minimize premature gelling. The compressive strength of the concrete samples are shown in Table 57.5.

Addition of colloidal silica increases the 1-day strength by up to 30% and the 28-day strength by up to 15%. Colloidal silica of type B may be somewhat more effective than type A, although the increase of the 1 day strength is only 4% at 0.20% of type B, as compared to 30% at only 0.15% of the same type of silica sol. Obviously, judicious choice of the average particle size and the particle size of silica sols makes it possible to fine-tune the pozzolanic activity of the silica so that significant increases of both the early stage strength and the final strength of the concrete can be accomplished.

Tables 57.6 and 57.7 show that addition of colloidal silica to a concrete mixture will substantially reduce chloride ion permeability and enhance sulfate resistance.

Greenwood et al. [15] showed that the smaller particles in the sol provided most of the sulfate resistance whereas the larger particles provided the chloride resistance, but the two particle size regions appeared to interact and gave rise to significant synergism.

TABLE 57.6
Effect of Colloidal Silica on the Chloride Ion Permeability of Concrete

| Silica, % | 0 | 0.1 | 0.15 | 0.20 |
|------------------------------------|------|------|------|------|
| Chloride ion permeability, coulomb | 3600 | 3200 | 2400 | 1700 |

Source: Adapted from reference [14].

The availability of modern workability additives, e.g., superplasticizers such as polycarboxylates, has made it possible to develop highly fluid concrete, HFC, which does not bleed or segregate in use. Self-compacting concrete, SCC, (in the U.S.: self-consolidating concrete) is a particular type of HFC, which achieves significant benefits and advantages in many types of constructions. Thus, by using SCC it is possible to fill the mould completely and uniformly, even moulds of difficult and complicated shapes. There is no need to vibrate the material so as to eliminate voids and holes formed when conventional, often sluggish concrete is poured into the form. Moreover, the quality of the concrete surface is often very good, minimizing the need for expensive and time-consuming after-treatment.

Skarp et al. [14], however, pointed out that poor stability, that is bleeding or segregation, and loss of workability are two main concerns when working with SCC. A concrete mixture is said to be workable if it can be maintained in fluid form until the casting moment. The term workability time is defined as the time the concrete mixture remains workable. They attribute the instability to deficiencies in mix design and the loss of workability to incompatibility between the cement and the superplasticizer.

Greenwood et al. [16] showed that small amounts, 0.2% by weight of SiO₂, of colloidal silica of small particle size, corresponding to a specific surface area of 900 m² g⁻¹, significantly increased the workability time

TABLE 57.7
Effect of Colloidal Silica on the Sulfate Resistance of Concrete

| Weeks | Control % expansion | Sol A, 0.13% SiO ₂ , % expansion | Sol B, 0.13% SiO ₂ % expansion |
|-------|---------------------|---|---|
| 4 | 0.01 | <0.01 | <0.01 |
| 8 | 0.021 | <0.01 | <0.01 |
| 12 | 0.036 | 0.015 | 0.014 |
| 16 | 0.050 | 0.017 | 0.016 |

Source: Adapted from reference [14].

of concrete mixtures containing polycarboxylates as superplasticizers. It required much larger amounts of colloidal silica of larger particle size, corresponding to a specific surface area of $80 \text{ m}^2 \text{ g}^{-1}$, 1.25% by weight of SiO_2 , or of fumed silica, 10% by weight of SiO_2 , to achieve the same results. In contrast to the control, containing no silica, the concrete mixtures containing either colloidal or fumed silica showed no bleeding.

Aluminum-modified sols, compared with unmodified sols of the same specific surface area, as additives in concrete mixture containing polycarboxylates as superplasticizers achieved not only increased workability time but also improved strength, Greenwood et al. [17].

COLLOIDAL SILICA AS RETENTION AID IN PAPER MAKING

Colloidal silica was introduced as retention aid in paper making less than 25 years ago. The home page of Compozil[®] states that in year 2000, 347 paper machines all over the world with a combined production of 26.3 million metric tons of paper and paper board used colloidal silica as retention aid, which probably makes it the largest application of colloidal silica today. Otterstedt and Brandreth [18] described the use of colloidal silica as retention aid in paper making and compared it with other types of retention aids. This section is a substantially abbreviated version of their work, but supplemented with the most recent developments of colloidal silica as retention aid in paper making.

The word paper is derived from papyrus, a sheet made in ancient times by pressing together very thin strips of an Egyptian reed, cyperus papyrus. The modern material, paper) consists of sheet materials that are comprised of bonded, flexible, cellulose fibers which, while very short) 0.5–4 mm, are about 100 times as long as they are wide. Small particle fillers or pigments, in the form of clays or other inorganic materials are used to improve the properties of paper, that is, opacity, brightness and printability, or to improve the economics of the papermaking process. In this chapter we will focus on the use of small particles as process aids to improve retention and dewatering on paper machines.

FILLERS

Mineral fillers in the form of small particles are used in paper for various reasons. There has always been the economic incentive to substitute low-cost fillers and extenders for some high-cost fibers in paper, but there is also the incentive to improve several of the properties of paper. The use of fillers increases opacity and brightness of the paper and also improves printability by making printing ink absorption more uniform, gives higher gloss after calendering and leads to better “feel” and dimensional stability.

The disadvantages of using fillers in paper are reduced mechanical strength, caused by the filler particles interfering with the hydrogen bonding between the cellulose fibers, heavier paper, greater wear on the wire of the paper machine, and higher content of fine material in the circulating water system.

Pigments, which are also small particles of inorganic materials, are used to improve the optical properties of paper and are usually more expensive than cellulose fibers. Pigments are also often made synthetically, whereas most fillers are ground minerals. The most common types of fillers are kaolin or clay, the most important filler, ($\text{Al}_2\text{O}_3 \cdot 2 \text{ SiO}_2 \cdot 2 \text{ H}_2\text{O}$), talc ($3\text{MgO} \cdot \text{H}_2\text{O}$), calcium carbonate (CaCO_3), gypsum ($\text{CaSO}_4 \cdot 2\text{H}_2\text{O}$) and mica ($3\text{Al}_2\text{O}_3 \cdot \text{K}_2\text{O} \cdot 6 \text{ SiO}_2 \cdot 2 \text{ H}_2\text{O}$).

PAPER-MAKING

Different paper machines have various configurations at the wet end of the machine, but Figure 57.1 shows schematically a representative setup. In the mixing chest fibers and paper chemicals are mixed to an aqueous slurry, the furnish, containing about 0.5–2% fiber. Some of the chemicals may be added at a later stage, for example, to the machine chest or before, or into a pump. From the head box, the furnish is filtered on a wire screen, where the fibers adhere weakly to one another. When more water is removed from the mat formed on the screen by suction, the sheet becomes stronger, but is still relatively weak. When the sheet is dried it becomes still stronger, and becomes the material known as paper. Modern paper machines produce an endless paper sheet, up to 10 m wide, at a speed of over 20 m/sec, that is, one hectare (more than two acres) every 50 sec. The machine is

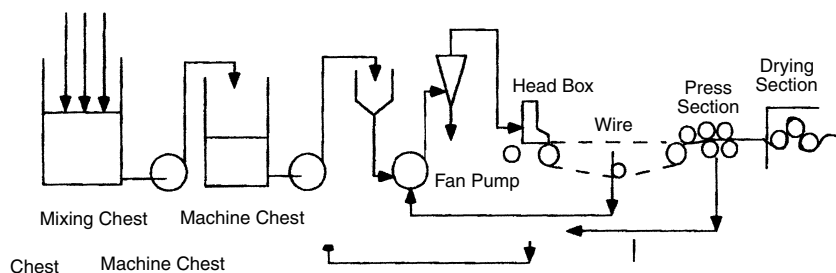


FIGURE 57.1 The wet end of a paper machine. From Otterstedt and Brandreth, [18]. Courtesy Plenum Press.

more than 100 m long and produces about 250,000 metric tons per year.

Environmental and economic pressures have reduced water usage in paper production in the last 30–40 yr from 80 to 90 m³ per metric ton to less than 10 m³/ton. During the last decade many efforts have been made to reduce the use of water even more with the ultimate objective of achieving a paper mill that is 100% closed.

THE PROBLEM

The achievement of a closed or nearly closed paper mill with respect to water usage is intimately related to the retention of fiber fines and chemicals and other additives in the furnish on the wire. Poor retention will cause the fines and other small particles to go through the wire with the water and make reuse of the back water difficult or impossible; see Figure 57.1. The nature of the problem is further illustrated by Figure 57.2, showing the dimensions in the wet end, and Figure 57.3, which compares the size of the holes in the wire with the sizes of the cellulose fibers, fines, filler particles and the various chemical additives present in the furnish.

The difficulty in retention is further aggravated by the fact that all the particles of the furnish are negatively charged and therefore have no bonding to each other to form aggregates large enough not to pass through the holes of the wire.

The obvious solution to the problem is therefore to put into the system particles or additives of opposite charge to cause agglomeration of the paper components to larger clumps that cannot go thorough the wire. This is accomplished by so-called retention aids.

RETENTION, RETENTION MECHANISMS AND RETENTION AIDS

The term retention refers to the holding back of the components of the stock during dewatering. The fibers are retained on the wire whereas fillers, fines, and additives of colloidal size may be washed through the mat formed

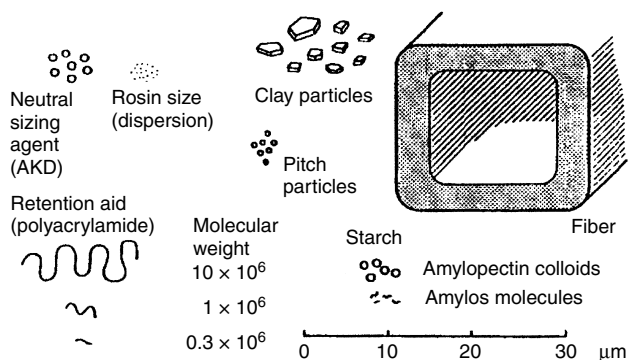


FIGURE 57.2 Dimensions in the wet end of the papermaking process. From Otterstedt and Brandreth, [18]. Courtesy Plenum Press.

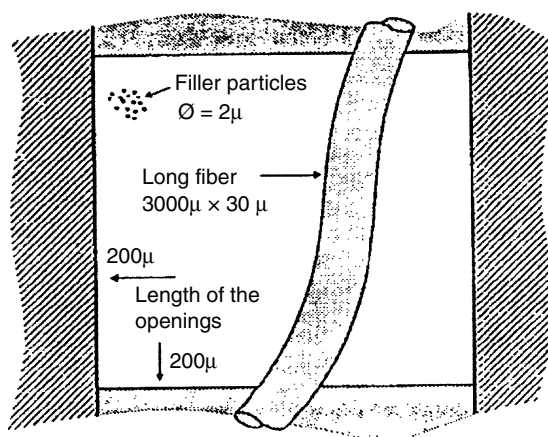


FIGURE 57.3 Small particles on the wire in the papermaking process. From Otterstedt and Brandreth [18]. Courtesy Plenum Press.

on the screen. Retention is accomplished by a combination of mechanical means, i.e., filtration, and the physico-chemical mechanism of agglomeration or flocculation.

Mechanical retention during sheet formation on the wire may be considered a filtration process. The fibers in the stock, which are 500–4000 μm long and 20–100 μm thick, are captured on the wire and form a three-dimensional network consisting of 2–100 layers of fibers on the wire. As the layers form, they capture progressively smaller fibers and other colloidal particles in the stock suspension, making the pore structure gradually finer with the largest pores on the wire side and the finest on the top side. Mechanical retention is least efficient in the beginning of the sheet formation and, although it becomes more effective as more layers form, it cannot retain a satisfactorily high proportion of the finest components of the stock. The losses for newsprint are typically about 50%.

By adding special chemicals, retention aids, to the stock, the fines and other colloidal components can be made to flocculate or aggregate into agglomerates too large to go through the wire. Retention aids may consist of either one component or two components. They can act by changing the electrostatic repulsion forces between colloidal particles or affect the stability of colloids by adsorbing on two or more particles causing them to form larger aggregates.

Although good retention is most likely attained by the joint action of more than one mechanism and a given retention aid may act by several mechanisms, it is still useful to distinguish between some principal types of aggregation mechanisms.

There are no sharp distinctions between the terms of coagulation and flocculation, but here coagulation denotes aggregation by the action of low molecular weight electrolytes whereas flocculation means aggregation brought about by polymers, which can be natural or synthetic.

In high-speed modern paper machines the floc is subjected to high shear, which may tear the floc apart. The trend toward reduced water usage in the production of paper increases the amounts of soluble anionic wood polymers and electrolytes in the stock, which will also affect the retention on the wire.

The principal types of retention mechanisms are:

1. *Charge neutralization*: Electrolytes are the simplest kind of coagulants that can be used to improve retention. They act fully in accord with the DLVO theory by screening the charges and compressing the electrolytic double layer of the negatively charged particles of the stock, thus allowing attractive forces to come into play and aggregate the particles. Aggregation by charge neutralization is a fairly slow process which has lost some of its importance as the speed of paper machines has become ever faster.
2. *Hetero-coagulation*: This mechanism involves adsorption of oppositely charged particles, e.g., complexes of resin acids and aluminum sulfate, on the surfaces of fibers and filler particles. Hetero-coagulation is sensitive to soluble anionic wood polymers and electrolytes, with which cationic sizing particles, preferentially interact.
3. *Patch flocculation-Patching*: Patching resembles charge neutralization, but is different. In this mechanism cationic polymers are strongly adsorbed in a flat configuration on the negative surfaces of the particles, on which they form cationic patches. Adsorption leads to partial charge neutralization and electrostatic attraction between oppositely charged patches on different particles leads to flocculation. If the cationic polymer is small and the patches are smaller in size than the thickness of the electrolytic double layer—which depends on the concentration of electrolytes—aggregation will take place by the mechanism of charge neutralization.

A characteristic difference between charge neutralization and patching is that the rate of coagulation for the former mechanism increases with electrolyte concentration. Once an optimal electrolyte concentration has been attained, however, the rate of flocculation by patching will decrease with electrolyte content due to the fact that the electrolyte cations will force the polymer from the particle surface.

Relatively short-chained cationic polymers of average molar mass and high charge density are suitable for patch flocculation. Modified polyethylene imines, polyamines, and polyamide-amine-epichlorohydrin resins are in this category.

4. *Bridging*: In this mechanism flocculation is accomplished by long-chain, i.e., high molar mass, polymers forming binding bridges between particles. For effective bridging to occur, it is very important that the polymers adsorbing on the surface of the particles form loops and tails that protrude into the solution. To what extent this happens depends on the type of polymers, contact time, and properties of the surface of the particles to be flocculated. Suitable polymers are weakly charged or non-ionic, that is, high molecular-mass polyacrylamide and polyethylene oxide. Flocs made by bridging are large but fairly easily broken by shearing, which may tear the bridging polymers and retard the process of re-flocculation.
5. *Complex flocculation*: Flocculation by any of the four mechanisms described above can be accomplished by only one flocculant or retention aid. Much more effective flocculation and retention can be achieved by using combinations of retention aids. The most common combinations are between oppositely charged retention aids, which can form complexes of varying strength with each other. It is, however, also possible to use combinations of nonionic retention aids that can form complexes by hydrogen bonding.

Some important types of retention aids are the following natural or synthetic polymers:

Polyethylene imines, PEI, are strongly cationic and strongly branched polymers with a molar mass between 100,000 and 1,000,000 (g/mole)

Polyethylene amines, contain secondary amine groups and are linear, strongly cationic polymers with a molar mass of about 100,000.

Polyacrylamides, PAM, are nonionic polymers with a molar mass of about 1,000,000.

Cationic polyacrylamides, CPAM, contain tertiary amine groups which can be quaternized. Molar mass is about 1,000,000.

Anionic polyacrylamides, A-PAM, can be synthesized by co-polymerizing acrylamide with acrylic acid. It contains anionic carboxyl groups and has a molar mass of about 1,000,000.

Polyethylene oxide, PEO, is nonionic and has a molar mass of about 1,000,000.

Cationic starch is modified natural polymer. Molar mass about 100,000,000.

DUAL RETENTION AID SYSTEMS

Cationic natural and synthetic polymers have long been used to improve retention of fines and fillers on the wire

of paper machines. Such polymers, that is, cationic starch or cationic polyacrylamide, produce a high degree of flocculation in the furnish. This floc, however, is not very strong and is easily broken and redispersed by hydraulic shear. Furthermore, when long-chain polymers are used, chain rupture and rearrangement of the polymer fragments on the particle surfaces may occur. Nevertheless, single-component retention aids improve the first-pass retention, though not to the same degree as dual retention aid systems.

Such systems have been used in the paper industry for many years. Component one, a cationic polymer, usually of the patching type, is first added to the furnish, followed by the addition of the second component, an anionic polymer of the bridging type. Figure 57.4 schematically compares single component and dual retention aid systems. The application of retention aids has been optimized in the sense that the retention maximum in the figure corresponds to a zeta potential of value zero, i.e., the charges on the positive components in the system exactly balance the charges on the negative component, which may be difficult to accomplish in an actual situation. When an optimal amount of cationic component, in this case cationic starch, in the single-component system, is added, the furnish system has no charge and flocculation and retention are maximized. In the dual system cationic starch has to be present in the furnish so as to reach zero-potential after the given amount of the second component, an anionic polymer, has been added. Thus, the maximum in flocculation and retention is not only higher than for the single component system, but it also occurs at larger dosages of cationic starch, which is beneficial since starch is not only a retention aid, but is also an additive that increases the dry strength of paper.

In the last 10–15 years a special kind of dual retention aid, a micro particle — containing flocculant system, often referred to as microparticulate retention/dewatering aid, was developed. In one of the commonly used commercial systems, the so-called Compozil® system, comprise

colloidal silica in combination with cationic starch or cationic synthetic polymers. Andersson and Larson [19] and Andersson and Lindgren [20]. In this system, the cationic polymer is added first and the extensive flocs then formed are broken down and partially redispersed by high-shear forces. The anionic microparticles are added just before the paper is formed and cause final flocculation of the furnish. A dual retention system, having colloidal silica as the anionic component has the following characteristics [21]:

- strong, reversible flocculation,
- more effective dewatering in the wire and press sections,
- formation on the wire yields sheets of higher porosity and permeability.

The Compozil® system was recently studied by Andersson and Lindgren [20]. They used a Britt Dynamic Drainage Jar to investigate the retention effects of combinations of various types of anionic colloidal silica, ACS, with either cationic starch or polyacrylamides of different charge density. The furnish consisted of a 60/40 mixture of fully bleached birch and pine sulfate pulps with 30% (based on total solids) chalk as the filler. The solids content and pH of the furnish were 0.5% and 8.1, respectively. The polyacrylamides had charge densities between 2 and 25% cationicity, corresponding to between 0.25 and 3.0 meq/g, and a molecular weight of 5×10^6 . The cationic starch had a degree of cationic substitution of 0.4, corresponding to 0.25 meq/g.

The anionic colloidal silica used in this study was either monodisperse colloidal silica with a particle size of about 4 nm or so-called structured colloidal silica, consisting of linear aggregates of about 4 nm particles. Structured colloidal silica is, like monodisperse colloidal silica, characterized by its specific surface area and charge density, which decreases with pH but can be maintained high even at pH as low as 3 and 4 by aluminizing the

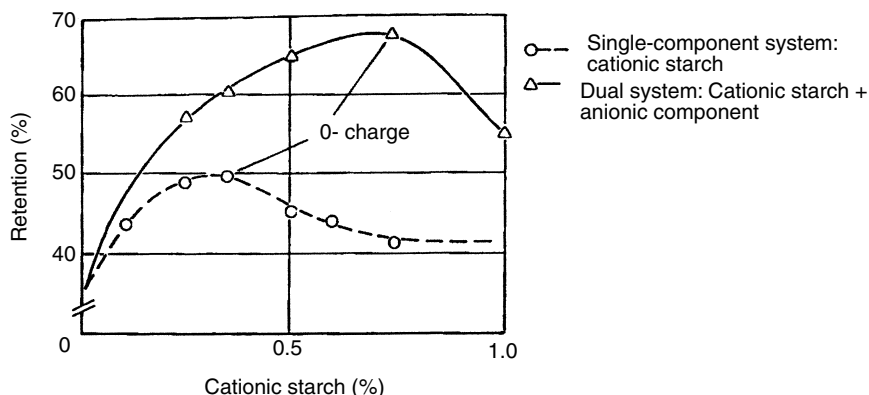


FIGURE 57.4 Single-component and dual retention aid systems. From Andersson and Larsson [19]. Courtesy Arbor Publications.

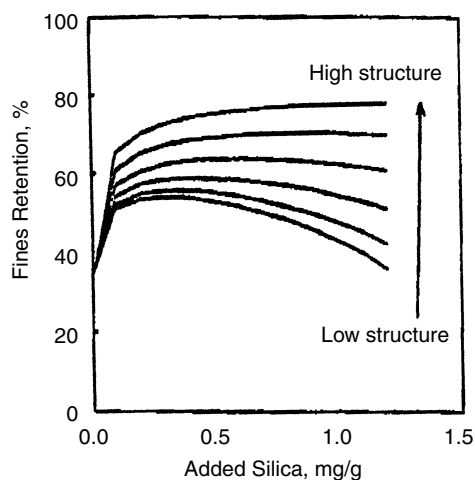


FIGURE 57.5 Retention model for the CPAM-ACS system. From Andersson and Lindgren [20]. Courtesy Arbor Publication.

colloidal silica with sodium aluminate, but also by some other properties. One is the S-value, which is defined as the percentage of silica in the dispersed phase and can be obtained from viscosity measurements [22]. A high S-value indicates well-dispersed, non-aggregated colloidal particles, whereas a low value suggests that the primary particles have formed microaggregates, perhaps linear structures containing up to 7–8 primary particles. Another one is the average size of the microaggregates, A , as determined by dynamic light scattering, DLS. Other ones are the length, L , and the width, W , of the microaggregates as determined by DLS and viscosity measurements.

From their results, Andersson and Lindgren concluded that for both the cationic starch-ACS and CPAM-ACS systems the main flocculation mechanisms were electrostatic interactions, for example, charge neutralization and bridging.

They also used their data to construct a model for the system CPAM-ACS, shown in Figure 57.5 for a constant dosage of CPAM. Each curve shows the predicted retention for an ACS with a constant S-value. As expected, maximum retention increases with increasing structure, or degree of microaggregation, of the ACS.

Greenwood et al. [23] showed that chemical modification of ACS, comprising stabilization of structured colloidal silica by amines instead of by NaOH, which is the most common method, not only improved the retention but also the dewatering on the wire of the paper machine, see Figure 57.1. They found that quaternary amines gave the best results, followed by tertiary and secondary amines.

COLLOIDAL SILICA IN LEAD-ACID BATTERIES

Lead-acid batteries are one of the most common type of batteries. Most lead-acid batteries are flooded, that is,

they have a liquid electrolyte as in standard car batteries, but a significant and growing number have a solid electrolyte. Some of the advantages of a solid electrolyte in lead-acid batteries are little or no spill or splashing of highly corrosive sulphuric acid in case of accidents, no leakage if the battery is placed sideways or even upside-down and longer life time, because no accumulation of precipitated lead at the bottom of the battery, which may cause discharge, can occur.

There are two different methods of immobilising the electrolyte, a solution of lead sulfate, that is, making a solid electrolyte, in VRLA, that is, *valve-regulated lead-acid* batteries. In AGM-VRLA batteries, the electrolyte is immobilized by being absorbed in *absorptive glass-fiber mats*, placed between the electrodes. This type of batteries can produce high starting currents and be rapidly recharged, and are used in for example, uninterrupted power supply systems (UPS). In GEL-VRLA batteries, the electrolyte is immobilized by being absorbed within the very fine pores of a silica gel, which can be made from different silica materials. GEL-VRLA batteries have long life span, good cycling characteristics and relatively low current, and they are used in applications such as telecommunication and solar energy devices and motive power applications, for example, golf cars, wheel chairs and loading trucks [25]. GEL-VRLA batteries are predicted to be used as a second battery in cars to supply steady, nonsurging power to the increasing number of electronic components in modern cars.

Silica gels can be made from different starting materials, for example, sodium silicate solutions, fumed silica or silica sols. Judging from the patent literature, fumed silica appears to be the most common starting material for making silica gels for GEL-VRLA batteries, but recently, in the last several years, some very promising work has been reported on making silica gels for batteries from colloidal silica in the form of silica sols.

GELLING OF SILICA SOLS

At the ACS National Meeting, in Washington, D.C., 1990, Paul Yates gave a talk on the “Kinetics of Gel Formation of Silica Sols” [24]. He described that the gellation of silica sols is kinetically quite different from that of soluble silicates although the same factors are important, that is silica concentration, pH, salt content, temperature and particle size of the sols. Expressions were derived for the quantitative prediction of the gel times of colloidal silica dispersions over a wide range of these variables. The following exposé is a summary of Yates presentation.

Types of Gels

There are three types of silica gels, of which the first results from neutralizing dilute aqueous solutions of a silicate and is formed by the polymerization of silicic acid.

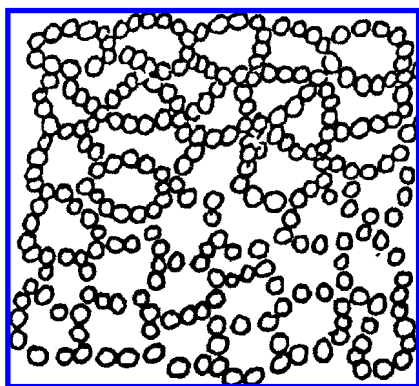


FIGURE 57.6 Structure of collision gel. From Yates [24].

The polysilicate ions extend as a three-dimensional cross-linked network throughout the solution.

The second type results from the collision of pre-formed colloidal silica particles to form three-dimensional chains of such particles, bonded at their junction points with siloxane bonds; see Figure 57.6.

The third type is a hybrid of the first two with polysilicic acid chains joining preformed colloidal silica particles. Hybrid gels are formed by neutralization of mixtures of silicates and colloidal silica sols.

Common Features in Gel Formation

Although the quantitative kinetic expressions for each of the three types of gel are different, they respond qualitatively in a similar way to most important variables. For all types of gels, gel times become shorter at higher temperatures, at higher concentrations, and in the presence of increasing concentrations of neutral salts.

The effect of pH is complex. Starting with strongly acid (low pH) systems, gel times initially decrease rapidly as the OH^- concentration is increased, then pass through a minimum and finally increase rapidly as the pH continues to increase. For all types of gels, the effect of salts in decreasing gel times is much more pronounced on the basic side than on the acid side, and the location of the minimum in the gel time versus pH curve is a very sensitive function of the neutral salt content and even of the specific salt employed.

The Central Mechanism in Gel Formation

The similarities described exist because the central polymerization mechanism is essentially the same for all types of gels. This mechanism also shows the key role played by the hydroxyl ion.

The First Role of Hydroxyl Ions — As a Catalyst

A silicon atom in silicic acid or at a surface normally has a coordination number of 4. The coordination number can

be momentarily expanded by adsorption of a hydroxyl ion simultaneously with adsorption of a sixth group such as a silanol group belonging to another silicic acid molecule or colloidal particle. This transition complex is unstable and water condenses out between the two silanol groups to form a permanent siloxane bond. The coordination number drops back to four and the hydroxyl ion is desorbed, regenerating it to continue its catalytic role elsewhere in the solution.

The Second Role of Hydroxyl Ions — Charge Repulsion

If the only role played by hydroxyl ions were a catalytic one, gel times would continuously decrease as the pH increased. The observed minimums in gel times and their rapid increase at high pH shows that the hydroxyl ion plays a dual role in the mechanism of formation of silica gels.

Silicic acid and silanol groups on the surface of colloidal silica particles are weak acids, and lose protons in basic solutions, thereby acquiring a negative electrostatic charge. This charge repels other negatively charged groups which attempt to approach. The charge increases rapidly as the pH increases.

For polysilicic acid, charge repulsion interferes with polymerization when the charged groups on the polysilicic acid polymer repel the negatively charged hydroxyl ion catalyst, which must be adsorbed on the already negatively charged polymer to perform its function.

In the collision of colloidal silica to form gels, the dominant charge repulsion is between the two negatively charged silica particles, which must collide before siloxane bonds can be formed at their surfaces.

The charge repulsion term will not be mathematically same for these different types of polymerization, but the effect on all three types of gels is that charge repulsion opposes the favorable catalytic effect of the hydroxyl ions, and at a sufficiently high pH, counterbalances it to lead to a minimum in the gel time.

The Role of Neutral Salts — Screening of Charge Repulsion

The reason why gel times are always decreased by the addition of a neutral salt is that when negatively charged groups of polysilicic acid, or surface groups on the colloidal particles, can be screened by a swarm of positively charged cations from neutral salts, their repulsion of approaching negatively charged species is substantially decreased. Higher the concentration of neutral salts, higher will be the probability of a number positive ions being located in screening positions around a negatively charged group.

Specific Salt Effects — Effect of Cations

The specific effects of salts come from differences in their screening ability. The larger size of the hydrated positively charged cation in the neutral salt, the more efficiently it can screen and the more rapid the gel time. The effect is particularly pronounced with large organic cations such as guanidine, tetramethylammonium, and tetraethanolammonium ions.

Effect of Anions

Even the anion of a neutral salt shows some specific salt effects. It probably does this through an indirect mechanism.

If the cations of a neutral salt are to be preferentially adsorbed as a double layer in the vicinity of the negatively charged groups of colloidal silica particles or polysilicic acid molecules, they will have to be recruited from the otherwise homogeneous mixture of anions and cations of the salt in the solution. This can only take place by removing them from the charge field of their own anions. The higher this charge field is, the less likely are they to concentrate around the polymer or colloid, and the less effective the salt will be in screening.

Neutral salts containing highly charged anions such as sulfate are not as effective screening agents as those containing monovalent anions such as chloride. Acetate salts are better screening agents than sodium chloride.

The Salt Effect Is Proportional to the pH

From the explanation just given, it is obvious that the salt effect will not be very strong on the acid side, since silicic acid polymers or colloidal silica surfaces do not have a high charge at low pH. It becomes more and more pronounced as the pH increases, since as the charge increases, the importance of screening will also increase.

The Effect of Temperature

The effect of temperature was not specifically studied in this work, but previous work in the literature shows that the activation energy for the central polymerization mechanism is about 80,000 J/mole. This means that the temperature coefficient will be about a factor of two in the gel time for every 10°C. change in the temperature. Activation energies will probably be different on the acid and the basic side, since the temperature coefficient for the charge repulsion effect will enter into the total activation energy in basic solution.

Differences between the Polymerization and Collision Mechanisms of Gel Formation

Although many of the features are common to both mechanisms they will not be mathematically the same. In the

case of the formation of gels by means of collision of colloidal silica particles, the important charge repulsion is that between two colloidal silica particles, whereas in silicic acid polymerization the charge repulsion is between the charged groups on the silicic acid polymer and the hydroxyl ion. Screening effects of neutral salts will also be quantitatively different.

Collision gels are extremely sensitive to the surface chemistry and surface composition of the colloidal particles. Small amounts of aluminum, for example, can greatly change the rates of collision. This is because such changes in surface chemistry strongly influence the charge on the colloidal silica particles, and thus the repulsion to be expected between two of them at any particular pH.

The basic structural units, which are doing the polymerization, are different in the two cases also, and the relationship of the concentration of silica to the polymerization rate will not be the same.

Kinetics of Collision Gels

Gels formed by the collision of colloidal silica particles in solutions containing only traces of silicate ions have entirely different kinetics than the other two types of gels. Under comparable conditions, gel times are 100 to several thousand times as long. The quantitative response to variables such as concentration, salt content, pH, and the surface area silica is also quite different.

The equation derived by Yates [24] for gels prepared from deionized "Ludox HS" mixtures of varying concentrations, pH values, and salt contents is given below as Equation (57.1).

$$\begin{aligned} \log t = & 5.85 - \text{pH} - \log (\Phi / (1 - 2.58\Phi)) \\ & + (1.333 - 1.482\Phi)(0.032 - 0.1183 \log c) \\ & \times (\text{pH} - 2.34)^2. \end{aligned} \quad (57.1)$$

Where t = gel time in minutes; Φ = volume fraction of silica; c = salt concentration.

This equation reproduced the gel times of 39 gels from solutions containing 10, 20, 30 and 40 wt.% SiO₂, at pH values of 3.5, 5.0, 6.0, 7.0, and 8.5, and salt concentrations of .01, .03, 0.1, and 0.3 N, with an average error of 0.11 units in the log gel time value. This is within the probable experimental reproducibility of this data.

Figure 57.7 shows the ability of this equation to reproduce gel times at a constant (0.1 N) salt concentration over a range of pH and silica concentrations. The solid lines were calculated from Equation (57.1).

It might be appropriate to review the physical meaning of each term in Equation (57.1). This will be done to indicate qualitatively how each of the variables affect this type of gel formation.

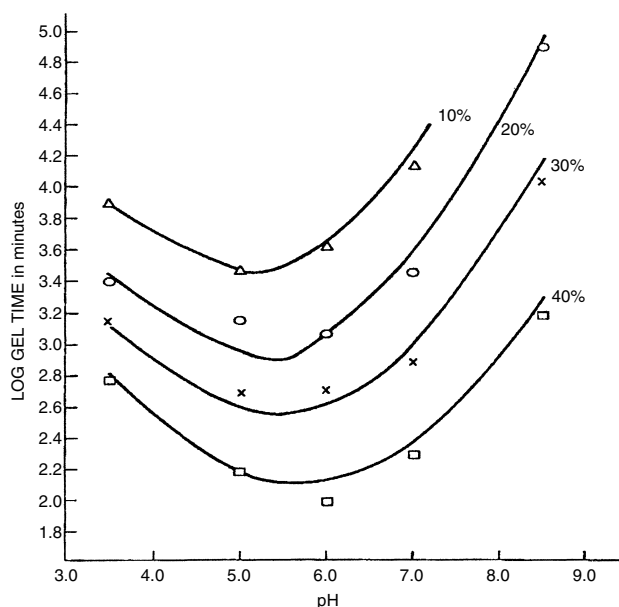


FIGURE 57.7 Effect of silica concentration on the gel time of collision gels at 0.1 normal salt concentration. From Yates [24].

The first term is a constant which includes the specific reaction rate constant for siloxane bond formation, the ionization product constant for water, the viscosity of water, and other miscellaneous numerical constants.

The second term, $(-pH)$ expresses the catalytic effect of the hydroxyl ion in decreasing gel time.

The third term, which involves Φ (the volume fraction of silica), expresses the effect of increasing the silica concentration in decreasing the gel time. The expression $\Phi/(1 - K\Phi)$ is used instead of Φ itself as a concentration variable, since the particles will physically touch one another long before the silica volume fraction becomes one (corresponding to a 100% concentration). The constant in the denominator of this expression, which has the value of 2.58 for the particular sample of deionized "Ludox" used in these gelling experiments, is identical to the constant, which appears in the Einstein–Mooney equation for the viscosity of spherical colloidal particles. This will vary with the degree of hydration and aggregation, or the % solids in the dispersed phase, of the silica particles.

The last and most complicated term in Equation (57.1) is the electrical repulsion term. As can be seen, for a fixed surface area (or particle size) of the colloidal silica, the charge repulsion is a function of the pH, the volume fraction, and the concentration of neutral salt.

The term $(pH-2.34)^2$ occurs because the electrical potential of the silica surface is proportional to the amount of (OH^-) adsorbed, and therefore is inversely proportional to the (H^+) ion concentration. The number 2.34 represents the zero point of charge for this particular colloidal silica, or the pH at which substantially no hydroxyl

ions are adsorbed. If some other sol were used, which had a different concentration of aluminum or other impurity atoms at the surface, this zero point of charge might occur at a different pH. This is the case, for example, with aluminum-modified "Ludox", which probably has a zero point of charge somewhere around a pH of 1.00 or lower. This term in the pH is squared because we are dealing with a charge repulsion between charged particles which are essentially identical to each other.

The term $(0.032-0.1183 \log c)$ accounts for the screening effect at the salt in decreasing charge repulsion. It will be noted that screening increases only with the logarithm of salt concentration, indicating much less sensitivity to variation in salt content than for the previous type of gels where the slope of the electrical repulsion term was proportional to the reciprocal of the salt concentration.

The constant .032 in the expression is proportional to the slope the charge repulsion term would have in a one molar salt solution when $\log c$ would equal 0.

The number 0.1183 in front of $\log c$ determines how rapidly the slope of the repulsion term changes for a given change in salt concentration. This will probably vary with both the chemical nature and the valence type of the neutral salt as was observed for the other types of gels.

The last term $(1.333-1.482\Phi)$ expresses how the charge repulsion or the electrical work of bringing the particles together will vary with the volume fraction of particles. It is perhaps not immediately obvious why the work of repulsion should depend on the volume fraction. This can be explained by reference to Figure 57.8, which is a schematic plot of the charge repulsion as a function of the distance between the particles. The difference between the bottom of the curve in Figure 57.8 and the top shows the electrical work which must be performed to bring widely separated particles into the gel configuration where the maximum repulsion will exist when the particles are in actual physical contact at tangent points between them. The difference between the top and other marks corresponding to silica sol concentrations represents the electrical work of repulsion involved in bringing the sol particles, each from their equilibrium distances apart, into a gel structure. It is obvious that the electrical work is less if a more concentrated sol is used. To put it simply, a significant part of the work of electrical repulsion to bring the particles into a gelling configuration has already been done in the process of concentrating the sol.

The constant 1.333 in this expression represents the maximum electrical work which might be found if sols were used which were so dilute that their electrical fields did not overlap. The slope 1.482 is proportional to the rate at which the electrical work changes per unit change in the volume fraction of particles.

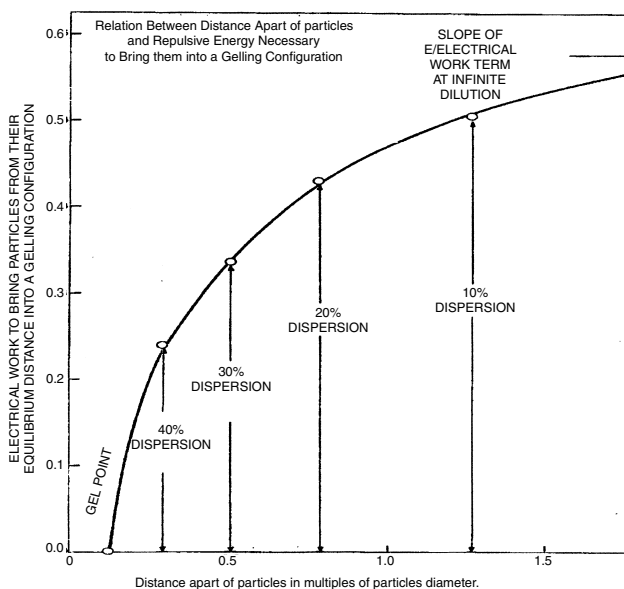


FIGURE 57.8 From Yates [24].

The slope of the repulsive energy term will also be a function of the particle size or surface area of the sol, since the repulsion between particles depends on size as well as on distance apart, charge, and salt content. This did not appear explicitly in Equation (57.1), since all of the data for evaluation of this equation came from sols of the same surface area.

Equation (57.1), and analogous equations for polymerisation and hybrid gels but not shown here, is very useful for predicting the gelling behavior of silica sols above the point of zero charge of silica. Silica gels for batteries, however, are made at pH well below 0. Thus, Lambert et al. [25] reported that they prepared a gel of this kind by mixing a silica sol, with a particle diameter of 12 nm and a silica concentration of 40% by weight, with concentrated sulfuric acid, 98% by weight. The concentration of sulfuric acid was more than 10 molar and the pH < -1. Using a pH value of -1 and electrolyte, SO_4^{2-} , concentration of 1 m, Equation (57.1) predicts that the gelling time would be less than a minute (the higher the anion concentration the shorter the gelling time), when it in an actual experiment was >12 h. Obviously, Equation (57.1) is at best only heuristically useful at very acidic condition. At these conditions, the various terms in the equation will be the same, but the actual values of the constants would have to be recalculated in order to make the equation fit experimental data more closely.

Wang [26] claimed that a solid electrolyte, in the form of a gel containing about 20% by weight of silica and made by mixing a de-ionized silica sol, adjusted to pH between 8 and 14, with sulphuric acid, compared with a conventional

fluid electrolyte consisting primarily of sulfuric acid, increased the capacity of lead-acid storage batteries by more than 30%.

Sielemann et al. [27] compares solid electrolytes, consisting of collision gels made from either silica sols with a specific surface area between 100 to 500 m^2g^{-1} or from fumed silica, in lead-acid batteries. The solid electrolyte made from the silica sol was prepared directly in the battery container, whereas the one made from fumed silica had to be made in separate step. The fumed silica, in the form of very light, fluffy powder, was mixed with the sulfuric acid and the other components of the solid electrolyte in a special vessel. The slow-gelling mixture was then poured into the battery container where it eventually solidified. The performances of lead-acid batteries containing the two different types of solid electrolyte were very similar, perhaps with a slight edge for the silica sol battery since it had a somewhat higher 20*1₀ discharge current.

Lambert et al. [25] have made a comparative study of solid electrolytes made from silica sol and fumed silica and claim the following advantages for electrolytes made with silica sol:

- Simplified handling and mixing of the electrolyte
- No liquid separates from the gel after solidification
- High silica concentration in gelling additive
- Increased residual gel strength
- Controlled gel time
- Less impurities (e.g. iron and chloride)
- Lower cost (~USD 2.60–3.50/kg pure silica from silica sol versus ~USD 9.00–18.00/kg fumed silica)

COLLOIDAL SILICA IN COATINGS

The coating process modifies the surface of a material, providing a gradual difference in composition or property between the surface and the bulk.

Iler [3] gives 36 references to how colloidal silica can be used in coatings on various substrates. Organic coating compositions with improved adhesion, hardness and durability can be obtained by adding colloidal silica in the form of silica sols to organic polymer dispersions. Inorganic coatings may use silica as the main component or as a binder in the coating composition.

Here we will highlight some very recent applications of colloidal silica in coating compositions.

SHOP PRIMERS FOR STEEL SUBSTRATES

Steel used in the shipbuilding industry and for other large-scale structures such as oil production platforms is often exposed to the weather during storage before construction and during construction, and it is generally protected

against corrosion by a coating called “shop primer” or “preconstruction coating”. Although the main purpose of the shop coating is to provide temporary corrosion protection during construction it is preferred that the primer can remain on the steel surface during and after fabrication. Thus, steel coated with shop primer must be weldable and compatible with and have good adhesion to the different types of anticorrosive coatings used on ships and other steel constructions.

Many modern shop primers are solvent borne and based on prehydrolyzed tetraethyl orthosilicate binders and zinc powders. They contain substantial amounts of volatile organic solvents, typically about 650 g per liter, to stabilize the paint binder and allow the primer to be applied as a thin film, about 20 μm thick. Obviously, the use of such primers will give rise to environmental concerns.

Much effort has therefore been expended to develop water-based shop primers with the advantages but without the disadvantages of organic solvent-based primers. In one approach, alkali silicate binders, e.g. aqueous solution of 3.3 ratio sodium silicate, were used. However, such binders contain relative large amounts of alkali metal cations, which remain in the coating after it has dried and after subsequent coatings have been applied to the steel surface. Exposure to water, for instance seawater, may cause blistering, that is, local delamination, due to the presence of too much alkali metal ions in the primer.

In a series of patent applications [28–31] Davies et al. show that the problems caused by high amounts of alkali metal ions could be overcome by using silica sols as the water-based binder instead of solutions of alkali silicates. The preferred sols had a particle size between 5 and 10 nm and a $\text{SiO}_2/\text{Na}_2\text{O}$ mole ratio of about 50:1. They also found that they could increase the pot life of the shop primer by using aluminum-modified silica sols.

INORGANIC PAINTS

Silicate coatings are used in construction to provide protective and decorative coatings on concrete and mortar. Such coatings may be completely inorganic in nature but may also contain up to 5% by weight of organic material, for example, in the form of a polymer latex. The binder, often a solution 3.3 molar ration sodium silicate, is mixed with pigments and fillers of different kinds. In the case of completely inorganic paints there is a problem with stability toward gelling and such paints are sold as two-component systems, one component consisting of the silicate binder solution and the other consisting of a dry powder of the other components of the paint. The two components are mixed prior to use and the resulting paint has a pot life of a few days.

An important property of inorganic paints is their resistance to water. A silicate based paint based on e.g. 3.3 molar ratio sodium silicate will have poor water resistance immediately and some time after the application of the paint, although it will improve with time, as alkali gradually becomes neutralized by the carbon dioxide in the atmosphere, that is, the $\text{SiO}_2/\text{Na}_2\text{O}$ molar ratio of the silicate binder slowly increases. The silicates in a silicate-based coating can also react with Ca^{2+} in a cementitious substrate and form insoluble calcium silicates, which also contributes to improved water resistance. In theory, the molar ratio of a silicate solution may be increased by mixing it with a silica sol. However, if an 3.3 ratio sodium silicate solution is mixed with an alkali-stabilized silica sol coagulation and gelling occurs, but Iler [32] reports that this does not happen if potassium silicate is used. Stable mixtures of colloidal silica and potassium silicate can be prepared with a silica concentration of 15–30 wt.% and with $\text{SiO}_2/\text{K}_2\text{O}$ molar ratios of 11:1 to 24:1. Greenwood and Otterstedt [33] studied such mixtures of silica sols and solutions of potassium silicate as binders in silicate paints and found that the pot life of the paint could be increased to about two months, but that it gelled after that time.

Heiberger and Schl affer [34] claim an inorganic paint with excellent water resistance and a pot life of at least 6 months. In a typical preparation they mix a potassium silicate solution, with a solids content of 30 wt.%, a silica sol, having a particle size of 9 nm and containing 20 wt.% SiO_2 , in such proportions that the $\text{SiO}_2/\text{K}_2\text{O}$ molar ratio is 10:1, and an aqueous solution of N,N' -Di(2-hydroxypropyl)- N,N' -tetramethylhexylenediamin. Next, they stir into this mixture pigment, filler and a butylacrylate-methylmetacrylate copolymer. The high water resistance of this paint is most likely due to the high $\text{SiO}_2/\text{K}_2\text{O}$ molar ratio of the silicate binder.

HARD, SCRATCH-RESISTANT THIN COATINGS

Many substrates, for example, many wood products, are provided with protective and decorative coatings of organic polymers, for example, radiation- or heat-curable polyacrylates, polyacrylate copolymers, polycarbonates or terephthalic resins, so as to improve gloss, dryness (no tack), and abrasion resistance and scratch resistance.

In many applications, the inherent properties of coating polymers are not adequate to meet very demanding specifications on for example, surface hardness, transparency and scratch resistance. Much work has therefore been expended to develop high-quality surface coatings an improvements of surface properties have been achieved by incorporating colloidal silica and silanes in the coating formulation.

In one particularly interesting development Jacquinet and Eranian [35] and Wilhelm et al. [36] prepare an

organosol of silica particles with a particle size between 10 and 50 nm in a reactive organic solvent also containing a photo-initiator and a vinylsilane, about .01 to 0.1 millimole of silane per m^2 of silica surface, as a coupling agent. The reactive solvent may be an acrylic monomer such as tripropylene glycol diacrylate or ethoxylated trimethylolpropane triacrylate. The preparation of the organosol is for instance described in patent example 1 [36]. 122 g of a silica sol, containing 40 wt.% SiO_2 with an average particle size of 50 nm, which has been de-cationized to pH of 2 with an ion exchange resin in the acid form, is mixed with 396.4 g isopropanol, 26 g vinyltrimethoxysilane (corresponding to 0.53 g silane per m^2 of silica surface) and 125 g ethoxylated trimethylolpropane triacrylate. The mixture is vacuum distilled at a pressure between 50 and 110 mbar and a temperature of 35°C for about 4 hours. After filtration the organosol is a slightly yellow, transparent liquid containing 30 wt.% SiO_2 and 0.3 wt.% water and having a viscosity of 304 mPa.s at 20°C.

In patent example 5 [36] it is described how a coating formulation is prepared by mixing 50 parts by weight of the organosol of patent example 1 with 50 parts by weight of urethane-acrylate oligomer and 5 parts by weight of a photo-initiator. A polycarbonate support is coated with 50 g m^2 of the formulation and the coating is cured by exposure to ultraviolet radiation. Abrasion and scratch resistance were measured and compared with those of a reference sample of polycarbonate coated with the formulation from which the silica organosol had been excluded. Optical transmission was 100% after abrasion in a Taber abrasion test as compared to only 70% for the reference. Scratch resistance was measured according to the pencil hardness test and was found to be 7 H versus 4 H for the reference.

COLLOIDAL SILICA IN POLYMER LATICES

In DuPont's brochure on Ludox[®] Colloidal Silica it is described that incorporation of silica particles in the form of a silica sol in polymer latices will improve abrasion resistance and modulus of polymer coatings. Greenwood and Otterstedt [37] studied the effect of mixing silica sols of different particle sizes with various water-based wood lacquers. The modulus of films made from latices of copolymers of urethane-acrylates containing up to 50 wt.% SiO_2 , based on the polymer weight, could be increased by several hundred percent. As expected, the reinforcing effect increased with decreasing particle size and increasing concentration of silica. However, the stability of the latex-silica sol mixture toward gelling decreases with decreasing particle size. Moreover, the stability towards gelling is very sensitive to the particular surfactant system used to make the latex and there are systems that do not form stable mixtures with silica sols of any particle size. From the point of

view of stability and also of ensuring a uniform distribution of silica particles in the coating, it would obviously be advantageous if the silica sol was present during the polymerisation of the latex particles, each one of which would then be a nano-composite consisting of nano-sized silica particles distributed in a polymer matrix.

Actually, one of the first nanocomposites of this kind, although the purpose was not to improve the mechanical properties of polymers, was prepared by Kirkland, and Iler and McQueston, [38] when they synthesized polymer-silica composites with average diameters ranging from 500 nm to 20 μm by copolymerisation of either melamine or urea with formaldehyde in the presence of a silica sol. Calcination yielded microporous silica spheres, which were used as chromatographic column packing under the trade name Zorbex[®].

Percy and coworkers [39,40] synthesized colloidal dispersions of polymer-silica nanocomposite particles by homopolymerizing 4-vinylpyridine or copolymerizing 4-vinylpyridine with either methyl methacrylate, styrene, n-butyl acrylate or n-butyl methacrylate in the presence of fine-particle silica sols using a free-radical in aqueous media at 60°C. No surfactants were used and a strong acid-based interaction was assumed to be a prerequisite for nanocomposite formation. The nanocomposite particles had comparatively narrow size distributions with mean particle diameters of 150–250 nm and silica contents between 8 and 54 wt.%. The colloidal dispersions were stable at solids contents above 20 wt.%.

Percy and Armes [41] showed that poly(methyl methacrylate)-silica nanocomposite particles can be readily prepared in aqueous alcoholic media at around ambient temperature without using either auxiliary comonomers such as 4-vinylpyridine or surfactants. In this work the silica sol was an organosol of 20 nm silica particles in isopropyl alcohol with a solids content of 30 wt.%.

COLLOIDAL SILICA AND INK JET

Imaging devices such as ink jet printers are well known methods for printing various information on different substrates or receptors, which can be transparent (e.g. polymer films) or opaque (e.g. sheets of paper and paper board). Imaging with either ink jet printers or pen plotters involves depositing ink on the surface of the receptors. Many types of ink consist of an organic dye dissolved in a mixture of water with a water miscible organic liquid having a boiling point of at least 150°C. There are also inks available, in which pigments instead of dyes are used as the coloring agent. Imaging devices normally utilize inks that can be exposed to air for long time without drying. It is therefore desirable that the surface of the receptors be dry and non-tacky to the touch, even after absorption of significant amounts of ink, soon after imaging. Receptors must thus have a rapid absorption rate of ink to give uniform

TABLE 57.8
Colloidal Silica in Coatings for Ink Jet Applications

| Reference | Coating system | Silica sol | Comments |
|-----------|--|--|--|
| [42] | Silica sol + polymeric binder + silane coupling agent + high boiling solvent | Elongated(structured) or spherical particles. Average particle size: up to 200 nm | Polymeric binder: e.g., PU-dispersion Advantage: quick drying of ink, low haze, reduced image bleeding, improved shelf-life |
| [43] | Silica sol + PVA 100 parts SiO ₂ to 25 parts PVA on dry bases | Agglomerated particles. Agglomerated surface area: 100–400 m ² /g | Highly transparent porous coating |
| [44] | Fumed silica + silica sol + PVA | Particle size: 22, 35 and 50 nm SiO ₂ from sol (on dry bases): about 20 wt.% | Glossy coating, high liquid absorption capacity, crack resistant, non-brittle surface |
| [45] | Silica sol + water-soluble resin, e.g.PVA. 15 parts PVA to 100 parts SiO ₂ (on dry bases) | Particle size: <200 nm Particle charge: anionic and cationic | High gloss, high ink absorption, excellent water resistance, "photo quality coating" |
| [46] | Silica sol + polymeric binder + silane coupling agent = image recording Layer | Particle size: 22 nm Ammonium stabilized | Porous solvent absorbing polyolefin layer + image recording layer: Improved color retention Higher optical density |
| [47] | 2 layers of "chain"-silica sol + ink-receiving layer | Primary particle size: 3–40 nm "chain" length: 40–200 nm | Excellent ink absorption High color density Good color reproducibility |

print, free from coalescence and banding. This can be accomplished, if the receptor is nonporous or not porous enough, by providing the surface of the receptor with a thin, porous coating.

In the last 20 years, there has been an intensive development of coating formulations for ink jet receptors, and colloidal silica plays a very significant role in this development work. Thus, a patent search, covering the period from 1971 to 2002 and using the search words "Ink Jet and Colloidal Silica," gave 1382 hits.

We have selected six patents or patent applications between 2000 and 2002, which demonstrate the use of colloidal silica in coatings for ink jet applications, and compiled the relevant information in Table 57.8, and one patent application describing the use of silica sols in pigmented inks.

Aluminum-modified silica sol with a particle size of 12 nm in a pigmented ink-jet ink formulation gave a print with improved optical density and superior rub resistance compared with a reference ink [48].

COLLOIDAL SILICA AS POLISHING AGENT FOR ELECTRONIC PRODUCTS

The advancement of high technology products, including computers, has been remarkable in recent years, and

parts to be used in such products have been developed for ever higher integration and speed. Paralleling this progress, the design rules for semiconductor devices have been increasingly refined. The depth of focus in a process tends to be shallow and the requirements for the planarization of the pattern-forming surface are becoming increasingly severe.

Electronic devices made on silicon chips must be connected to each other by means of interconnecting metallic tracks to constitute the desired electronic circuit. Interconnected metallic levels are electrically insulated from each other by being encapsulated in a dielectric layer. The interconnecting metallic tracks are often made by a metal reactive ionic etching procedure. Sputtering is used to deposit an aluminum or aluminum alloy film, approximately 10–12 μm thick. The design is transferred onto the film by photolithography and the metallic tracks are created using reactive ionic etching. The tracks are next covered with a dielectric layer of silica, about 2 μm, obtained by decomposition of tetraethylorthosilicate in the vapor phase. Chemical-mechanical planarization is used to planarize the dielectric layer.

Chemical-mechanical planarization, "CMP", processes are widely used to remove material from the surface of a substrate in the production of a wide variety of microelectronics. In a typical CMP process, the

TABLE 57.9
Colloidal Silica as Polishing Agent for Microelectronic Products

| Reference | Substrate | Silica sol | Slurry | Comments |
|-----------|---|--|-------------------------------|--|
| [49] | Display grid Al,Cu,W | Ammonium stabilized Average particle size: 25 nm Size range: 12–50 nm Solids: 30% pH: 9–11 | pH: 9–11 | Well controlled polishing rates over large surfaces |
| [50] | Cu | Average particle size: 35 nm Size range: 10–100 nm Solids: 30% pH: 2–3.5 | pH: 2–3.5 | Homogeneous and regular polishing No dishing |
| [51] | Ni–P plated substrate of Al alloy (Hard disc) | Average particle size: 35 nm pH: alkaline | pH: 2–5% SiO ₂ : 7 | Buffer solution is important High stock removal rate No surface defects |
| [52] | Polymer with low dielectric constant | Cationic sol Average particle size: 25 or 50 nm | pH: 3.5 | Good polishing speed Uniformity of polishing No scratching of polished surface |
| [53] | Cu, Ta | Silica sol + fumed silica Average particle size: <20 nm | pH: 2–5% SiO ₂ : 5 | Improved polishing selectivity for Cu and Ta Suppressed polishing of insulating layer |

surface to be polished is pressed against a polishing pad in the presence of a slurry under controlled conditions of chemistry, pressure temperature and velocity. The slurry generally contains small particles that abrade the surface, and chemicals that etch and/or oxidize the newly formed surface. The polishing pad is usually a planar pad made of a polymeric material, for example, polyurethane. As the pad and substrate move relative to each other, material is removed from the surface mechanically by the abrasive particles and chemically by the etchants and/or oxidants in the slurry.

Just like in the case of coating formulations for jet ink receptors, intensive efforts have been made in the last 15 to 20 years to develop polishing formulations for microelectronic products containing colloidal particles of different compositions. The final step in most polishing processes usually employs colloidal particles of silica. We have summarized information on colloidal silica as polishing agent from an number of recent patents in a table, Table 57.9.

REFERENCES

- Griessbach, R. *Chem. Ztg.* **1933**, 57, No.26, pp 253–260, 274–276.
- Iler, R.K. *The Colloidal chemistry of Silica and Silicates*; Cornell University Press: New York, **1955**, p 89.
- Iler, R.K. *The Chemistry of Silica*; Wiley-Interscience: New York, **1979**, pp 415–438.
- Otterstedt, J-E. and Brandreth, D.A. *Small Particles Technology*; Plenum Press: New York, **1998**, pp 432–433.
- Cotterill, R. *Material World*; Cambridge University Press: Cambridge, **1985**, pp 124–131.
- Bergqvist, H.; Chandra, S. U.S. Patent 5,932,000, **1999**
- Inglis, G.E. *Trans. Inst. Nav. Archit.* **1913**, 55, p 219
- Eka Chemicals; *Technical Bulletin on Cembinder products* No.2, **2000**
- Hara, N.; Inoue, N. *Cem. Concr. Res.* **1980**, 10, p 677
- Papadakis, V. G. *Chem. Concr. Res.* **1999**, 29, pp 79–86
- Iler, R.K. *The Chemistry of Silica*; Wiley-Interscience: New York, **1979**, p 312
- Bergna, H.E. *The Colloid Chemistry of Silica*; Advances in Chemistry Series 234; American Chemical Society: Washington D.C., **1994**, p 30
- Wagner and Hauk *Hochsch. Archit. Bauwes-Weimar*, **1994**, 40, 5/6/7, pp 183–187
- Skarp, U.; Sarkar, S. *Proceedings from the World of Concrete*, Las Vegas, **2001**, February 27–March 2.
- Greenwood, P.; Bergqvist, H.; Skarp, U. U.S. Patent Application 2002/0011191, **2002**
- Greenwood, P.; Bergqvist, H.; Skarp, U. U.S. Patent 6,387,173, **2002**
- Greenwood, P.; Bergqvist, H.; Skarp, U. PCT WO 01/98227, **2001**
- Otterstedt, J-E. and Brandreth, D.A. *Small Particles Technology*; Plenum Press: New York, **1998**, pp 407–429
- Andersson, K.; Larsson, H. *Nordisk Cellulosa* **1984**, No.1, p 57
- Andersson, K.; Lindgen, E. *Nordic Pulp and Paper Research Journal* **1996**, Nr.1, p 15

21. Lindström, T.; Hallgren, H.; Hedborg, F. *Nordic Pulp and Paper Research Journal* **1989**, 4:2, p 99
22. Dalton, R. L.; Iler, R. K. *J. Phys. Chem.* **1956**, 60, p 955
23. Greenwood, P.; Linsten, M. O.; Johansson-Vestin, H. E. U.S. Patent 6,379,500, **2002**
24. Yates, P. C.; "Kinetics of Gel Formation of Colloidal Silica Sols", *Ralph K. Iler Memorial Symposium on the Colloidal Chemistry of Silica*, ACS National Meeting, Washington D.C., **1990**
25. Lambert, W. H.; Greenwood, P.; Reed, M. C. *Journal of Power Sources*, **2002**, 107, pp 173–179
26. Wang, W. U.S. Patent 6,218,052, **2001**
27. Sielemann, O.; Niepraschk, H.; Nemeč-Losert, P. U.S. Patent 5,664,321, **1997**
28. Davies, G. H.; Jackson, P. A.; McCormack, P. PCT WO 00/55260, **2000**
29. Davies, G. H.; Jackson, P. A. PCT WO 02/22746, **2002**
30. Davies, G. H.; Jackson, P. A.; McCormack, P.; Banim, F. PCT WO 00/55261, **2000**
31. Davies, G. H.; Greenwood, P.; Jackson, P. A. PCT WO 02/22745, **2002**
32. Iler, R.K. *The Chemistry of Silica*; Wiley-Interscience: New York, **1979**, p 145
33. Greenwood, P.; Otterstedt, J-E. Unpublished results, **1995**
34. Heiberger, F.; Schläffer, H. PCT WO 01/53419, **2001**
35. Jacquinet, E.; Eranian, A. U.S. Patent 6,136,912, **2000**
36. Wilhelm, D.; Eranian, A.; Vu, N.C. U.S. 2001/0027223, **2001**
37. Greenwood, P.; Otterstedt, J-E. Unpublished results, **1996**
38. Kirkland, J.J. U.S. Patent 3,782,075, **1974**; Iler, R.K.; McQueston, H.J. U.S. Patent 4,010,242, **1977**
39. Percy, M.J.; Barthet, C.; Lobb, J.C.; Khan, M.A.; Lascelles, S.F.; Vamvakaki, M.; Armes, S.P. *Langmuir* **2000**, 16, pp 6913–6920
40. Amalvy, J.L.; Percy, M.J.; Armes, S.P. *Langmuir* **2001**, 17, pp 4770–4778
41. Percy, M.J.; Armes, S.P. *Langmuir* **2002**, 18, pp 4562–4565
42. Paff, A.; Miller, A. PCT WO 00/71360, **2000**
43. Noguchi, T.; Tajiri, K. EP 1 118 584 A1, **2001**
44. Darsillo, M.S.; Fluck, D.J.; Laufhutte, R. U.S. Patent 6, 284,819, **2001**
45. Liu, B.; Nemoto, H.; Ikezawa, H. U.S. 2002/0034613, **2002**
46. Chu, L.; Romano, C.E.; Chen, C.C. EP 0 983 867, **1999**
47. Otani, T.; Ono, A.; Ilmorì, Y.; Chatani, A.; Kondo, N.; Ueno, T.; Kuruyama, Y. EP 1 016 546, **1999**
48. Martin, T.W.; Bugner, D. EP 0 976 797, **1999**
49. Alwan, J.J.; Carpenter, C.M. U.S. Patent 6,271,139, **2001**
50. Jacquinet, E.; Letourneau, P.; Rivoire, M. U.S. Patent 6,302,765, **2001**
51. Shemo, D.S.; Rader, W.S.; Owaki, T. U.S. Patent 6,332,831, **2001**
52. Jacquinet, E.; Letourneau, P.; Rivoire, M. U.S. Patent 6,362,108, **2002**
53. Ina, K.; Rader, W.S.; Shemo, D.S.; Hori, T. U.S. Patent 6, 355,075, **2002**

Paper VI

LIGHT SCATTERING IN PIGMENTED COATINGS: EXPERIMENTS AND THEORY,
W.E Vargas, P. Greenwood, J.E. Otterstedt and G. A. Niklasson, Solar Energy, 2000, Vol. 68,
No. 6, pp. 553–61.



LIGHT SCATTERING IN PIGMENTED COATINGS: EXPERIMENTS AND THEORY

W. E. VARGAS*, P. GREENWOOD**, J. E. OTTERSTEDT** and G. A. NIKLASSON***†

*Department of Physics, University of Costa Rica, San José, Costa Rica

**Department of Engineering Chemistry, Chalmers University of Technology, S-41296 Göteborg, Sweden

***Department of Materials Science, The Ångström Laboratory, Uppsala University, Box 534,
S-75121 Uppsala, Sweden

Communicated by JOACHIM LUTHER

Abstract—Small silica particles uniformly coated by a shell of titania, were produced by wet chemical methods. The pigments were dispersed in polymeric binders and were applied as paints to glass substrates. Total reflectance and transmittance were determined by integrating sphere measurements. Luminous and solar reflectance of paints containing the novel pigments were comparable with paints containing commercial titania. The spectral transmittance and reflectance of the paints were modelled by a four-flux radiative transfer theory. Theory and experiment could be brought into good agreement, if it was assumed that the particles were slightly porous. The studied pigments may find applications in sunscreens or in foils for daylighting and radiative cooling. © 2000 Elsevier Science Ltd. All rights reserved.

1. INTRODUCTION

Light scattering is of importance in various energy related applications, such as sunscreens, pigmented polymer foils for radiative cooling (Nilsson and Niklasson, 1995) and daylighting, infrared energy barriers (Berdahl, 1995), as well as thermotropic materials (Wilson and Eck, 1993; Wilson et al., 1994). Solar cell design may also benefit from a thorough understanding of the light scattering occurring, for example, in photo-electrochemical cells with nanostructured electrodes (Usami, 1997; Ferber and Luther, 1998). Foils containing white pigments can be used to minimize the solar absorption of a material. Currently titanium dioxide is the most used commercial white pigment. For environmental reasons it is desirable to minimize the amount of titania used in the pigment (Hsu et al., 1993), for example by using inexpensive cores coated with titania. Another advantage is the very good control of particle size and size distribution possible with chemical coating methods. This makes optimization of the optical properties easier. A good understanding of multiple light scattering in pigmented materials is a necessary prerequisite for optimization and design of coatings for the above-mentioned applications.

Multiple light scattering from pigment particles dispersed in paints, paper, polymer foils or electrolytes can be described by radiative transfer theory (Chandrasekhar, 1950; Ishimaru, 1978; van de Hulst, 1980; Reiss, 1988). Rigorous solutions often require numerical implementation (van de Hulst, 1980; Stamnes et al., 1988). Approximate approaches are based on the concept of radiation exchange between different directions or flux channels in the coating (Mudgett and Richards, 1971, 1972; Whitney, 1974). Radiative transfer models characterized by a low number of channels are simple and surprisingly accurate methods for describing the optical properties of light scattering and absorbing materials (Kubelka and Munk, 1931; Reichman, 1973; Maheu et al., 1984). Diffusion models are appropriate when considering optically thick materials in which multiple scattering effects lead to isotropic distributions of the scattered radiation (Yoo et al., 1990). We have recently provided a theoretical framework for various approximative analytical methods and have derived generalizations of two-flux and four-flux theories (Vargas and Niklasson, 1997b,c; Vargas, 1998). In these models the anisotropic diffuse radiation is characterized by effective average pathlength parameters (APP), ξ . The fraction of energy that a particle scatters into the forward hemisphere is given in terms of forward scattering ratios (FSR): σ_c for an impinging collimated flux, and σ_d for an impinging anisotropic diffuse radiation flux. We have devised

† Author to whom correspondence should be addressed. Tel.: +46-18-4713-101; fax: +46-18-500-131; e-mail: gunnar.niklasson@angstrom.uu.se

methods to calculate these parameters (Vargas and Niklasson, 1997d,e).

In this paper we focus on the visible and near infrared optical properties of pigmented polymer coatings. They were composed of SiO₂ (silica) or commercial TiO₂ (rutile titania) pigments hosted in a polymeric matrix. The solar and luminous reflectance were compared to that of films containing TiO₂ (anatase titania) coated SiO₂ pigments. We have also compared the experimental data with a four flux theory using one APP, and one FSR each for the collimated and diffuse parts. Hence the direction dependence of these parameters is neglected. By the extended Hartel approximation (Vargas and Niklasson, 1997b,e), we evaluate ξ and σ_a and take into account their dependence on wavelength, particle relative refractive index, particle size, and film thickness. Here we present the first comparisons of this model with experimental data. Good agreement between measured and computed reflectances and transmittances is displayed when pigment porosity is taken into account.

2. EXPERIMENTS

Pure TiO₂ (rutile) pigments were obtained from commercial sources; namely: Flexonyl White R 100 VP supplied by the Hoechst company, and W6206K from Nordsjö (Akzo-Nobel Inc.). Colloidal suspensions of silica particles were produced by the Stöber synthesis (Stöber *et al.*, 1968). The reaction temperature was varied to obtain different diameters between 0.3 and 0.5 μm . After introduction of aluminosilicate sites on the particle surfaces, charge reversal and a heat treatment, a solution of titanium tetrachloride was added at a rate of 0.2 mmol/m² of core surface per hour. Uniform TiO₂ coated SiO₂ particles were obtained, with the content of titania per particle given by the deposition time. The particles were given a stabilising negative charge to prevent agglomeration. Then the sols were mixed with a binder, a copolymer latex of ethylene vinylic acetate (Bindoplast, from Nordsjö, Akzo-Nobel Inc.) and coatings were prepared on 2 mm thick glass plates by using a doctors blade with a clearance of 200 μm . Coatings with thicknesses between 25 and 80 μm and particle weight fractions from 0.05 to 0.50 were obtained. Film thicknesses were measured by using a Tencor-Alpha-Step 200 surface profiling instrument. A JEOL JSM-5200 scanning electron microscope was used to determine the size distribution of the pigments. The mean diameter of the commercial

titania pigments was about 0.3 μm . The diameters of the composite particles were between 0.35 and 0.65 μm with very narrow size distributions. X-ray diffraction showed that the titania in the composite particles consisted of the anatase phase. It is not possible to obtain a rutile coating with this or a similar method, as far as we are aware. For the composite pigment sols, light scattering measurements with a particle size analyser (Brookhaven BI-90 particle sizer) were carried out. Comparisons of the obtained hydrodynamic diameters with the electron microscopy results showed that the particles were well dispersed with very little aggregation. The density of the silica was measured as 2.0–2.2 g/cm³, i.e. somewhat lower than in the bulk. The anatase titania values, although more uncertain, were close to bulk values. Further details of the preparation and characterization are given by Greenwood (1998).

Optical measurements were carried out for wavelengths in the solar spectral range (from 0.3 to 2.5 μm). Total reflectance and transmittance spectra of the pigmented coatings were measured by a Beckman Acta 5240 spectrophotometer equipped with an integrating sphere and using barium sulphate as the reflectance reference. In such measurements losses of scattered radiation through the open edges of the glass substrate can occur and lead to serious errors (Nitz *et al.*, 1998). For strongly backscattering samples such as ours the errors should mainly affect the transmittance. In our case the difference in transmittance for light incident onto the coating and light incident onto the backside of the substrate could be as much as five percent of the signal. If edge losses are significant, an artificially high absorption would be measured. This is to be compared to the weak absorption of the binder, that is clearly significant for the coating thicknesses that we consider. Indeed, we do not consistently observe higher measured absorption than predicted theoretically from the known properties of the binder. For characterizing the optical properties of the pigmented coatings it is necessary to know the spectral dependence of the refractive index of the binder in which the particles are hosted, and of the glass substrate on which the coatings are deposited. We obtained this information from measured near-normal reflectance and transmittance of an uncoated glass substrate and of a pure binder film supported on a glass substrate. The bulk refractive indices of the silica (Malitson, 1965), rutile (Ribarsky, 1985) and anatase (Demyriont, 1985) were taken from literature, and used to estimate the refractive indices of

the pigments. The bulk mass densities of silica [$\bar{\rho} = 2.30 \text{ g/cm}^3$], rutile [$\bar{\rho} = 4.245 \text{ g/cm}^3$], and anatase [$\bar{\rho} = 3.90 \text{ g/cm}^3$] were also used.

3. THEORY

In order to treat the effects of multiple scattering, boundary internal reflections inside the film, substrate properties, as well as absorption by the particles, we have extended the four flux model developed by Maheu et al. (1984) and Maheu and Gouesbet (1986). In this radiative transfer model, the radiation field inside the film is considered to consist of four contributions: two collimated intensities (I_c and J_c) and two diffuse radiation intensities (I_d and J_d), as indicated in Fig. 1. Perpendicular illumination is assumed, and the film is characterized by smooth interfaces with air and a substrate. The intensities of the collimated beams decay due to scattering and absorption by the particles. The intensity of the diffuse beam I_d is decreased by absorption, and scattering into the backward hemisphere (relative to the direction of the impinging radiation); and it is increased by scattering of the I_c , J_c and J_d contributions into the forward hemisphere. The same analysis can be done for the other diffuse beam J_d . Consequently, the differential equations for the intensities are

$$\frac{dI_c}{dz} = -(\alpha + \beta)I_c, \tag{1a}$$

$$\frac{dJ_c}{dz} = (\alpha + \beta)J_c, \tag{1b}$$

$$\begin{aligned} \frac{dI_d}{dz} = & -\xi\beta I_d - \xi(1 - \sigma_d)\alpha I_d + \xi(1 - \sigma_d)\alpha J_d \\ & + \sigma_c\alpha I_c + (1 - \sigma_c)\alpha J_c, \end{aligned} \tag{1c}$$

$$\begin{aligned} \frac{dJ_d}{dz} = & +\xi\beta J_d + \xi(1 - \sigma_d)\alpha J_d - \xi(1 - \sigma_d)\alpha I_d \\ & - \sigma_c\alpha J_c - (1 - \sigma_c)\alpha I_c. \end{aligned} \tag{1d}$$

Here z is a linear coordinate, measured from the illuminated side and perpendicular to the interface, $\alpha(\beta)$ is the scattering (absorption) coefficient per unit length which, within the independent scattering approximation, is evaluated as the particle volume fraction (f) times the volumetric scattering (absorption) cross section of the particle [C_{sca}/V (C_{ab}/V) where V is the particle volume]. The forward and backward diffuse radiation arises from multiple scattering processes and their path through the coating is on the average longer than for the collimated radiation. This difference is characterized by the average path-length parameter (APP), ξ : the average pathlength travelled by the diffuse beams as compared to the collimated ones. The fractions of energy that each particle scatters into the forward hemisphere are given by the forward scattering ratios (FSR), for collimated and (anisotropic or isotropic) diffuse incident radiation, σ_c and σ_d , respectively. By means of

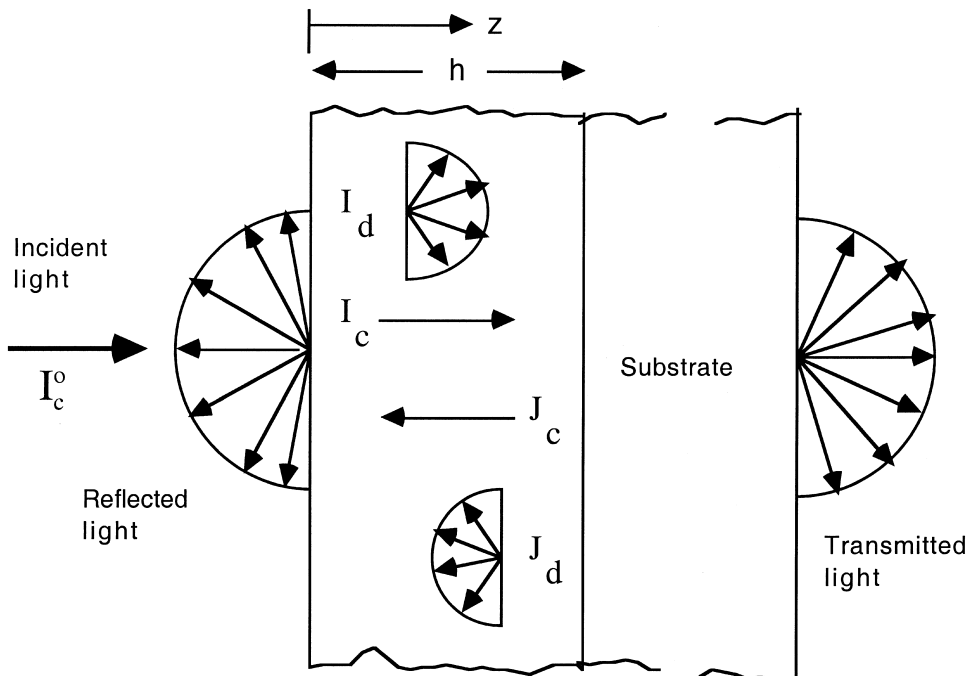


Fig. 1. Electromagnetic radiation fluxes inside an inhomogeneous film of thickness h , which is normally illuminated.

the APP and σ_d the anisotropy of the propagating diffuse radiation was taken into account.

By applying boundary conditions at the interfaces of the film, in terms of reflection coefficients and intensities of the fluxes, the solutions for the system of differential equations lead to explicit expressions for the collimated and diffuse components of the reflectance and transmittance. The expressions for these quantities are readily available in Vargas and Niklasson (1997a) and will not be repeated here. We now shortly describe the evaluation of all parameters entering into the four flux theory. Volumetric scattering and absorption cross sections of the pigments, C_{sca}/V and C_{abs}/V with V as the particle volume, as well as the forward scattering ratio for collimated incident radiation, were evaluated from the Lorenz–Mie theory (Bohren and Huffman, 1983). The APP and the FSR for diffuse incident radiation were evaluated from an extension of the Hartel theory (Hartel, 1940). We take into account the dependences $\xi = \xi(\lambda_o, x, m, h)$ and $\sigma_d = \sigma_d(\lambda_o, x, m, h)$ where λ_o is the free space wavelength of the impinging radiation, $x = 2\pi r/\lambda_o$ is the size parameter with r as the particle radius, m is the particle relative refractive index, and h is the film thickness. Our approach to obtain explicit expressions for ξ and σ_d is based on expansions of the single-particle phase function, $p(\mu, \mu')$, and the diffuse intensity, $I(\tau, \mu')$, in terms of Legendre polynomials. The coefficients involved in the expansions of $p(\mu, \mu')$ are obtained from the Lorenz–Mie theory (Chu and Churchill, 1955). The coefficients specifying the expansion of the diffuse intensity are obtained by the analytic solution of a system of differential equations obtained from an order-of-scattering expansion. The details of the extended Hartel theory have been published previously (Vargas and Niklasson, 1997b,e). The evaluation of the APP and the FSR are finally carried out from

$$\xi(\tau) = \frac{\int_0^1 I(\tau, \mu) d\mu}{\int_0^1 \mu I(\tau, \mu) d\mu},$$

$$\sigma_d(\tau) = \frac{\int_0^1 d\mu' \int_0^1 I(\tau, \mu') p(\mu, \mu') d\mu}{\int_0^1 d\mu' \int_{-1}^1 I(\tau, \mu') p(\mu, \mu') d\mu} \quad (2)$$

where $\tau = (\alpha + \beta)h$ is the optical thickness of the coating, and $\mu = \cos \theta$ ($\mu' = \cos \theta'$), $\theta(\theta')$ being a polar angle measured from the normal to the film interfaces.

It is well known that optical constants of thin films depend on their internal structure (Pulker *et al.*, 1976; Harris *et al.*, 1979; Laux and Richter, 1996). The Lorenz–Lorentz or Clausius–Mossotti relation has been used to describe the effect of thin film porosity on the optical constants (Pulker, 1979), and it has also been used in connection to optical constants of pigments or powders (Böttcher, 1945). Porous particles are characterized by decreased scattering, a mass density and complex refractive index (ρ_p and m_p) lower than the corresponding bulk values ($\bar{\rho}_b$ and \bar{m}_b). The optical constants of the particles depend on the porosity, which was obtained from a fit to the experimental spectra. We used the particle relative mass density ($p = \rho_p/\bar{\rho}_b$) as a fitting parameter to minimize the function

$$G(p) = \sum_{i=1}^N \{ |R_{\text{exp}}(\lambda_i) - R_{\text{calc}}(\lambda_i, p)|^2 + |T_{\text{exp}}(\lambda_i) - T_{\text{calc}}(\lambda_i, p)|^2 \}, \quad (3)$$

where N is the number of measurements carried out to obtain the reflectance and transmittance (R_{exp} and T_{exp}) at different wavelengths, $R_{\text{calc}}(\lambda, p)$ and $T_{\text{calc}}(\lambda, p)$ are the corresponding theoretical values calculated from a four-flux model by varying the particle refractive index according to the Clausius–Mossotti equation. The details are given by Vargas and Niklasson (1997a).

It should be realized that close approaches between particles may result from the deposition procedure, even if the sol is well-dispersed. Particles with separations less than a third of the wavelength give rise to dependent scattering (Reiss, 1988). In this case the scattering efficiency decreases just as for porous pigment particles.

4. COMPARISON OF THEORY AND EXPERIMENTS

Fig. 2 depicts reflectance and transmittance spectra for coatings containing rutile titania (Flexonyl) pigments with different particle weight fractions. The particle volume fraction, f , is related to the particle weight fraction, F , by

$$f = \frac{1}{1 + \frac{\rho_p}{\rho_b} \left(\frac{1-F}{F} \right)}, \quad (4)$$

where ρ_p (ρ_b) is the mass density of the particle

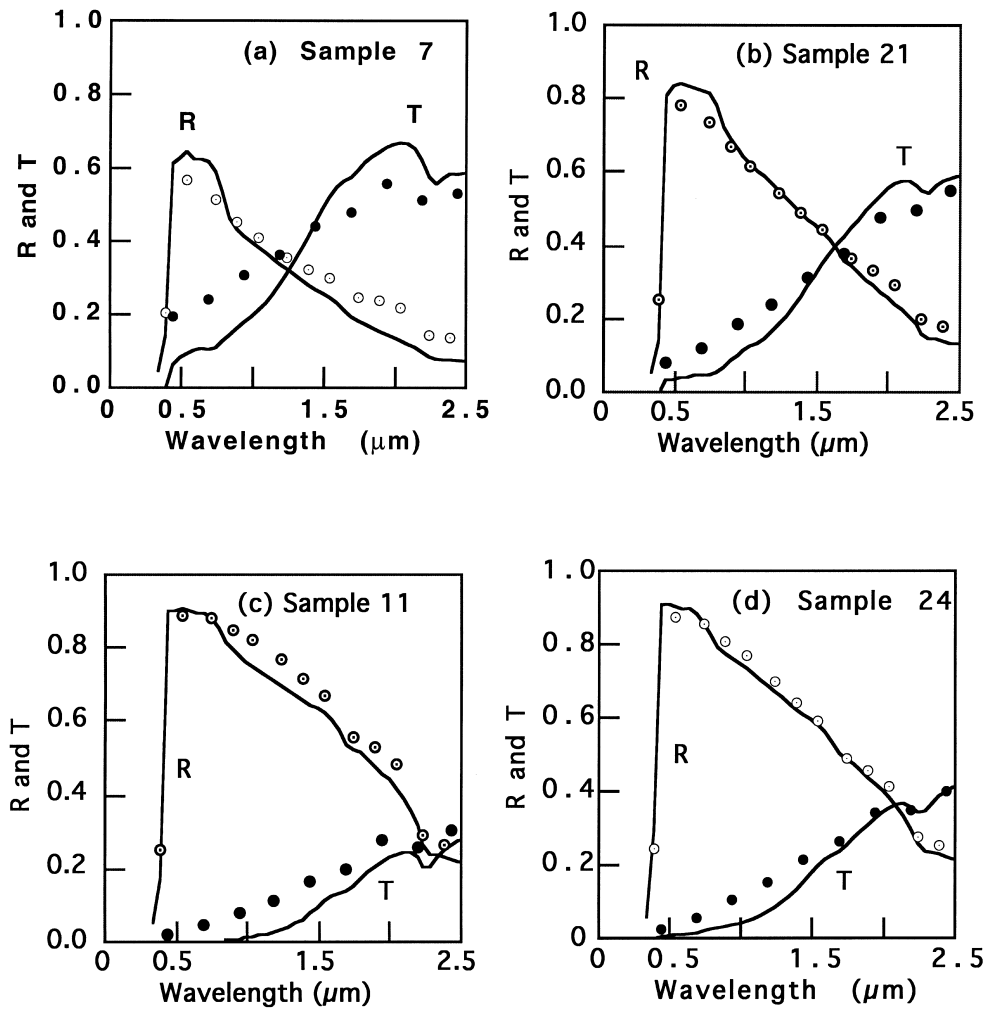


Fig. 2. Comparisons between measured total reflectance (circles) and transmittance (dots) with the corresponding predicted values obtained from four-flux calculations (solid lines), for pigmented films containing 300 nm TiO_2 (rutile) particles in a polymer binder. The particle weight fractions, F , and film thicknesses, h , were (a) $F=0.05$, $h=63 \mu\text{m}$, (b) $F=0.20$, $h=33 \mu\text{m}$ (c) $F=0.40$, $h=62 \mu\text{m}$ and (d) $F=0.50$, $h=40 \mu\text{m}$. The fitted values of pigment porosity were 0.91, 0.94, 0.92 and 0.83, respectively.

(binder). It is seen that rutile titanium dioxide pigmented films have high reflectance values in the visible wavelength range where the scattering cross section of the particles reaches the highest values. The reflectance decreases and the transmittance increases towards longer wavelengths. The strong absorption in the near ultraviolet is due to indirect allowed transitions (Grant, 1959) at about 3.02 eV. The samples containing the W6206K pigments had somewhat lower reflectance values than the samples in Fig. 2. This may be due to a higher degree of particle aggregation leading to dependent scattering effects. The weak absorption band around 2.2 μm is caused by the binder. In contrast, the spectra of films containing silica particles are characterized by low reflect-

ance values due to the weak scattering from these particles. The best fit to theory was obtained for $\rho(\text{SiO}_2)=0.84$ which gives a pigment mass density of 1.93 g/cm^3 . This value is between 1.80 g/cm^3 , the one characterizing silica particles produced by Stöber synthesis (Coenen and Kruijff, 1988) and our experimental values for heat treated samples.

Fig. 3 depicts reflectance and transmittance spectra for coatings containing composite pigments consisting of a silica core coated with a titania (anatase) shell. The spectra are qualitatively similar to those of the titania pigmented coatings in Fig. 2. The coatings are characterized by the ratio between titania and silica mass per particle, $m(\text{TiO}_2)/m(\text{SiO}_2)$, as well as the diam-

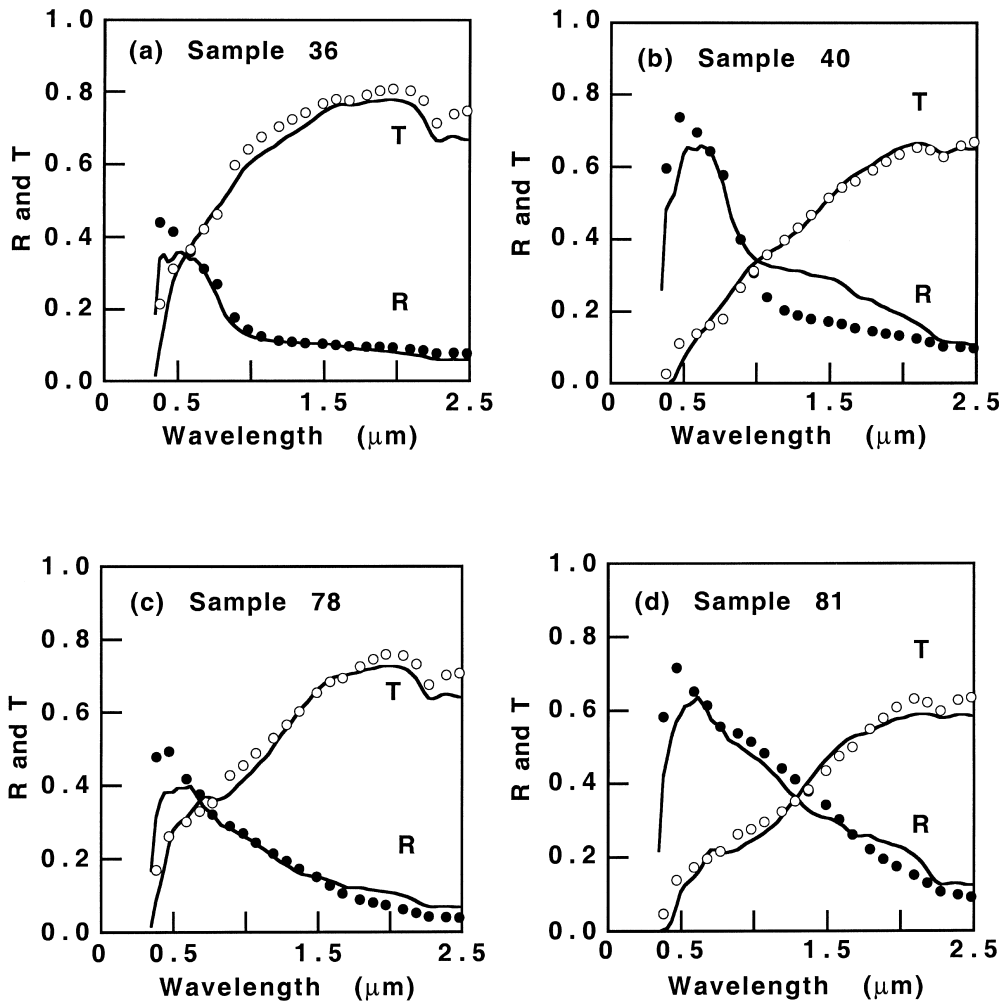


Fig. 3. Comparison of computed reflectance and transmittance spectra (solid lines), with measured ones (dots and circles) from polymer coatings containing anatase titania coated silica pigments. The particle weight fractions, F , and film thicknesses, h , were (a) $F=0.05$, $h=46 \mu\text{m}$, (b) $F=0.40$, $h=33 \mu\text{m}$ (c) $F=0.10$, $h=47 \mu\text{m}$ and (d) $F=0.40$, $h=38 \mu\text{m}$. Mass ratios of titania to silica in the particles were (a,b) 1.50 and (c,d) 1.38. The diameters of the silica cores were (a,b) 300 nm and (c,d) 500 nm. The particle diameters were (a,b) 370 nm and (c,d) 630 nm. The fitted values of pigment porosity were 0.84, 0.83, 0.73 and 0.73, respectively.

eter of the silica core, d_o , obtained from SEM measurements. The particle diameter was evaluated from

$$d = d_o \left[1 + \frac{\rho(\text{SiO}_2)}{\rho(\text{TiO}_2)} \frac{m(\text{TiO}_2)}{m(\text{SiO}_2)} \right]^{1/3}, \quad (5)$$

taking into account pigment porosity. The anatase phase of titanium dioxide is characterized by an absorption edge, at about 3.5 eV, due to direct allowed transitions (Krishna *et al.*, 1993). Measured reflectances of films containing TiO_2 (anatase) coated SiO_2 pigments are smaller than those obtained from films containing rutile pigments with similar sizes. This is mainly due to that anatase pigments have a lower refractive index

and hence are less scattering than rutile ones. It was found that the reflectance increases with the amount of titania per particle, as expected.

In Figs. 2 and 3 we also present fits to the experimental data by use of the theory described in Section 3. In general the agreement between theory and experiment is good, although minor quantitative discrepancies remain. It can be seen that a fairly good agreement between computed results and measurements can be obtained even in the case of coatings with high particle concentrations. Titania pigmented films (Fig. 2) are characterized by large values of the diffuse radiation intensity, especially in the mid-visible. Our calculations show that, at the absorption edge, the diffuse radiation intensity is small with a peaked

forward anisotropic distribution ($\xi \cong 1$ and $\sigma_a \cong 1$). Beyond the absorption edge, in the visible wavelength range, both ξ and σ_a display a structure because of the excitation of low multipolar orders. In the near infrared the diffuse radiation pattern becomes nearly isotropic with ξ increasing towards 2 and $\sigma_a \approx 0.5$. The best fits to experiments were obtained for slightly porous particles with $p(\text{rutile})$ between 0.9 and 1. The values were often even lower for samples with the highest weight fraction, $F=0.5$. We do not regard the fitted pigment density ($3.9 \pm 0.3 \text{ g/cm}^3$) to be significantly different from the bulk value. Rather, the sample-to-sample variation in $p(\text{rutile})$ is probably due to different particle aggregation in the samples, leading to decreased scattering efficiency. Such dependent scattering effects should also be more pronounced at large weight fractions.

The quality of the fit to the optical properties of films containing composite pigments (Fig. 3) is similar, but the interpretation is more problematic. In most of the spectral range there is a rather good agreement between measurements and computed results. Around $0.50 \mu\text{m}$, just after the absorption edge, there is a discrepancy because the ripple structure characterizing the scattering parameters of the single particles is missing in the experimental spectra. The reason for this is a fine roughness on the surface of the composite pigments, seen in SEM measurements. In order to estimate the relative mass density of the anatase shell, $p(\text{anatase})$, we assumed that the relative mass density of the silica core is $p(\text{SiO}_2)=0.84$. Then $p(\text{anatase})$ was used as a fitting parameter to minimize the function $G(p)$ given in Eq. (3). The particle volume fraction, f , was evaluated from Eq. (4), where ρ_p now becomes the average mass density of the particle. The $p(\text{anatase})$ -values are scattered between 0.7 and 0.9, but values close to unity were sometimes obtained for samples with $F=0.5$. The average mass density of the anatase shell estimated from the majority of the results is much lower than, and inconsistent with, the experimental determinations of the density. The reason for this is not clear. The contributions of particle aggregation, particle surface roughness and the surface roughness of the coating need to be carefully evaluated. Edge losses may be a problem as noted above, but the measured absorption (Fig. 3) appears to be roughly on the same level as the computed one.

It should be noted that preliminary computations with a more general theory than in the present paper displayed worse agreement with the

experiments (Vargas and Niklasson, 1998). Using a theory with different APP and FSR in forward and backward directions (Vargas and Niklasson, 1997d,e) leads to pronounced spectral structures not seen in the experimental data.

SOLAR AND LUMINOUS REFLECTANCES

Finally we consider the performance of the coatings as white, solar reflecting surfaces. From the spectrophotometric measurements we have calculated solar [R_{sol}] and luminous [R_{lum}] reflectances of films containing commercial rutile titania pigments, and the novel anatase titania coated silica ones, at different concentrations. The solar spectrum AM1.5 has been used (Bird et al., 1983). Fig. 4 depicts the results as a function of Fh , where F is the pigment weight fraction and h denotes the film thickness. It is seen that the reflectance increases steeply at low values of Fh , and approaches a constant for $Fh > 15 \mu\text{m}$. Films containing commercial rutile titania pigments display larger values of solar and luminous reflectance than films pigmented with composite particles. The effect becomes small at large Fh . The refractive index of anatase is lower than that of rutile, hence films containing composite pigments are less scattering, which leads to a lower diffuse reflectance. As expected, by increasing the amount of titania per particle in the composite pigments, the diffuse reflectance increases, as seen from Fig. 4c,d. The best solar reflectances were close to 0.7 for the coatings with composite pigments and between 0.75 and 0.8 for coatings with commercial rutile pigments.

CONCLUSIONS

Optical properties of polymeric films containing novel anatase titania coated silica pigments have been compared to films pigmented with commercial titania particles. The novel pigments are less scattering than homogeneous rutile titania ones, but the difference is not very large. A four-flux model has been used to predict the optical properties of the particulate polymeric films and good agreement was achieved by assuming the particles to be slightly porous. However the porosity obtained from the fits was unreasonably large in the case of coatings containing composite pigments. Further analyses taking into account aggregation and surface roughness effects are needed in order to obtain a better agreement between theory and experiment.

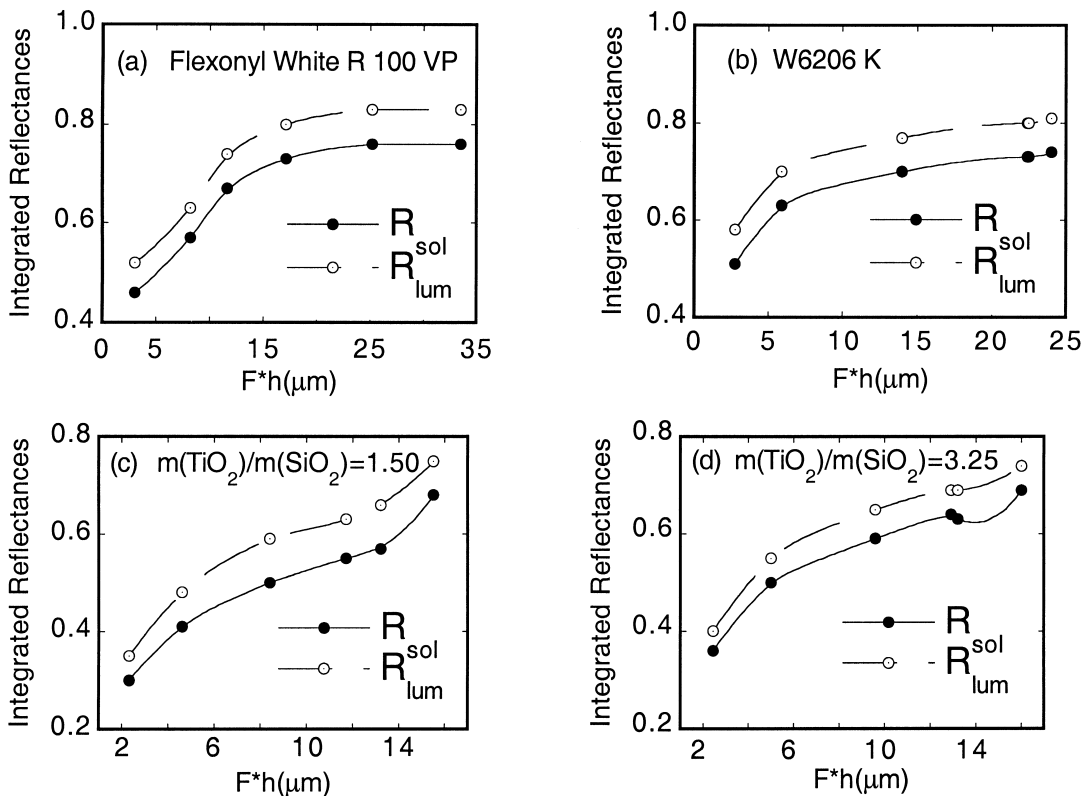


Fig. 4. Solar and luminous reflectance of particulate coatings containing commercial titania pigments (a and b) where the particle diameter is around 300 nm, and novel titania coated silica particles (c and d) where the diameter of the silica core is around 300 nm. The mass ratios of titania to silica are given in (c) and (d).

Acknowledgements—This work was financially supported by the Swedish Foundation for Strategic Environmental Research (MISTRA) through the Ångström Solar Center, Uppsala University. Additional support was obtained from the University of Costa Rica.

REFERENCES

- Berdahl P. (1995). *J. Heat Transfer* **117**, 355–358.
- Bird R. E., Hulstrom R. L. and Lewis L. J. (1983) Terrestrial solar spectral data sets. *Solar Energy* **30**, 563–573.
- Bohren C. F. and Huffman D. R. (1983). *Absorption and Scattering of Light by Small Particles*. Wiley, New York.
- Böttcher C. J. F. (1945) The dielectric constant of crystalline powders. *Rec. Trav. Chem.* **64**, 47–51.
- Chandrasekhar S. (1950). *Radiative Transfer*. Oxford, London.
- Chu C. M. and Churchill S. W. (1955) Representation of the angular distribution of radiation scattered by a spherical particle. *J. Opt. Soc. Am.* **45**, 958–962.
- Coenen S. and Kruijff C. G. (1988) Synthesis and growth of colloidal silica particles. *J. Colloid Interface Sci.* **124**, 104–110.
- Demyrion H. (1985) Optical properties of SiO_2 - TiO_2 composite films. *Appl. Opt.* **24**, 2647–2650.
- Ferber J. and Luther J. (1998) Computer simulations of light scattering and absorption in dye-sensitized solar cells. *Solar Energy Mater. Solar Cells* **54**, 265–275.
- Grant F. A. (1959) Properties of rutile (titanium dioxide). *Rev. Mod. Phys.* **31**, 646–674.
- Greenwood P. (1998). *TiO₂-Belagda Kärnor av Kiselsyra Som Starkt Ljusspridande Kompositpigment*. Licentiate thesis, Chalmers University of Technology, Gothenburg.
- Harris M., Macleod H. A., Ogura S., Pelletier E. and Vidal B. (1979) The relationship between optical inhomogeneity and film structure. *Thin Solid Films* **57**, 173–178.
- Hartel W. (1940). Zur Theorie der Lichtstreuung durch trübe Schichten besonders Trübgeläser. *Licht* **10**, 141–143, 165, 190, 191, 214, 215, 232–234.
- Hsu W. P., Yu R. and Matijevic E. (1993) Paper whiteners I. Titania coated silica. *J. Colloid Interface Sci.* **156**, 56–65.
- Ishimaru A. (1978). *Wave Propagation and Scattering in Random Media*. Academic Press, New York.
- Krishna M. G., Rao K. N. and Mohan S. (1993) Properties of ion assisted deposited titania films. *J. Appl. Phys.* **73**, 434–438.
- Kubelka P. and Munk F. (1931) Ein Beitrag zur Optik der Farbanstriche. *Z. Techn. Phys.* **12**, 593–601.
- Laux S. and Richter W. (1996) Packing-density calculation of thin fluoride films from infrared transmission spectra. *Appl. Opt.* **35**, 97–101.
- Maheu B., Letoulouzan J. N. and Gouesbet G. (1984) Four-flux models to solve the scattering transfer equation in terms of Lorenz–Mie parameters. *Appl. Opt.* **23**, 3353–3362.
- Maheu B. and Gouesbet G. (1986) Four-flux models to solve the scattering transfer equation: Special cases. *Appl. Opt.* **25**, 1122–1128.
- Malitson I. H. (1965) Interspecimen comparison of the refractive index of fused silica. *J. Opt. Soc. Am.* **55**, 1205–1209.

- Mudgett P. S. and Richards L. W. (1971) Multiple scattering calculations for technology. *Appl. Opt.* **10**, 1485–1502.
- Mudgett P. S. and Richards L. W. (1972) Multiple scattering calculations for technology II. *J. Colloid Interface Sci.* **39**, 551–567.
- Nilsson T. M. J. and Niklasson G. A. (1995) Radiative cooling during the day: Simulations and experiments on pigmented polyethylene cover foils. *Solar Energy Mater. Solar Cells* **37**, 93–118.
- Nitz P., Ferber J., Stangl R., Wilson H. R. and Wittwer V. (1998) Simulation of multiply scattering media. *Solar Energy Mater. Solar Cells* **54**, 297–307.
- Pulker H. K., Paesold G. and Ritter E. (1976) Refractive indices of TiO₂ films produced by reactive evaporation of various titanium–oxygen phases. *Appl. Opt.* **15**, 2986–2991.
- Pulker H. K. (1979) Characterization of optical thin films. *Appl. Opt.* **18**, 1969–1979.
- Reichman J. (1973) Determination of absorption and scattering coefficients for nonhomogeneous media. 1: Theory. *App. Opt.* **12**, 1811–1815.
- Reiss H. (1988). *Radiative Transfer in Nontransparent Dispersed Media*. Springer-Verlag, Berlin.
- Ribarsky M. W. (1985) Titanium dioxide (rutile) (TiO₂). In *Handbook of Optical Constants*, Palik E. D. (Ed.), pp. 795–804. Academic Press, New York.
- Stamnes K., Tsay S. C., Wiscombe W. and Jayaweera K. (1988) Numerically stable algorithm for discrete-ordinate-method radiative transfer in multiple scattering and emitting layered media. *Appl. Opt.* **27**, 2502–2509.
- Stöber W., Fink A. and Bohn E. (1968) Controlled growth of monodispersed silica spheres in the micron size range. *J. Colloid Interface Sci.* **26**, 62–69.
- Usami A. (1997) Theoretical study of application of multiple scattering of light to a dye-sensitized nanocrystalline photo-electrochemical cell. *Chem. Phys. Lett.* **277**, 105–108.
- van de Hulst, H. C. (1980). *Multiple Light Scattering*. Academic, New York.
- Vargas W. E. (1998) Generalized four-flux radiative transfer model. *Appl. Opt.* **37**, 2615–2623.
- Vargas W. E. and Niklasson G. A. (1997a) Pigment mass density and refractive index determination from optical measurements. *J. Phys. Condens. Matter* **9**, 1661–1670.
- Vargas W. E. and Niklasson G. A. (1997b) Forward scattering ratios and average pathlength parameters in radiative transfer models. *J. Phys. Condens. Matter* **9**, 9083–9096.
- Vargas W. E. and Niklasson G. A. (1997c) Applicability conditions of the Kubelka–Munk theory. *Appl. Opt.* **36**, 5580–5586.
- Vargas W. E. and Niklasson G. A. (1997d) Generalized method for evaluating scattering parameters used in radiative transfer models. *J. Opt. Soc. Am. A* **14**, 2243–2252.
- Vargas W. E. and Niklasson G. A. (1997e) Intensity of diffuse radiation in particulate media. *J. Opt. Soc. Am. A* **14**, 2253–2262.
- Vargas W. E. and Niklasson G. A. (1998). Light scattering in pigmented coatings: Theory and experiments. *Proc. Eurosun 98 Conf.*, Portoroz, Slovenia, Vol. 2, Paper III, 1, 18.
- Whitney C. (1974) Efficient stream distributions in radiative transfer theory. *J. Quant. Spectrosc. Radiat. Transfer* **14**, 591–611.
- Wilson H. R. and Eck W. (1993) Transmission variation using scattering/transparent switching films. *Solar Energy Mater. Solar Cells* **31**, 197–214.
- Wilson H. R., Ferber J. and Platzner W. (1994) Optical properties of thermotropic layers. *Proc. SPIE* **2255**, 473–484.
- Yoo K. M., Liu F. and Alfano R. R. (1990) When does the diffusion approximation fail to describe photon transport in random media? *Phys. Rev. Lett.* **64**, 2647–2650.



The aim with this work was to develop methods of modifying the surface of colloidal silica, to develop new applications, as well as to improve some existing applications. Aqueous silica sols have been used in a variety of applications over the years and there are an increasing number of applications for these kinds of materials, many of them environmentally driven. To give some examples; the development of waterborne low VOC coatings has led to the need of silane modified colloidal silica that can enhance coating properties, being used as pigments dispersants and also fulfil the demands on shelf-life of such coating formulations. Lead-acid batteries with solid electrolyte are gaining new markets with the development of telecommunication and solar energy where such batteries are used as power sources/storage. The handling and working environment are significantly improved by using silica sols instead of fumed silica as a gelling agent for the acid.

Another example where the “green drive” has given opportunities for colloidal silica dispersions is in the construction field. The recycling of old concrete, increasing amounts of e.g., limestone fillers in concrete, and also the use of the cement kilns as incinerators for waste are producing cements of poorer quality, paving the way for concretes which are susceptible for bleeding, segregation and slow strength development. Addition of colloidal silica may remedy these shortcomings.